

EPA/600/3-86/070

DECEMBER

NOVEMBER 1986

COMPREHENSIVE FIELD STUDY PLAN TO RELATE POLLUTANT
SOURCES TO ACIDIC DEPOSITION
A Preliminary Study of Uncertainties

ATMOSPHERIC SCIENCES RESEARCH LABORATORY
OFFICE OF RESEARCH AND DEVELOPMENT
U.S. ENVIRONMENTAL PROTECTION AGENCY
RESEARCH TRIANGLE PARK, NORTH CAROLINA 27711

COMPREHENSIVE FIELD STUDY PLAN TO RELATE POLLUTANT
SOURCES TO ACIDIC DEPOSITION
A Preliminary Study of Uncertainties

by

D.A. Stewart, J.E. Langstaff, G.E. Moore, S.M. Greenfield, and M.K. Liu
Systems Applications Incorporated
101 Lucas Valley Road
San Rafael, California 94903

and

D.J. McNaughton, N.E. Bowne, R. Kaleel, and M.K. Anderson
TRC Environmental Consultants, Inc.
800 Connecticut Boulevard
East Hartford, Connecticut 06108

Contract No. 68-02-4081

Project Officer

Francis Pooler, Jr.
Meteorology and Assessment Division
Atmospheric Sciences Research Laboratory
Research Triangle Park, North Carolina 27711

ATMOSPHERIC SCIENCES RESEARCH LABORATORY
OFFICE OF RESEARCH AND DEVELOPMENT
U.S. ENVIRONMENTAL PROTECTION AGENCY
RESEARCH TRIANGLE PARK, NORTH CAROLINA 27711

NOTICE

The information in this document has been funded wholly by the United States Environmental Protection Agency under Contract No. 68-02-4081 to TRC Environmental Consultants, Inc. It has been subject to the Agency's peer and administrative review, and it has been approved for publication as an EPA document.

Mention of trade names or commercial products does not constitute endorsement or recommendation for use.

PREFACE

Design of the comprehensive experiments (COMPEX) was an evolutionary process involving a large group of scientists on the design team. As the result of preliminary design discussions, studies were begun on several issues of uncertainty identified as being significant. These studies progressed along parallel path with the COMPEX design report and the results are presented here. Some of the studies undertaken in support of the preliminary plan may incorporate assumptions which differ slightly from those of the final experimental plan but the general results still provide a valuable contribution in determining feasibility and expected results of the experiments.

The following report was produced in large part by Systems Applications, Inc., as the major contributor to Sections 2 through 5. As prime contractor, TRC contributed summary subsections to tie the uncertainty studies to the COMPEX design plan as well as contributing to the uncertainty studies described in Section 6.

This research has been funded as part of the National Acid Precipitation Assessment Program by the Environmental Protection Agency.

ABSTRACT

An experimental program was designed to empirically relate acidic deposition to precursor emissions. Several technical issues requiring further study prior to field experiments were raised. Preliminary estimates of uncertainty were made in order to assess confidence in the experimental design. The five general areas studied included uncertainties in measurements, local scale data analyses, regional scale data analyses, model simulations and data analyses for regional experiments.

Measurement uncertainties are large compared to deposition losses for gases on the local scale. On a regional scale the existing ambient sulfate measurement network has a resolution of order 500 km which is adequate, but characteristic spacing of SO₂ patterns requires resolution of less than 100 km. Model simulations indicated the frequency of tracer detectability at a receptor from a specific source was small and limited by meteorology. Also the frequency of detectability is dependent on source strength. Local source modulations were modeled and attainable modulation signals were found to be of insufficient magnitude to be detected over background concentrations when measurement uncertainties were considered. Results from these analyses of the effects of uncertainty were considered in the final experimental design.

EXECUTIVE SUMMARY

The Atmospheric Sciences Research Laboratory of U.S. Environmental Protection Agency funded a program to design an experimentally based study to provide empirical relationships relating acidic deposition in ecologically sensitive areas to sources of precursor emissions. In addition, the experiments are to provide a data base for evaluation of regional acidic deposition models. The program has been named the comprehensive experiment or COMPEX and the design plan is presented in a companion report entitled, "Comprehensive Experimental Design Plan to Relate Pollutant Sources to Acidic Deposition." In the course of designing the program, several questions arose on technical issues requiring further study prior to conducting the experiments. This report describes preliminary studies performed to clarify these issues and increase the confidence in success of the COMPEX plan. Studies are divided into five general areas: 1) summary of measurement uncertainties, 2) local scale data analyses, 3) regional scale data analyses, 4) model simulations, and 5) data analyses from the regional experiments.

A primary consideration in COMPEX is the ability to design a program which would provide empirical source/receptor relationships within reasonable uncertainty levels. The first component of the uncertainty studies is a review of uncertainties associated with measurement techniques required in the design. COMPEX requires new experimental techniques or new applications of previously used techniques. The report summarizes information on uncertainties associated with systems to be used in the study with the exception of PMCP perfluorocarbon tracer measurements proposed for use. Feasibility experiments proposed in the COMPEX design include studies of this tracer.

The second element of the uncertainty studies involved examination of local scale data to better understand the temporal and spatial characteristics of concentrations and the relationships among pollutants and tracers. The study analyzed data from the Electric Power Research Institute's (EPRI) Plume Model Validation and Development (PMV+D) experiments within 20 km of the Kincaid power plant. Results can be summarized as follows:

- Within local scale distances (<20 km), ambient concentrations of sulfur dioxide, oxides of nitrogen, and inert tracers are strongly related when there is no interference from background. Ambient concentrations respond to variations in emission rates.
- Close agreement of concentration data among pollutants and tracers indicates that depositional losses within 20 km of sources are negligible and within the measurement uncertainty.
- Uncertainty in experimental measurements is large.

Primarily, the results indicate the difficulty in detecting deposition effects over short distances and the need, when simulating sources, to match the tracer release rates to the actual source emissions rates.

Ambient concentration data are available on a regional scale from the EPRI Sulfate Regional Experiment (SURE) and the data provides a data base for studying concentration relationships on a regional scale. The primary product of the regional data analysis is an evaluation of the scale of the spatial concentration patterns and the required resolution for sampling in a program such as COMPEX. The spatial resolution of the ambient sulfate concentrations is of the order of 500 km which indicates the adequacy of both the SURE network and the proposed COMPEX monitoring grid. SURE data were not of adequate resolution to determine the characteristic spacing of the SO₂ patterns. Data indicate that the scale of patterns is less than 100 km. The SURE data analysis also allowed an estimate of the uncertainties in

representing spatial concentrations with mean values from point measurements. The analysis provided a means of studying the errors involved with spatial averaging but also indicated difficulties in detecting concentrations changes resulting from local source modulation experiments.

Numerous uncertainty questions were studied using regional model simulations. First, relative to the long range tracer experiments, the simulations indicated that point source releases of tracers in transport studies did not adequately describe the resultant tracer or emissions distributions from large emission areas. In addition, the simulations suggested tracer release rates which are adequate to assure detection at large source/receptor separation distances. The frequency of detectability was analyzed as a function of these rates and multiples of concentration over background levels. The frequency of detectability or the frequency of source receptor interactions is in general small and limited by meteorology. The frequency is reduced when emission levels for the tracers are reduced. The rate of reduction is larger for tracer releases which are intermittent rather than continuous.

Smaller scale simulations were performed to evaluate the feasibility of local source modulation and deposition experiments. Results indicated that planned emissions modulation may not be of sufficient magnitude to be detected over background concentrations. Supplementary results indicate that the time series analyses of the modulation patterns may likewise be insufficient to provide a detectable modulation signal over temporal cycles in the concentration data. Model simulations relative to source depletion and mass balance techniques for estimation of dry deposition rates may also be hampered by problems with the detectability of deposition losses over local to mesoscale distances.

Analyses of data from other more specialized experimental programs were performed to evaluate aspects of the COMPEX design. Limited data available for analysis from the CAPTEX program was used to evaluate the feasibility of using ground level tracer concentration data to estimate trajectories for the transmittance approach described in the COMPEX plan. The CAPTEX tracer data indicated that the tracer data could be used to provide trajectory information using a sampler network with the resolution of that proposed for the COMPEX experiments.

Data from the SURE program and the MAP3S precipitation chemistry program were analyzed to examine the representativeness of a one year experimental program in generating empirical source/receptor relationships and potential categories for use in statistical analyses. The data suggest that the use of a single year period for an empirical analysis may not be satisfactory. Meteorological categorization schemes require additional study and need to consider broad classes of data to provide adequate sample sizes. Data collection activities in the COMPEX program require both modifications to increase the statistical data base and to relate the program to previous data collection efforts.

The last element of the uncertainty analysis is an analysis of data from the ACURATE experimental program to determine the frequency of source/receptor interactions. ACURATE examined the long-range transport of krypton-85 releases over a one and one half year period. The data show a surprisingly small frequency of interaction between a point release and single receptors. The relationship decreases with distance which emphasizes the need for program modifications to increase the sample size of the COMPEX data base.

The uncertainty studies were performed in parallel with modifications of the COMPEX plan. Numerous suggestions from the studies were incorporated in the plan, particularly in the areas of distributed tracer releases, release rates, release configuration, and sampling resolution.

CONTENTS

PREFACE	iii
ABSTRACT	iv
EXECUTIVE SUMMARY	v
 1. INTRODUCTION AND SUMMARY	 1
Components of the COMPEX Program	1
Topics for Uncertainty Studies	4
Summary	6
Report Outline	8
2. REVIEW OF MEASUREMENT UNCERTAINTY	10
Perfluorocarbon Tracer	10
Sulfur Hexafluoride (SF ₆) Tracer	14
Isotopic Sulfur (³⁴ S) Tracer	16
Sulfur Dioxide	17
Sulfate	20
Implications to the Experimental Design	22
3. LOCAL DATA ANALYSIS	24
Characteristics of the Kincaid Data Base	25
Conservation of Tracer/Pollutant Concentration Ratios	27
Comparison of SO ₂ and NO _x Concentration Time Series	27
Comparison of SF ₆ and SO ₂ Concentrations	42
Statistical Nature of Concentration Fluctuations	44
Implications for Experimental Design	48
4. REGIONAL DATA ANALYSIS	54
Description of the EPRI SURE Data Base	54
Spatial Scale of Concentration Data	57
Analysis of One-Hour SO ₂ Concentrations	57
Analysis of 24-Hour SO ₂ Concentrations	69
Analysis of 24-Hour Sulfate Concentrations	69
Temporal Characteristics of Concentration Data	79
Spatial Representativeness of Single Station Concentration Measurements	83
Analysis of Network Uncertainties	86
Implications for Experimental Design	97
5. MODEL SIMULATION ANALYSIS	100
Modeling Approach	101
Uncertainties in Long-Range Experiments	107
Estimation of Regional Tracer Release Rates	110
Tracer Release Configuration	121
Uncertainties in Short-Range Experiments	133
Local Source Modulation Experiments	133
Local Reactive Tracer Experiments	151
Implications in Experimental Design	171

CONTENTS
(Continued)

<u>SECTION</u>	<u>PAGE</u>
6. Additional Uncertainty Analyses	174
Analysis of Long Range Pollutant Transport Using Tracer Data. .	174
Summary of CAPTEX Program	175
Analysis Results	176
General Observatoins on the CAPTEX Experiments	176
Climatological Analysis of the Experimental Design	177
Duration of Wet Deposition Events	177
Climatological Characterization of Deposition Events. .	178
Analysis of the Adequacy of a One-Year Monitoring Program	190
Potential for Pollutant Transport as Indicated by Source/ Receptor Pair Data	195
References.	200

FIGURES

<u>NUMBER</u>		<u>PAGE</u>
3-1	Time series of hourly concentrations at the stack on 25 May 1981	29
3-2	Time series of five-minute average SO ₂ and NO _x concentrations	31
3-3	Time series of hourly concentrations at station 1422, 28 May 1981	32
3-4	Time series of five-minute average SO ₂ and NO _x concentrations for station 1118 on 25 May 1981.	35
3-5	Time series of hourly concentrations at the stack on 28 May 1981	36
3-6	Scatter plots of five-minute average SO ₂ concentrations versus NO _x concentrations for various EPRI MVD&D monitoring sites for tracer tests conducted 12 May to 1 June 1981	38
3-7a	Hourly Average SO ₂ , SF ₆ , and NO _x Concentrations at Station 1422: 28 May 1981	39
3-7b	Hourly Average SO ₂ , SF ₆ , and NO _x Concentrations at Station 1422: 25 May 1981	40
3-8	Scatter Plots of Hourly Average Concentrations of SO ₂ and NO _x for Two EPRI PMV&D Monitoring Sites at Kincaid, Illinois, Where the Background NO _x was not Sufficient During Tracer Tests Conducted Between 12 May and 1 June 1981	43
3-9	Scatter Plot of Normalized Hourly Averaged SO ₂ Concentrations (10 ⁻⁷ s/m ³) Versus Hourly Averaged SF ₆ Concentrations (10 ⁻⁷ s/m ³). Sample Size is 51 Cases, and the Shaded Region Indicates the 90 Percent Confidence Level	45
3-10	Concentration Spectra Recorded at Station 1422, 11-31 May 1981	47
3-11	Cumulative Distributions of 5 Minute Averaged SO ₂ for Two EPRI PMV Sites at Kincaid. The Intermittency Factor, λ, is Approximately 0.05 for Both Sites. The Intermittent Exponential CDF Function was Fitted to Both Sites	50

FIGURES (Continued)

<u>NUMBER</u>		<u>PAGE</u>
4-1	The EPRI SURE Network of Monitors. Sites Numbered 1-9 Are Class I Stations	55
4-2	Cumulative Distribution of 1-Hr Averaged SO ₂ at EPRI/SURE Station 4 on Lognormal Probability Paper	60
4-3	Autocovariance of Hourly Averaged SO ₂ Concentration Observed at the Scranton, PA site (EPRI/SURE Site #2)	62
4-4	Observed Spatial Correlatins of Hourly SO ₂ Versus Distance. .	63
4-5a	Spatial Distribution of Correlations Between Station Pairs: Western Region	64
4-5b	Mid Region	65
4-5c	Eastern Region.	66
4-6	A Map of the EPRI/SURE Site Locations Occurring Within the Two Study Areas	67
4-7	Scatter Plot of 24-Hour Average SO ₂ Correlations as a Function of the Distance Between Stations	71
4-8	Observed Spatial Correlations of 24-Hour SO ₄ Versus Distance	73
4-9	The Variation in the Correlation Coefficient of 24-Hour Average SO ₄ as a Function of Station Pair Separation. The Error Bars are for the 95% Confidence Interval	74
4-10	The Increase in 24-Hour Average SO ₄ MSE as a Function of Separation Between Station Pairs.	75
4-11	Geographic Distribution of the Mean Sulfate Concentrations (µg/m ³) for Each of the 54 EPRI SURE Monitoring Sites	77
4-12	Inter-Comparisons of Power Spectrums of 24-hr Averaged SO ₂ at the EPRI/SURE Stations	81
4-13	Observed 24-hour SO ₄ (C _x - C _y) ² Versus Distance	88
4-14	Observed 24-hour SO ₄ Root Mean Square Errors Vs. Distance	89

FIGURES (Continued)

<u>NUMBER</u>		<u>PAGE</u>
5-1	Illustration of the Modeling Domain Showing the Nested Coarse-Resolution Grid Region, the High-Resolution Grid Region, and Isolated Point Sources Chosen for Tracer Detectability Simulations	103
5-2	Diagram Illustrating the Use of Model Information and Ancillary Information in the Analysis of Detectability and Uncertainties.	106
5-3a, 5-3b	Schematic Illustration of the Frequency of Exceedence of (a) the Normalized Concentration, χ/Q , as a Function Z , and (b) a Detectable Concentration, χ_d , as a Function of Tracer Emission Strength, Q . In the Illustration $A < B < C$	109
5-4	Distribution of χ/Q from the "Ohio" Single Source and Associated Source Cluster Over all Adirondack Receptor Points.	111
5-5	Distribution of χ/Q from the "Kentucky" Single Source and Associated Cluster over All Nine Adirondack Receptor Points.	112
5-6	Distribution of χ/Q for Continuous and Modulated (One Day On, Two Days Off) Tracer Emissions for (a) the "Ohio" Cluster of Point Sources and (b) the "Kentucky" Cluster of Point Sources	115
5-7	Detectability of 6-hour PMCP Concentrations over the Adirondacks as a Function of (a) Continuous and (b) Modulated Tracer Emission Rates from the "Ohio" Cluster of Point Sources	116
5-8	Detectability of 6-hour PMCP Concentrations over the Adirondacks as a Function of (a) Continuous and (b) Modulated Tracer Emission Rates from the "Kentucky" Cluster of Point Sources	117
5-9	Detectability of 6-hour PMCH Concentrations over the Adirondacks as a Function of (a) Continuous and (b) Modulated Tracer Emission Rates from the "Ohio" Cluster of Point Sources	119
5-10	Detectability of 6-hour PMCH Concentrations over the Adirondacks as a Function of (a) Continuous and (b) Modulated Tracer Emission Rates from the "Kentucky" Cluster of Point Sources	120

FIGURES
(Continued)

<u>NUMBER</u>		<u>PAGE</u>
5-11	Geographic Distribution of Monthly Mean χ/Q Resulting From a Continuous Tracer Release for the "Ohio" Cluster of Point Sources. (Units are 10^{-12} s/m ³)	123
5-12	Geographic Distribution of χ/Q Bias (Cluster Release Minus Major Point Source Release) resulting from a Continuous Tracer Release from the "Ohio" Emission Region. (Units are 10^{-12} s/m ³)	124
5-13	Geographic Distribution of χ/Q Correlation Coefficient Between the "Ohio" Cluster and Single Major Point Source Emission for a Continuous Tracer Release	125
5-14	Geographic Distribution of Monthly Mean χ/Q Resulting from a Continuous Tracer Release from the "Kentucky" Cluster Point Sources. (Units are 10^{-12} s/m ³)	126
5-15	Geographic Distribution of χ/Q Bias (Cluster Release Minus Major Point Source Release) Resulting from a Continuous Release from the "Kentucky" Emission Region. (Units are 10^{-12} s/m ³)	127
5-16	Geographic Distribution of χ/Q Correlation Coefficient Between the "Kentucky" Cluster and Single Major Point Source Emission for a Continuous Tracer Release.	128
5-17	Geographic Distribution of Monthly Mean χ/Q Resulting from a Modulated Tracer Release from the "Ohio" Cluster of Point Sources. (Units are 10^{-12} s/m ³)	130
5-18	Geographic Distribution of χ/Q Bias (Cluster Release Minus Major Point Source Release) Resulting from a Modulated Tracer Release from the "Ohio" Emission Region. (Units are 10^{-12} s/m ³)	131
5-19	Geographic Distribution of χ/Q Correlation Coefficient Between the "Ohio" Cluster and Single Major Point Source Emission for a Modulated Tracer Release	132
5-20	Time Series of Predicted Hourly July (a) SO ₂ and (b) SO ₄ Concentrations at the centroid of the Southwest 80 km Grid Cell Within the Adirondack Region. Light Shading Indicates the Concentrations from Area Sources and all Point Sources Not Modeled With the Plume Segment Approach. The Unshaded Portion Represents the Contribution from the 21 Large Point Sources Treated with the Plume Segment Modeling Component. Finally the Dark Shading Represents the Contributions from the 3 New York Point Sources Assuming Continuous Emission .	136

FIGURES
(Continued)

<u>NUMBER</u>		<u>PAGE</u>
5-21	Predicted (a) SO ₂ and (b) SO ₄ Concentration Time Series Due to the Three New York Point Source Emission Only Over the Same Receptor Point as in Figure 3-23. Shaded Portions Refer to Concentration Predicted for the Modulated Emission Configuration.	137
5-22	Percentage of Time During July 1978 that SO ₂ Concentrations Due to (a) Continuous and (b) Modulated SO ₂ Emissions from the Three New York Point Sources are Detectable.	139
5-23	Percentage of Time During July 1978 that SO ₄ Concentrations Due to (a) Continuous and (b) Modulated SO ₂ Emissions from the Three New York Point Sources are Detectable.	140
5-24	Percentage of Time During January 1978 that SO ₂ Concentrations Due to (a) Continuous and (b) Modulated SO ₂ Emissions from the Three New York Point Sources are Detectable	144
5-25	Predicted Average SO ₂ Concentration Distribution During the (a) Odd-Week and (b) Even-Week Periods. Part "c" Illustrates the Difference in Average SO ₂ Concentrations Over These Two Samples (i.e., Odd-Week Average Minus Even-Week Average). Units are µg/m ³	146
5-26	Predicted RMS SO ₂ Concentration Distribution During the (a) Odd-Week and (b) Even-Week Periods. Part "c" Illustrates the Difference in RMS SO ₂ Concentrations Over These Two Samples (i.e., Odd-Week Average Minus Even-Week Average). Units are µg/m ³	147
5-27	Predicted Average SO ₂ Concentration Distribution Over the Odd-Week Period (a) With, and (b) Without the Contribution from the Three New York Point Sources. Part "c" Illustrates the SO ₂ Concentration Deficit Resulting from the Modulated Emissions. Units are µg/m ³ . . .	149
5-28	Predicted RMS SO ₂ Concentration Distribution Over the Odd-Week Period (a) with, and (b) Without the Contribution From the Three New York Point Sources. Part "c" Illustrates the RMS SO ₂ Concentration Dificit Resulting from the modulated Emission. Units are µg/m ³	150

FIGURES
(Continued)

<u>NUMBER</u>		<u>PAGE</u>
5-29a	(a) Percentage of Initial Sulfur Mass Removed Through SO ₂ and Sulfate Dry Deposition; (b) Difference in Percentage of Initial Sulfur Mass Removed Through SO ₂ and Sulfate Dry Deposition Considering the Uncertainties in Oxidation and Dry Deposition Rate Constant Specification. See Text for Further Details.	156
5-30	Minimum Mass Flux Measurement Precision (i.e., C _v -Upper Limit) Required for Sulfur Deposition Detection (a) Without, and (b) With Consideration of the Uncertainties in Oxidation and Dry SO ₂ and Sulfur Deposition Rates. These Values, Expressed as a Percentage, Are Calculated From the Simple Mass Balance Approach. See Text for Further Details.	161
5-31	Spatial Distribution of Hourly Average SF ₆ X/Q for 1500-1600 EST, July 6, 1978 (Milliken Power Plant, Central New York State)	165
5-32	Spatial Distribution of Hourly Average Sulfur 34 X/Q For 1500-1600 EST, July 6, 1978 (Milliken Power Plant, Central New York State).	166
5-33	Spatial Distribution of Hourly Average Ratio of 34 _s X/Q' to SF ₆ X/Q for 1500-1600 EST, July 6, 1978 (Milliken Power Plant, Central New York State).	167
6-1	Air Mass Classification Scheme Used in SURE Data Analysis SOURCE: Mueller and Hidy (1983)	181
6-2	Variations of Arithmetic Mean Values for Individual Areometric Parameters for Class I Stations in the Northeast Coast Region. SOURCE: Mueller and Hidy (1983) .	183
6-3	Precipitation (Top) and Sulfate Ion Concentration in Precipitation (Bottom) as a Function of the Directional Sector Through Which the Air Parcel Passed to Reach Whiteface Mountain, New York in 1978. SOURCE: Wilson, et al, (1982)	187
6-4	Frequency of Occurrence of Krypton 85 Concentrations as a Function of Distance for Concentration Levels \geq Background Upper Limit (BUL), $\geq 10 \times$ BUL and $\geq 100 \times$ BUL. . . .	197

TABLES

<u>NUMBER</u>		<u>PAGE</u>
2-1	Properties and Costs (Except Cost of Sampling and Analysis) of Gaseous Conservative Tracers	12
2-2	Summary of Uncertainty Estimates for Ambient SO ₂ Measurements	21
3-1	Uncertainty in the Hourly Averages of the Various Stack Parameters for the Kincaid Site During 1981	26
3-2	Uncertainty in the Hourly Averages of SF ₆ , SO ₂ , and NO _x Concentrations Observed at Rockwell's Monitors at Kincaid During 1981	28
3-3	The Median Five-Minute Average SO ₂ and NO _x Data at the Rockwell Sites, May 11, 1981 Through May 31, 1981	33
3-4	A Summary of Statistical Measures Comparing the 5-Minute Average SO ₂ and NO _x Observations During Specific Tracer Tests and at Stations Where the NO _x Background Concentration was not Significant	37
3-5	A Comparison of Hourly Average SO ₂ and NO _x Statistics for Stations Where the NO _x Background Concentration was not Significant	41
3-6	Comparison of SO ₂ and SF ₆ Normalized Concentrations (X/Q), IN 10 ⁻⁷ s/m ³	46
3-7	The Average and Standard Deviation of the Coefficient of Variation as a Function of Averaging Period. All Coefficients of Variation Statistics are Estimated From Sets of 5-Minute Averages	49
4-1	The Number of Hourly SO ₂ Observations Available for Selected EPRI/SURE Sites	56
4-2	The Number of Station Pairs as a Function of the Distance of Separation	58
4-3	A Summary of the Accuracy of SO ₂ and SO ₄ Observations Made at the Class I EPRI/SURE Network	59
4-4	The Variance of SO ₂ (ppb ²) for Various EPRI/SURE Stations as a Function of Averaging Time	70

TABLES
(Continued)

<u>NUMBER</u>		<u>PAGE</u>
4-5	Comparison of the Observed Mean Square Error (MSE) in 24-Hour Average SO ₄ Concentrations as a Function of Station Separation Versus the MSE Computed Using a Single Variogram Model Described by Equation 4-6. Variance for all Stations is 36 µg/m ³	78
4-6	A Summary of the Maxima in the SO ₂ -SO ₄ Gain Function, as a Function of Period and Station SO ₂ /SO ₄ Pairing (Band Width is 0.0675)	82
4-7	Parameters Fitted to Hourly SO ₂ and 24-Hour SO ₄ Data	85
4-8	Comparison of Observed 24-Hour SO ₄ With Predictions of Equation 4-10	87
4-9	The Expected Root Mean Square Error (RMSE) of Estimating a Spatial Mean Over a 57,600 km ² Region, Varying the Station Spacing	95
4-10	The Expected Root Mean Square Error (RMSE) of Estimating a Spatial Mean Over a 57,600 (240 x 240 km) Region With a Station Spacing of 60 km, for Increased Averaging Times	96
5-1	Difference in Ratios of Normalized ³⁴ S to Normalized SF ₆ Concentrations as a Function of the Distance Between Sampling Arcs. Differences are Expressed as the Percentage of the Average Ratio Across the Interval Between Arcs	169
6-1	Duration of Precipitation/Deposition Events	179
6-2	Annual Percentage of Event Days by Air-Mass Category	184
6-3	Yearly Percent Deviations From 4-Year Mean Precipitation and Sulfate Deposition Amounts at Brookhaven National Laboratory, Upton, LI, NY	192
6-4	Yearly Percent Deviation From 3-Year Mean Precipitation and Total Sulfur Deposition Amounts at 4 MAP 3S Locations	192
6-5	Annual Mean and Monthly Percent Deviations From Annual Mean Concentration, Precipitation, and Deposition Values for Charlottesville, Virginia, 1977-1978	193

SECTION 1

INTRODUCTION AND SUMMARY

This report describes uncertainty and feasibility studies related to the comprehensive experiment (COMPEX) designed under the sponsorship of the U.S. Environmental Protection Agency Atmospheric Sciences Research Laboratory. The objective of the design program was to design experiments which will:

- 1) Relate empirically mass transfer from acid pollutant (and precursor) source areas to acidic deposition.
- 2) Provide a data base to aid in the development and evaluation of regional acidic deposition models.

The objectives of this study were to study critical issues related to the COMPEX design and to support, where possible, modifications of the design which improve its potential for success. The work reported in this document was performed in parallel with refinements of the design document. Some results, summarized in Section 1.3, are incorporated into the design report.*

1.1 Components of the COMPEX Program

The comprehensive experimental program consists of three experimental components and an analysis designed to provide source/receptor relationships and the data base for model evaluation. In the COMPEX design document, the components are referred to as the combined experiments because only in combination can they provide sufficient data for developing the required relationships. The components of COMPEX are:

Long Range Tracer Experiments

The major objectives of the long range tracer study are to simulate transport and dispersion of pollutants using inert tracers and to determine

*Comprehensive Experimental Design Plan to Relate Pollutant Sources to Acidic Deposition.

the mass distributions and balances of the tracers in a receptor area. Tracer releases will be made at major emission source areas. These will be selected for study on the basis of SO₂ emissions and forecast meteorological conditions (i.e., expected transport routes). The source areas are located 500 to 1000 km from the Adirondacks Region of New York State which was identified as the primary receptor area for the study. From these source areas, inert tracers will be released and tracked by means of a ground-level sampling network covering the northeast. A fine resolution ground level sampling grid will be established in the Adirondacks Region where aircraft sampling will be conducted to support studies of deposition and transmittance in a small area.

Short Range Experiments

A series of short range experiments is proposed to provide information on plume depletion. This is an important process in the transmittance approach. Current estimates are only available on a local scale and are associated with a high degree of uncertainty. To overcome these uncertainties, a combination of three types of experiments are proposed:

- Reactive Tracer Deposition Experiments - Sulfur-34 tracer studies will be performed to provide information on deposition and plume depletion. The experiments will represent a variety of meteorological and surface conditions. Experiments will include releases of sulfur-34 and two additional inert tracers. The tracer samples will provide deposition estimates by plume depletion and tracer ratio techniques.
- Deposition Experiments - Experiments will be conducted to determine deposition rates using fixed deposition monitoring sites in conjunction with aircraft eddy correlation techniques for ozone. Fixed site data will be used to determine the relationships of ozone and sulfur and nitrogen oxide fluxes. These data will then be available for use in extrapolating aircraft ozone eddy correlation measurements to estimate sulfur and nitrogen oxide deposition for large areas.

- Source Modulation Experiments - The last type of short range experiments proposed are local source modulation experiments. Data from these studies will provide a direct measure of local source attribution and plume depletion as a test for derived source/receptor relationships.

Routine Monitoring and Support Data Collection

This component of the combined experiment will provide the primary data base for model evaluation. It will provide wind and concentration data to help determine transport trajectories and transmittances associated with long-range transport. In addition, the data will be used to study the variability of acidic species and precursors as a function of meteorological and emissions patterns and to provide a historical perspective for these patterns relative to past or ongoing programs. An important role of the data collected under the routine monitoring component will be to provide a limited data set for analysis of the chemistry of deposition processes. Support meteorological and emissions data from other programs will be collected as part of this component.

Analysis

Analyses of the data collected by the three components will characterize deposition episodes. More importantly they will provide fractional transmittance functions, tracer transport statistics, and deposition estimates. Combination of these derived values will provide an estimate of the mass arriving at a receptor and the potential for depositing that mass, thus completing the source/receptor relationships.

The combined experimental program is designed to meet the data requirements of a transmittance approach. Data collected under the program will also be sufficient for additional parallel analyses including analyses using upgraded versions of current regional models, and analyses by statistical inference.

The plan utilizes some untested methods and unproven combinations of techniques. Therefore, success of the design must be gauged in pilot experiments and uncertainty assessments which examine these approaches. This use of pilot and preliminary studies to assess the adequacy of the plan is termed a staged approach and is an integral part of the plan. The studies described in the following sections represent the first phase of a staged approach. The studies use existing data and regional air quality models to evaluate several program components.

1.2 Topics For Uncertainty Studies

The work plan for uncertainty studies was established based on preliminary COMPEX designs. The areas of concern were in two broad classes, the detectability of tracers and pollutants for various components and the representativeness of the data. The specific uncertainty topics under these broad classes include:

Detectability

- Uncertainties involved with source modulation experiments and the feasibility of such experiments.
- Uncertainties involved with mass flux and mass balance techniques.
- Tracer release rates required to assure detectable plumes of perfluorocarbon and sulfur-34 tracers.
- Space/time relationships for parameters measured by the program.

Representativeness

- Representativeness of subgrid scale measurements.
- The impact of non-uniform sampling areas on measurement uncertainties.
- Meteorological categories to be used for analysis.

As the plan developed and initial comments were received, the critical areas of concern for analysis were refined as:

- The feasibility and representativeness of dry deposition and precipitation measurements.
- Tracer use and application.
- Statistical uncertainties and the feasibility of emissions modulation experiments.

Analyses presented in this report are derived from these two lists.

Topics included are:

- 1) Uncertainties associated with measurement techniques.
- 2) Local scale studies to examine:
 - Losses of chemical concentrations during travel;
 - The effects of uncertainty and background variations on concentration statistics;
 - The nature of concentration fluctuations.
- 3) Regional scale studies to examine:
 - The spatial scales of concentration data relative to network spacing;
 - Temporal characteristics of regional pollutant measurements;
 - The spatial representativeness of concentration data;
 - Uncertainties in network design.
- 4) Modeling studies to examine:
 - Release rates for tracer experiments;
 - The frequency distributions of source/receptor interactions from point and distributed sources;
 - The detectability of local source modulations;
 - Local scale mass balance and concentration ratio techniques for source depletion estimates.

- 5) Studies of long range tracer study data to examine the frequency of source/receptor interactions and the feasibility of using ground level tracer concentration measurements in trajectory calculations.
- 6) A review of air and precipitation chemistry data to examine the categories for statistical analyses and the adequacy of a one year program in providing sufficient data to develop empirical source/receptor relationships.

1.3 Summary

Specific conclusions are provided in each section. The study results in these sections are generally not conclusive since the models and data bases for analyses were not designed for this application. For example, two data sets were evaluated to determine the spatial scale of SO₂ patterns to aid in the selection of COMPEX sampling sites. One data set provides concentration data for a network with spacing of more than 100 km while the other provides data on a dense network which only extends 20 km from the source under study. Measurement of SO₂ concentration patterns will require concentration measurements with a resolution somewhere in this range.

Study results are informative in a number of areas and since they were developed in parallel with the COMPEX design effort, some of the results contributed to the modifications of the design plan. Results were not adequate to determine the overall feasibility of COMPEX but they do suggest a need for further studies in a phased or staged approach. Major findings of the studies are as follows:

- 1) Frequency of sources/receptor interactions. Results of modeling studies and analyses of tracer experiment data indicate that the frequency with which a single point source influences a single receptor is very low, on the order of 10 percent of the time or less. One set of tracer data indicated that the frequency decreases with separation distance between the source and receptor. This indicates that plume transport direction is more important than dispersion in determining the frequency of transport.

The frequency of source influence increases when a group or distributed configuration of sources is considered rather than a point source. Frequencies also increase when the impact on receptor areas is considered rather than a single receptor point. As a result of these findings, several modifications were included in the COMPEX plan including the use of distributed tracer source configurations, use of multiple tracer release areas under meteorological forecast control, and enhanced resolution of sampling grids.

- 2) Spatial resolution of concentration data. The spatial resolution of SO_2 was determined to be less than 100 km. Sulfate concentrations are adequately described by the resolution of the COMPEX sampling resolution of approximately 100 to 150 km. SO_2 which is a primary pollutant might be expected to be similar in near-source concentration patterns as inert tracers. This leaves open some question as to whether tracer sampling resolution is sufficient near source areas. This topic needs to be investigated along with the design element of using five tracer release points to represent emissions areas with a scale of 100 km.
- 3) Trajectory determination from tracer data. Results of a previous long range tracer study indicated that transport position and trajectories could be determined with ground-level concentration data although coarse grid resolution, missing data, and unexpectedly narrow plumes of tracer material are a problem. In response, the grid resolution for COMPEX sampling was increased.
- 4) Release rates and configuration. Model results indicated that the frequency of source/receptor influence increases for distributed emissions. The frequency does not vary linearly with detected concentration when expressed as a multiple of background concentration. These results confirm the benefits of planned tracer releases in a distributed configuration. In addition, tracer release rates are determined with reference to a multiple of approximately 10 to 20 times background rather than 100 times specified in initial COMPEX plans.
- 5) Uncertainties. Results of study surveys and analyses include a compilation of measurement uncertainties for some of the parameters specified in the COMPEX design. Suggestions were made and examples provided for methods to estimate uncertainties associated with network data.
- 6) Short range experiments. Two aspects of the short range experiments were examined, the source depletion estimates by reactive tracer experiments and the local source modulation experiments. Success of both experiments is dependent on the detectability of a signal over natural variability or background. Results of the reactive tracer analyses indicate that differences in concentrations or concentration ratios may not be sufficient to determine plume depletion over distances of approximately 10 to 50 km. Results from model simulations indicate that the fraction of mass depleted over these distances may not be sufficient to exceed measurement uncertainties, particularly those related to SF_6 in

sulfur-34 to SF₆ ratios. Confirmation of this conclusion would require a pilot experiment and a cost benefit analysis of this component of the study. Results of source modulation exercises indicate that in the COMPEX, network configuration of the modulation of sources near the fine mesh grid area would probably not provide sufficient signal for analysis. This conclusion based on a modeling analysis, may not be true if the experiments are of long enough duration that time series analysis methods could be used for analysis. In addition, the analyses did not consider modulation of larger sources in areas of low background concentrations.

- 7) Categorization of data and the representativeness of a one year program. A review of past studies did not provide a categorization scheme for statistical analysis of data. These studies did not include an analysis of both concentration and wet and dry deposition data. Wet deposition is highly episodic and single episodes have the potential of providing a large portion of annual deposition as a receptor. A scheme to analyze a one year data set, particularly when tracer releases are not performed every day, must be very simple with few categories or data collection must be performed in such a way that the data from the one year program can be tied to previous studies. In the COMPEX design, monitoring sites are proposed for some locations previously used in monitoring experiments in hopes that the needed long term relationship can be developed from a combination of current and past program data.
- 8) Tracer use. An analysis of short range SO₂ and tracer data indicates the importance of matching emission fluctuations of a study pollutant to the tracer used in the study.

1.4 Report Outline

The uncertainty report which follows is divided into five sections:

- Section 2, Review of Measurement Uncertainty - This section discusses measurement techniques and related uncertainty estimates for tracers or pollutants which will be measured in the COMPEX program.
- Section 3, Local Data Analysis - This section reports analyses of a very complete local scale data set developed for evaluation of air quality models applied within 20 km of a source. The analyses focus primarily on using the spatial and temporal characteristics of tracers and pollutants and their interrelations to evaluate the tracer use in the COMPEX experiments.

- Section 4, Regional Data Analyses - This section discusses sampler spacing and the representativeness of point observations for areal averages.
- Section 5, Model Simulation Analysis - A series of model simulations are reported covering a range of topics related to the required tracer release rates for long range tracer experiments, the frequency of source/receptor interactions, and the detectability of tracers and pollutants for experiments designed to determine deposition rate and mass balances.
- Section 6, Additional Uncertainty Analyses - The last section consists of descriptions of analyses using experimental and network data to examine the feasibility of long range tracer experiments and to suggest categories for data analysis in COMPEX.

SECTION 2

REVIEW OF MEASUREMENT UNCERTAINTY

Species of interest to this plan include several perfluorocarbons; sulfur hexafluoride (SF_6), isotopic sulfur (^{34}S), sulfur dioxide (SO_2), and sulfates (SO_4^{2-}). With the exception of a few of the potentially useful perfluorocarbon tracers, successful measurement techniques for each of the species have been demonstrated in past field experiments (Dietz and Senum, 1984). A summary of the tracer characteristics, measurement methods, and associated uncertainties for these species are presented below.

2.1 Perfluorocarbon Tracer (PFT)

Perfluorocarbon tracers (PFT's) are under consideration for long-range transport and dispersion field experiments because they meet the following criteria:

- The tracers are nondepositing and nonreactive resulting in long residence times.
- Low background concentrations permit the release of relatively small quantities of the tracer while maintaining instrument detectability.
- The tracers are non-toxic and cause no adverse environmental impacts.
- Limited industrial use insures that a detected tracer is unambiguously identified with the source from which it was released.
- Tracers are available at relatively low cost in the quantities required for detectability.
- They are detectable with high sensitivity down to ambient levels at relatively low cost.

In a recent review of gaseous tracer capabilities and applications, Dietz and Senum (1984) list four perfluorocarbons currently available for use in a long-range tracer experiment. Their physical and chemical properties and

relative costs (based on simple dispersion estimates) are presented in Table 2-1. Perfluoromethylcyclohexane (PMCH) and perfluoromethylcyclopentane (PMCP) are proposed for use in the COMPEX experiments.

Because of the liquid state of the perfluorocarbon tracers, their release requires atomization and complete evaporation into a gas stream. The common methods of dispensing the tracers are through pressurizing the storage tank or withdrawing the liquid by a metered pump. Atomization is accomplished through the use of a high-pressure hydraulic nozzle. The droplets produced are subsequently entrained into a heated air stream where complete vaporation occurs.

Detection of the four currently available PFTs consists of collecting an air sample and performing a gas chromatographic analysis on the four compounds. Sampling of the PFTs is performed using one of two generic sampling apparatuses. Whole-air samplers consist of pumps or syringes and collection bags or bottles. Samples are collected in the field and shipped to a laboratory for analysis. The advantage of simplicity in the whole-air sampling technique is partly offset by the main disadvantage of the technique, namely the potential for sample degradation during shipping and handling.

The other collection method utilizes adsorbent samplers, which consist of an adsorbent material enclosed by a containment tube in contact with the air. Two types of adsorbent samplers have been developed specifically for collecting PFT samplers. The Brookhaven Atmospheric Tracer Sampler (BATS) is a commercially manufactured, programmable PFT sampler consisting of an array of 23 sampling tubes, each containing an adsorbent that can retain all the PFTs in more than 30 liters of air. The portable unit is designed to take sequential samples at preprogrammed frequencies and durations. The sampling time is controlled by the rate at which air is drawn through the tubes

TABLE 2-1

PROPERTIES AND COSTS (EXCEPT COST OF SAMPLING AND ANALYSIS) OF GASEOUS CONSERVATIVE TRACERS

Distance = 100 km, desired concentration = 100 times background at centerline, release time = 3 hours
(from Dietz and Senum, 1984)

Tracer	Symbol	Formula	Molecular Weight	Phase at 20°C	Boiling Point (°C)	Supplied Form	Ambient Concentration (f1/l) ^A	Cost (\$/kg)	Released Quantity (kg)	Relative Tracer Cost (\$1000)
Perfluorodimethylcyclohexane	PDCH	C ₈ F ₁₆	400	Liquid	102	Liquid	26	120	82	9.8
Perfluoromethylcyclohexane	PMCH	C ₇ F ₁₄	350	Liquid	76	Liquid	3.6	100	10	1.0
Perfluoromethylcyclobutane	PDCB	C ₆ F ₁₂	300	Liquid	45	Liquid	0.35	500	0.83	0.42
Perfluoromethylcyclopentane	PMCP	C ₇ F ₁₄	350	Liquid	48	Liquid	2.7	100	9 ^C	0.9
Sulfur hexafluoride	SF ₆	SF ₆	146	Gas	-64	Liquid gas	2000 ^B	10	2320	23.2

^A 1000 f1/l equals p1/l or one part per trillion.

^B Near-urban SF₆ is 2000 f1/l or more in many locations because of significant use; tropospheric background is 850 f1/l.

^C Based on ~85 percent purity, which is readily available.

and is adjustable from one minute to one week per tube. After each tube has collected the specified volume of air, the PFTs are recovered from the adsorbent by heating and are subsequently passed from the tube through an automated electron capture detector-gas chromatograph (EDC-GC) system, which is capable of analyzing the 23-tube array in about three hours. This sampling system has been used in several intermediate- and long-range tracer experiments with successful results (e.g., Ferber et al., 1981; Fowler and Barr, 1983; Clark et al., 1984).

Another type of adsorbent sampler collects the tracer by Fickian diffusion toward the adsorbent material. This passive sampling device, developed originally for indoor tracer studies, has also been used in atmospheric tracer studies (Dietz et al., 1983). The sampler, known as the Capillary Adsorption Tube Sampler (CATS), is best suited to sampling tracers over extended periods of time. The sampling rate for the passive collector was recently determined from a comparison of samplers to be equivalent to 232 ml air/day for PMCH and 217 ml air/day for PDCH (Dietz et al., 1983).

Perfluorocarbon sampling devices have also been developed to sample concentrations aloft. The main sampling methods consist of either airborne sampling using whole-air or adsorbent samplers, or sampling through a group of tubes suspended by a balloon. PFT samples are currently capable of being analyzed in the laboratory and in situ, by semi-continuous and continuous analyzers. Analytical techniques are similar for both bag samples and those collected by adsorption. The samples are first processed to concentrate the tracer and subsequently passed through a gas chromatograph system. Detectability limits and measurement precision depend on the collection and analysis methods.

The range of detection for laboratory analysis spans six orders of magnitude, i.e., a minimum of 0.5 - 5 fL/L up (femtoliters per liter) to 5000

pL/L (Ferber et al., 1981; Dietz et al., 1983), whereas semi-continuous and continuous analyzers in situ have greater minimum detectable limits (Dietz and Dabberdt, 1983). Continuous analyzers used to detect PFTs in recent local/mesoscale studies revealed a practical detection limit of approximately 10 pL/L, clearly not sensitive enough to detect PFTs from long-range tracer experiments, where the emphasis is on sub pL/L concentration levels. A semi-continuous dual-trap analyzer, which periodically processes samples on a four-minute basis, currently exhibits a 1 fL/L detection limit (Dietz and Senum, 1984), suitable for airborne sampling on a regional scale.

The programmable BATS sampler has detected background concentration levels of PDCB (0.35 pL/L) with a precision of ± 10 percent, PMCH (3.6 pL/L) with a precision of ± 3 percent, and PDCH (26 fL/L) with a precision of ± 5 percent from 25-liter samples. With adjustable sampling rates of 0.5 - 40 ml/min, these precision measures correspond roughly to a 10-hour minimum sample.

The CATS passive PFT sampler has a demonstrated detection precision for background PMCH and PDCH concentrations of ± 10 percent. However, these precision measurements correspond to 30-day sampling periods due to the slow sampling rate (0.14 ml/min) of the passive sampling method. Both CATS and BATS samplers have measured nearly identical background PMCH and PDCH levels, indicating the low variability of background levels and high accuracy of the gas chromatography detection procedure.

The long-range tracer component of the combined experiment will use the semi-continuous dual trap analyzer for aircraft measurements. Ground level sampling will be performed using the BATS adsorbent samplers with analysis of the samples performed in a central automated laboratory.

2.2 Sulfur Hexafluoride (SF₆) Tracer

Use of sulfur hexafluoride (SF₆), the first electron-attaching compound used for atmospheric tracing, dates back to the mid-1960s. Its continued

widespread use is due to its ease of detectability in GC analyzers and its availability in the liquified gas state, which simplifies the release procedure. The physical properties of SF₆ and relative costs are shown in Table 2-1. The high background levels of SF₆ restrict its use to local/mesoscale (i.e., <100 km) field experiments.

Sampling of SF₆ is typically accomplished using a variety of whole-air or adsorbent samplers, with both ground-level and airborne sampling methodologies currently well established. Portable gas chromatographs are commercially available for analyzing whole air samples with detection limits of 5 pL/L. Processing the sample prior to analysis, i.e., using a precut column technique (Dietz and Cote, 1971) and concentrator (Dietz et al., 1976a), have yielded lower detectable limits and higher precision. For example, Dietz and co-workers (1976b) demonstrated detectable limits of 0.5 pL/L with \pm 3 percent precision from 40 ml whole-air samples passed through a molecular sieve trap cooled to dry ice temperatures.

Detection limits of about 7 pL/L have been produced by a semi-continuous SF₆ monitor sampling at downwind distances of 90 km, whereas the detection limits of truly continuous analyzers, used in short range (~10 km) field experiments, are typically 10 to 30 pL/L (Dietz and Dabberdt, 1983).

During the recent short-range SF₆ tracer experiments associated with the EPRI PMV&D Kincaid field measurement phase, the SF₆ measurement uncertainties were assessed by analyzing numerous colocated samples, performing analyses on duplicate samples, and auditing the performance of the sampling and analysis procedures. Results from these QA procedures indicate that for ground-level SF₆ concentrations less than 100 pL/L (i.e., 100 ppt), the overall measurement uncertainty is within \pm 10 pL/L 90 percent of the time. Measured concentration values exceeding 100 pL/L were generally within \pm 10 percent of the mean concentration, 90 percent of the time (Smith et al., 1983).

2.3 Isotopic Sulfur (^{34}S) Tracer

With the development of the Isotope Ratio Tracer Method (Manowitz et al., 1970; Newman et al., 1971), the use of sulfur isotope ratios as tracers has become feasible. The two most predominant isotopes of sulfur, ^{32}S and ^{34}S , occur approximately in the ratio $^{34}\text{S}/^{32}\text{S} = 4.502 \times 10^{-2}$ in meteoritic sulfur. This ratio has been accepted as the standard against which measured ratios in the environment are compared. Newman and others (1975a and b) present data suggesting that the average isotopic ratio in atmospheric sulfur is 4.515×10^{-2} , with a range of 4.500×10^{-2} to 4.534×10^{-2} and a standard deviation of 9.18×10^{-3} . In terms of the percentage abundance of ^{34}S relative to total sulfur, the average, range, and standard deviation are 4.319 percent, 4.3060-4.3373 percent, and 0.0091 percent, respectively. The very low background variability suggests that only small quantities of enriched ^{34}S , enough to exceed the natural variability, are required to serve as an atmospheric tracer.

The process by which isotopic tracers are monitored in the field involves collection of SO_2 and sulfate particulates on suitable filters and performing isotopic mass spectrography. The basic collection technique, described by Forrest and Newman (1973), has been used in several programs (e.g., Newman et al., 1975a and b; Hitchcock and Black, 1984). To obtain a precision of ± 0.02 percent from the mass spectrometer, a minimum quantity of sulfur oxide is required. The sensitivity of the spectrometer used during the mid-1970 studies required a minimum sample size of 1 mg of sulfur oxides (Forrest and Newman, 1973) to achieve this precision.

Precision sulfur dioxide samples are typically collected on a series of alkaline (carbonate) impregnated filters mounted back-to-back behind glass fiber pre-filters in a hi-vol sampler. The filters are subsequently processed to isolate the sulfur sample, which is then analyzed for isotope fractions.

The precision achieved for the ratio measurement procedure is approximately 0.01 percent of the isotopic ratio (Hitchcock and Black, 1984).

Available evidence suggests that sulfur oxides produced by biological processes may exhibit different isotope signatures than the sulfur from geological sources (Kaplan and Rittenberg, 1964). There is also some empirical evidence suggesting that the isotopic ratio is altered by atmospheric chemical reactions, particularly aqueous phase SO_2 oxidation (Newman et al., 1975). This evidence would imply that the sulfur isotopic ratio distribution within aerosols may be variable and dependent on the available ambient oxidants. Furthermore, if the fractionation varies with particle size, for example due to a relationship between oxidation rate and droplet pH, then dry deposition processes could influence the isotope ratio of ambient airborne sulfur. However, the differences in isotope ratios, which are thought to be associated with these processes, are of the order of 2 percent of the $^{34}\text{S}/^{32}\text{S}$ ratio (Hitchcock and Black, 1984), and thus could conceivably result in a slightly higher variability than the data of Newman and co-workers (1975) and Forrest and Newman (1973) would indicate. Use of the isotope tracer in the combined experiments will be over limited distances and will minimize these effects. Further studies are required to quantify the significance of variable fractionation accompanying the atmospheric transport of an isotopic sulfur tracer. However, even the larger estimates of the ratio variability indicate a nearly constant proportionality, and hence, determining suitable ^{34}S emission rates based on detection above the background variability, as suggested by Hicks (1984) and appear entirely adequate.

2.4 Sulfur Dioxide

Methods specified for the combined experiments combine hi-vol sampling of SO_2 on alkaline impregnated cellulose filters with subsequent extraction and

analysis. A review of the varied techniques used to sample ambient SO₂ concentrations and their associated uncertainties is not attempted here. Instead, SO₂ sampling methods employed in the recent SURE program (Mueller and Hidy, 1983) and ERAQS program (Mueller and Watson, 1982)* are described. Uncertainties estimated from these programs can be considered upper limits for those specified in the COMPEX program.

Under the previous SURE and ERAQS field experiments, hourly averaged SO₂ measurements were taken with a commercially available flame-photometric sulfur analyzer (Meloys Labs, Models 185 and SA 285). Since the flame-photometric measurement principle responds to any sulfur-containing species reaching the flame, particulate sulfate is filtered at the analyzer inlet. Other sulfur-containing species, such as hydrogen sulfide, carbonyl sulfide, and organic sulfur compounds, typically occur at concentrations below the level of parts per billion and hence do not significantly affect the accuracy of background SO₂ levels.

The relative uncertainty was determined for a limited number of instruments over a limited time period during the ERAQS program (Mueller and Watson, 1982). Results of this audit suggested that SO₂ measurement uncertainty was approximately ± 15 percent for 85 percent of the data and ± 10 percent for 71 percent of the data.

Under the SURE program, a more comprehensive uncertainty analysis was performed. When considering the SO₂ measurements from all ground-level stations continuously operated from August 1977 through October 1979 (i.e., the Class I stations), the relative uncertainty at the 90th percentile of

*The ERAQS (Eastern Regional Air Quality Study) conducted between 1 January 1979 and 4 March 1980 served to extend some of the regional air quality measurements of the SURE (Sulfate Regional Experiment) program conducted between 1 August 1977 and 31 December 1978.

concentrations (i.e., 17 ppb) was 18 percent and that at the 50th percentile (3.5 ppb) was 86 percent. These large uncertainties at lower concentrations were attributable to numerous SO₂ measurements at or below the quantifiable limit. These large uncertainties may not be a problem in the COMPEX program where filter sampling techniques are expected to provide a limit of detection at 10 ppt.

Under the SURE measurement program, airborne SO₂ measurements were also obtained over selected sites during intensive measurement periods (Blumenthal et al., 1981). The SO₂ monitors aboard the two aircraft used in the study were Meloy Lab flame-photometric analyzers (Model 285).

Continuous measurements were made in several spiral flight paths upwind and downwind of the particular ground-level station. These data were then averaged over 15 m vertical segments below 1500 m (above mean sea level) and over 30 m segments above 1500 m. Ascent and descent rates were nominally 60 m/min below 1600 m and 120 m/min above 1600 m. Measurement data were thus representative of approximately 15-second averages. An instrument time response of 90 seconds (to 90 percent of concentration) (Blumenthal et al., 1981) indicates that the concentration profiles are considerably smoothed over the higher frequencies. Thus, uncertainties in continuous airborne SO₂ sampling have an additional response-time component. The uncertainties in SO₂ concentration measurements from aircraft therefore require a very detailed analysis of the accuracy of the high-resolution concentration field.

During the EPRI PMV&D Kincaid field measurement program, a large number of quantitative audits of all the ambient air quality measurements were performed. SO₂ measurements were obtained routinely over 5-minute and hourly averaging times. Since the monitoring network was established within 20 km of a power plant, the measured SO₂ concentration levels and uncertainty estimates are more applicable to the proposed COMPEX short-range

experiments than are the ambient SO₂ measurements of the SURE and ERAQS programs.

A summary of the audit information and estimated measurement uncertainties for hourly SO₂ measurements are shown in Table 2-2, as reported by Smith and co-workers (1983). Although the uncertainty estimates indicate improved precision with increasing concentration, a representative maximum precision at the highest observed levels (in terms of the coefficient of variation, C_v) is roughly 5 to 6 percent. Overall, a representative measurement precision is approximately 10 percent.

2.5 Sulfate

As with SO₂, the sulfate monitoring methods and associated uncertainties can be summarized with respect to the measurements achieved during the recent field measurement programs. Under the SURE and ERAQS programs, SO₄²⁻ concentrations were analyzed from hi-vol particulate samples on a daily-average basis and from sequential filter samplers (SFS) during limited periods on a 2-hour basis (ERAQS) and a 3-hour basis (SURE). The hi-vol samplers collect total suspended particulate matter with an aerodynamic diameter less than approximately 30 μm. The SFS collects particles in the inhalable size range (<11 μm) and, when used with a cyclone preseparator, collects refined particulate matter less than 2 μm. Filters used with the hi-vol and SFS instruments during the SURE and ERAQS programs consisted of Teflon-coated glass fiber filters, which met stringent flow rate, ion content, collection efficiency, and appearance criteria (Mueller and Hidy, 1983).

The precision of the SO₄²⁻ measurements is obtained by propagating the uncertainties associated with the measured sulfate concentration on the collection filters, and the measured flow rate. Volumetric flow rate

TABLE 2-2
SUMMARY OF UNCERTAINTY ESTIMATES FOR
AMBIENT SO₂ MEASUREMENTS

Variable	Concentration (ppb)	LDL (ppb)	Bias (%)	CV (%)	90 Percent CI (%)
SO ₂ , PMV&D Network	50 >100	9	-6 0	10 7.5	-22 to + 10 -13 to +13
SO ₂ , D&M Network	50 100 >300	16	+2 -2 -3.5	18 8.8 5.8	-29 to +33 -17 to +13 -13.5 to +6.5

Key:

PMV&D Plume Model Validation and Development (EPRI)
D&M Dames and Moore
LDL Lower Detectable Limit
CV Coefficient of Variation
CI Confidence Interval

Source: Smith et al., 1983

uncertainties of the Hi-vols pertaining to individual SURE sites ranged from less than 1 percent to about 20 percent, with a representative value over the entire network (Class I and II stations) of approximately 8.7 percent. Slightly higher precision was achieved for the nine sites under the ERAQS program. The precision of the flow rate measurements for the Class I SFS instruments averaged about 3 percent during the SURE and ERAQS programs.

The uncertainty in sulfate measurements from hi-vol filter samples typically ranged from about 8 percent for ambient concentrations of approximately $4 \mu\text{g}/\text{m}^3$ to about 1 percent for ambient concentrations of approximately $40 \mu\text{g}/\text{m}^3$. Similar precision values were derived for both sampling programs. Sulfate measurements from sequential filter samples ranged from 6 percent for low ambient sulfate levels to about 1 percent for higher ambient levels (Mueller and Watson, 1982).

Considering the sulfate variability in blank filters along with the volumetric flow rates, the hi-vol sulfate measurement precision was 8.4 percent for the median concentration values ($6.8 \mu\text{g}/\text{m}^3$) during the SURE measurement program. SFS sulfate measurement precision for the median concentration level of $5.4 \mu\text{g}/\text{m}^3$ was 9.7 percent (Mueller and Hidy, 1983). Under the ERAQS program, typical precision considering all measurement and laboratory uncertainties was 8 percent for hi-vol samples, 22 percent for SFS samples in the inhalable particle sizes, and 6 percent for SFS in refined ($<2\mu\text{m}$) size range. These values correspond to typical SO_4^{2-} concentration levels of $10 \mu\text{g}/\text{m}^3$ (Mueller and Watson, 1982).

2.6 Implications to the Experimental Design

Precision of tracer and airborne SO_2 and SO_4^{2-} concentration measurements can only serve as a rough guide in estimating the "measurement uncertainty." For perfluorocarbon tracers, the information is incomplete,

consisting only of a limited number of sample intercomparisons, and only at background levels. Data for PMCP are not available. The high precision of $^{34}\text{S}/^{32}\text{S}$ ratio detection is based on the precision of the mass spectrographic analysis technique, provided the sample size of sulfur oxides is sufficient for analysis.

Finally, SO_2 and sulfate measurement precision is a function of ambient concentration levels and the individual sampling instruments and analytic procedures, and exhibits some variability. Concentration measurements under the proposed COMPEX program should be performed using detailed QA/QC procedures. Analyses of measurement precision should also be performed to quantify the uncertainties associated with the various measurements, as was performed under the SURE and the PMV&D programs.

SECTION 3

LOCAL DATA ANALYSIS

The Electric Power Research Institute's (EPRI) Plume Model Validation and Development (PMV&D) field study at the Kincaid power plant provides a data base with which to examine the behavior of inert tracers for distances within 20 km of a source. Observations of several trace gases made using 18-20 collocated instruments offer a good opportunity to explore the statistical characteristics of concentration time series for several different chemical species in order to:

- 1) Determine if the proportions of the chemical concentrations remain constant during travel from the stack to monitors within 20 km,
- 2) Examine and quantify the effects of measurement uncertainty and background concentrations in the statistics and conclusions drawn from the observations,
- 3) Determine if physical processes such as surface deposition, or differences in the stack gas concentration fluctuations introduce noticeable effects near (< 20 km) the stack, and
- 4) Analyze the statistical nature of concentration fluctuations that arise in the concentration time series at and near (< 20 km) of the stack.

Analysis of these topics provides an evaluation of how well tracers represent emission sources and how variations in sampling and averaging times affect these simulations.

The Kincaid power plant is a typical large (>1200 MW) elevated, buoyant point source of a variety that is thought to contribute a major portion of the sulfur in the sulfate deposited to the surface over large regions such as the northeast United States. The Kincaid PMV&D observations used in this study consist of:

- a) Short-term average (5 minute) concentrations of both SO₂ and NO_x at 18 sites for 34 weeks at distances ranging from 5 to 20 km from the source, and

- b) Over 100 hours of hourly averaged collocated SF_6 and SO_2 observations from 20 co-located sites (excluding mobile observations).

The usefulness of the data base was established with careful quality assurance procedures followed in the field, and quantitative estimates of observational uncertainties. Such numerical analyses are valuable in determining whether or not specific conclusions can be drawn from the data.

The present analyses was built on a study of collocated SF_6 , SO_2 , and NO_x , data reported by Bowne (1982). Bowne's findings were implemented and additional analysis of the effects of measurement uncertainty was performed using comparisons of five-minute observations of SO_2 and NO_x concentrations. The effects of background on conclusions are discussed along with the question of the usefulness of inert tracer releases for studying near source SO_2 and NO_x dispersion.

3.1 Characteristics of the Kincaid Data Base

The data base selected for analysis is a subset of the Kincaid experiment data base (Bowne, 1982) and includes emissions and stack parameters, including the release rates of tracers, and ambient concentrations of SO_2 and NO_x . Processing of the data included the development of analysis statistics and relative concentrations.

The SO_2 and NO_x stack observations were gas concentrations drawn from the stack. Observations were reported as five-minute averages. When the monitoring instruments were not operating, the SO_2 and NO_x were computed for hourly averages using the plant load data. SF_6 releases were recorded as mass flow rates based on instantaneous flow readings taken from a rotormeter at least once every hour. The stack gas velocity measuring device did not operate properly so hourly averages were obtained using plant input data. The uncertainties for the stack parameters are presented in Table 3-1.

TABLE 3-1

UNCERTAINTY IN THE HOURLY AVERAGES OF THE VARIOUS
STACK PARAMETERS FOR THE KINCAID SITE DURING 1981
(Source: Smith et al., 1983)

Parameter	Units	Uncertainty Interval (90 Percent)
SO ₂ (measured)	ppb	SO ₂ (true) = 1.04 SO ₂ (obs) ± 0.1 SO ₂ (obs)
NO _x	ppb	NO _x (true) = 1.10 NO _x (obs) ± 0.15 NO _x (obs)
V _s	m/sec	V _s (true) = 1.03 V _s (obs) ± 0.17 V _s (obs)
Q _{SO₂}	g/sec	Q _{SO₂} (true) = Q _{SO₂} (obs) ± 0.05 Q _{SO₂} (obs)
SO ₂ (calculated)	g/sec	SO ₂ (true) = 1.06 SO ₂ (calc) ± 0.18 SO ₂ (calc) ^a
Q _{SO₂}	g/sec	Q _{SO₂} (true) = Q _{SO₂} (calc) ± 0.27 Q _{SO₂} (calc) ^b
Q _{NO_x}	g/sec	Q _{NO_x} (true) = Q _{NO_x} (calc) ± 0.32 Q _{NO_x} (calc) ^b

^aUsing measured stack SO₂ values.

^bComputed by using bias-corrected SO₂, NO_x, and V_s, otherwise bias is + 0.07 SO₂ and + 0.13 NO_x.

Ambient SO₂ and NO_x samples were drawn from a single sampling manifold at a height of 3 m. The data polling rate was once every 10 sec for both species. The major differences between SO₂ and NO_x instruments is that the SO₂ instrument rise time was much larger than that of the NO_x device. Rise time was exponential and took over 20 minutes to reach 95 percent of an input step (189 ppb) in concentration. This effect causes an underestimate in the average SO₂ concentration of about 16 percent for a concentration spike lasting for five minutes or less. In analyses, care should be taken to avoid selecting periods when the elevated concentrations persist for only a single five-minute averaging period. The observations of both SO₂ and NO_x were routinely stored as five-minute average observations.

The SF₆ observations were made from the same air volume as the SO₂ and NO_x observations. The sample consisted of a one-hour integrated sample of two-second air samples made every 20 seconds. The sampling technique introduces some artificial sampling "diffusion" where peaks are reduced and some zero concentrations are made slightly non-zero. The hourly average uncertainties are summarized in Table 3-2.

3.2 Conservation of Tracer/Pollutant Concentration Ratios

3.2.1 Comparison of SO₂ and NO_x Concentration Time Series

The underlying hypothesis in any dispersion analysis for conservative pollutants is that a puff of air being sampled at a downwind receptor contains the same proportion of constituents as it did when it left the stack. Under normal plant operations, the time series of SO₂ and NO_x concentrations at the stack varies slightly over the course of 6 to 10 hours as demonstrated by Figure 3-1. The concentration time series at a downwind monitoring site is substantially more variable and intermittent at averaging periods of 5 minutes. Two questions were addressed: 1) does the proportion of SO₂ to

TABLE 3-2

UNCERTAINTY IN THE HOURLY AVERAGES OF SF₆, SO₂, and NO_x
 CONCENTRATIONS OBSERVED AT KINCAID MONITORS DURING 1981
 (Source: Smith et al., 1983)

Parameter*	Uncertainty Interval (90 Percent)
SF ₆	$SF_6 \text{ (true)} = SF_6 \text{ (obs)} \pm 10 \text{ ppt, } SF_6 \text{ (obs)} < 100 \text{ ppt}$ $SF_6 \text{ (true)} = SF_6 \text{ (obs)} \pm 0.10 SF_6 \text{ (obs), } SF_6 \text{ (obs)} > 100 \text{ ppt}$
SO ₂	$SO_2 \text{ (true)} = 0.94 SO_2 \text{ (obs)} \pm 0.16 SO_2 \text{ (obs), at } 50 \text{ ppb}$ $SO_2 \text{ (true)} = SO_2 \text{ (obs)} \pm 0.13 SO_2 \text{ (obs), } SO_2 \text{ (obs)} > 100 \text{ ppb}$ $SO_2 \text{ (true)} = 1.33 SO_2 \pm 0.63 SO_2 \text{ (obs), at } 9 \text{ ppb}$
NO _x	$NO_x \text{ (true)} = 0.98 NO_x \text{ (obs)} \pm 0.29 NO_x \text{ (obs), at } 50 \text{ ppb}$ $NO_x \text{ (true)} = 0.98 NO_x \text{ (obs)} \pm 0.19 NO_x \text{ (obs), at } 100 \text{ ppb}$ $NO_x \text{ (true)} = 0.98 NO_x \text{ (obs)} \pm 0.15 NO_x \text{ (obs), } NO_x \text{ (obs)} > 300 \text{ ppb}$

*Lowest detectable limit for SO₂ is 9 ppb and for NO_x 11 ppb. TRC suggested a value for SF₆ of 2 ppt.

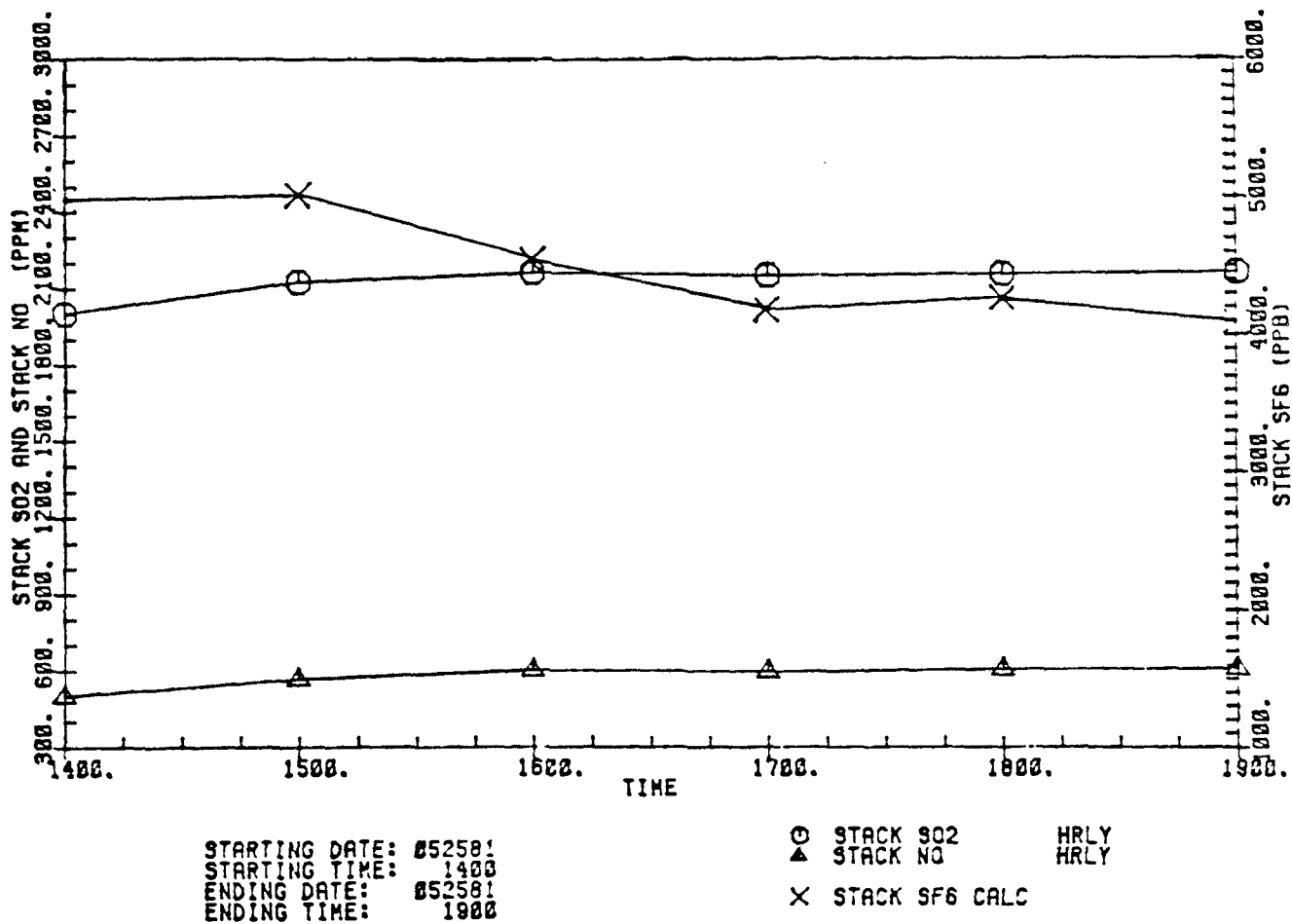


FIGURE 3-1. Time series of hourly concentrations at the stack on 25 May 1981.

NO_x present at the stack change between the stack and a nearby monitoring site, and 2) do the SO₂ and NO_x time series correlate very closely with one another? Answers to these questions aid in understanding over what distances pollutants can be simulated by tracers.

Preliminary evidence to answer the questions was gathered by visually inspecting time series co-plots of SO₂ and NO_x at various monitoring sites. The travel time for plume material is less than an hour so chemical transformations and surface deposition are not expected to be significant. Under such conditions, SO₂ and NO_x time series should agree closely. Figure 3-2 demonstrates that a close agreement does in fact occur between the two time series at a site. In fact, over 30 time series plots at various sites and times all demonstrate a close correspondence between SO₂ and NO_x concentrations when they are significantly above the background concentrations.

The background concentrations arise from several sources. For NO_x, the background concentration varied widely among the 18 monitoring sites. The background concentration fluctuations are more constant with time (Figure 3-3). Background can easily be removed by visual inspection. However, an objective method of removal is somewhat more difficult, particularly as the averaging times become longer and the ratio of the concentration standard deviation to the average background (σ_c/c_b) approaches one. In the present analysis, either a station where background was not significant was selected for analysis, or else background was removed as a long-term average when the concentration averaging time was relatively short, e.g., <1 hour. The SO₂ and NO_x background as the median concentration at each station is compiled in Table 3-3.

The proportion of SO₂ to NO_x at the stack in Figure 3-1 was found to be 3:1. when a background of 10 ppb of NO_x was subtracted from the NO_x in Figure 3-2, a constant ratio between SO₂ and NO_x at the downwind monitor

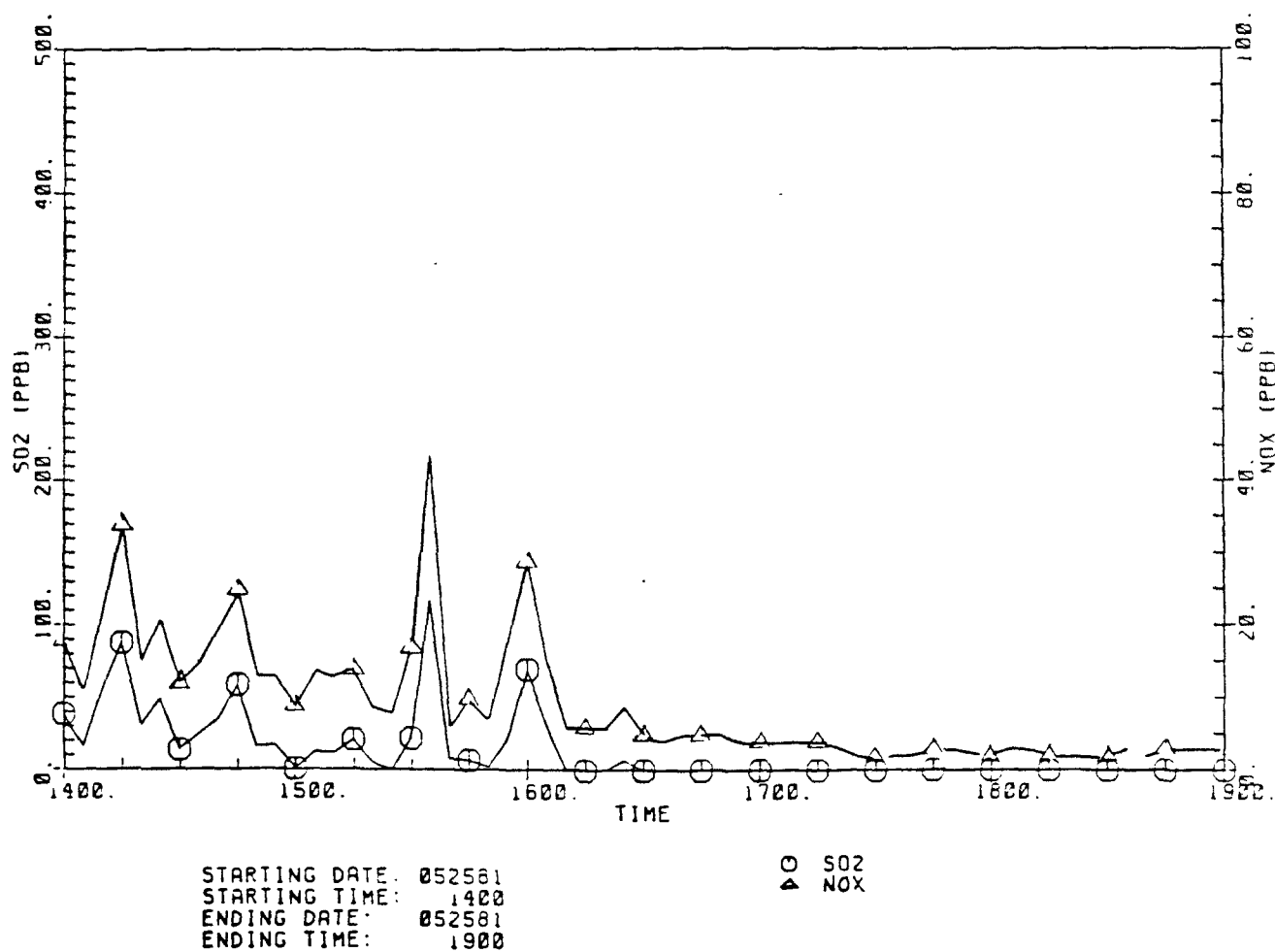


FIGURE 3-2. Time series of five-minute average SO_2 and NO_x concentrations for station 1422 on 25 May 1981.

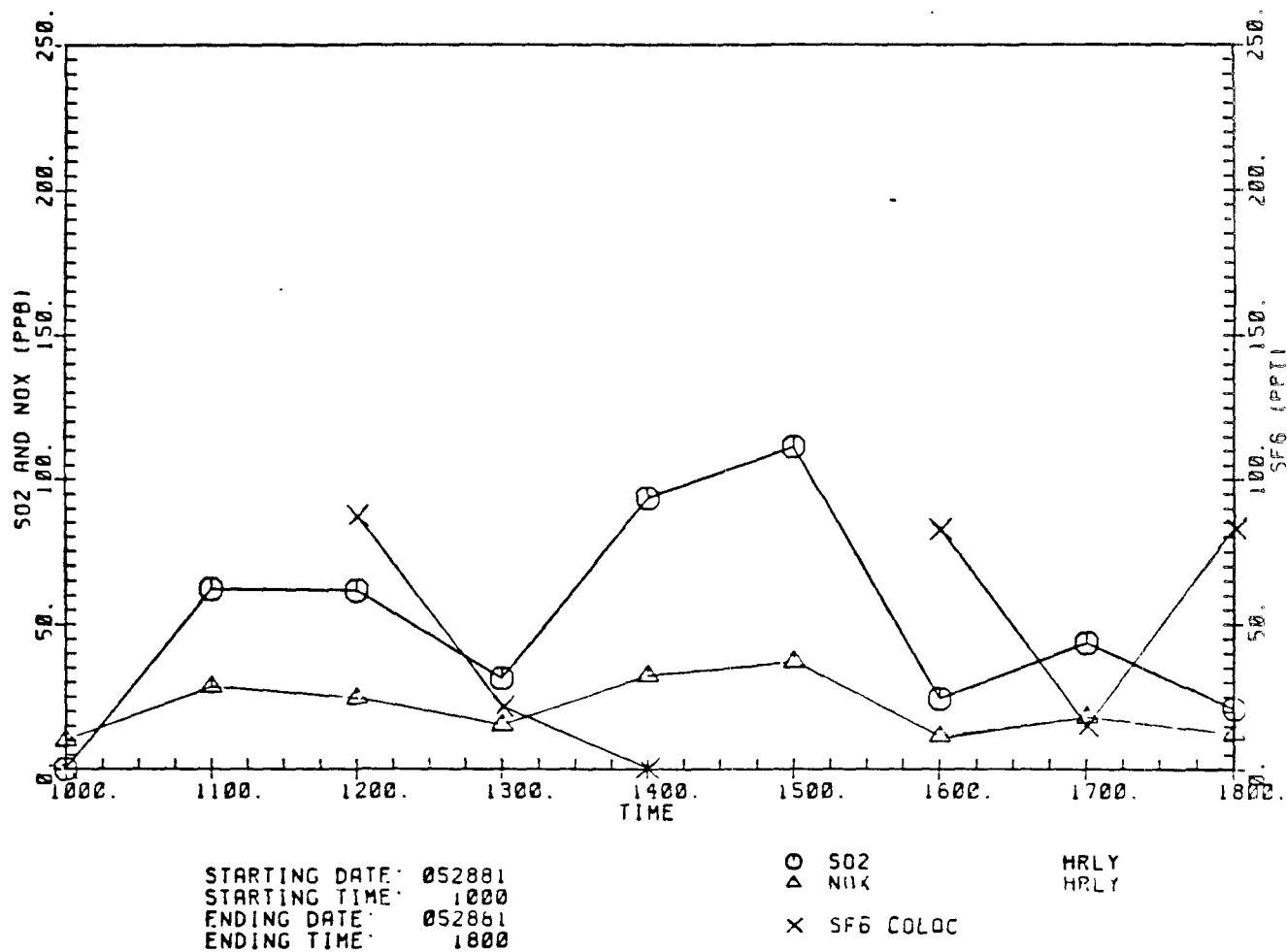


FIGURE 3-3. Time series of hourly concentrations at station 1422, 28 May 1981.

TABLE 3-3

THE MEDIAN FIVE-MINUTE AVERAGE SO₂ AND NO_x DATA AT THE
ROCKWELL SITES, MAY 11, 1981 THROUGH MAY 31, 1981

Station Number	SO ₂	NO _x
0424	0.0	5.0
1118	0.0	8.0
1160	0.0	7.0
1244	0.0	1.0
1335	0.0	9.0
1422	0.0	6.0
1650	0.0	13.0
1713	0.0	1.0
2019	0.0	0.0
2744	0.0	12.0
2832	0.0	5.0
3829	0.0	4.0
5146	0.0	8.0
5318	0.0	7.0
5623	0.0	1.0
5745	3.0	4.0
6052	0.0	4.0
7134	0.0	0.0

was also 3:1. Figure 3-4, showing five-minute concentrations for a different day and station (28 May 1981 -- Station 1118), indicates similar results when observations are compared with the stack concentrations in Figure 3-5. Results show a one-to-one correspondence between NO_x and SO_2 concentration maxima and minima, and an SO_2 -to- NO_x ratio of 4:1 at both stations and the stack.

The strong agreement of the five-minute averages is apparent when statistics are performed on the five-minute averages for tracer tests and SO_2 and NO_x are available at the same times and locations. Table 3-4 presents a summary of these statistics. The most notable features are as follows:

- The correlations, particularly for monitoring stations unaffected significantly by the NO_x background, are in excess of 0.90.
- The higher-order statistical moments of the concentration probability density function (pdf), such as skewness and kurtosis, are remarkably similar for SO_2 and NO_x .

The SO_2 and NO_x concentration variations correlate closely (Figure 3-6) despite the fact that the proportion of SO_2 to NO_x from the source can change. This agreement suggests that for short travel times NO_x is a good tracer for SO_2 , and that the proportion of SO_2 to NO_x does not change greatly at Kincaid.

The close tracking of SO_2 and NO_x is not as apparent in hourly averages. Figure 3-7 shows a time series comparison of hourly SO_2 , NO_x , and SF_6 for the two days previously discussed using five-minute average data. The SO_2 and NO_x curves are roughly parallel, but the concentrations have been reduced by averaging so that they do not show as great a difference with the background. Table 3-5 shows several sets of station statistics that are not significantly affected by the NO_x background. In this case, the SO_2

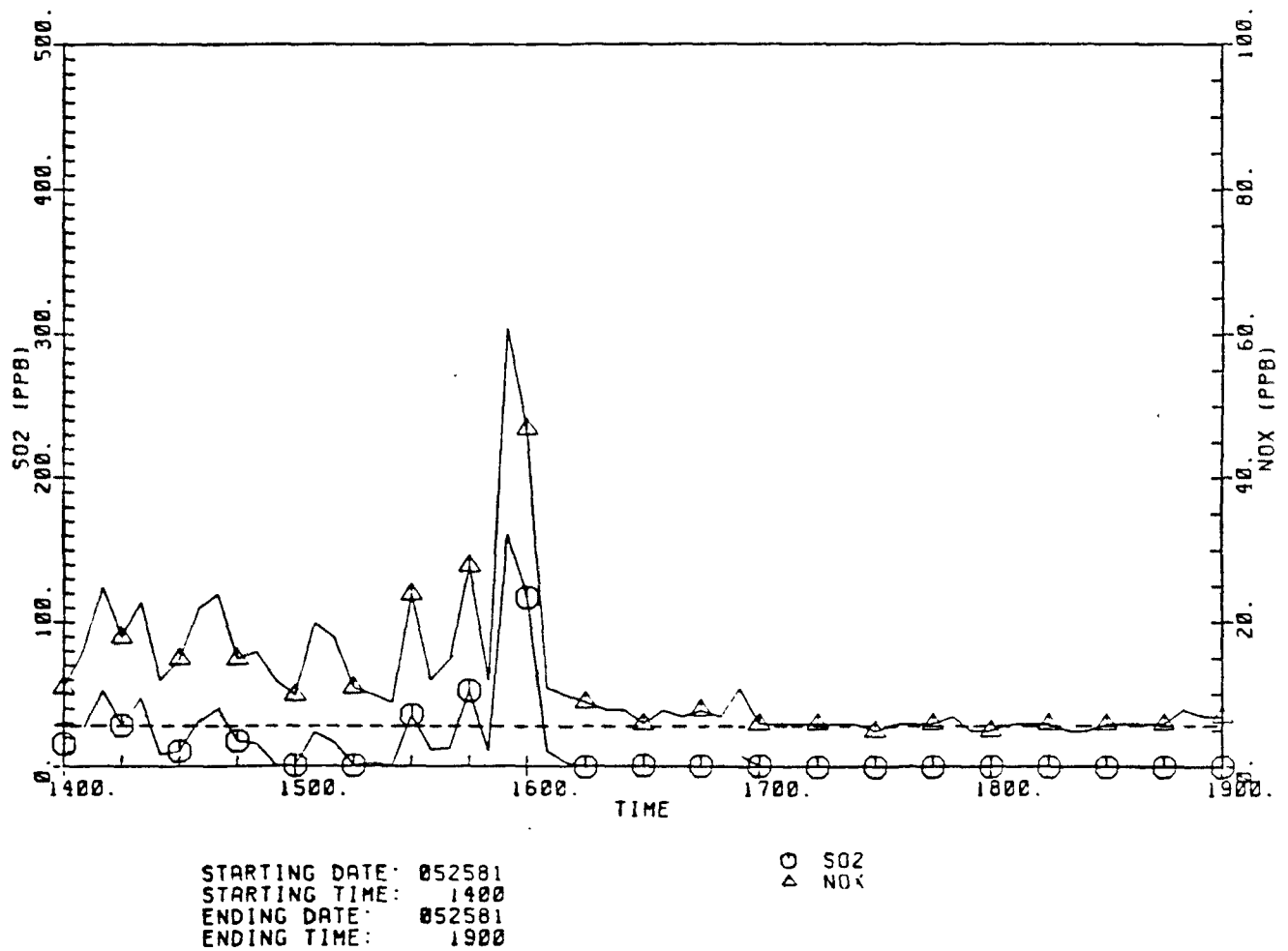


FIGURE 3-4. Time series of five-minute average SO₂ and NO_x concentrations for station 1118 on 25 May 1981. Background concentration^x is denoted by the dashed line.

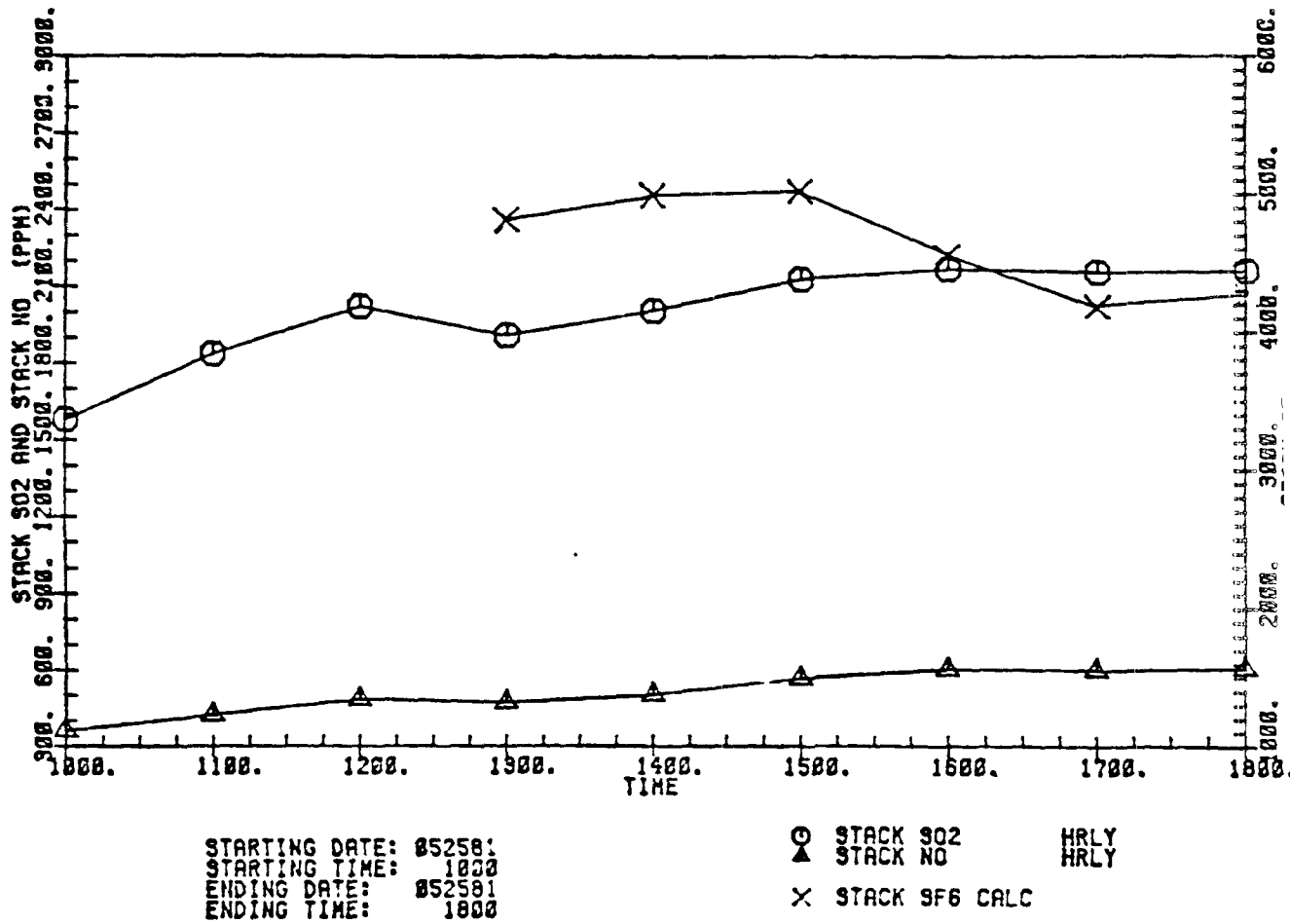


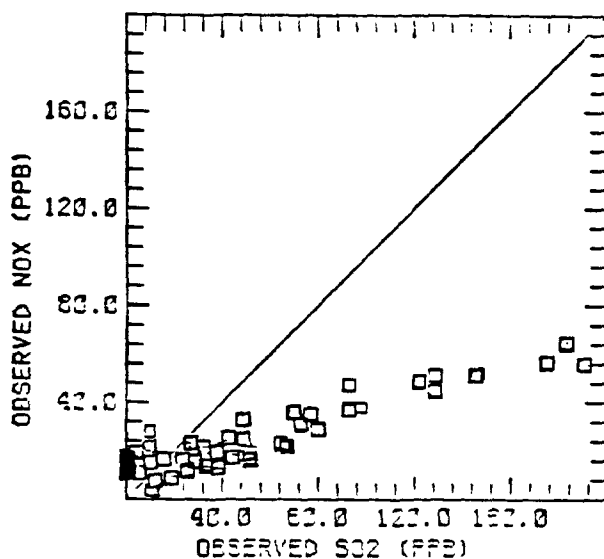
FIGURE 3-5. Time series of hourly concentrations at the stack on 28 May 1981.

TABLE 3-4

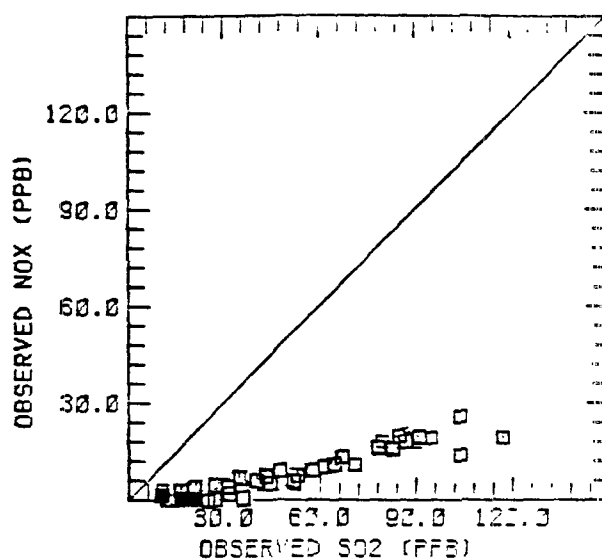
A SUMMARY OF STATISTICAL MEASURES COMPARING THE 5-MINUTE AVERAGE SO₂ and NO_x OBSERVATIONS DURING SPECIFIC TRACER TESTS AND AT STATIONS WHERE THE NO_x BACKGROUND CONCENTRATION WAS NOT SIGNIFICANT
(Units for SO₂, NO_x are ppb)

Date	Station No.	Sample Size	Median		Max		Correlation Coefficient	Skewness		Kurtosis	
			SO ₂	NO _x	SO ₂	NO _x		SO ₂	NO _x	SO ₂	NO _x
5/12/81	5318	27	9.0	11.0	36.0	19.0	0.93	0.8	1.3	-0.9	0.3
5/13/81	5318	57	10.0	12.0	129.0	51.0	0.98	3.2	3.6	13.3	15.2
5/22/81	5318	40	34.0	15.0	190.0	65.0	0.97	1.3	1.3	0.5	0.2
5/13/81	6052	22	22.0	13.0	75.0	29.0	0.97	0.2	0.4	-1.7	-1.4
5/28/81	1118	80	4.0	11.0	11.0	13.0	0.81	0.2	0.4	-1.1	-1.0
5/25/81	1118	33	18.0	16.0	162.0	61.0	0.99	1.8	1.8	2.5	2.7
5/28/81	1118	71	53.0	23.0	223.0	75.0	0.99	0.7	0.8	-0.7	-0.5
5/28/81	1713	25	58.0	19.0	155.0	54.0	0.90	0.3	0.7	-1.0	0.0
5/25/81	1422	27	25.0	16.0	123.0	46.0	0.96	1.1	1.4	0.9	1.3
5/20/81	1422	59	37.0	16.0	191.0	62.0	0.98	0.8	0.9	-0.1	0.0
5/28/81	2019	49	45.0	6.0	104.0	26.0	0.96	0.3	0.6	-1.1	-0.7
5/28/81	1335	26	52.0	15.0	135.0	52.0	0.92	0.8	1.5	0.2	1.8
5/28/81	1244	56	40.0	14.0	108.0	30.0	0.88	0.5	0.2	-0.7	-0.8
5/28/81	2832	36	21.0	15.0	81.0	37.0	0.91	0.7	1.1	-0.4	-0.3

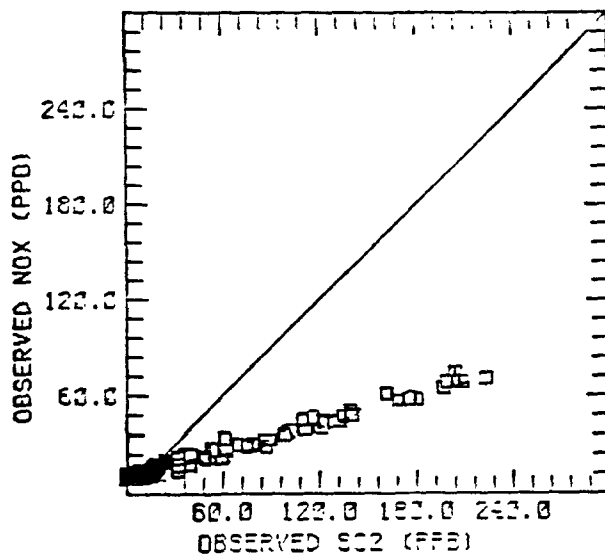
A. Station 5318 (N = 194)



B. Station 2019 (N = 61)



C. Station 1118 (N = 219)



D. Station 1422 (N = 114)

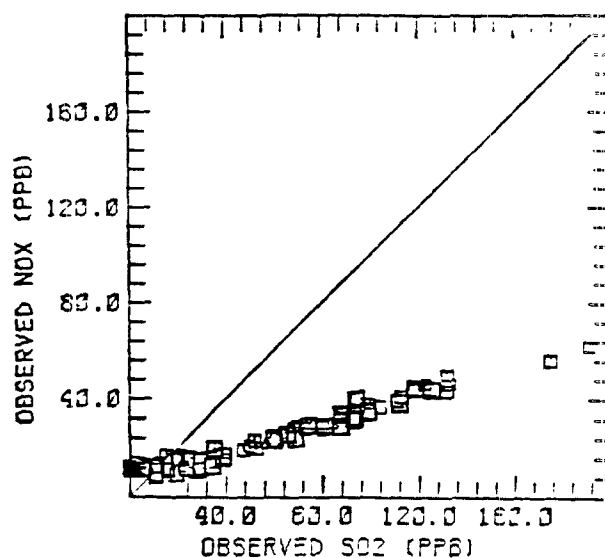


FIGURE 3-6. Scatter plots of five-minute average SO_2 concentrations versus NO_x concentrations for various EPRI PMV&D monitoring sites for tracer tests conducted 12 May to 1 June 1981.

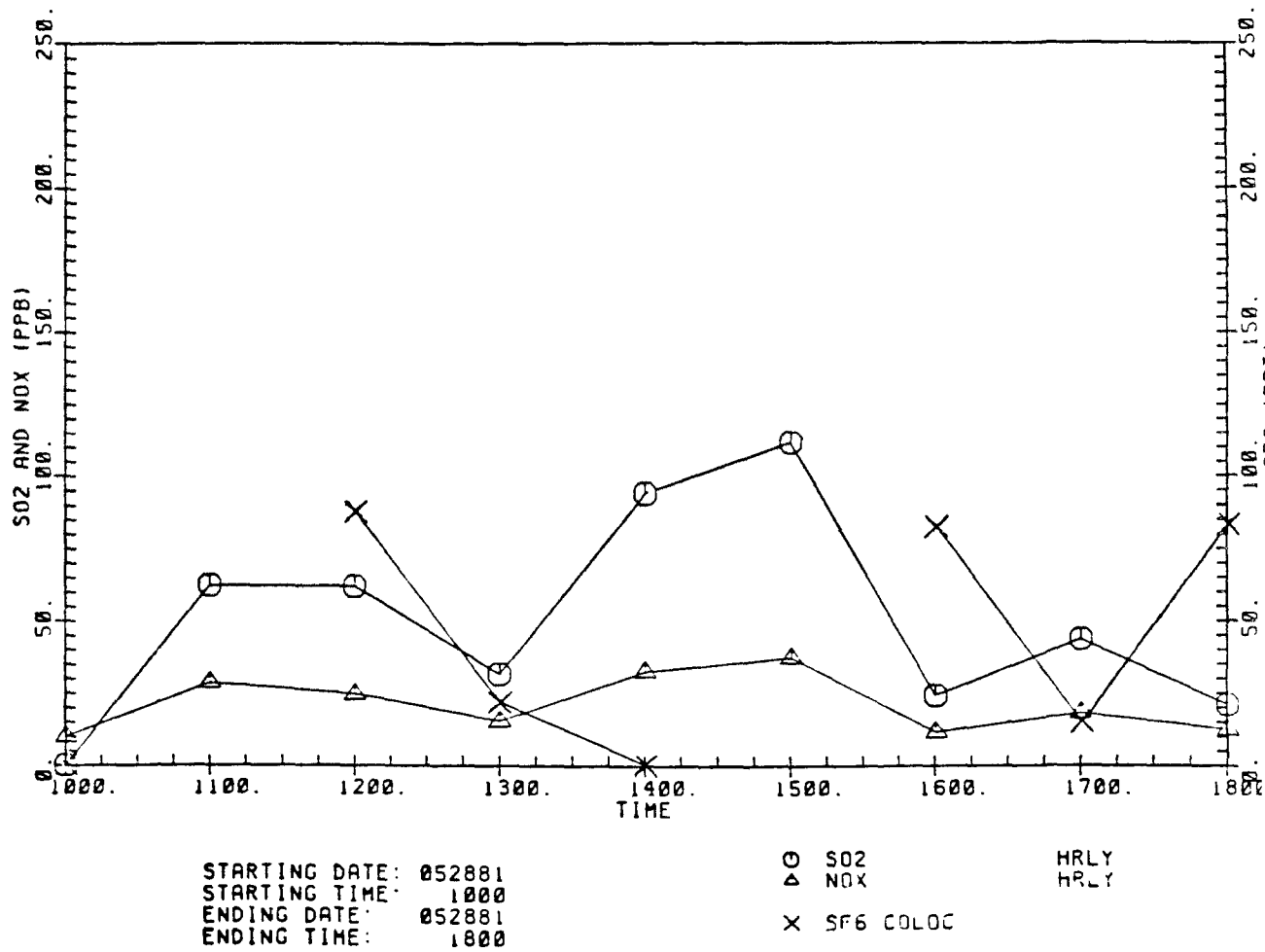


FIGURE 3-7a. Hourly average SO₂, SF₆, and NO_x concentrations at station 1422: 28 May 1981.

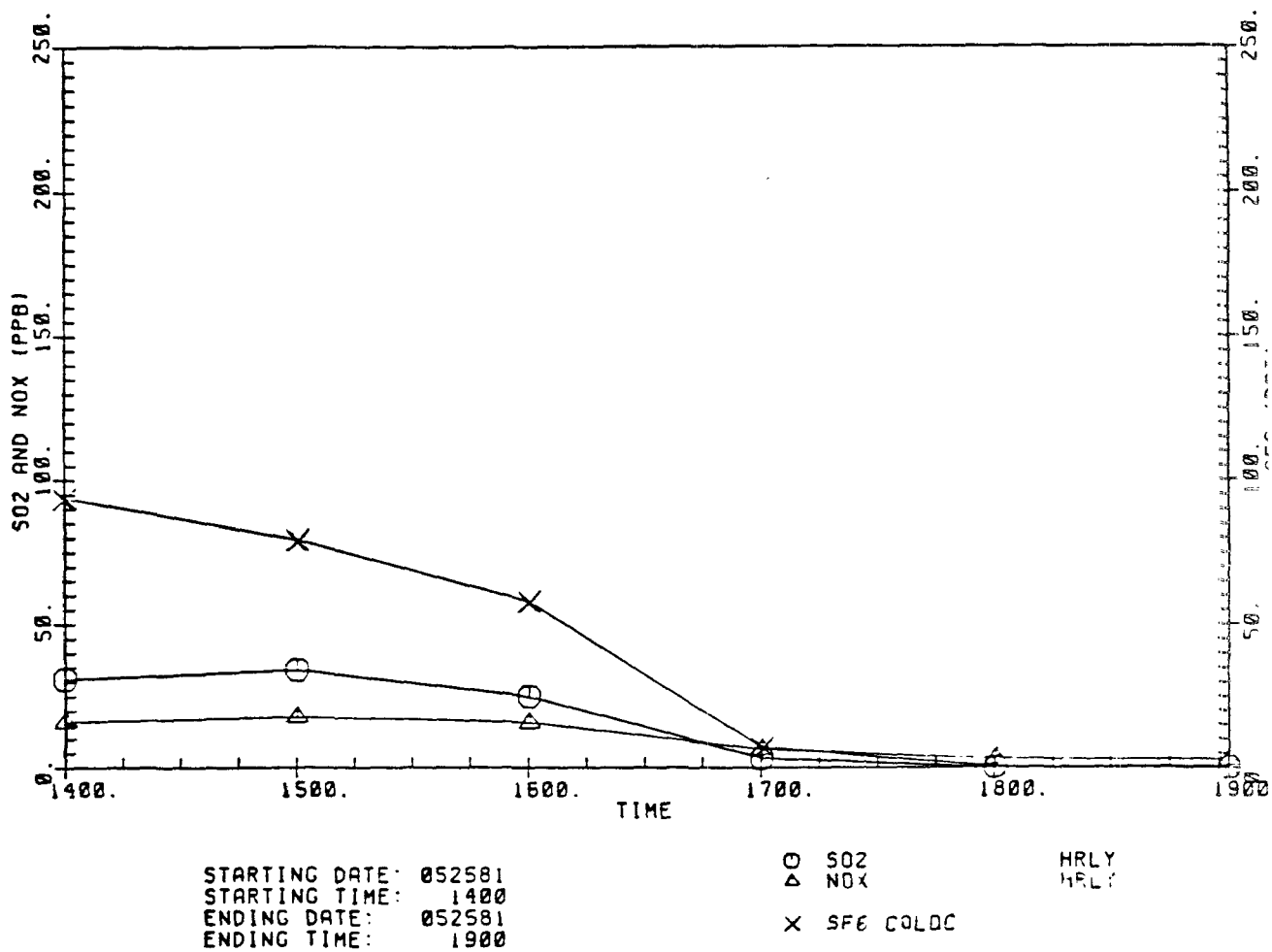


FIGURE 3-7b. 25 May 1981

TABLE 3-5

A COMPARISON OF HOURLY AVERAGE SO₂ AND NO_x STATISTICS
FOR STATIONS WHERE THE NO_x BACKGROUND CONCENTRATION WAS NOT SIGNIFICANT
(Threshold is 10 ppb for SO₂ and NO_x)

Station No.	Sample Size	Median		Max		Correlation Coefficient	Skewness		Kurtosis	
		SO ₂	NO _x	SO ₂	NO _x		SO ₂	NO _x	SO ₂	NO _x
7134	56	11.0	10.0	242.0	68.0	0.88	2.94	2.86	8.73	8.84
1118	10	37.6	19.5	144.8	49.1	0.99	1.19	1.10	-0.09	-0.19
5318	9	25.8	16.6	67.5	24.1	0.97	0.55	0.35	-1.41	-1.70
1244*	15	21.7	11.8	81.3	25.1	0.80	0.88	0.22	0.12	-1.46
1422*	14	24.5	13.0	93.8	32.5	0.98	1.07	0.89	0.54	0.22
2019*	9	21.6	2.8	44.8	8.3	0.98	-0.01	0.15	-1.87	-1.69

*Thresholds were set at 1.0 ppb.

$_2/\text{NO}_x$ correlations are in excess of 0.90 and the higher moments of the concentration distribution agree closely. The scatter plot in Figure 3-8 shows similar agreement as that obtained for the five-minute averages. The major difference between hourly and five-minute averages for SO_2 and NO_x is that the influence of background concentrations becomes more significant for the hourly averages. In low background areas, the NO_x could still act as a suitable tracer for SO_2 .

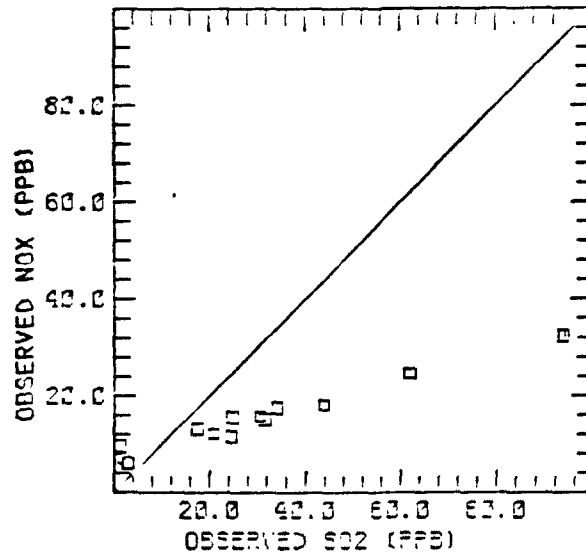
3.2.2 Comparison of SF_6 and SO_2 Concentrations

Analyses have compared normalized concentrations (χ/Q) of SO_2 and SF_6 at the same times and locations (collocated observations). The main finding of the analysis is that a large scatter occurred in the co-plot of χ/Q (for SO_2) even when questionable data points were screened (correlation coefficients of 0.72 were estimated). The report did not resolve all of the questions about the suitability of SF_6 as a surrogate for SO_2 . Clearly, if the proportion of an inert tracer to an inert pollutant (SO_2 for the short travel times) cannot be maintained in a parcel of air, then the whole experimental rationale for using a tracer becomes questionable. The question of the usefulness of the SF_6 tracer at Kincaid is reevaluated in this section.

The approach used in this analysis is to factor in the influence of measurement uncertainty in both χ and Q . The 90 percent confidence intervals were used to plot confidence regions around each relative SF_6 concentration/relative SO_2 concentration pair. Additional screening removed observations:

- Where large gradients of tracer concentration (>50 ppt/km) occurred (timing errors become significant).
- Where the ratio of emission rate of SF_6 to SO_2 changed rapidly (e.g., 1300-1500 of May 13, 1981).

A. Station 1422 (N = 14)



B. Station 5318 (N = 17)

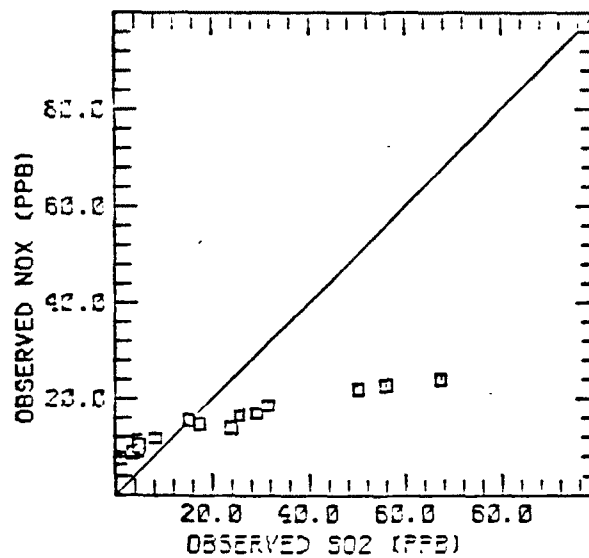


FIGURE 3-8. Scatter plots of hourly average concentrations of SO₂ and NO_x for two EPRI PMV&D monitoring sites at Kincaid, Illinois, where the background NO_x was not significant during tracer tests conducted between 12 May and 1 June 1981.

- Where SO_2 observations contain position biases.
- Where background concentrations were appreciable.
- Where the SO_2 peaks were temporary (<10 min) (the SO_2 instrument may not have responded properly).

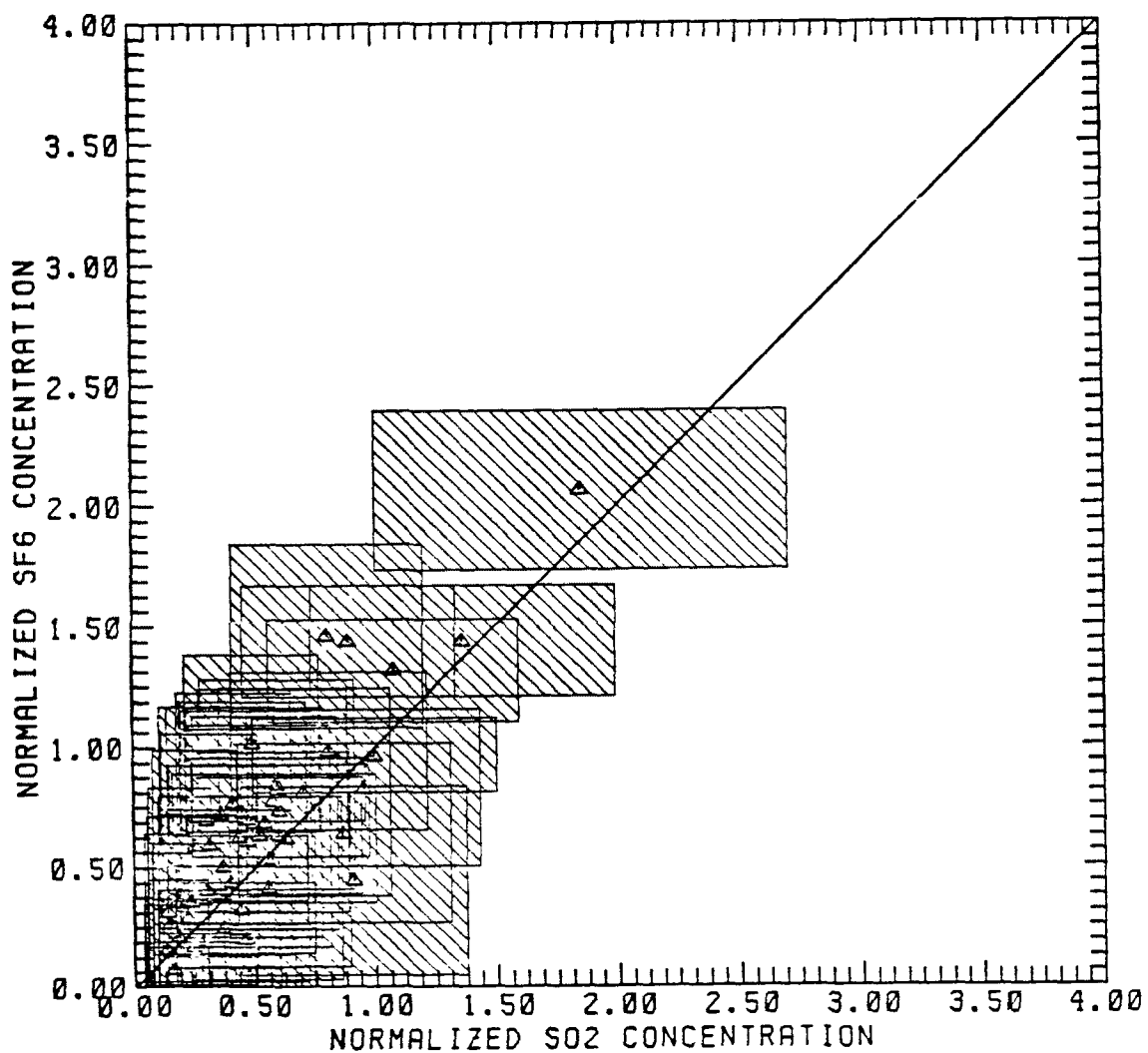
Removal of these χ/Q observations resulted in a set of 51 observations, which are plotted with their 90 percent confidence intervals in Figure 3-9. Despite the scatter, very few observations have confidence regions that do not intercept the one-to-one correspondence line. The confidence regions are so large as to still allow an appreciable amount of scatter (Figure 3-9).

The χ/Q statistics for both SF_6 and SO_2 are compared in Table 3-6. This table shows that the bias is not significant at the 95 percent level and that the correlation coefficient is 0.85. The Kolmogorov-Smirnov test reveals that the two distributions of χ/Q are similar at the 96 percent confidence. The statistics all suggest that within 20 km of the source, on the average, the proportion of SO_2 to SF_6 in a parcel of air remains constant and SF_6 acts as a suitable tracer.

3.3 Statistical Nature of Concentration Fluctuations

A power spectrum of fluctuation of both SO_2 and NO_x was computed from three weeks of five-minute averages during the third intensive (May 11, 1981 through May 31, 1981) of the PMV&D study. The spectra of the two species are shown in Figure 3-10 for one station. They do not exhibit a substantial background contribution. The most important feature that emerges is that the two spectra are parallel to one another over essentially the entire range of frequencies (periods of 10 minutes to 3 weeks).

The natural uncertainty in estimating hourly or longer averages was examined using SO_2 averaging periods up to 24 hours. The approach used ignored serial correlation and nonstationary effects and estimated a lower



SCATTER PLOT OF NORMALIZED SO2 VS SF6 CONCENTRATION

FIGURE 3-9. Scatter plot of normalized hourly averaged SO₂ concentrations (10^{-7} s/m³) versus hourly averaged SF₆ concentrations (10^{-7} s/m³). Sample size is 51 cases, and the shaded region indicates the 90 percent confidence level.

TABLE 3-6
COMPARISON OF SO₂ AND SF₆ NORMALIZED
CONCENTRATIONS (χ/Q), IN 10⁻⁷ s/m³

Statistic	SO ₂	SF ₆	95 Percent Confidence Interval
Sample size	51	51	
Average	0.52	0.63	
Standard deviation	0.33	0.39	
Skewness	1.61	1.31	
Kurtosis	3.54	2.16	
Correlation Coefficient			(0.74 < 0.85 < 0.91)
Average residual			(-0.23 < -0.11 < 0.01)

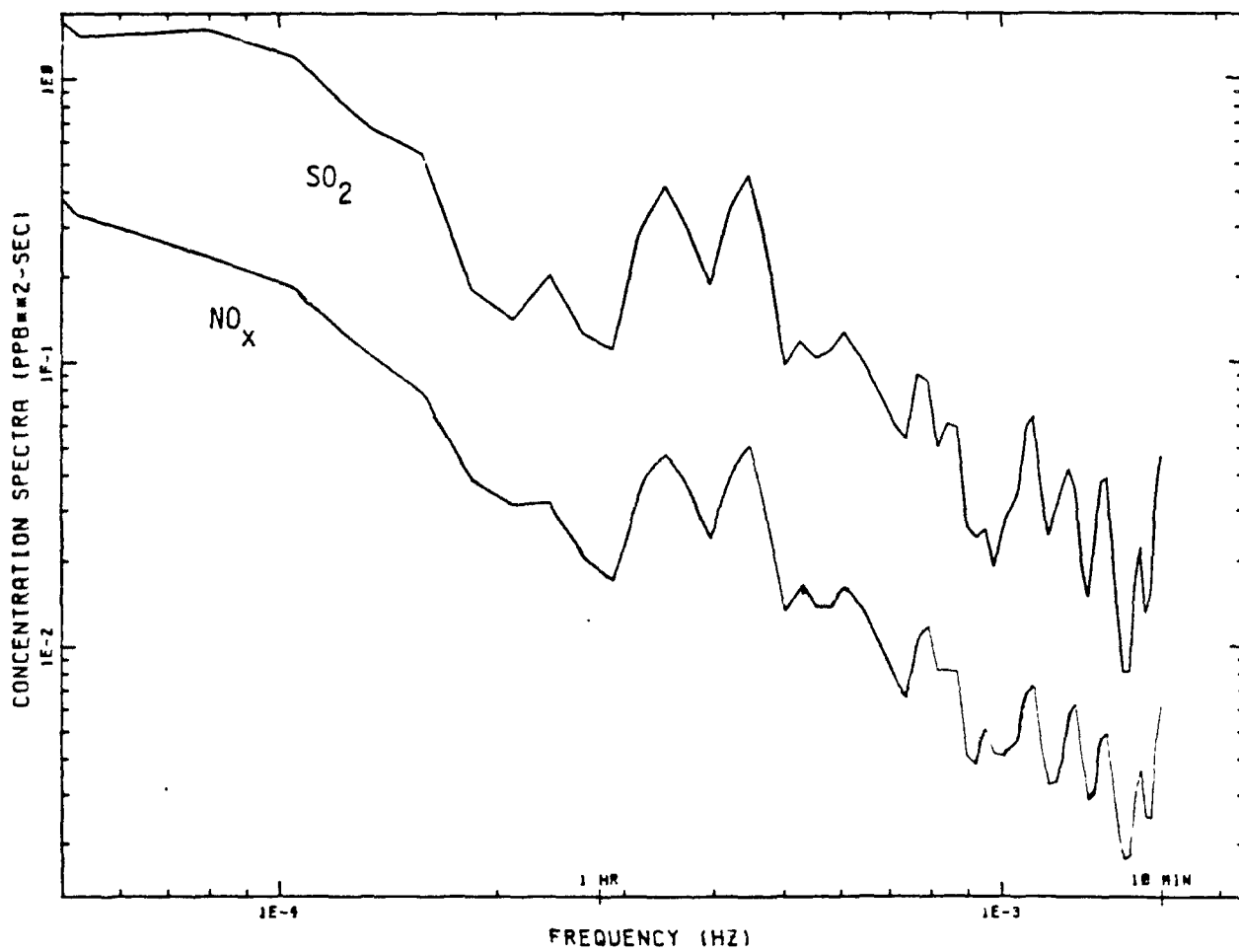


FIGURE 3-10. Concentration spectra recorded at station 1422, 11-31 May 1981.

limit on the confidence interval of the mean using Student's t statistics. The coefficients of variation for the averages are tabulated for selected monitoring sites in Table 3-7. There seems to be no systematic change in the natural uncertainty with downwind distance. The natural uncertainty remains relatively constant for all averaging periods.

The probability density functions (pdf) of the five-minute averaged SO₂ concentrations at a near-source site and a far-source site were fitted to an intermittent exponential distribution like that suggested by Barry (1974). The corresponding best fit for three weeks of data indicates an intermittency factor of 0.05 for the near-source site, and 0.05 for the far-source site. The pdfs and the fitted model are shown in Figure 3-11. The fit of the pdfs suggests that the intermittency and the peak concentrations do not systematically decrease with increasing downwind distance between 7 to 20 km.

3.4 Implications for Experimental Design

A local data analysis was performed to evaluate the interrelationships of pollutants and tracers and their spatial and temporal characteristics. The analyses were directed at determining the ability to use tracers in experimental programs such as COMPEX. From an analysis of portions of the EPRI PMV&D data base, consisting of SF₆, SO₂, and NO_x concentrations distributions within 20 km of the Kincaid Generating Station, the following results have been obtained:

- 1) The 5-minute and 1-hour average SO₂ concentrations and those NO_x concentrations in excess of the 5-15 ppb NO_x background correlate quite closely and show no systematic phase lag.
- 2) When data from biased monitoring sites, low concentrations, spatially isolated concentrations, and other justifiably untrustworthy data are removed, the normalized concentrations (X/Q) of the SO₂ and SF₆ measured at the same site and time agree indicating no measurable depletion on a local scale.

TABLE 3-7

THE AVERAGE AND STANDARD DEVIATION OF THE COEFFICIENT OF VARIATION
AS A FUNCTION OF AVERAGING PERIOD. ALL COEFFICIENTS OF VARIATION
STATISTICS ARE ESTIMATED FROM SETS OF 5-MINUTE AVERAGES.

Station	1 hour	Average			Standard Deviation			
		3 hour	6 hour	12 hour	1 hour	3 hour	6 hour	12 hour
0424	2.1	3.4	5.3	7.6	1.2	2.0	2.7	3.5
0118	1.3	2.0	3.2	4.5	1.0	1.6	2.5	3.7
1160	1.7	2.6	3.9	5.7	1.0	1.7	2.3	3.2
1422	1.6	2.9	4.3	6.3	1.0	2.1	2.6	3.7
1650	1.6	3.0	5.1	7.1	1.0	1.8	2.4	3.3
Average	1.7	2.8	4.4	6.2	1.0	1.9	2.5	3.5
	(1.7)	(2.4)*	(4.2)	(5.9)				

*Coefficient of variation assumes uncertainty is constant with averaging period.

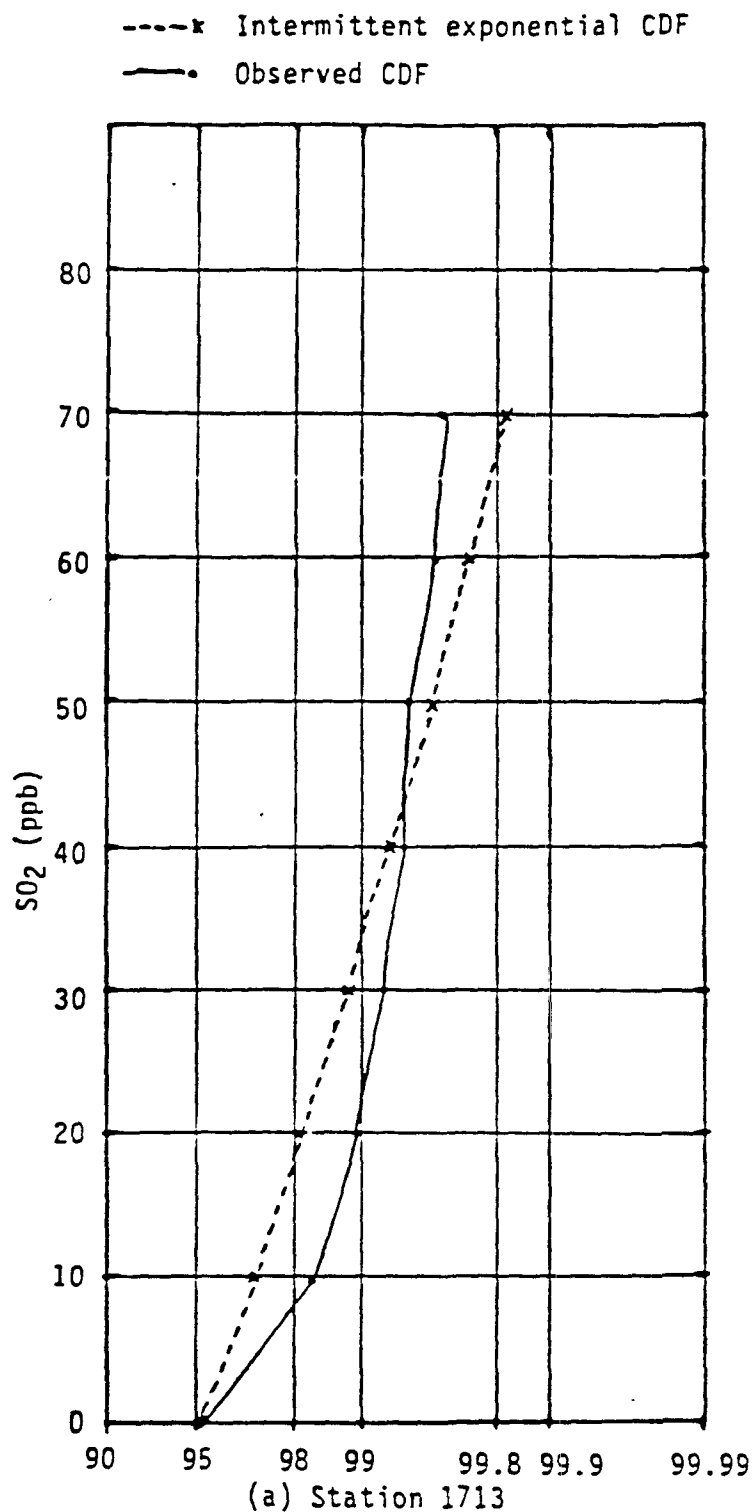


FIGURE 3-11. Cumulative distributions of 5 minute averaged SO₂ for two EPRI PMV&D sites at Kincaid. The intermittency factor, λ , is approximately 0.05 for both sites. The intermittent exponential CDF function was fitted to both sites.

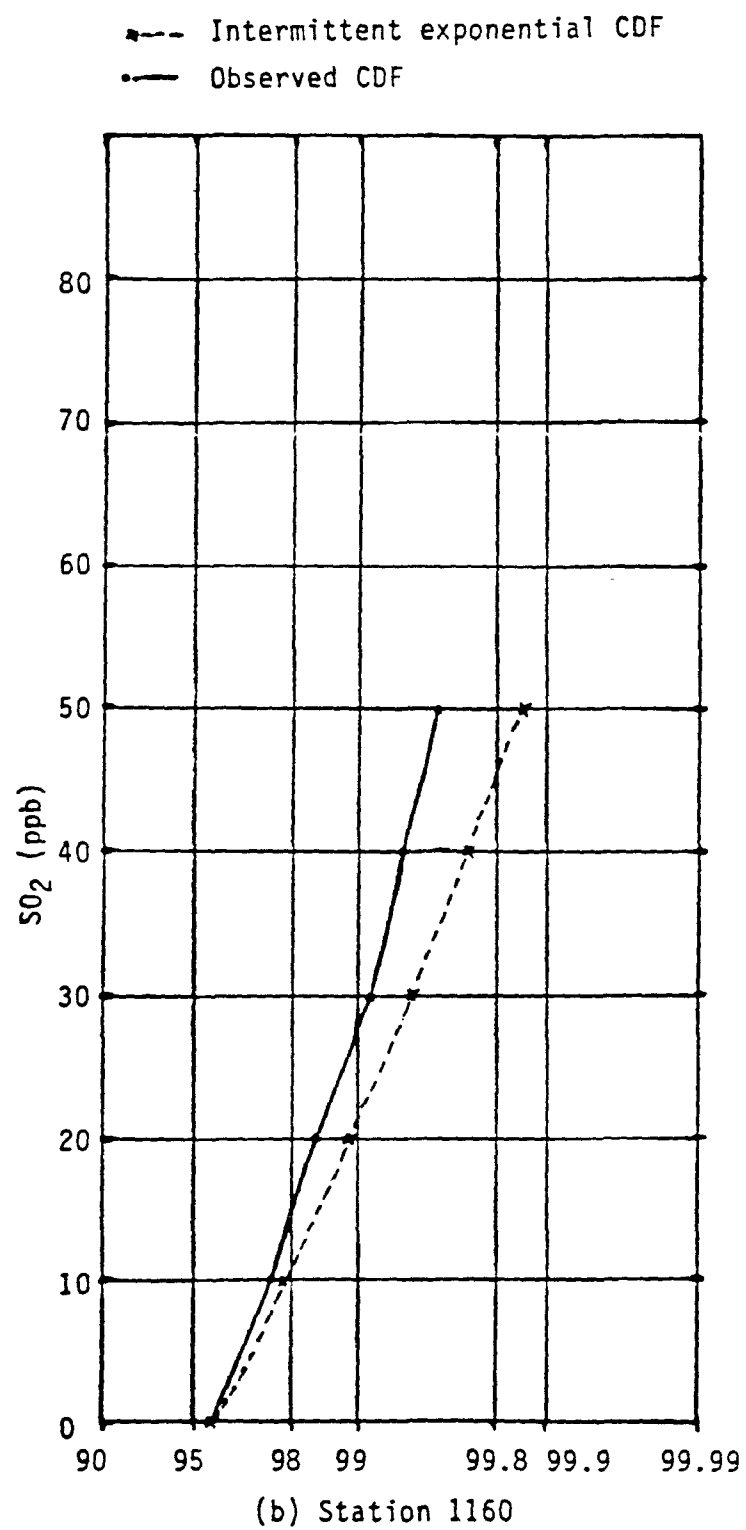


FIGURE 3-11.(concluded).

- 3) There is a large degree of uncertainty in the estimates of X/Q due to measurement uncertainty.
- 4) There seems to be no significant systematic decrease in SO_2 concentrations due to dry deposition with downwind distances ranging from 7-20 km, nor does the statistical intermittency of surface concentration time series vary substantially with downwind distances. Additionally, the analysis indicates that the proportion of NO_x to SO_2 remains constant between the stack and downwind monitors.
- 5) The increase in averaging time does not significantly reduce the 90 percent confidence interval about the estimated mean. The presence of many zeroes in the concentration time series seems to contribute toward this result.

On the basis of these results, the strategy of tagging SO_2 emissions with inert or reactive tracers appears to be appropriate. However, it is important to carefully control the tracer emission rate so that its variability accurately reflects the variability in SO_2 emissions. Additionally, thorough quality assurance and quality control measures, including frequent instrument audits and replicate sampling should be implemented during the monitoring activities in order to accurately characterize the measurement uncertainties.

SECTION 4

REGIONAL DATA ANALYSIS

The analysis of the Kincaid data set discussed in the previous section was beneficial in describing the local scale spatial and temporal variability of pollutants and the feasibility of tracer use in small scale experiments. To establish a suitable sampling network on a regional scale it is important to understand the important temporal and spatial scales for SO_2 and SO_4^{2-} . The most notable regional pollutants study was the EPRI Sulfate Regional Experiment (SURE). This section describes the SURE data set and analyses of the data to provide information on:

- The spatial scale of concentration data.
- The temporal characteristics of concentration data.
- The spatial representativeness of single station concentration measurements.
- Uncertainties in network design.

Implications of the findings on experimental design are also discussed.

4.1 Description of the EPRI SURE Data Base

The EPRI/SURE monitoring network consisted of 54 monitoring sites distributed over the eastern United States as shown by Figure 4-1. Monitoring started in August 1977 and it ended on October 31, 1978. Of the 54 sites, the first nine were designated as Class I (primary) sites where additional aerometric and meteorological variables were observed over the remainder or Class II sites. A summary of the number of observations for selected stations is presented in Table 4-1. Generally, the Class I stations have about three times as many observations as the remaining stations. Most of the EPRI/SURE sites were located in a position that on the average is either upwind, or

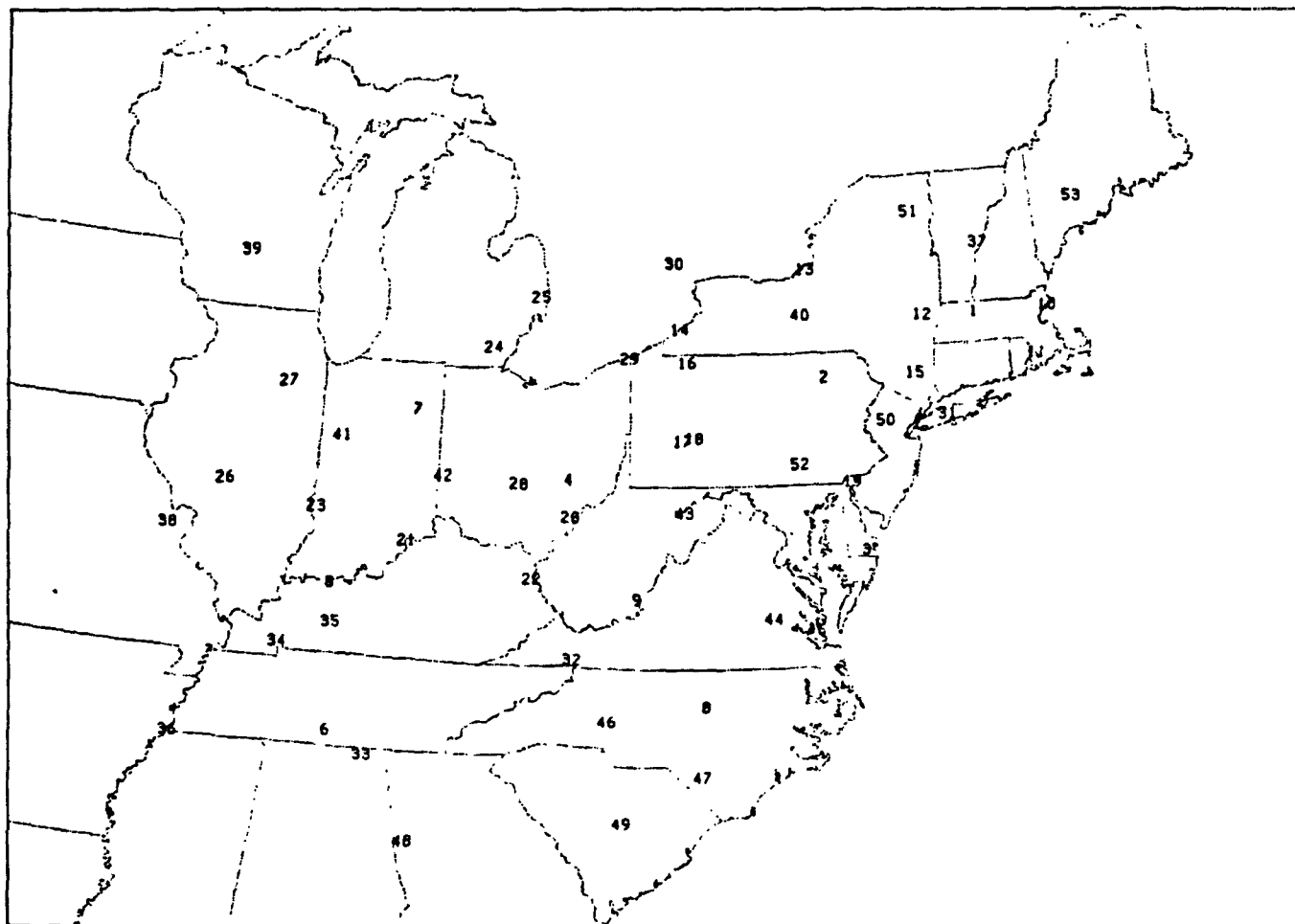


FIGURE 4-1. The EPRI SURE network of monitors. Sites numbered 1 - 9 are class I stations.

TABLE 4-1

THE NUMBER OF HOURLY SO₂ OBSERVATIONS AVAILABLE
FOR SELECTED EPRI/SURE SITES

Station	Class	Number of Observations	
1	I	9545	
2	I	7031	
9	I	9558	8660 observations average per station
12	I	8512	
13	II	3640	
15	II	3651	
18	II	3789	
20	II	4431	
22	II	3699	
28	II	4031	3334 observations average per station
37	II	1455	
40	II	2627	
42	II	2308	
43	II	4005	
51	II	2099	

remote from large point sources of SO_2 . The individual sites are described in some detail by Mueller and Hidy (1982). The distances between sites range from 28 km to 2371 km. The number of pairs of stations that fall within certain ranges of distance are presented in Table 4-2.

The accuracies of the various measurements of interest in the present study are summarized in Table 4-3. The 24-hour particulate SO_4^{2-} concentrations were slightly biased since only particles exceeding a certain diameter were collected efficiently. The external data quality audits and comparisons of the data with data from other programs are reported by Mueller and Hidy (1983).

4.2 Spatial Scale of Concentration Data

Hourly SO_2 concentrations and 24-hourly SO_2 and sulfate concentrations are provided for the 54 stations of the SURE network. Correlation and autocorrelation techniques are used in the following three subsections to examine the spatial scale of concentration data and the representativeness of concentration measurements.

4.2.1 Analysis of One-Hour SO_2 Concentrations

The one-hour averaged SO_2 concentrations at the nine Class I sites were examined for their statistical characteristics. Large concentrations were rarely encountered, which confirms that their placement was far away from large point sources. The probability density function of 1-hour average SO_2 concentrations at many of the sites seems to follow an intermittent lognormal distribution like that described by Netterville (1979). The intermittency factor ranges typically from 0.5 to ~1.0 for the Class I stations. Figure 4-2 shows the frequency distribution for site 4 as an example.

TABLE 4-2

THE NUMBER OF STATION PAIRS AS A FUNCTION
OF THE DISTANCE OF SEPARATION

Range	Number	Percent
0-200 km	81	5.6
200-400 km	219	15.3
400-600 km	250	17.4
600-800 km	235	16.4
800-1000 km	182	12.7
1000-1200 km	140	9.8
>1200 km	<u>324</u>	<u>22.6</u>
Total	1431	100

TABLE 4-3

A SUMMARY OF THE ACCURACY OF SO₂ AND SO₄ OBSERVATIONS
MADE AT THE CLASS I EPRI/SURE NETWORK
(Excerpted from Mueller and Hidy, 1983)

Station	1-Hour Average SO ₂ (LQL = 3ppb) ^a		24-Hour Average Hivol SO ₄ ⁻ (LQL = 8.4 µg/m ³) ^b	
	Bias (%) [*]	90% Confidence Interval (%)	Bias (%) [*]	90% Confidence Interval (%)
1	8.0	4.3	-3.6	5.4
2	5.7	3.4	-3.0	6.4
3	1.7	4.6	-5.3	3.3
4	4.3	9.7	-4.6	6.2
5	0.4	2.3	-8.4	10.0
6	8.4	5.7	-15.2	1.9
7	1.4	4.4	-8.1	7.7
8	-2.9	2.3	-3.0	2.2
9	-9.6	4.8	-2.7	4.6

* Bias (%) = 100 (ERT-EPA)/EPA

^a Concentrations range from 30-500 ppb

^b Assume accuracy is determined by volume flow rate rather than lab analysis.

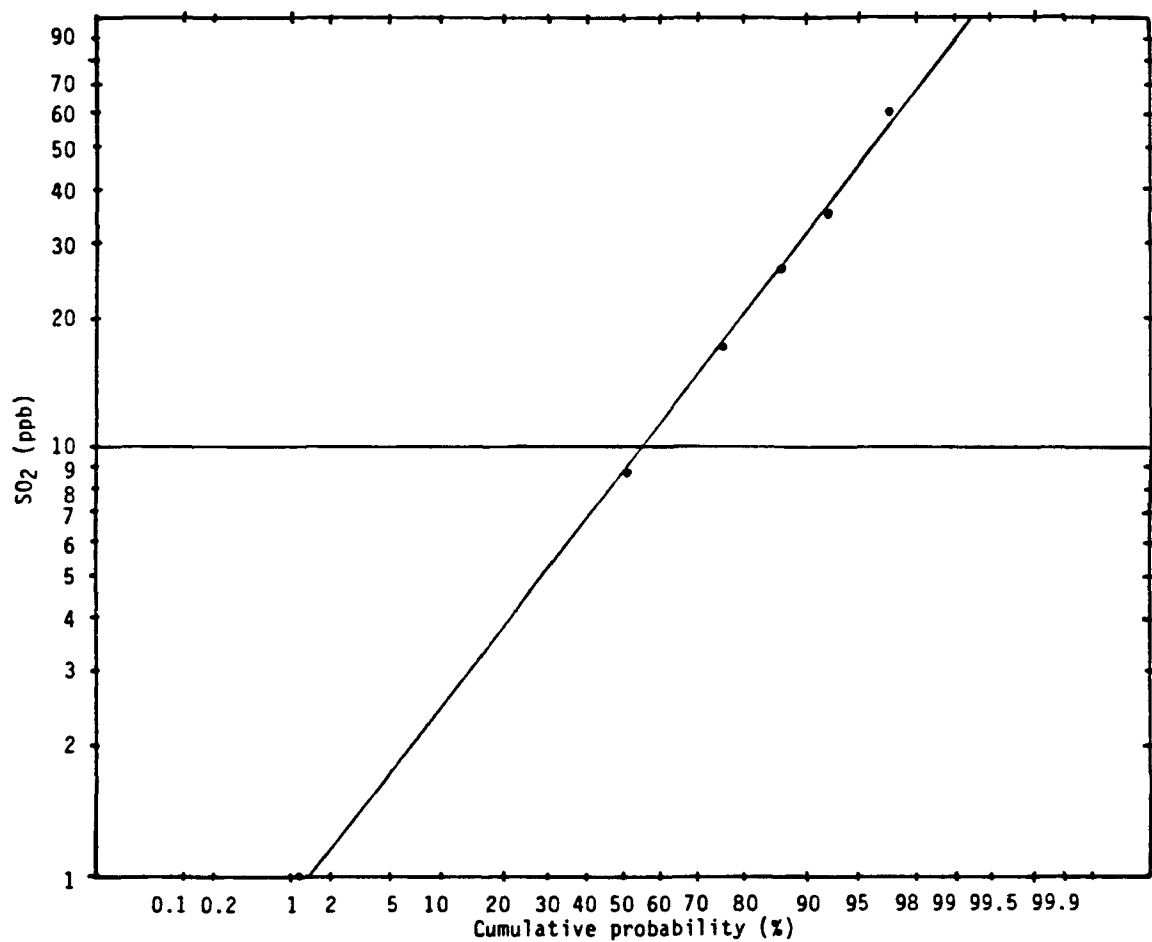


FIGURE 4-2. Cumulative distribution of 1-hr averaged SO₂ at EPRI/SURE station 4 on lognormal probability paper.

Some of the EPRI/SURE stations exhibit signs of cycle in the SO₂ concentrations, as shown in the autocovariance plot for the Scranton, Pennsylvania site (Figure 4-3). The autocovariance indicates that the fluctuation is a 12-hour cycle. Such variations were discovered at several of the class I sites. Presence of the cycles could possibly mask spatial correlations in SO₂ concentrations over large distance scales and should be considered in analyses.

The correlations of the one-hour average SO₂ concentrations between pairs of SO₂ monitoring sites were estimated for all possible station pairs of the 54 stations. Correlations averaged over 200 km station separation categories are shown in Figure 4-4 as a function of the site separation distance. The maximum correlation coefficients are approximately 0.6. It appears that the SURE network resolution is insufficient to fully describe the relationship of correlation with distance. Visual examination of the spatial correlations such as those shown in Figure 4-5 leads to the speculation that the scale of SO₂ variations changes with location in the EPRI/SURE network. An analysis to group stations by geographic region was pursued, but no statistically significant systematic changes were found in the shape of the autocorrelation function for various station groupings.

An analysis was done to examine how accurately a number of SO₂ observations made at several points within the region can be used as an estimator of the true spatial mean within the region. This is another means of estimating the spatial representativeness. For this analysis two arbitrary regions were selected in order to do the estimates. These two regions consist of the Ohio River valley region and a region covering New York and western New England (Figure 4-6). Eight stations within each of the regions were used in the analysis. The average concentration as well as the coefficient of

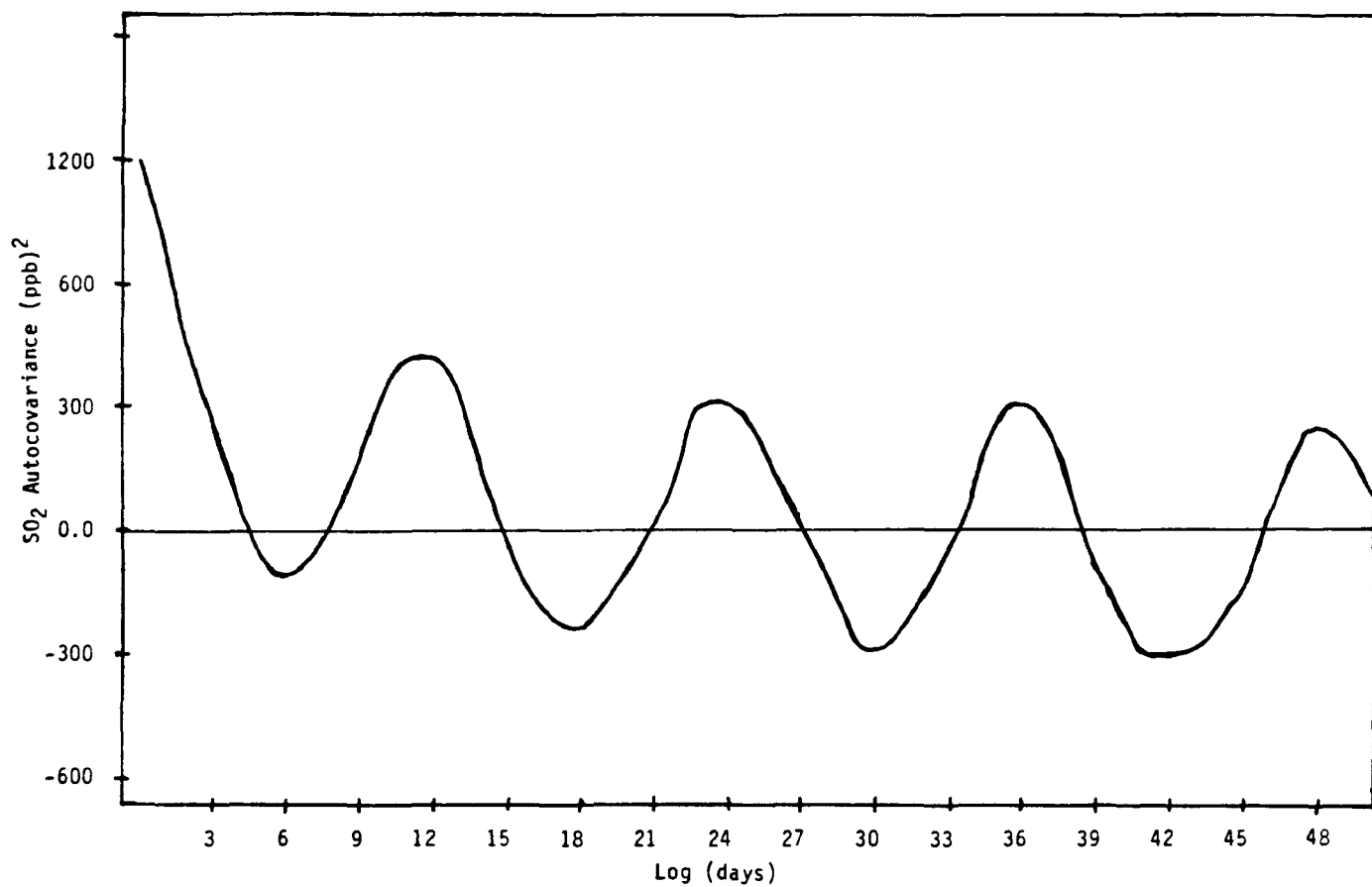


FIGURE 4-3. Autocovariance of hourly averaged SO_2 concentration observed at the Scranton, Pennsylvania site (EPRI/SURE site #2).

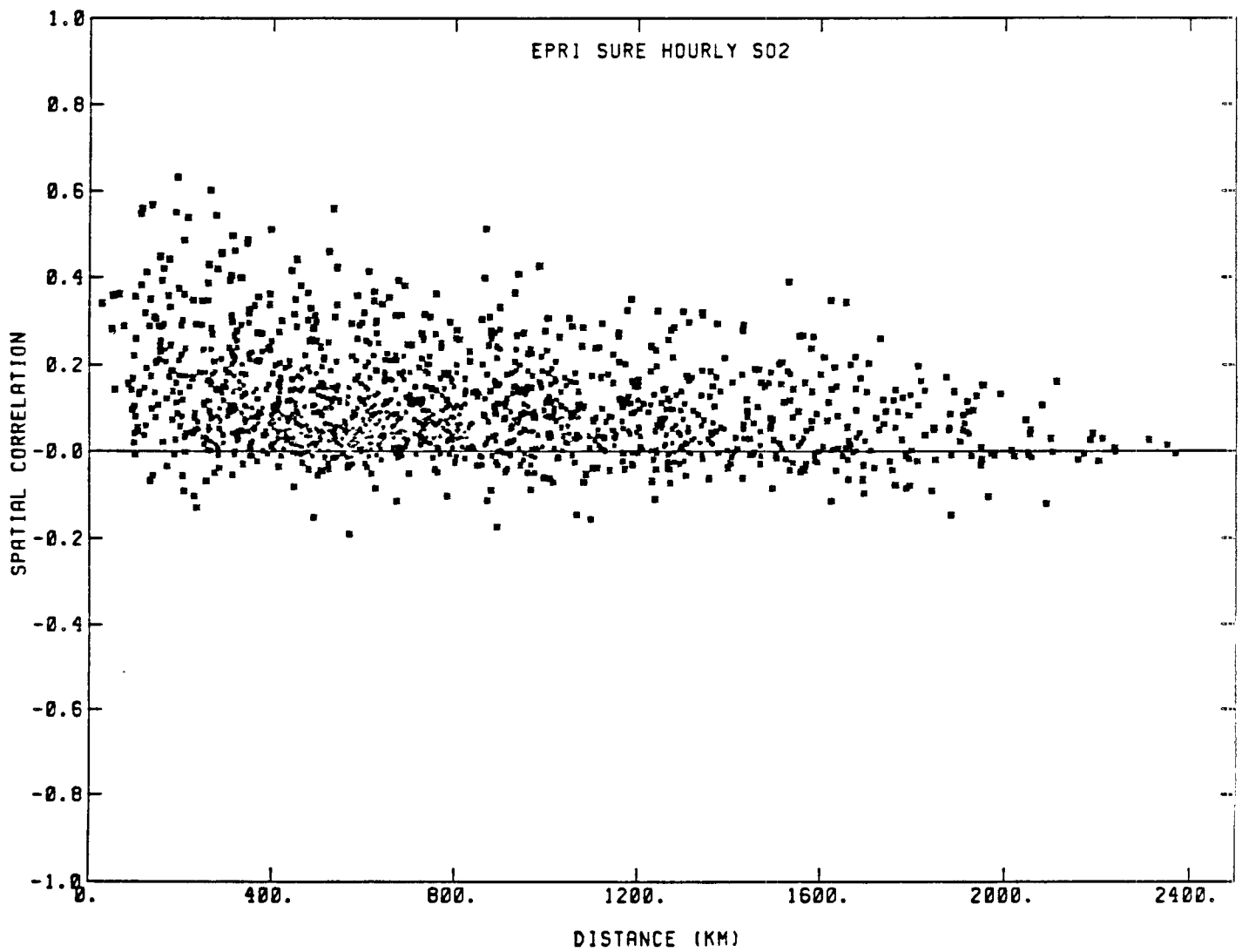


FIGURE 4-4. Observed spatial correlations of hourly SO₂ versus distance.

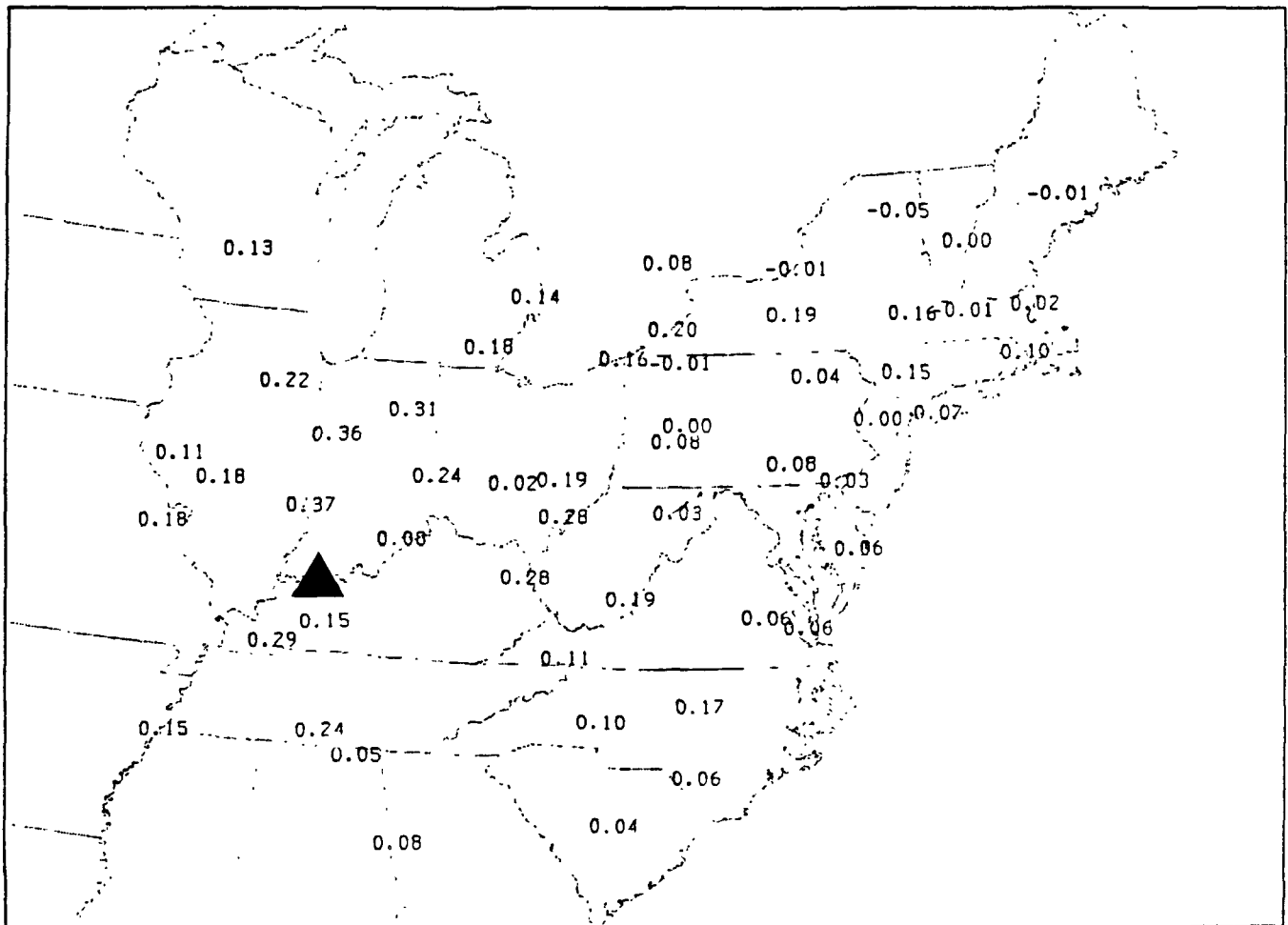


FIGURE 4-5a. Spatial distribution of correlations between station pairs: western region (the reference station is indicated by ▲).

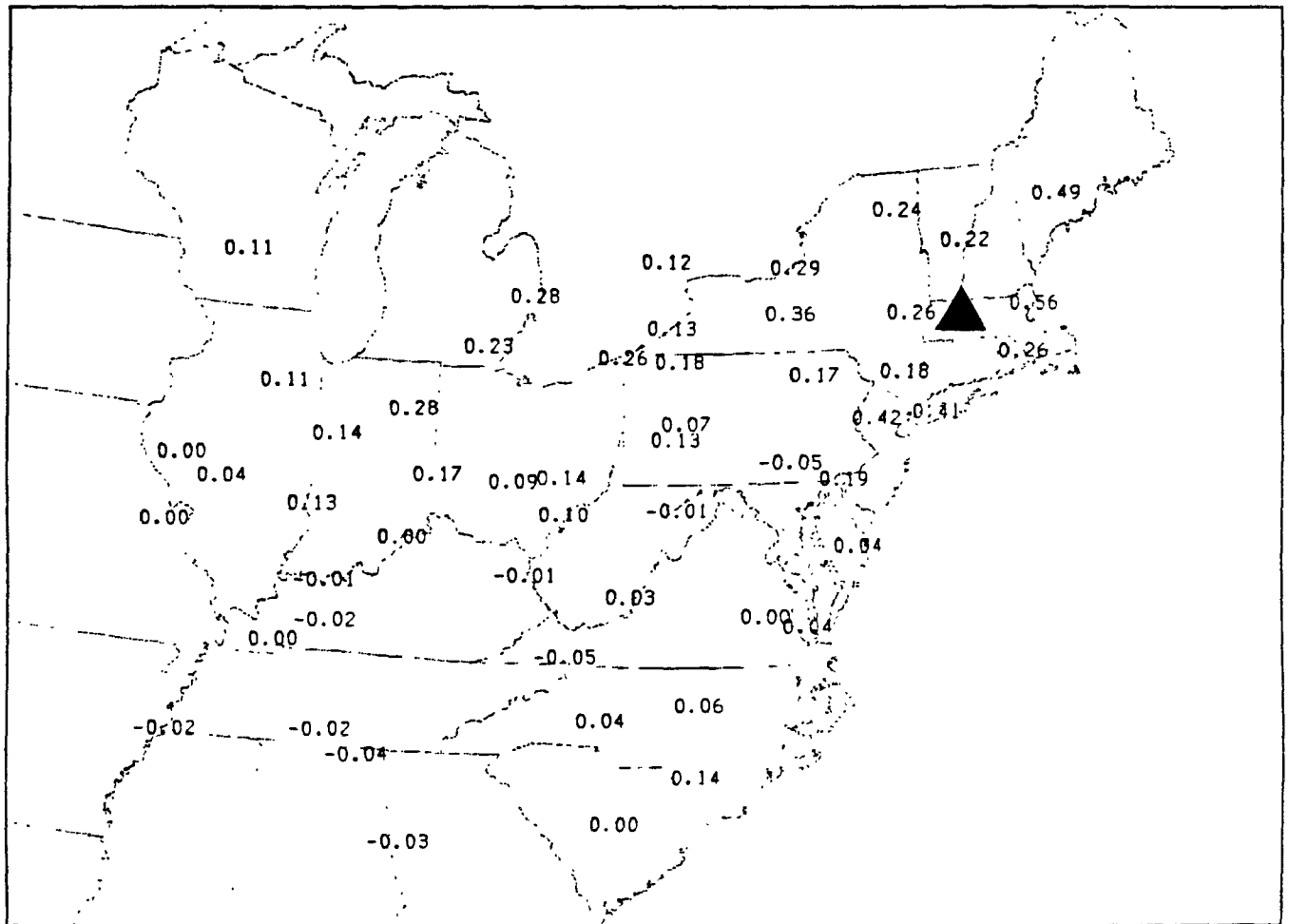


FIGURE 4-5c. Eastern region (the reference station is indicated by ▲).

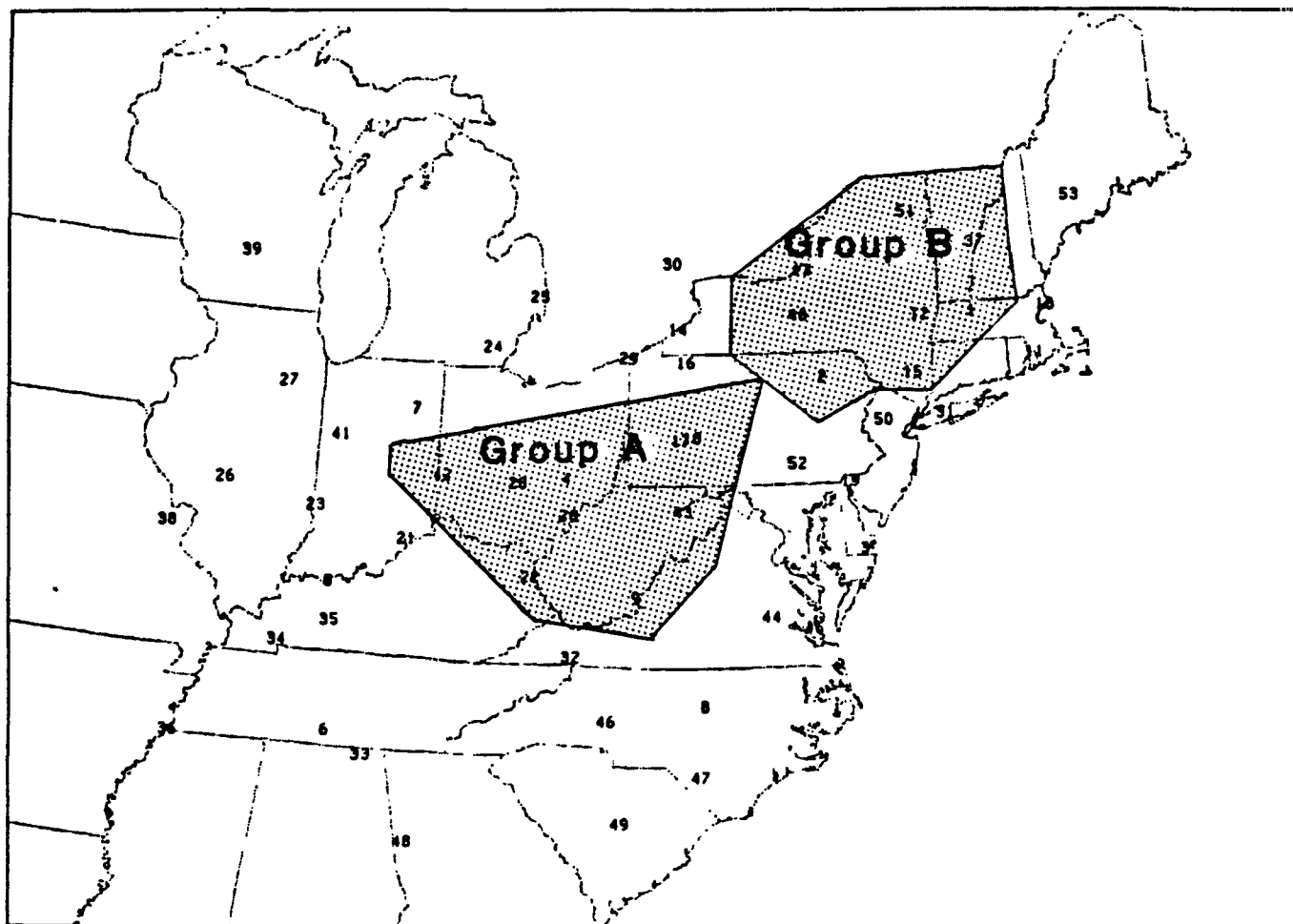


FIGURE 4-6. A map of the EPRI/SURE site locations occurring within the two study areas.

variation (cov), estimated as $\sigma_c \langle c \rangle$, were computed for all eight stations. The true average over the region is given by a weighted sum of the observations, where the weights could be dependent on the area where each point measurement is assumed to hold. Determination of the weights can introduce one source of uncertainty into the analysis. Another source of uncertainty arises from the degree of confidence that one can make in determining the true mean from the eight observations on either regular or irregular spaced grids. If the observations have no persistence (serial correlation) then the 95 percent confidence interval for the estimate of the mean can be computed using Student's t statistic as:

$$\langle c \rangle_{obs} [1 - 0.72 \cdot cov] \leq \langle c \rangle_{true} \leq \langle c \rangle_{obs} [1 + 0.72 \cdot cov]. \quad (4-1)$$

Serial correlation increases the confidence interval (Morris and Ebey, 1984) so the range given in Equation 4-1 represents a lowest limit on the uncertainty. The average value of $0.72 \cdot cov$ is 0.62 for the New York region and 0.66 for the Ohio River valley region. The standard deviation of $0.72 \cdot cov$ is large, typically 1.5.

Several averaging periods are being suggested for the various trace gases of interest in COMPEX. For example, hourly averaged SO_2 concentrations and six-hour averaged tracer observations are design possibilities. As the averaging period increases, the short-term variations are smoothed out, leading to a reduction in the variance. An obvious design question is how rapidly the variance changes with the averaging rate. In order to study this question, the SO_2 data were averaged over 6-, 12-, and 24-hour periods. The results indicate that in general the SO_2 variance follows as relationship of the form:

$$\text{Var}(\text{SO}_2 \text{ N-hour average}) = \text{Var}(\text{SO}_2 \text{ 1-hour average})/N^\alpha \quad (4-2)$$

where α ranges from 0.1 to 0.2. A summary of the variance for the averaging periods and stations is presented in Table 4-4.

4.2.2 Analysis of 24-Hour SO₂ Concentrations

Averaging of hourly SO₂ data for 24-hour periods provides a data base in which diurnal cycles are removed and which can be used for correlation analysis and comparison to 24-hour average sulfate concentrations. The correlations between all possible pairs of the 54 EPRI/SURE stations were computed. A scatter plot of these correlations as a function of distance between station pairs shows much scatter and only a slight variation of the correlation coefficient with downwind distance (Figure 4-7). As in the hourly case, grouping stations by geographical region did not provide any significant reduction of scatter. A model for the correlation coefficient of the form:

$$\rho(d) = \exp(-d/d_0),$$

where d is the distance between stations and d_0 is some characteristic distance, did not provide a satisfactory fit. Estimates of the mean squared error (MSE) are relatively constant at all ranges of station pair separation distance. The results suggest that for 24-hour averaging the spatial variation in SO₂ concentrations is quite large even for separations of the order of 150 km. Data for smaller spatial scales are not available from SURE.

4.2.3 Analysis of 24-Hour Sulfate Concentrations

Although both 3- and 24-hour average SO₄ observations were made, the 3-hour average SO₄ data only was collected for six months at the class I sites and the analyses were performed only on the 24-hour averaged SO₄ data.

TABLE 4-4

THE VARIANCE OF SO₂ (ppb) FOR VARIOUS
EPRI/SURE STATIONS AS A FUNCTION OF AVERAGING TIME

Station	1 Hour	6 Hours	12 Hours	24 Hours
1	5.3	5.1	4.8	4.6
2	30.9	23.7	18.1	15.0
4	17.7	15.2	13.4	11.6
9	7.6	7.2	6.7	6.3
12	11.6	9.1	7.7	6.8
13	6.8	5.3	4.8	4.3
15	31.7	23.5	19.5	17.1
18	13.5	13.0	12.5	11.5
20	18.9	15.3	13.3	11.2
22	12.5	11.7	10.9	10.0
28	8.7	7.6	6.9	6.2
37	2.7	2.6	2.5	2.2
40	7.4	6.5	5.9	5.6
42	11.0	10.2	9.6	7.8
43	17.8	10.6	8.9	7.8
51	3.4	3.1	3.0	2.6

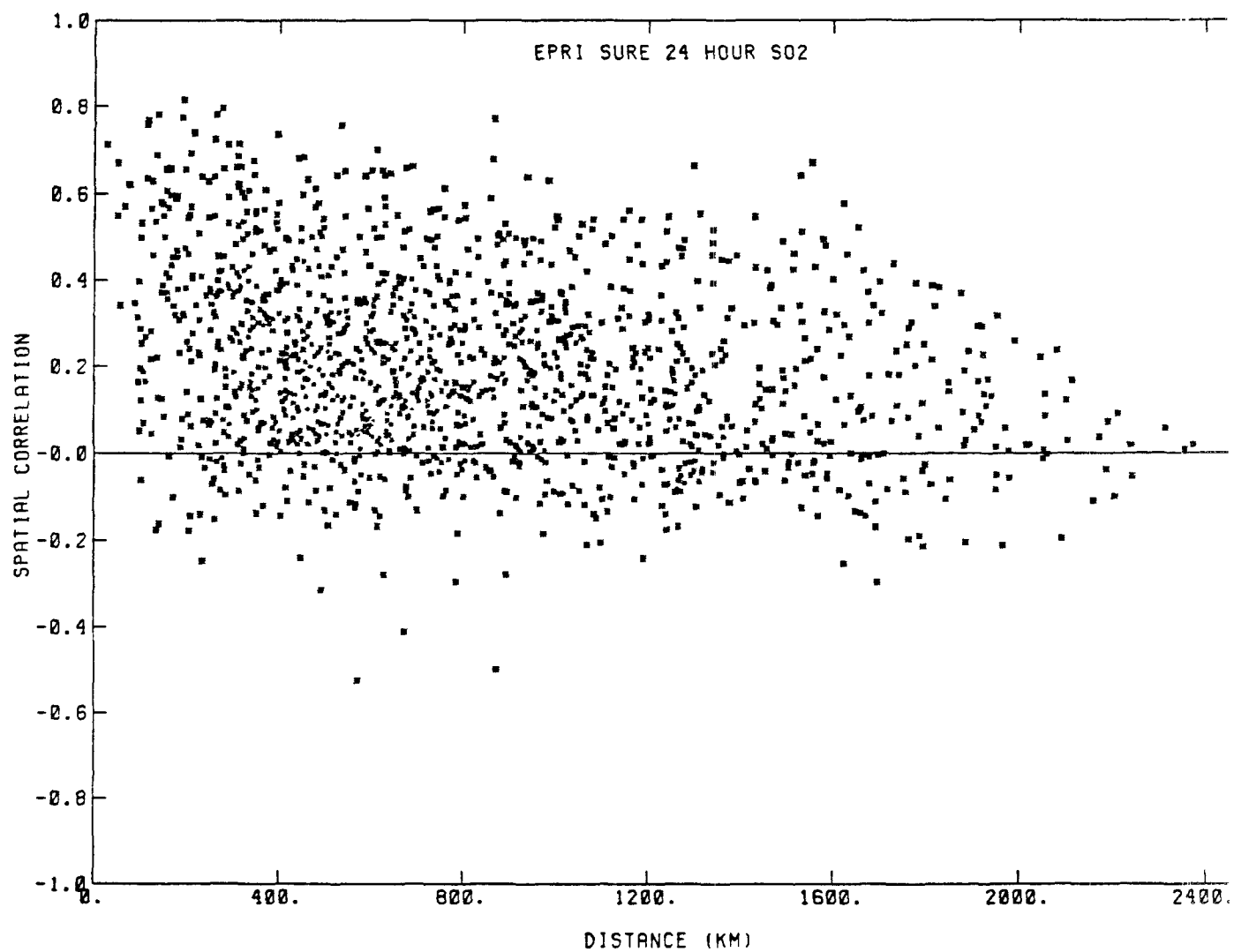


FIGURE 4-7. Scatter plot of 24-hour average SO_2 correlations as a function of the distance between stations.

The correlation coefficients were estimated for all possible station pairs and are presented as a function of distance separating the pairs (Figure 4-8). Despite the relatively large scatter, the average correlation coefficients seem to decrease systematically as a function of station separation. The average correlation coefficient was computed for ranges of station separation. The resulting curve with its confidence interval is shown in Figure 4-9. The curve suggests that a model of the form:

$$\rho(d) = \exp(-d/d_0), \quad d_0 = 660 \text{ km} \quad (4-3)$$

is a good fit of the curve in Figure 4-9. This result suggests that the spatial persistence of the SO_4 concentration patterns is much greater and extends over much larger scales than for SO_2 concentrations.

One parameter of interest to network design is the station separation that is necessary to keep the MSE of interpolation below some arbitrary level. The MSE of extending an observation at location X over a distance ΔX can be estimated directly from the pair station statistics. Figure 4-10 shows the rate of increase in the MSE with increasing ΔS . The MSE was fitted to a model of the form:

$$\text{MSE}(\Delta x) = 0.45 \Delta X^{0.45} \quad (\Delta X \text{ is in km}) \quad (4-4)$$

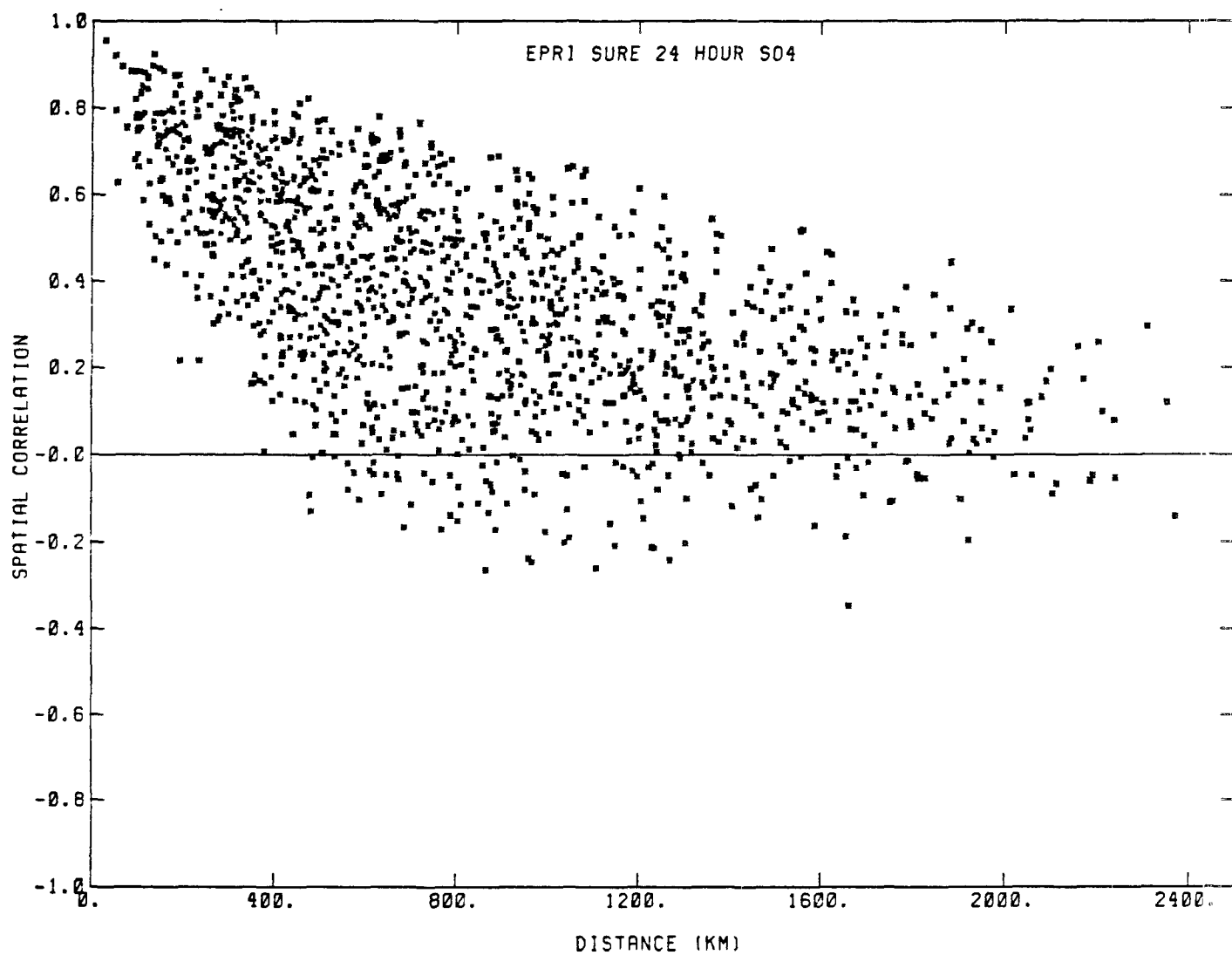


FIGURE 4-8. Observed spatial correlations of 24-hour SO₄ versus distance.

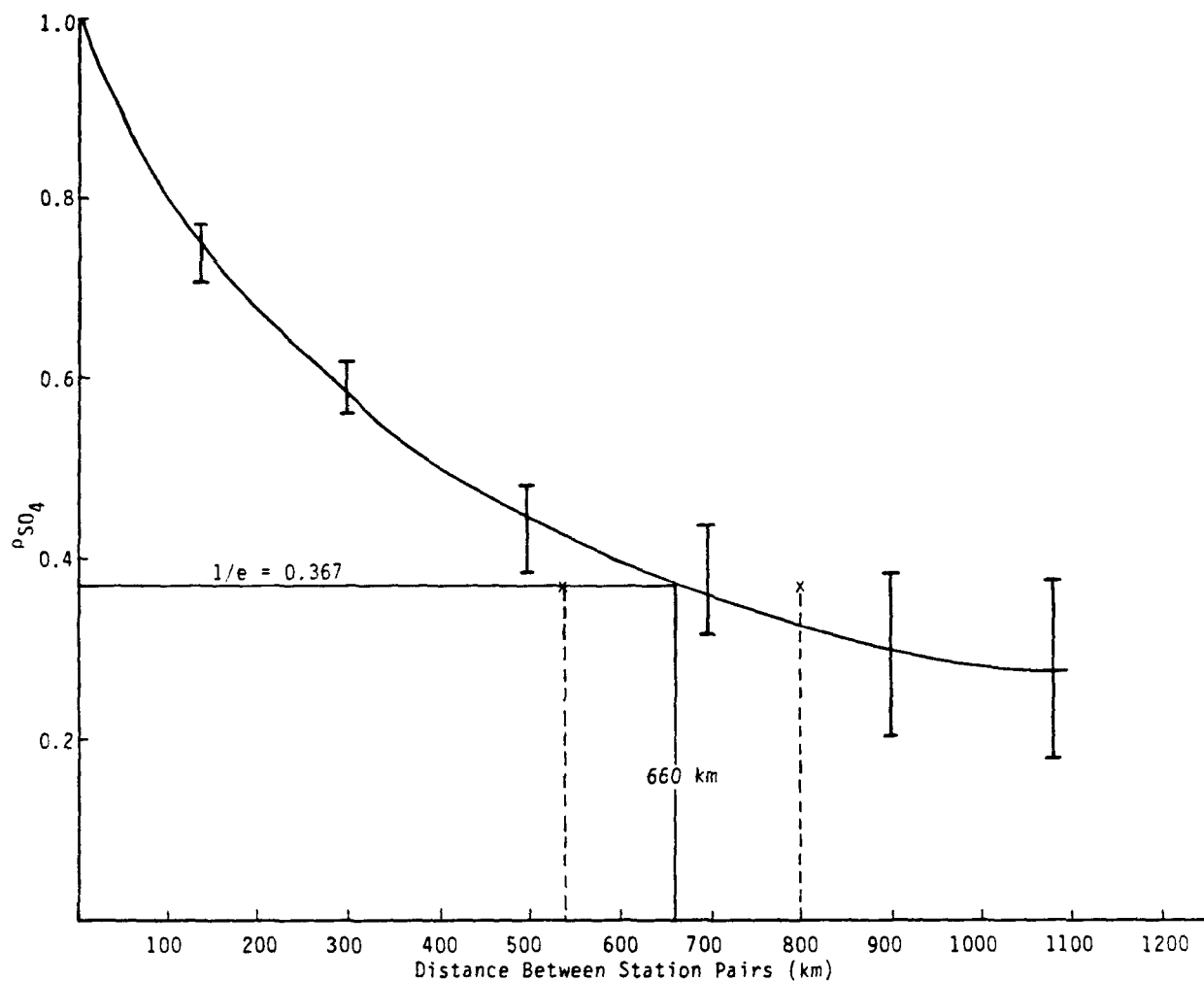


FIGURE 4-9. The variation in the correlation coefficient of 24-hour average SO_4 as a function of station pair separation. The error bars are for the 95% confidence interval.

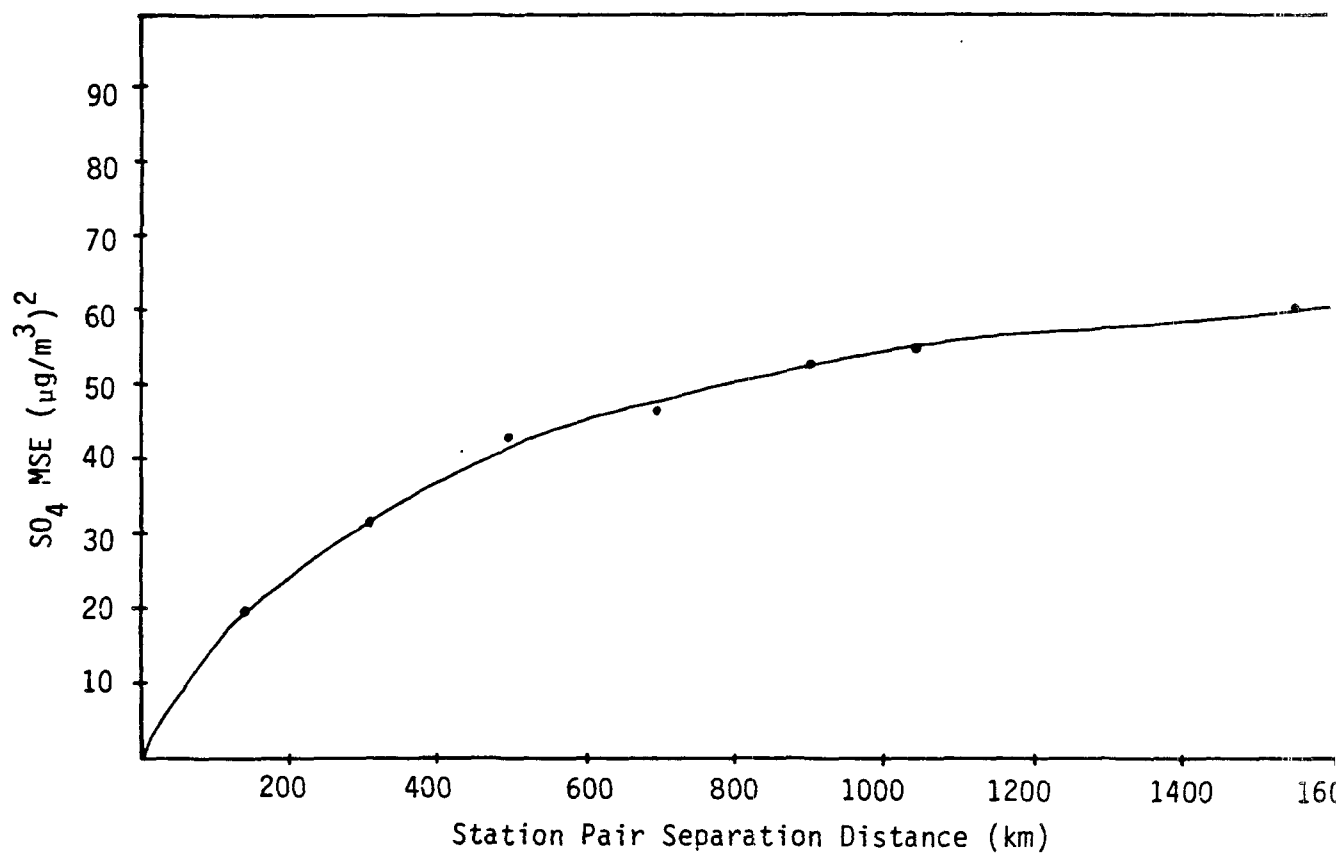


FIGURE 4-10. The increase in 24-hour average SO_4 MSE as a function of separation between station pairs.

The MSE can be used to define a signal to noise ratio (s/n) in terms of the reduction of variance, e.g.,

$$S/N(d) = 1.0 - MSE(d)/2 \text{ Var}(c) \quad (4-5)$$

where c is the SO_4 concentration. At a distance $d = 660$ km, the $S/N(d)$ is of the order 0.375.

According to the variogram model for the MSE that is discussed by Huijbregts (1975), the MSE can be related to the spatial autocorrelation function $\rho(d)$ by

$$MSE(d) = 2 \text{ Var}(c)[1 - \rho(d)] + \epsilon \quad (4-6)$$

if the SO_4 statistics over the EPRI/SURE network are stationary, then $\epsilon = 0$. Visual inspection of average SO_4 concentrations such as those displayed in Figure 4-11 indicates that the concentration averages vary with distance. One hypothesis advanced was that the term $\epsilon = (c_x - c_{x+\Delta x})^2$ is related to spatially and temporally averaged concentrations and rapidly approaches a constant value with increasing distance. This hypothesis was examined by computing the $MSE(d)$ from Equation 4-6 and comparing it with the observed $MSE(d)$. The results are summarized in Table 4-5 and show that the $(c_x - c_{x+\Delta x})^2$ term is relatively both constant and small. The term can be fitted to a model of the form

$$(c_x - c_{x+\Delta x})^2 = K\langle\bar{c}\rangle[1 - \exp(-d/d_0)] \quad (4-7)$$

where d_0 is less than 50 km and K is a constant of order unity.

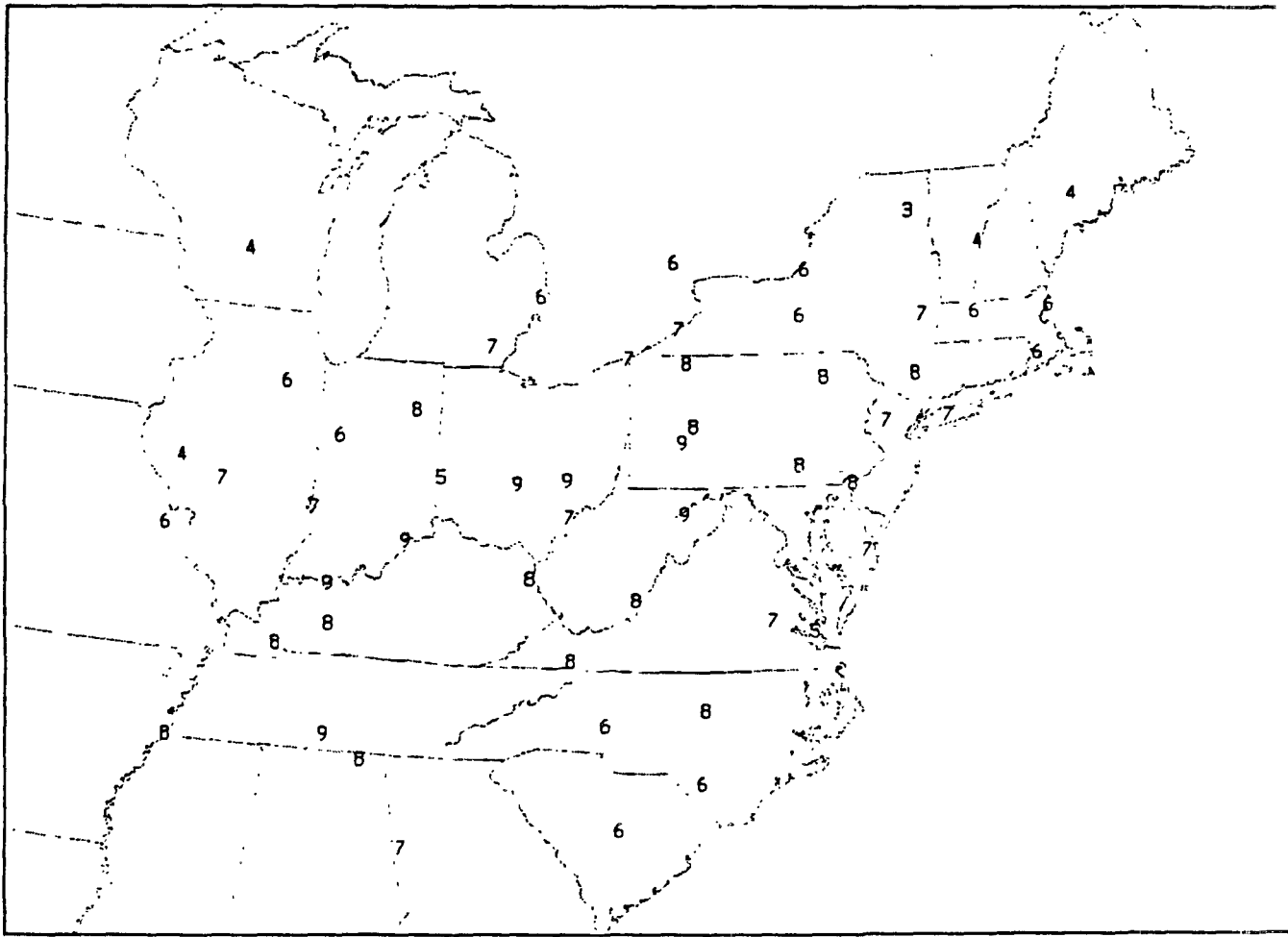


FIGURE 4-11. Geographic distribution of the mean sulfate concentrations ($\mu\text{g}/\text{m}^3$) for each of the 54 EPRI SURE monitoring sites.

TABLE 4-5

COMPARISON OF THE OBSERVED MEAN SQUARE ERROR (MSE) IN 24-HOUR AVERAGE SO_4 CONCENTRATIONS AS A FUNCTION OF STATION SEPARATION VERSUS THE MSE COMPUTED USING A SIMPLE VARIOGRAM MODEL DESCRIBED BY EQUATION 4-6. VARIANCE FOR ALL STATIONS IS $36 \mu\text{g}/\text{m}^3$.

Distance (km)	Observed MSE $(\mu\text{g}/\text{m}^3)^2$	Predicted MSE $(\mu\text{g}/\text{m}^3)^2$	Observed Minus Predicted (E)
140	19.8	19.1	0.7
306	31.6	29.7	1.9
496	43.1	41.5	1.6
695	46.5	45.0	1.5
903	52.9	51.6	1.3
1090	54.8	53.0	1.8
1551	60.3	59.8	0.5

4.3 Temporal Characteristics of Concentration Data

The temporal characteristics of the concentration data are important particularly in evaluating the feasibility of the source modulation component of the planned short-range experiments. The planned experimental program calls for the modulation of several SO₂ sources in a region. The modulated signal will be modified by the atmosphere and hopefully part of the signal will be detected at target receptor locations. This signal will have to compete with the SO₂ fluctuations caused by other sources. The signal takes a significant time to reach the receptors and is transported in a directionally biased fashion. Furthermore, the loss of signal can be highly nonlinear with distance due to processes such as rainout.

These considerations make it important to perform a frequency analysis of the relationships between daily average SO₂ and sulfate fluctuations. In the analyses, the 24-hour average ground-level SO₂ concentrations in the major source region is used as a surrogate for the SO₂ emitted into the air aloft. The reasoning is that if the ambient ground-level SO₂ concentrations are dominated by only the major point sources operating within about 100 km, then there is no effective time lag between emission rates and 24-hour average concentrations.

For the analysis, it would be good to know if there is a window of frequencies for which the source signal would propagate to the desired receptors with a minimum loss. This question can be estimated through the use of the frequency gain function, $G(\omega)$. The gain function is a measure of the fraction of a unit amplitude sine wave of frequency ω that reaches the receptor site. The function is generally bounded between 0 and 1 and is often expressed as a logarithm.

The gain function, $G(\omega)$, is defined as the cross power spectrum function of the transmitted signal (the 24-hour averaged SO_2 concentrations) derived by the power spectrum of the transmitted signal (the 24-hour average SO_4 concentrations), e.g.,

$$G(\omega) = \frac{\phi^2_{(\text{SO}_4 - \text{SO}_2)}(\omega)}{\phi^2_{\text{SO}_2}} \quad (4-8)$$

The gain function is useful when the emission from point sources in other regions are either white noise, or else their spectrum resembles that of the 24-hour average SO_2 concentrations from the areas of interest. The SO_2 spectrums are not constant with frequency and do not resemble that of a white noise signal. However, an analysis of the SO_2 sources from other regions are compared in Figure 4-12, with the finding that in general, the SO_2 power spectra are qualitatively similar.

Only the SO_2 and SO_4 observations at the nine class I sites could be analyzed since only these stations have enough data (>80 percent possible) to avoid significant bias due to missing data. All of the spectral analysis was done on time series where the missing data was replaced with an average over the whole time series. The gain function peaks at several frequencies as Table 4-6 shows. The most consistently strong peak occurs for periods between 4-5 days at the station pairs analyzed. A second peak occurs for a period ranging between 3-4 days. The results suggest that a source modulation frequency of 3 to 5 days would be appropriate.

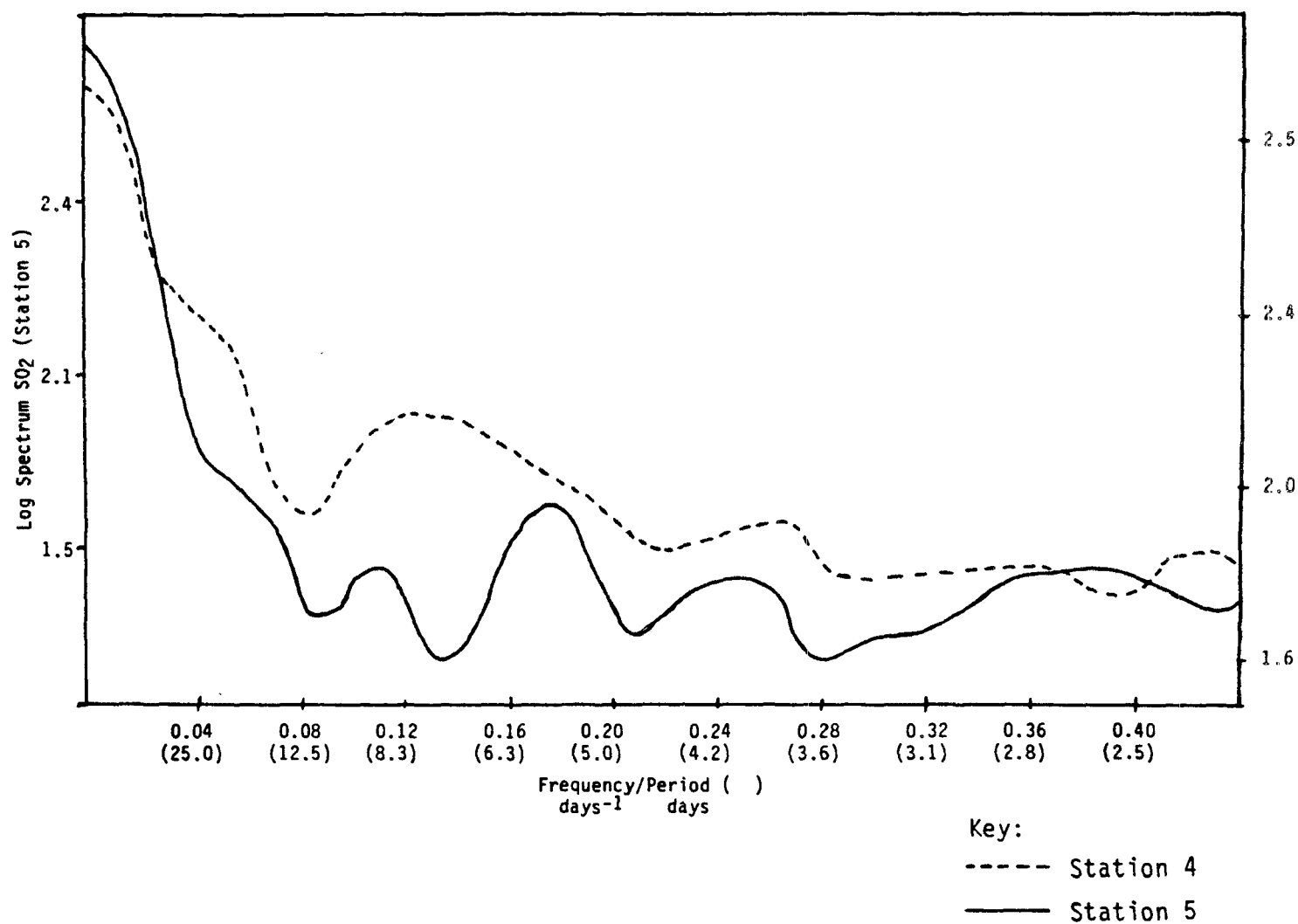


FIGURE 4-12. Inter-comparisons of power spectrums of 24-hr averaged SO₂ at the EPRI/SURE stations.

TABLE 4-6

A SUMMARY OF THE MAXIMA IN THE SO_2 - SO_4 GAIN FUNCTION, $G(\omega)$, AS A FUNCTION OF PERIOD AND STATION SO_2/SO_4 PAIRING (BAND WIDTH IS 0.0675).

SO_2 Station	SO_4 Station	Period (Days)	$-\log G(\omega)$
5	2	4.8	0.77
		9.0	1.15
		22.0	1.34
9	1	5.3	0.35
		3.3	1.27
		26.0	1.52
5	1	3.5	1.06
		26.0	1.20
		4.8	1.21
		7.6	1.38
4	1	4.8	1.35
		7.6	1.36
		11.8	1.46
		3.5	1.75

4.4 Spatial Representativeness of Single Station Concentration Measurements

The question of how representative the measured concentrations at monitoring sites are of the surrounding areas can be approached by looking at the expected errors of extrapolating the values at the site to neighboring locations. The station spacing required to provide adequate spatial coverage of a region is determined by examining the mean square error of predicting values at neighboring locations by the value at the single station, as a function of distance from the station. This is expressed by the mean square error:

$$MSE_{xy} = \frac{1}{n} \sum_{i=1}^n C_{xi} - C_{yi}^2 \quad (4-9)$$

$$= \text{var}(C_x) + \text{var}(C_y) + (\bar{C}_x - \bar{C}_y)^2 - 2 \text{cov}(C_x, C_y),$$

where

$C_{xi}, C_{yi}, i=1, \dots, n$ = the concentrations at locations x and y, at n times,

\bar{C}_x, \bar{C}_y = the mean concentrations at x and y,

$\text{var}(C_x), \text{var}(C_y),$ = the concentration variances at x and y,

$\text{cov}(C_x, C_y)$ = the covariance of the concentrations at x and y.

This can be simplified by assuming that the concentration variance does not vary greatly within the region of interest as in equation 4-6. In this case:

$$MSE_{xy} \sim 2 \text{var}(C) (1-r_{xy}) + (C_x - C_y)^2 \quad (4-10)$$

where

$\text{var}(C)$ = a typical value of the concentration variance within the region,
and

r_{xy} = the correlation of the concentrations at x and y.

r_{xy} and $(C_x - C_y)^2$ are modeled as functions of the distance between x and y , and then Equation 4-10 is used to express the mean square error as a function of distance. This approach assumes that the concentration field is approximately second-order stationary after the mean concentrations, or spatial trends, have been removed. The first term of Equation 4-10 is the contribution of the concentration fluctuations to the uncertainty associated with using the value measured at x as a surrogate for the value at y ; the second term is a measure of the uncertainty that results from spatial trends in the concentration field.

It should be noted that Equation 4-10 will overestimate the mean square error of interpolation from a network. Typically, more than one station is used for interpolation, and this can substantially reduce the error term due to spatial trends. However, as the station spacing is increased, the error of interpolation from multiple stations will approach the value of Equation 4-10.

This approach has been used for the EPRI/SURE hourly SO_2 and 24-hour SO_4 data collected at 54 stations in the eastern United States. This data base is described in Section 4-1. Using Equation 4-10, $\text{var}(C)$ is calculated as the mean of the concentration variances at the 54 stations, and r_{xy} and $(C_x - C_y)$ are given by:

$$r_{xy} = \exp(-d/d_0) \quad (4-11)$$

and

$$(C_x - C_y) = a[1 - \exp(-d/d_1)] \quad (4-12)$$

where d is the distance from x to y , and d_0 , d_1 , are constants, determined by fitting these models to the data. The fitted values are given in Table 4-7. The spatial variability of the hourly SO_2 data is of a scale

TABLE 4-7

PARAMETERS FITTED TO HOURLY SO₂ AND 24-HOUR SO₄ DATA.

Parameter	SO ₂	SO ₄
var(C)	216 (ppb) ²	35.5 (μg/m ³) ²
d ₀	137 (km)	680 (km)
d ₁	0 (km)	985 (km)
a	56 (ppb) ²	9.7 (μg/m ³) ²
s	5.64 (ppb)	1.65 (μg/m ³)
τ ₀	8.6 (hours)	3.5 (days)

less than the SURE network spacing. As a result, fitting of the models to the data was unsuccessful. The value of d_1 from the data was approximately zero and the correlation coefficients rapidly approached zero as the station separation distance increased. This was consistent with distribution of the observed correlations, mean differences squared, and root mean square errors versus distance.

Table 4-8 compares the SO_4 predictions of Equation 4-10 with the average values within each of seven distance classes of the observed mean square errors. The predicted values are calculated at a representative distance for each class. These distances are the midpoints of each class, except for the first and last classes, in which cases they are the mean distances within the classes. The second term of Equation 4-10 is also tabulated, so that the relative contributions of the two terms can be seen.

Figures 4-8 and 4-13 display the SO_4 sample correlations r_{xy} and the sample values of $(C_x - C_y)^2$, plotted against distance. Figure 4-14 shows the sample mean square errors (MSE_{xy}), plotted against distance. It can be seen that there is considerable scatter in all of these plots, and that Equation 4-10 is only estimating expected or mean values. This analysis shows that the spatial representativeness of 24-hour SO_4 at a station is of the order of 100 to 200 km. The spacing of the SURE network stations is not dense enough to adequately estimate the scale of representativeness of hourly SO_2 , except to say that it is less than 100 km.

4.5 Analysis of Network Uncertainties

This section describes a method for quantifying the uncertainties associated with monitoring networks, where the objective of the monitoring is to estimate spatial and/or temporal averages or to obtain point estimates of

TABLE 4-8

COMPARISON OF OBSERVED 24-HOUR SO₄ WITH PREDICTIONS OF EQUATION 4-10

Distance Class (km)	Average Observed MSE	Representative Distance (km)	Predicted MSE	Predicted (C _x - C _y) ²
<200	19.4	140	14.5	1.3
200-400	31.4	300	27.9	2.6
400-600	43.6	500	40.8	3.9
600-800	46.2	700	50.6	4.9
800-1000	53.3	900	57.9	5.8
1000-1200	54.8	1100	63.4	6.5
>1200	60.8	1550	71.4	7.7

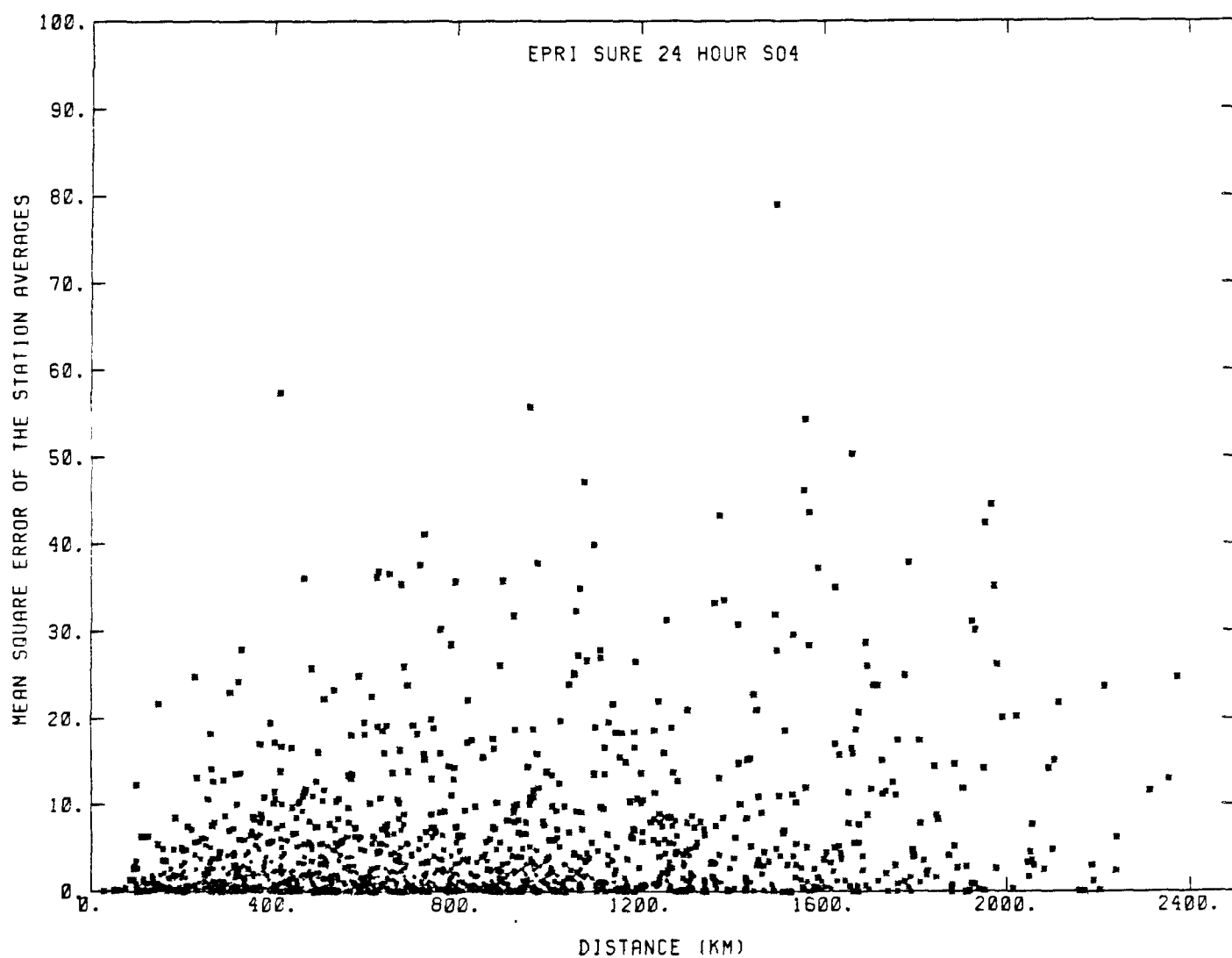


FIGURE 4-13. Observed 24-hour SO₄ $(\bar{C}_x - \bar{C}_y)^2$ versus distance.

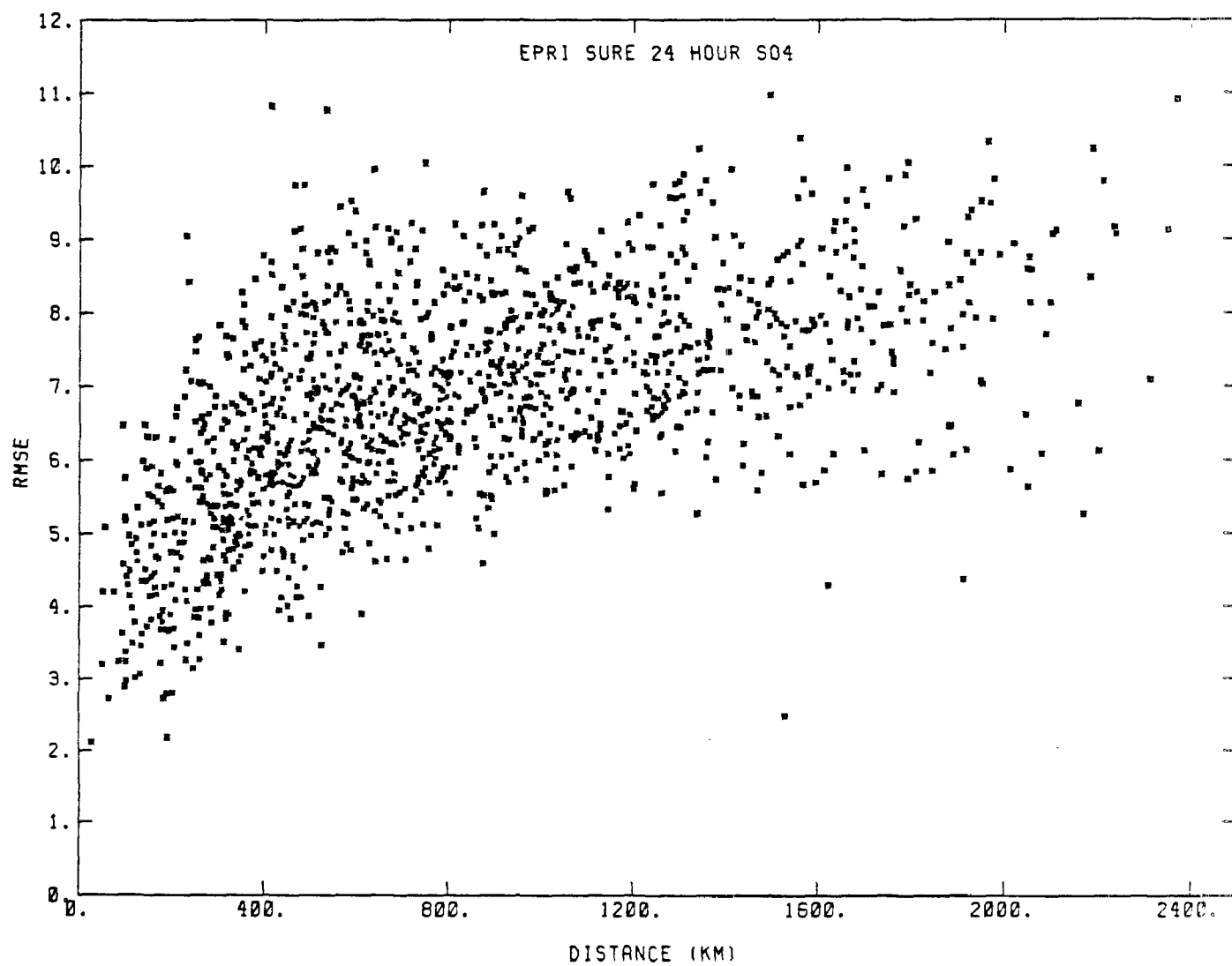


FIGURE 4-14. Observed 24-hour SO_4 root mean square errors versus distance.

the concentration by interpolation. First, the uncertainties inherent in making spatial averages from point estimates are discussed. A second analysis shows these uncertainties can be reduced by averaging over time.

Consider the problem of estimating the average concentration over a region, at a given time, from a discrete set of measured values. The uncertainty of this estimation can be addressed by looking at the expected mean square error of the estimate:

$$\text{estimated mean square error} = E(A - \hat{A})^2$$

where:

E = the expectation operator (over time)
 A = the true spatial average, and
 \hat{A} = the estimate of A .

$$A = \frac{1}{|\Omega|} \int_{\Omega} C(x) dx, \quad (4-13)$$

and

$$\hat{A} = \sum_{i=1}^n Y_i C(x_i), \quad (4-14)$$

where:

Ω = the region of interest,
 $|\Omega|$ = the area of the region,
 $C(x)$ = the concentration at location x ,
 n = the number of monitoring sites used to form the average,
 x_1, \dots, x_n = are the locations of the sites, and
 Y_1, \dots, Y_n = weights.

Measurement errors are neglected. For the special case where Ω is a single location x_0 , then $A = C(x_0)$, and the problem is one of interpolation.

The weights Y_i can be chosen to minimize the expected errors, by various methods, including the multivariate linear regression (Gandin, 1965;

Eddy, 1967) and Kriging (Huijbregts, 1975; Delhomme, 1978). If the spacing of the stations is fairly uniform in Ω and the covariance structure of the concentration field is fairly homogeneous, then taking the weights to be equal will be near optimal for estimating a spatial average. This will be the case for the combined experiments for which it is assumed that A is formed using equal weights $Y_i = 1/n$.

This gives:

$$\begin{aligned}
 E(A - \hat{A})^2 &= E \left[\frac{1}{|\Omega|} \int_{\Omega} C(x) dx - \frac{1}{n} \sum_{i=1}^n C(x_i) \right]^2 \\
 &= \frac{1}{n^2} \sum_{i=1}^n \sum_{j=1}^n V(x_i, x_j) - \frac{2}{n|\Omega|} \sum_{i=1}^n \int_{\Omega} V(x, x_i) dx \\
 &\quad + \frac{1}{|\Omega|} \int_{\Omega} \int_{\Omega} V(x, x') dx dx' \\
 &\quad + \left[\frac{1}{|\Omega|} \int_{\Omega} \bar{C}(x) dx - \frac{1}{n} \sum_{i=1}^n \bar{C}(x_i) \right]^2
 \end{aligned} \tag{4-15}$$

where $V(x, x') = E [C(x) C(x')]$ is the covariance of the concentrations at x and x' , and $\bar{C}(x) = E [C(x)]$ is the mean concentration at x .

This equation is analogous to Equation 4-10. The first three terms give the contribution to the error variance from the variance-covariance structure of the concentration field. The last term results from the structure of the mean concentration field.

In order to estimate the terms in Equation 4-15, the approach of the previous section is followed by modeling the spatial correlation as a

distance-dependent exponential and using a mean or typical value for the station variances to get:

$$V(x, x') = \text{var}(c) \exp (-d/d_0) \quad (4-16)$$

where:

d = the distance between x and x' ,
 $\text{var}(c)$ = the mean variance, and
 d_0 = a parameter to be determined.

In order to estimate the last term, it is assumed that the n stations are fairly uniformly distributed within the region of interest, in which case it is reasonable to suppose that $1/n \sum_{i=1}^n \bar{C}(x_i)$ is an unbiased estimator of the spatial average $1/|\Omega| \int_{\Omega} \bar{C}(x) dx$. The last term in Equation 4-15 is estimated by s^2/n , where s/\sqrt{n} is the standard error of:

$$1/n \sum_{i=1}^n \bar{C}(x_i)$$

as an estimate of the mean,

$$s^2 = \frac{1}{n-1} \left[\sum_{i=1}^n C(x_i) - \sum_{i=1}^n C(x_j) \right]^2 \quad (4-17)$$

$\text{Var}(c)$, d_0 , and s are estimated using hourly SO_2 and 24-hour SO_4 data; the values are given in Table 4-7.

The mean square error of the estimate A will be reduced by averaging the observations over time. In this case, the spatial-temporal averages are estimated by:

$$A_T = \frac{1}{T} \int_0^T \frac{1}{|\Omega|} \int_{\Omega} C(x, t) dx dt \quad (4-18)$$

$$\hat{A}_T = \frac{1}{m} \sum_{j=1}^m \frac{1}{n} \sum_{i=1}^n C_{ij} \quad (4-19)$$

where C_{ij} is the observed concentration at site i at time j . It is assumed that the times of measurement are equally spaced throughout the interval $[0, T]$, although not necessarily continuous. The error variance is reduced according to the following relationship (Papoulis, 1965; Thiebaut and Zwiers, 1984):

$$E(A_T - \hat{A}_T)^2 = E(A - \hat{A})^2 \frac{1}{m} \sum_{\tau=-(m-1)}^{m-1} (1 - |\tau|/m) \rho(\tau \Delta) \quad (4-20)$$

where:

m = the number of measurement times,
 $\rho(\tau)$ = the autocorrelation of A at lag τ , and
 Δ = the time interval between successive measurements.

The amplitude of a signal of cyclic nature is sought, then Δ can be taken to be equal to the period of the signal, and averages can be formed for different portions of the cycle; m would then be equal to the number of cycles available for averaging. $\rho(\tau)$ is modeled by:

$$\rho(\tau) = \exp(-|\tau|/\tau_0) \quad (4-21)$$

where τ_0 is a parameter, determined by fitting this function to the autocorrelations of the observed area-wide mean values (Table 4-7).

So far, any errors due to individual measurement inaccuracies have been neglected. It is reasonable to assume that these errors are independent, and therefore, to take this into account, the measurement error variance can be added to Equation 4-15. This error variance term is given by:

$$\frac{1}{n \cdot m} \sigma^2 \quad (4-22)$$

where $n \cdot m$ is the number of measurements, and σ^2 is the error variance of a single measurement.

Combining Equations 4-15 and 4-20 with the models given by Equations 4-16, 4-17, and 4-18 gives the expression for the expected mean square error of estimating A_i by A_i :

$$\begin{aligned}
 E(A_T - A_T)^2 = & \left\{ \text{var}(c) \frac{1}{n^2} \cdot \sum_{i=1}^n \sum_{j=1}^n \exp \left(- \frac{||X_i - X_j||}{d_0} \right) \right. \\
 & - \frac{2}{n|\Omega|} \sum_{i=1}^n \int_{\Omega} \exp \left(- \frac{||X - X_i||}{d_0} \right) dx \\
 & + \frac{1}{|\Omega|^2} \int_{\Omega} \int_{\Omega} \exp \left(- \frac{||X - X'||}{d_0} \right) dx dx' \\
 & + \frac{1}{n(n-1)} \sum_{i=1}^n \left[\bar{C}(x_i) - \sum_{j=1}^n \bar{C}(x_j) \right]^2 \Bigg\} \\
 & \cdot \frac{1}{m} \sum_{\tau=-(m-1)}^{m-1} \left(1 - \frac{|\tau|}{m} \right) \exp(-|\tau|/\tau_0) + \frac{1}{nm} \sigma^2
 \end{aligned} \tag{4-23}$$

This procedure was demonstrated by applying these results to the EPRI SURE 1-hour SO_2 and 24-hour SO_4 data. The expected mean square error is modeled by Equation 4-22, using the fitted parameter values given in Table 4-7. The values of measurement error variance used are 0.18 c for hourly SO_2 , 0.084 c for 24-hour SO_4 , with c taken to be the average concentration over the region, 8.74 ppb for SO_2 and 7.98 $\mu\text{g}/\text{m}^3$ for SO_4 . Results were calculated for a square region 240 x 240 km with monitoring sites located in a rectangular grid. This area approximates the fine grid area of the combined experiments. These results are tabulated in Tables 4-9 and 4-10 for varying station configurations and averaging times.

TABLE 4-9

THE EXPECTED ROOT MEAN SQUARE ERROR (RMSE) OF ESTIMATING A SPATIAL MEAN OVER A 57,600 km² REGION, VARYING THE STATION SPACING

Number of Monitoring Stations Within the Region	Spacing of the Monitoring Stations (km)	Estimated 1-Hour SO ₂ (ppb)	RMSE 24-hour SO ₂ (µg/m ³)
4	120	4.4	1.1
9	80	2.6	0.70
16	60	1.9	0.51
25	48	1.4	0.40
64	20	0.8	0.23

TABLE 4-10

THE EXPECTED ROOT MEAN SQUARE ERROR (RMSE) OF ESTIMATING A SPATIAL MEAN OVER A 57,600 (240 x 240 km) km² REGION WITH A STATION SPACING OF 60 km, FOR INCREASED AVERAGING TIMES

Species	Averaging Time	RMSE
SO ₂	1 hour	1.9 ppb
SO ₂	24 hours	1.3
SO ₂	1 week	0.65
SO ₄	24 hours	0.51 (µg/m ³)
SO ₄	1 week	0.41

4.6 Implications for Experimental Design

An analysis of portions of the EPRI/SURE data base, consisting of hourly SO_2 and 24-hour sulfate concentration measurements throughout the eastern third of the United States, reveal that the spatial coherence of sulfate is much greater than SO_2 . Additionally, the monitoring station spacing required to confine interpolation uncertainties to less than half of the variance in the observations is less than 200 km for SO_2 and greater than approximately 600 km for sulfate. SO_2 data available indicate the existence of spatial concentration patterns of a scale intermediate to the Kincaid and SURE experiments. This limits the ability to specify a characteristic scale of measurement to guide selection of sample resolution.

As would be expected, increasing the averaging time of SO_2 concentration results in reduced variance in the measurements. However, even for 24-hour averaged concentrations, the spatial structure is characterized by rapidly decaying spatial correlation fields. Although the EPRI/SURE network was designed to detect "rural" SO_2 concentration patterns, the data analysis leads to a recommendation of greater spatial resolution for SO_2 monitoring than that characteristic of the SURE program.

The spatial "structure" of 24-hour sulfate concentration patterns appears fairly well determined with a spatial resolution of approximately 500 km.

The 24-hour average SO_2 and SO_4 concentration time series for two stations were compared using spectral methods. The SO_2 concentration time series were used as input signals to the acidic deposition generation processes, while the SO_4 concentration time series at a remote site sufficiently downwind of the sources were considered the output signal. The amplitude response in the SO_4 concentrations due to variations in SO_2 concentrations, as expressed by a gain function, was found to produce maximum responses in SO_4 for a three- to five-day variation in the input SO_2

concentration time series. However, the implications of this result are not straightforward with regard to an appropriate modulation frequency. The three- to five-day cycle is likely dominated by synoptic weather fluctuations. A more rigorous analysis of the input and output time series is warranted.

A methodology has been presented for determining the typical spatial representativeness of monitoring stations and estimating the average mean square errors of calculating spatially averaged concentrations from data collected at a monitoring network. This is useful for two purposes. First, it allows one to determine the spacing of the monitors so that the objective of the study can be met in a cost-effective manner. Second, once the network is operational, this method will provide improved estimates of the uncertainties associated with estimates of spatial means. The methodology was used to investigate the monitoring requirements of hourly SO_2 and 24-hour SO_4 , using data collected at 54 EPRI/SURE stations to estimate the parameters involved.

The application involves calculating the average RMS error associated with forming a spatial mean over a 240×240 km region (comparable in size to the Adirondacks area) by varying the density of monitoring stations within the region. The results of this analysis indicate that spatially representative RMS errors are greater for SO_2 than sulfate. The magnitude of the SO_2 errors range from less than 1 ppb with a 20 km resolution to approximately 4.4 ppb with a 120 km resolution. Sulfate RMS errors range from approximately $0.2 \mu\text{g}/\text{m}^3$ to about $1.1 \mu\text{g}/\text{m}^3$ with a similar decrease in spatial resolution, i.e., 20 km to 120 km.

These errors may be too large for the successful detection of the effects of source modulation. The number of time periods averaged together may be increased to reduce the errors, both by contiguous sampling periods and, if a

cyclic signal amplitude is anticipated, by forming noncontiguous composite samples of time periods matched by the phase of the modulation. This has implications for the duration of a modulation experiment since a longer experiment will allow for more data values to be averaged. Once the proposed monitoring network is operational, it will be important to refine the estimates of the correlational structure of the monitored pollutants using the new data in order to improve the above estimates of the monitoring uncertainty.

Considering planned elements of the combined experiments, the following can be stated:

1. Sulfate monitoring can be successfully performed with the sample resolution suggested in the COMPEX plan.
2. SO₂ sampling may or may not be successful in describing spatial variability. A data base for analysis of sample resolution is apparently not available.
3. Inert tracers, like SO₂ are primary pollutants and analyses presented did not provide information on required resolution.
4. Analyses of the spatial representativeness of spatial averages suggests that errors may be too high to successfully detect effects of local source modulation.

SECTION 5

MODEL SIMULATION ANALYSIS

The uncertainties associated with a multi-faceted large scale field experiment, such as the proposed COMPEX, may be condensed into a series of statements expressing the accuracy with which various signals can be isolated from background noise. In this context, the term "signal" is loosely defined, and may represent a concentration or deposition value at a specific receptor, or a sum, product, or other combination of several "signals," such as a deposition rate, or area averaged deposition.

Regardless of the type of signal under scrutiny, the underlying assumption of the proposed field experiment is that the particular signal is associated with a specific source, and this signal is embedded within fluctuating background noise. The noise is associated physically with pollutants or tracers from multiple sources. An additional component of noise arises due to measurement uncertainties. The monitoring network design (i.e., spatial and temporal sampling intervals, averaging times, etc.) introduces noise as well, but this noise is related to stochastic natural variability.

An air quality or acid deposition model provides a very useful tool for addressing certain aspects of the uncertainty issue, primarily the detectability of signals against background variability arising from multiple sources. The acceptability of model results depends on the number of degrees of freedom (i.e., complexity of modeled processes and spatial and temporal resolution) incorporated into the model and the validity of the model formulation. However, it is important to emphasize that despite the complexity and sophistication of a model, its skill is ultimately limited by the irresolvable, and inherently stochastic processes of nature.

The objective of the modeling analysis is to examine some of the key uncertainty issues associated with various components of the proposed COMPEX

study. These issues are related to the detectability of a particular signal embedded in background noise arising due to multiple signal sources. The detectability is influenced by the signal's magnitude in relation to the noise and the precision with which the signal can be measured.

Four major experimental components of the COMPEX are examined--two pertaining to regional tracer experiments and two pertaining to short range tracer experiments. The regional-scale experimental uncertainty issues include examining the required inert tracer (perfluorocarbon) emissions rates necessary for tracer detection over regional scales and the degree to which single source emissions characterize diffuse emissions from an entire source region. The short-range experimental uncertainty issues include examining the nature of the fluctuating signal and noise resulting from a local and mesoscale source modulation experiment, and examining the detectability of sulfur-34 deposition by measuring the difference of inert and reactive tracer fluxes across an array of receptors.

5.1 Modeling Approach

In order to investigate the uncertainties associated with field experiments proposed under the comprehensive field plan, a modified regional transport model is used to simulate pollutant concentration and deposition patterns resulting from hypothetical inert and reactive tracer releases. The model formulation is described by Durran et al. (1979) and Liu et al. (1982), and an analysis of model performance is described by Stewart et al. (1983 a, b). The model simulations are designed to investigate the detectability of perfluorocarbon tracers over regional scales, and the detectability of SF₆ and isotopic sulfur (³⁴S) emissions over local scales and mesoscales. Within this section are presented discussions on the model configuration, the

hypothetical tracer emission distribution, and the simulation plans for the long-range and local/mesoscale detectability analysis.

Modeling Region Configuration

The modeling domain chosen for these analyses is subdivided into three regions (Figure 5-1). An outer region encompasses much of the northeast defined on the basis of a preliminary version of the comprehensive field study plan. Surrounding the Adirondack Mountains of New York State is an additional fine-resolution grid.

The point sources displayed in Figure 5-1 represent 21 of the largest SO₂ point sources within the modeling region and a group of three point sources within New York State, which represent candidate sources for local/mesoscale tracer experiments. The point sources external to New York are grouped into three categories. Seven point sources (denoted hereafter as the "Ohio" emissions) are clustered within approximately 700 km of the Adirondack receptor region, a cluster of nine point sources (denoted as "Kentucky" emissions) are situated roughly 1300 km away from the receptor region, and the remaining five sources are situated off the Ohio River-upstate New York axis. The shaded symbols for point sources within each of the two source clusters represent the largest SO₂ emitters within their respective clusters. The cluster names "Ohio" and "Kentucky" are derived from the locations of these major point sources.

The SO₂ emissions associated with the 21 large point sources identified in Figure 5-1 represent 7.1 million tons per year, or 35 percent of the emissions within the full modeling region. Within the "Ohio" point source cluster, 2.4 million tons of SO₂ are emitted per year. This represents

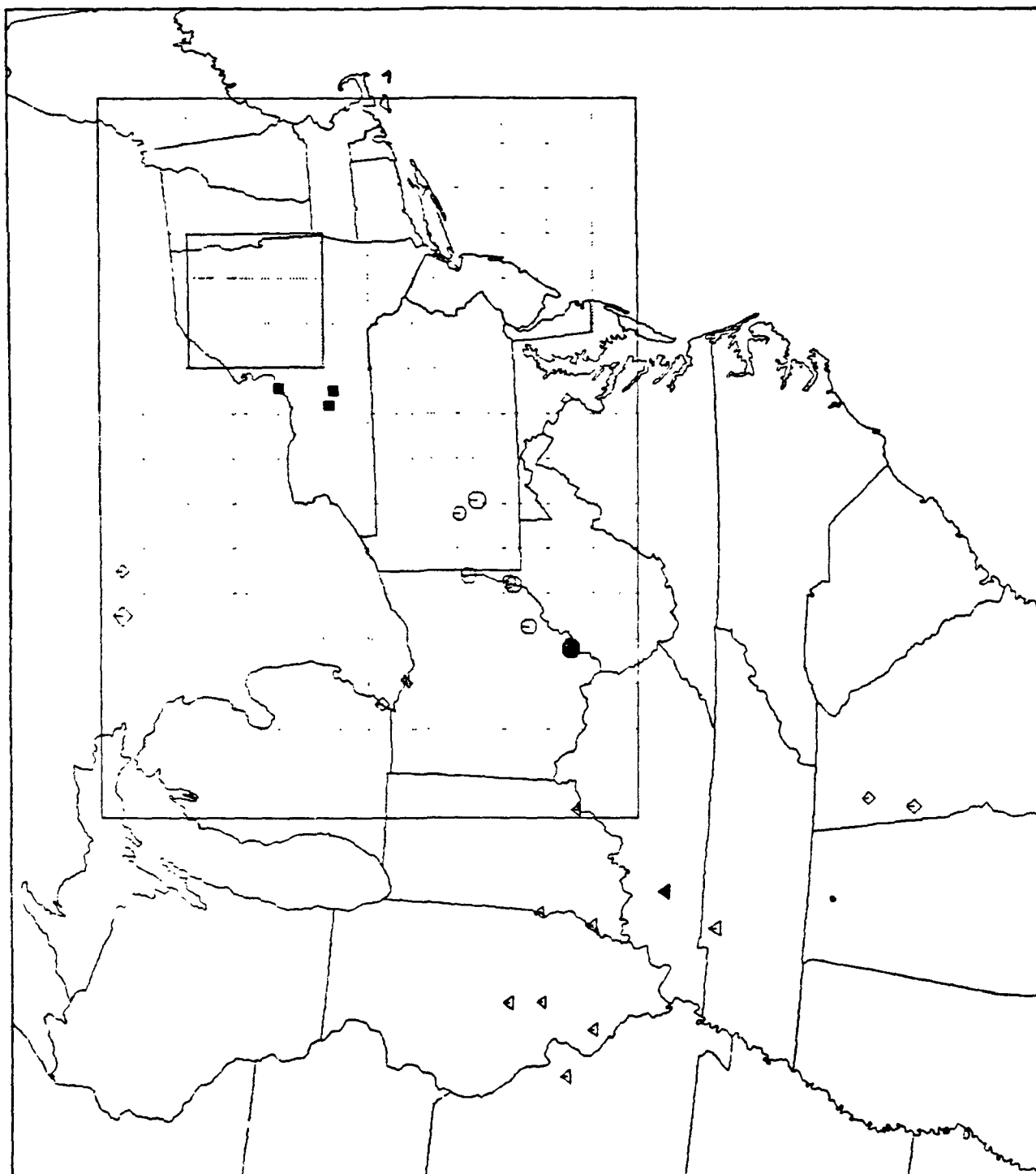


FIGURE 5-1. Illustration of the modeling domain showing the nested coarse-resolution grid region, the high-resolution grid region, and isolated point sources chosen for tracer detectability simulations.

about 75 percent of the total SO₂ emissions within the area encompassing the point source cluster. The largest point source in the "Ohio" cluster contributes 22 percent of the cluster's SO₂ emissions.

The area enclosing the "Kentucky" point source cluster emits roughly 3.6 million tons of SO₂ per year, of which 74 percent emanates from the cluster of 9 large point sources. The largest of this cluster emits 14 percent of the point source cluster's SO₂ emissions.

Processing of Model Simulation Results

Among the proposed experiments under the comprehensive field study plan are the release of tracers from major emission regions in the Midwest. At issue is the question of whether a single-point or a multiple-point tracer release provides the most information on pollutant transport between a specific emission region and the sensitive receptor. Also requiring investigation are the questions of what quantity of tracer and what release characteristics are necessary to ensure adequate detectability over regional scales.

To address these questions, the regional model is exercised in a Lagrangian mode over two one-month time spans (January and July, 1978). Output from the model consists of a time history of plume segment locations and ages, which can readily be combined with prescribed time varying tracer emission rates to produce time varying concentration predictions over an array of receptor locations (specifically, the coarse grid).

A similar plume segment location history pertaining to the three New York point sources is combined with specified SF₆ and ³⁴S emission rates to yield concentration histories over a series of high-resolution receptor coordinates situated within the Adirondack Region.

In addition to the Lagrangian simulations, the model is exercised over the entire modeling domain with a complete SO₂ emission inventory in order to examine the detectability of modulated SO₂ emissions from the three candidate New York point sources. Major point sources other than those illustrated in Figure 5-1 are treated in a manner consistent with routine application of the regional model. That is, their emissions are incorporated into the appropriate model layer (i.e., mixed layer or layer aloft) as determined by a plume rise algorithm. Minor point sources and area source emissions are incorporated within the mixed layer. SO₂ emissions from the 24 highlighted point sources undergo chemical transformation and wet and dry deposition consistent with the remaining SO₂ emissions treated within the grid framework. Deposition values from these sources and all others are accumulated within the appropriate coarse-resolution grid element.

The use of model simulation results in the analysis of uncertainty and detectability is illustrated in Figure 5-2. Enclosed within the thickline box are the specific analyses of perfluorocarbon detectability, modulated emission detectability, and uncertainties associated with mass balance calculations. Direct input to these analyses from the model simulation consist of concentration time series of SO₂, SO₄, SF₆, PFT, and ³⁴S over either the coarse grid or fine grid. These time series are generated from both the Lagrangian plume segment output and the full Eulerian model output. The time series pertaining to tracer concentrations are due either to continuous or modulated emission rates (1 day on, 2 days off). Similarly, the SO₂ and SO₄ time series due to the three New York point sources are modified by a selected modulation frequency.

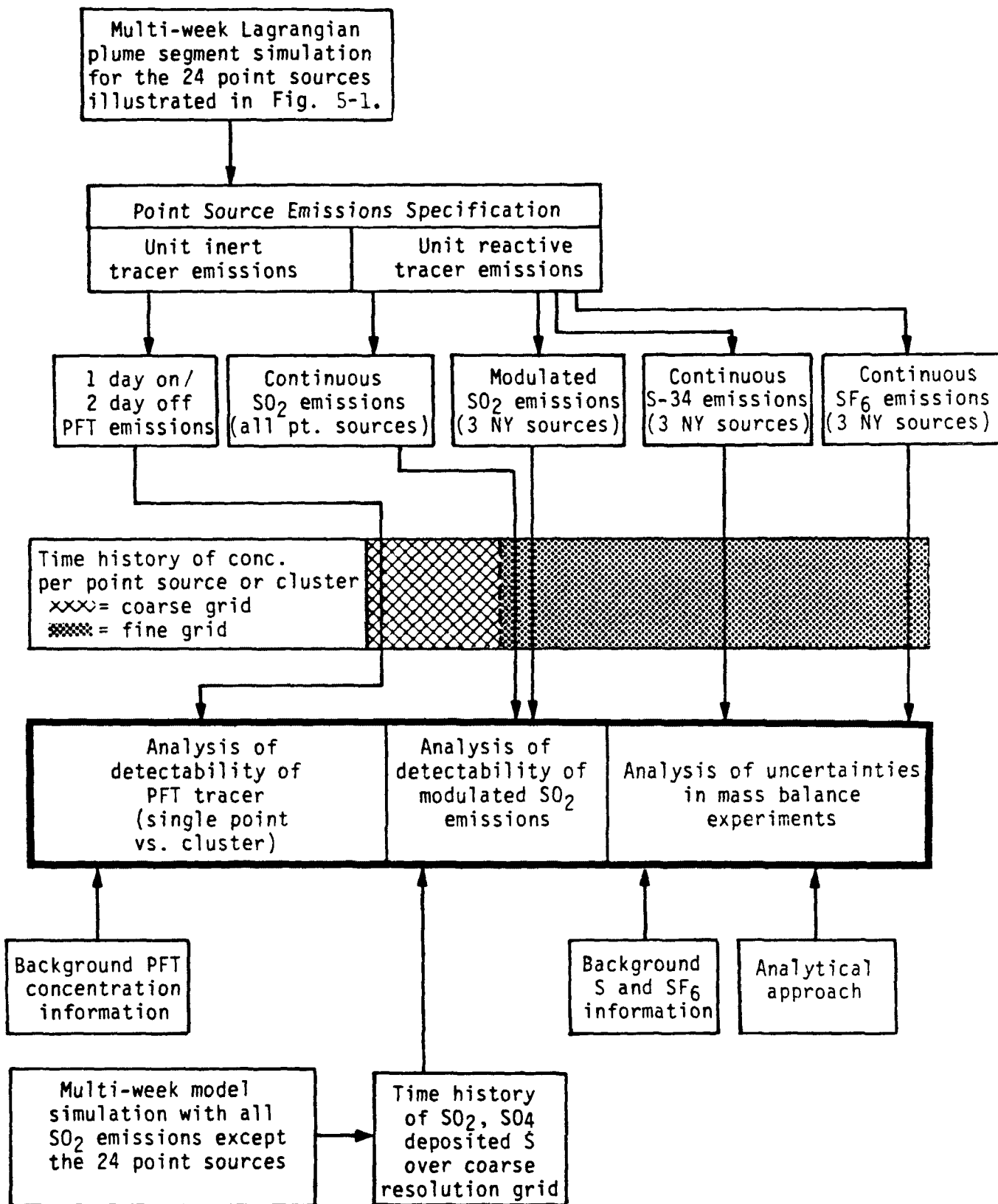


FIGURE 5-2. Diagram illustrating the use of model information and ancillary information in the analysis of detectability and uncertainties.

The ability to synthesize time series from model output relies on a linear superposition assumption, which is consistent with the transformation and deposition parameterization utilized within the model. While undoubtedly a simplification for SO_2 and SO_4 concentrations, the superposition assumption is valid for the inert tracer. The linearity assumption also permits the analysis of signal detectability directly from the statistics derived from the time series. Hence, minimal emission rates necessary to ensure a detectable signal are easily calculated.

Additional details on the procedures used to adapt modeling results to the analysis are presented in the following sections. Although the modeling analyses of long-range and short-range experiments have been performed using both the January and July simulations output, unless otherwise noted the results are discussed with reference to the July simulation only. During July 1978, the meteorological conditions resulted in a frequency of transport from the Midwest toward the Adirondack region that was slightly greater than in January. Hence, the frequency of detection of long-range tracer concentrations within the Adirondacks may represent slightly better than average conditions.

5.2 Uncertainties in Long-Range Experiments

Long-range tracer components of the combined experiments are designed to provide upper-bound estimates of pollutant impacts from major emissions sources, indicate the frequency of time that the receptor impacts are not attributable to the source region, and finally, provide the means by which deposition experiments are integrated into the source-receptor relationships. This section describes studies of uncertainty issues related to the long range component.

One aspect of uncertainty in the long range tracer experiments involves the determination of suitable tracer emission strengths to ensure a high frequency of detectability at selected monitoring sites over various transport conditions. Another issue related to detectability of tracer is that of tracer release strategies. The goal of the COMPEX experiment is to relate emissions from specific source regions to deposition over selected receptors. As pointed out by McNaughton and Bowne (1984), concentration patterns resulting from individual point source tracer releases may not be representative of those arising from a cluster of point sources. The larger spatial distribution of a cluster of tracer releases may require additional tracer quantities to produce the same frequency of detectability at a given monitoring station. Because of the increased logistics required from clustered tracer releases, a trade-off exists between various release strategies. While a comprehensive analysis of the cost-benefits of various strategies is beyond the scope of this study, an indication of the difference in concentration patterns resulting from single- and multiple-point releases and implications with regard to tracer quantity requirements are determined from a modeling exercise.

To investigate these aspects, normalized tracer concentration time series (i.e., χ/Q) are extracted on an hourly basis from an 80 km resolution model grid for the Adirondack receptor. The proposed PFT sampling duration is six hours. Accordingly, the time series were processed into non-overlapping six-hour average values. Both hourly and six-hour averages are analyzed to investigate detectability issues.

For each location in the coarse-grid region, the normalized concentration time histories are processed into a frequency distribution of χ/Q exceeding a given value as a function of that value, as illustrated in Figure 5-3a.

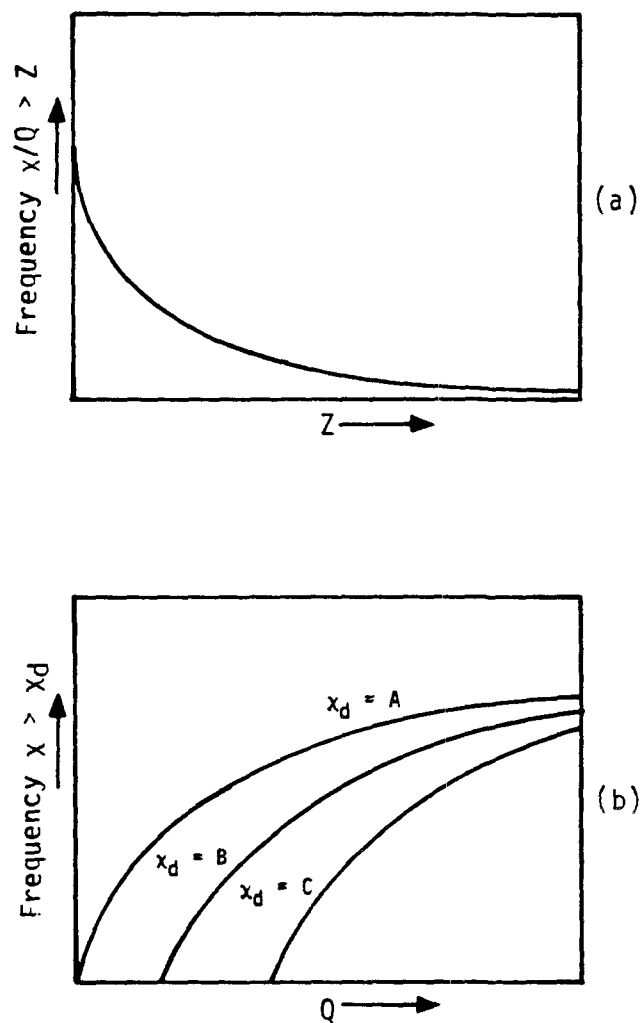


FIGURE 5-3. Schematic illustration of the frequency of exceedence of (a) the normalized concentration, x/Q , as a function Z , and (b) a detectable concentration, x_d , as a function of tracer emission strength, Q . In the illustration $A < B < C$.

From this distribution, the frequency with which the concentration exceeds a given detectable limit, χ_d is also calculated as a function of the tracer emission rate (Figure 5-3b). Plots of this type are used to estimate emission rates as a function of data recovery rate for time varying meteorological transport and dispersion conditions, and thus are a refinement over the steady-state dispersion method of estimating minimum emission rates.

Time series of PFT normalized concentrations resulting from a single point source and a cluster of sources over the entire coarse-resolution grid are processed in a similar fashion to determine the degree to which the signals compare. Additionally, the two sets of concentration patterns are compared via residual and correlation analyses to determine the representativeness of a single-point approximation to a clustered-release strategy. This analysis is performed for two clusters of point sources - those approximately 700 km and those approximately 1300 km away from the Adirondacks.

5.2.1 Estimation of Regional Tracer Release Rates

Figures 5-4 and 5-5 illustrate the frequency with which the relative tracer concentration (χ/Q) exceeds a given value, z , as a function of that value.* The frequency distributions, denoted $F(z)$, are displayed for the largest single sources in the clusters and the clusters of sources in "Ohio" and "Kentucky" both for one-hour average and six-hour average measurement times. Continuous tracer releases are assumed from all sources. The total tracer mass released from the single source equals the total mass released from the cluster. The concentration frequency represents the average of nine receptor sites in the Adirondack receptor region.

* The figure displays $F(z) = 1 - f(z)$, where $f(z)$ is the cumulative frequency distribution of z .

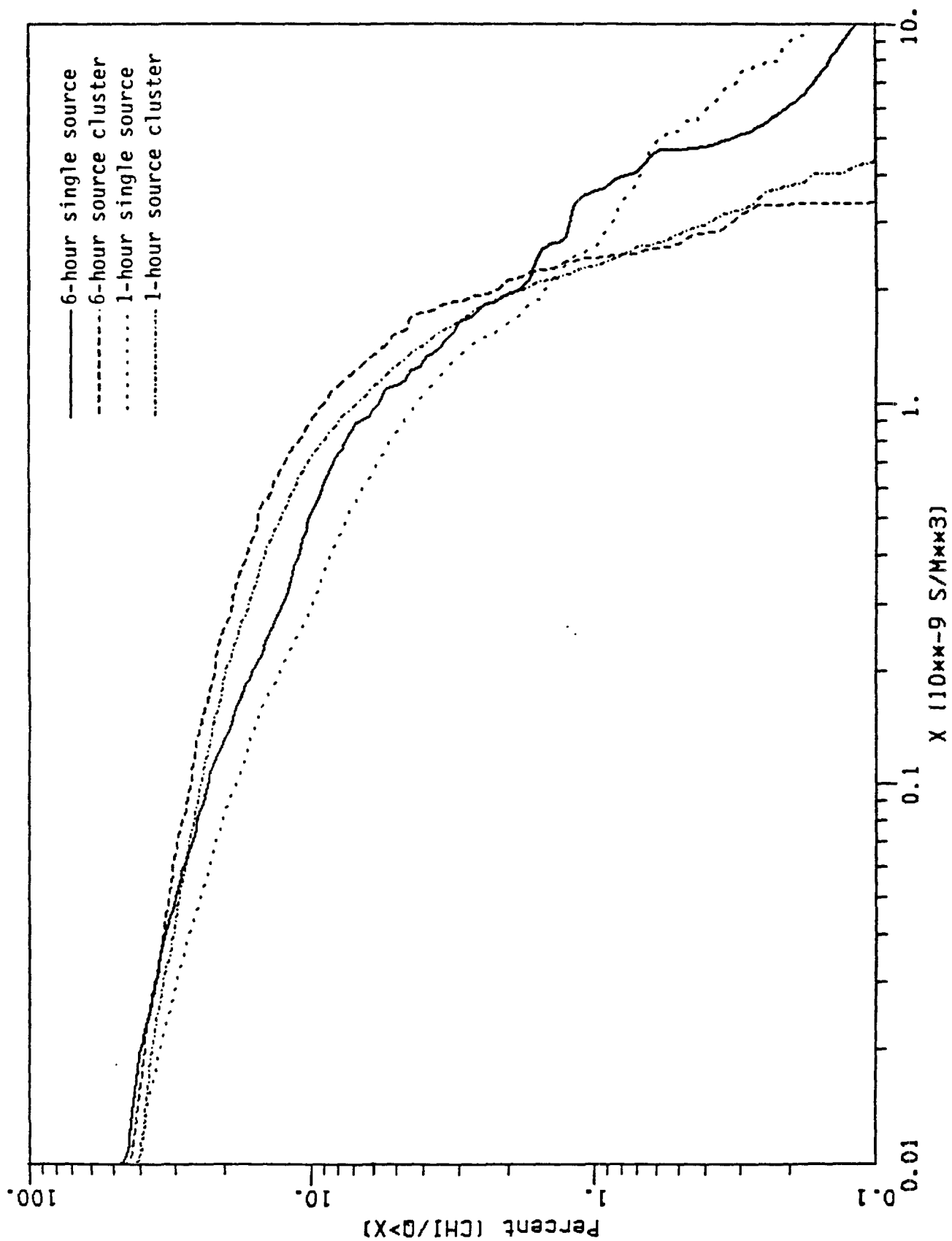


FIGURE 5-4. Distribution of x/Q from the "Ohio" single source and associated source cluster over all Adirondack receptor points.

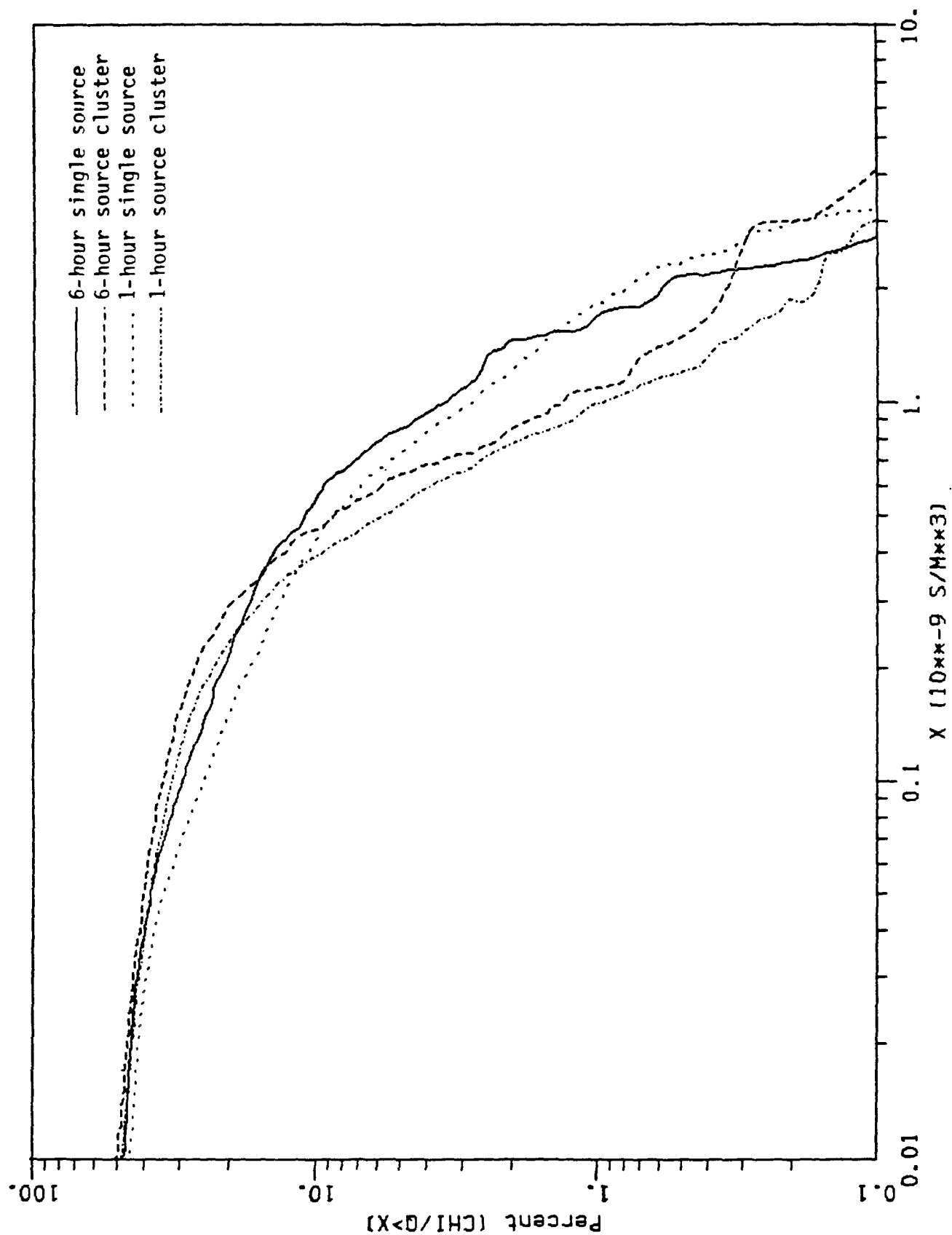


FIGURE 5-5. Distribution of x/Q from the "Kentucky" single source and associated cluster over all nine Adirondack receptor points.

Comparing the χ/Q frequency distributions arising from an "Ohio" clustered tracer release configuration to that from a single point release suggests that the more concentrated tracer pattern from the single source yields higher χ/Q values with a frequency of only 2 percent within the Adirondacks. A comparison of the "Kentucky" tracer impacts (Figure 5-5) suggests that a larger relative concentration impact from the single source occurs with a 20 percent frequency. This higher frequency is likely due to the more dispersed character of the "Kentucky" point source cluster relative to the "Ohio" cluster.

For both clustered and single source tracer releases from the "Ohio" region, only the highest 1 percent of hourly averaged χ/Q values exceed those produced from 6-hour averaging. For lower χ/Q values, the frequency of χ/Q exceedance is larger when concentrations are averaged over 6-hour periods. This result is qualitatively what one would expect from an intermittent but highly peaked time series. The temporal smoothing by six-hour averaging tends to increase the frequency of low χ/Q values by flattening the sharp concentration gradients at the "edge" of a concentrated plume. This smoothing also "clips" the peak concentrations, giving a lower frequency of exceeding the highest χ/Q values.

Figure 5-5 illustrates the 1-hour and 6-hour χ/Q exceedance frequencies for the single "Kentucky" point source and a cluster of nine sources. Although these point sources are nearly twice as far away from the receptor as the "Ohio" point source and associated source cluster, the frequency distributions show a similar 40-50 percent plume impact frequency for the month-long scenario. This is principally due to the well-organized large-scale transport episodes occurring during July 1978. The highest 1 percent of the χ/Q impacts from both the "Kentucky" point source and source cluster are predicted to be half the magnitude of the impacts from the single "Ohio" point source and source cluster.

The frequency of χ/Q values resulting from a modulated tracer release is compared with that resulting from continuous releases. The suggested release strategy of a one-day release followed by two days of no release is designed to conserve tracer and to assure detectability of discrete events so that an experiment of long duration is possible. Additionally, modulated emissions permit calculation of tracer transport times. Figure 5-6 illustrates the frequency exceeding values of χ/Q for continuous tracer releases versus modulated (i.e., 1-day on, 2-days off) releases from the "Ohio" and "Kentucky" clusters of point sources. As expected, the two-day period of no emissions reduces the frequency with which the Adirondack receptor is exposed to the entire range of χ/Q values. For high χ/Q values the frequency of exceedance is reduced by a factor of 6, whereas for low relative concentration impacts the reduction factor is about 3.5.

Frequency distributions of exceeding χ/Q can be transformed into diagrams of the frequency of tracer concentration detectability by determining, for each tracer emission rate (Q), the frequency with which χ exceeds χ_d , the detectable concentration. Because the exceeding χ/Q frequencies of 6-hour average concentrations are greater than the 1-hour values, results of the tracer detectability analysis are confined to the 6-hour average concentration impacts. Results also pertain to tracer emission released from the "Ohio" and "Kentucky" point source clusters rather than the single point sources.

Figures 5-7 and 5-8 illustrate the percentages of six-hour PMCP* concentrations that are detectable above a background concentration, χ_d , as a function of PMCP emission rate for the "Ohio" and "Kentucky" point source

*Two perfluorocarbon tracers are considered - PMCP and PMCH.

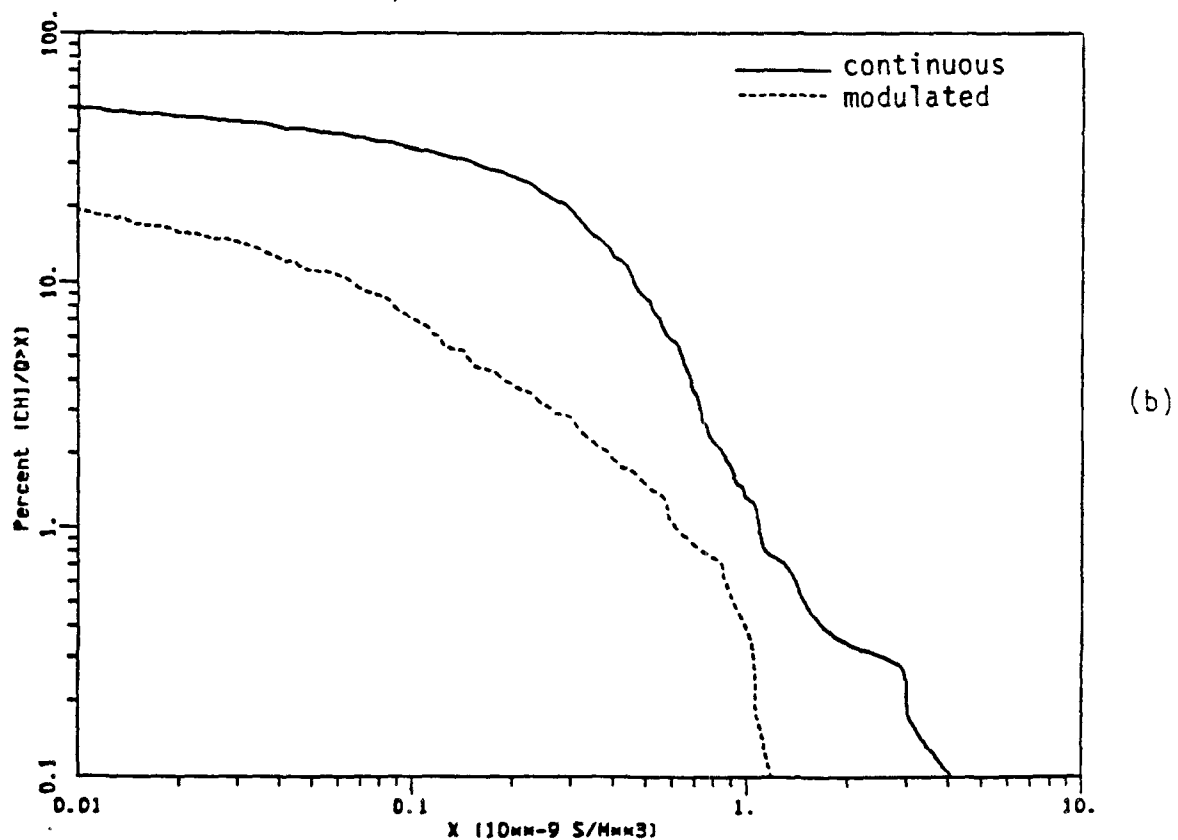
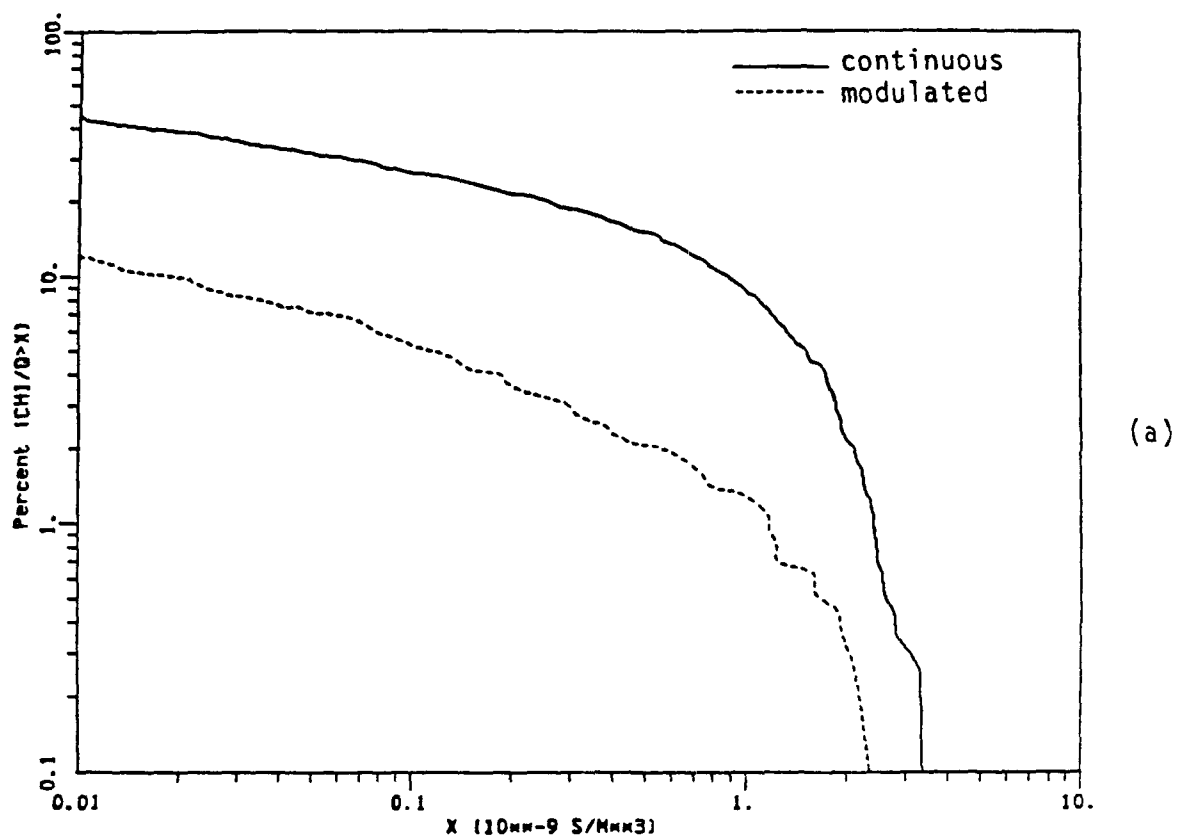


FIGURE 5-6. Distribution of x/Q for continuous and modulated (one day on, two days off) tracer emissions for (a) the "Ohio" cluster of point sources and (b) the "Kentucky" cluster of point sources.

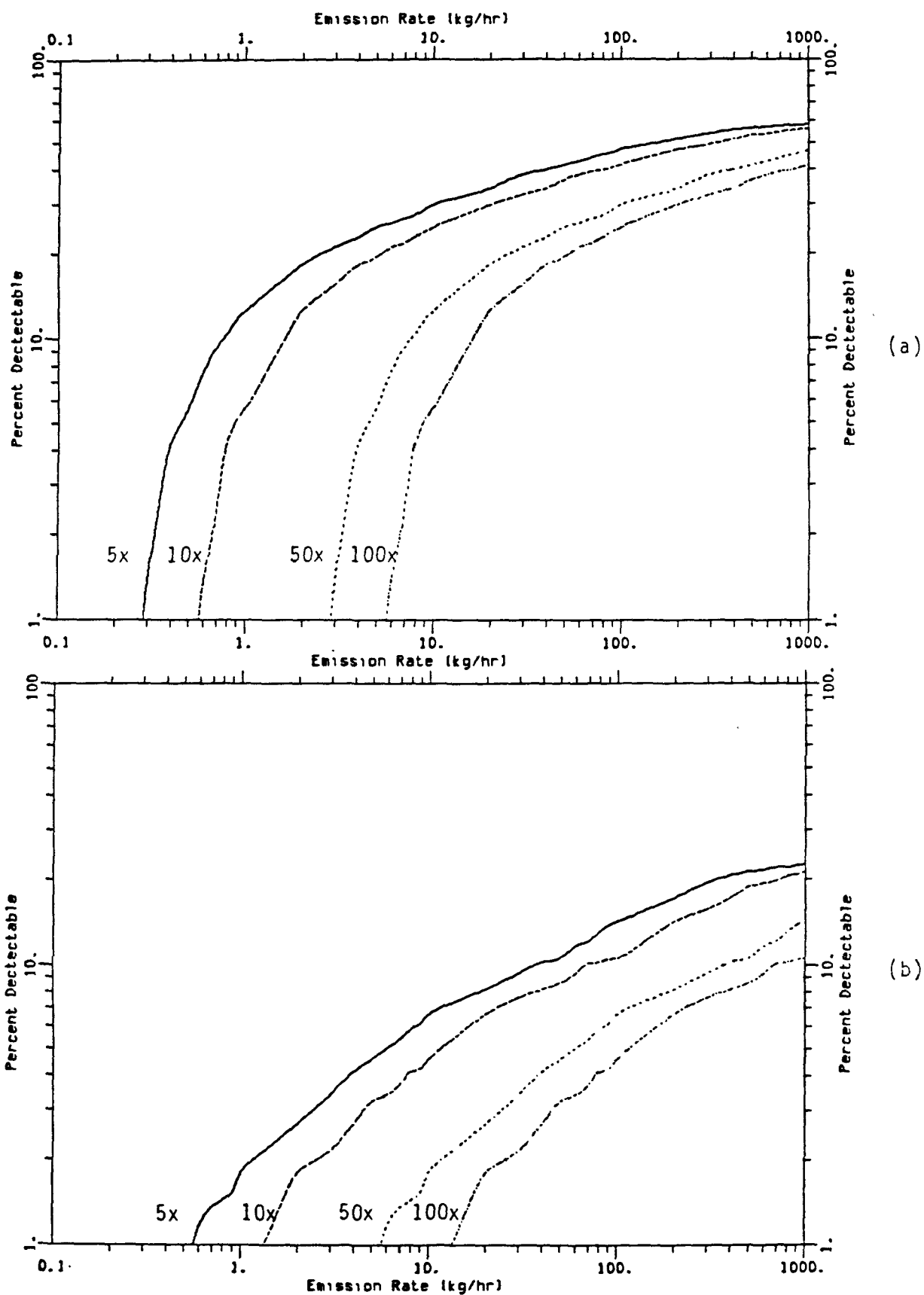


FIGURE 5-7. Detectability of 6-hour PMCP concentrations over the Adirondacks as a function of (a) continuous and (b) modulated tracer emission rates from the "Ohio" cluster of point sources.

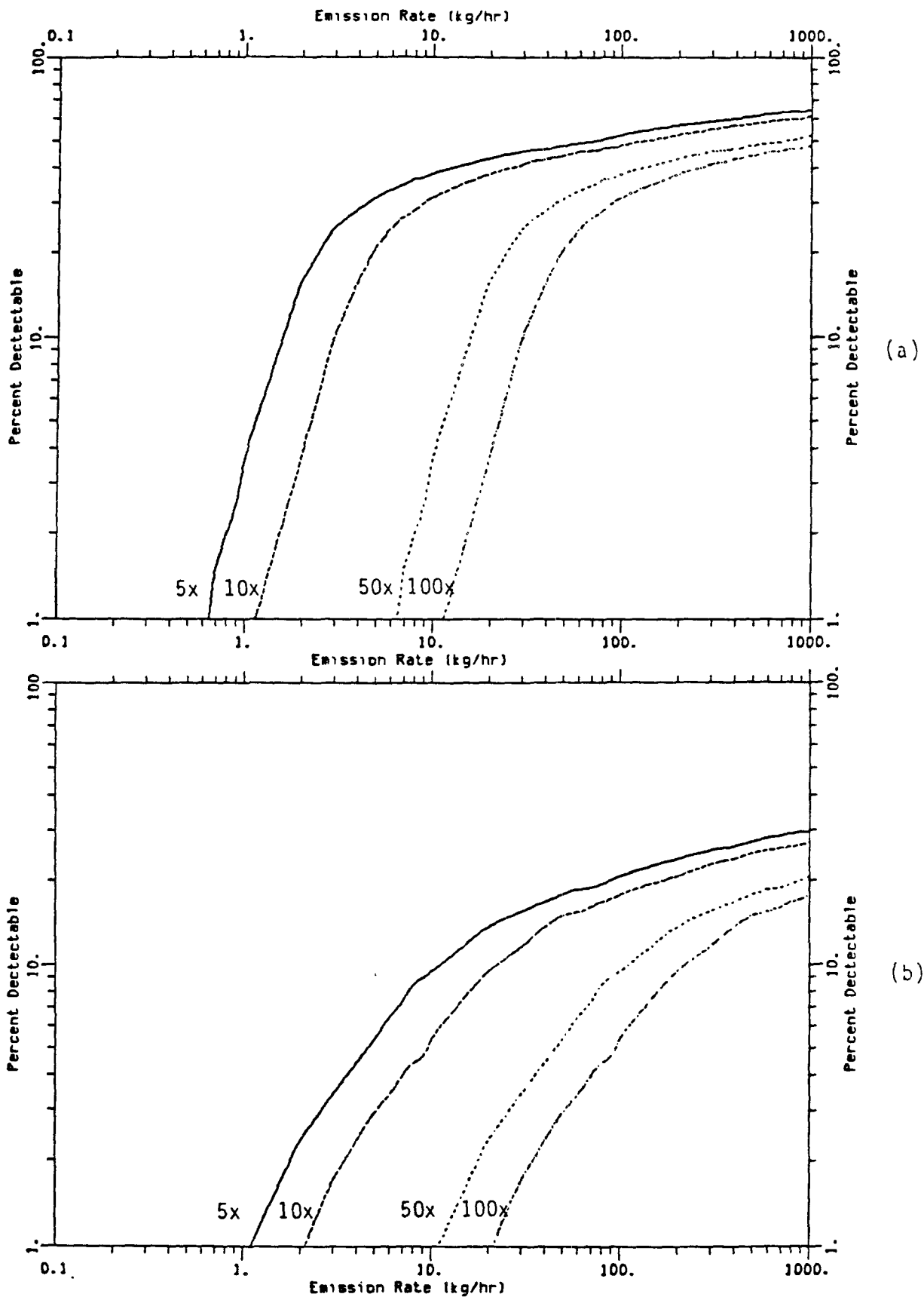


FIGURE 5-8. Detectability of 6-hour PMCP concentrations over the Adirondacks as a function of (a) continuous and (b) modulated tracer emission rates from the "Kentucky" cluster of point sources.

clusters. Part (a) of the figure illustrates to a continuous emission strategy, whereas part (b) refers to a modulated release strategy. Shown in the figure are four distribution functions pertaining to detectable PMCP concentrations (χ_d) of 5, 10, 50, and 100 times background concentrations (2.7 fl/l).

With continuous tracer emission rates, the two figures suggest that there are two distinct detectability regimes per unit emission increase. For example, for the "Ohio" cluster emissions, a doubling of the detectable concentration frequency accompanies a doubling of tracer emissions for detectability frequencies of less than 10 percent. For detectability frequencies exceeding 20 percent, a 15-fold increase in emissions is required to double the frequency of tracer concentration detection. For a tracer experiment focusing on the more distant "Kentucky" source region, the largest gain in detectability per unit emissions increase occurs at detection frequencies below approximately 20 percent. These results therefore imply that an upper bound on recommended tracer emission rates exists for the continuous tracer release strategy.

For a modulated tracer release strategy, the gain in frequency of detection per unit of emission increase is far lower throughout the range of emission release rates, averaging for the "Ohio" tracer experiment about the five- to 10-fold increase in emission for a doubling of detection frequency.

Figures 5-9 and 5-10 illustrate the frequency of PMCH concentration detection as a function of emission rates for the "Ohio" and "Kentucky" point source clusters, respectively.* These figures likewise illustrate the lower frequency of detection per unit of tracer emission under a modulated release strategy, as compared with a continuous release strategy.

*The background concentration of PMCH is assumed equal to 3.6 fl/l.

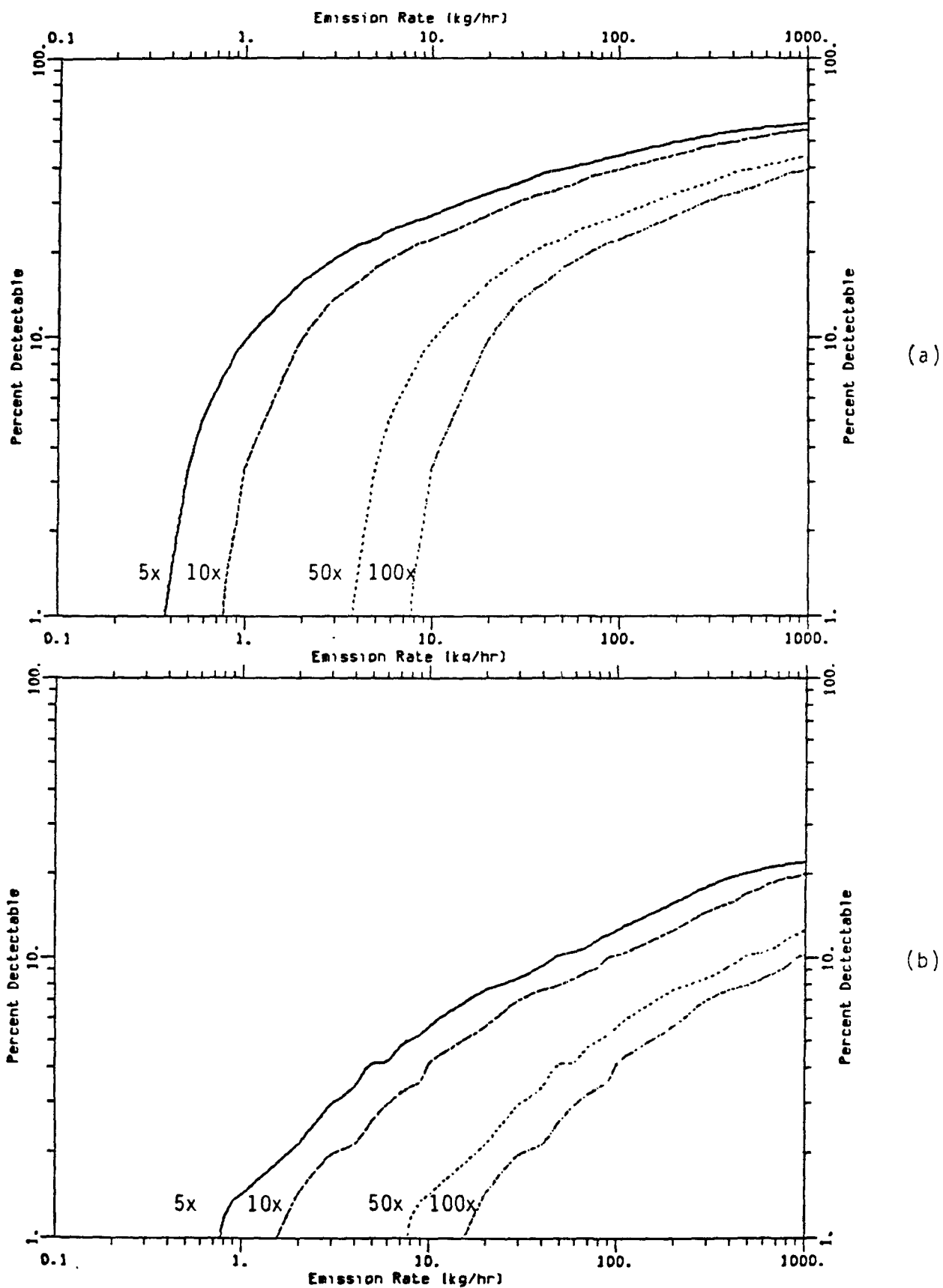


FIGURE 5-9. Detectability of 6-hour PMCH concentrations over the Adirondacks as a function of (a) continuous and (b) modulated emission rates from the "Ohio" cluster of point sources.

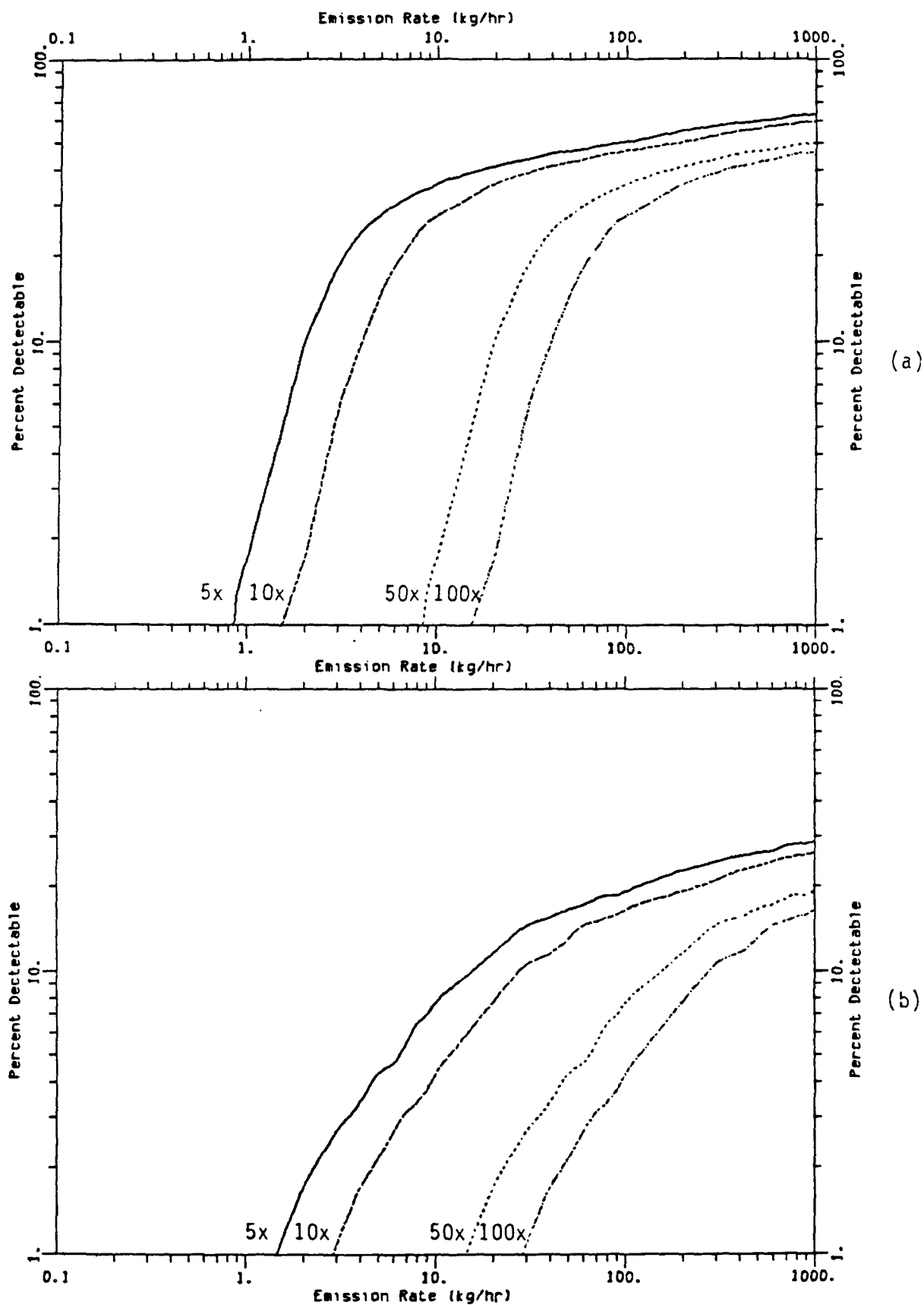


FIGURE 5-10. Detectability of 6-hour PMCH concentrations over the Adirondacks as a function of (a) continuous and (b) modulated emission rates from the "Kentucky" cluster of point sources.

Figures such as these should provide useful guides for selecting appropriate emission rates for planning a long-range tracer study. Selecting an appropriate release strategy (continuous versus modulated) requires a careful analysis of the gain in information resulting from a modulated release since the required tracer amounts increase rapidly with increasing demands on the desired frequency of detectable concentration.

It should be emphasized that the tracer detection frequencies discussed in this section are derived from a one-month model simulation characterized by several episodes of fairly well organized transport from the Ohio River valley region toward the Adirondack receptor region. Before a long-term (i.e., year-long) tracer experiment is designed, the simulation should be extended to cover longer periods of time so that more representative detection frequencies can be deduced.

5.2.2 Tracer Release Configuration

The frequency distribution of χ/Q presented in the previous subsection indicates that the Adirondack receptor region would receive more frequent low and moderate concentration impacts and less frequent high impacts when the tracer is released in the clustered configuration than when released from a single point source. The χ/Q frequency distributions also show that when the tracer is released in a modulated fashion, concentration impacts of all magnitudes are less frequent than when released in a continuous fashion.

This section examines whether the release configuration affects the spatial signature of the relative concentration, particularly over the Adirondack region. If the spatial pattern of inert concentration impacts differs widely between the cluster and single-source emission configurations,

a single-source release will not provide sufficient information to characterize the dispersion of the entire emission region.

Figures 5-11 through 5-13 illustrate the distributions of, respectively, the monthly mean χ/Q , χ/Q bias, and χ/Q correlation coefficients pertaining to continuous tracer emissions from the "Ohio" source region. The χ/Q bias is defined as the relative concentration from a clustered release configuration minus the relative concentration from a single point source emission. Locations of the cluster of point sources and the individual point source are indicated.

Figure 5-11 indicates that central Pennsylvania receives the greatest impact of monthly mean tracer concentration resulting from a clustered release. Within the Adirondack receptor region, a northwest-to-southwest factor of 6 gradient of concentration impact occurs. With an identical mass of tracer released continuously from a single source in southern Ohio, the relative concentration impact in the southern portion of the Adirondacks is about 25 percent lower than the impacts arising from a clustered release configuration (Figure 5-12). In the northern portion of the Adirondacks, the effects of tracer release configuration are smaller. Correlating the one-hour relative concentration impacts arising from the clustered release and those from the single point release indicates that the single point release is a rather poor surrogate for multiple point source emissions (in Figure 5-12, the correlation coefficient across the Adirondacks is roughly 0.4).

Considering next the distinction between concentration signals received from multiple point and single point emissions from a greater upwind distance (i.e., the "Kentucky" emissions), Figures 5-14 through 5-16 illustrate a similar lack of agreement. The χ/Q bias across the Adirondacks ranges from approximately +40 percent to -40 percent (Figure 5-15), whereas the

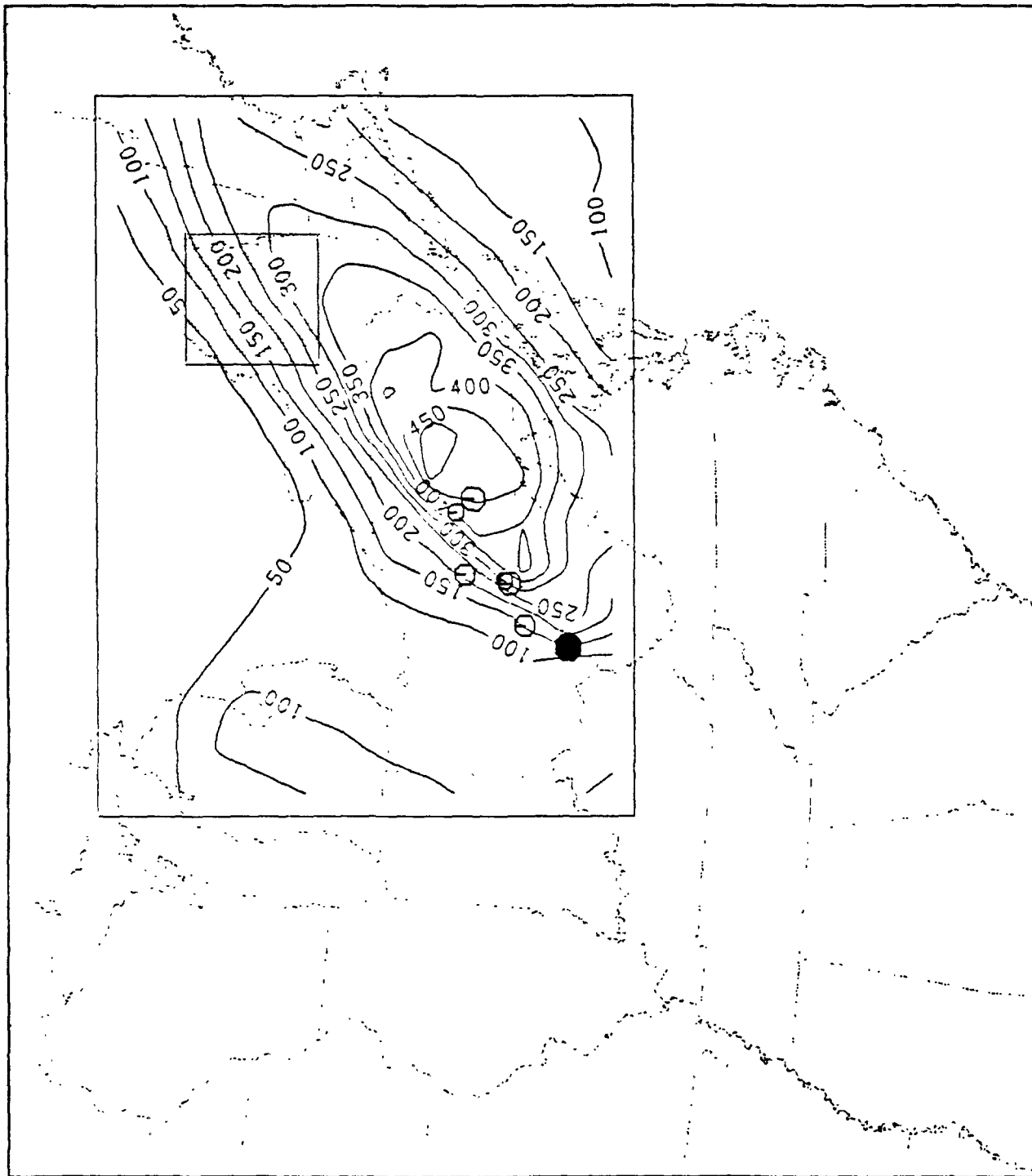


FIGURE 5-11. Geographic distribution of monthly mean x/Q resulting from a continuous tracer release from the "Ohio" cluster of point sources. (Units are 10^{-12} s/m^3)



FIGURE 5-12. Geographic distribution of x/η bias (cluster release minus major point source release) resulting from a continuous tracer release from the "Ohio" emission region (Units are 10^{-12} s/m³)

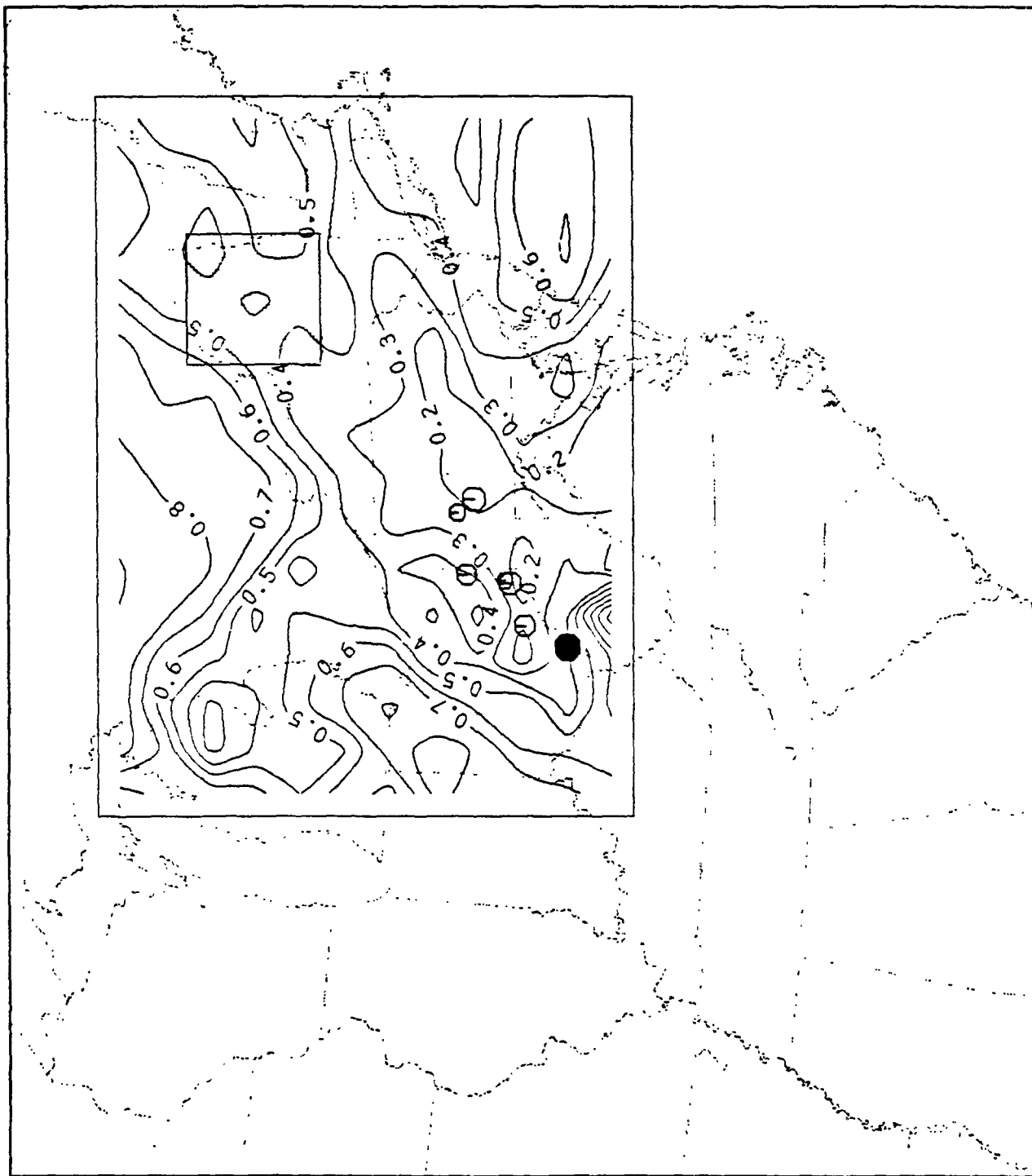


FIGURE 5-13. Geographic distribution of x/Q correlation coefficient between the "Ohio" cluster and single major point source emission for a continuous tracer release.

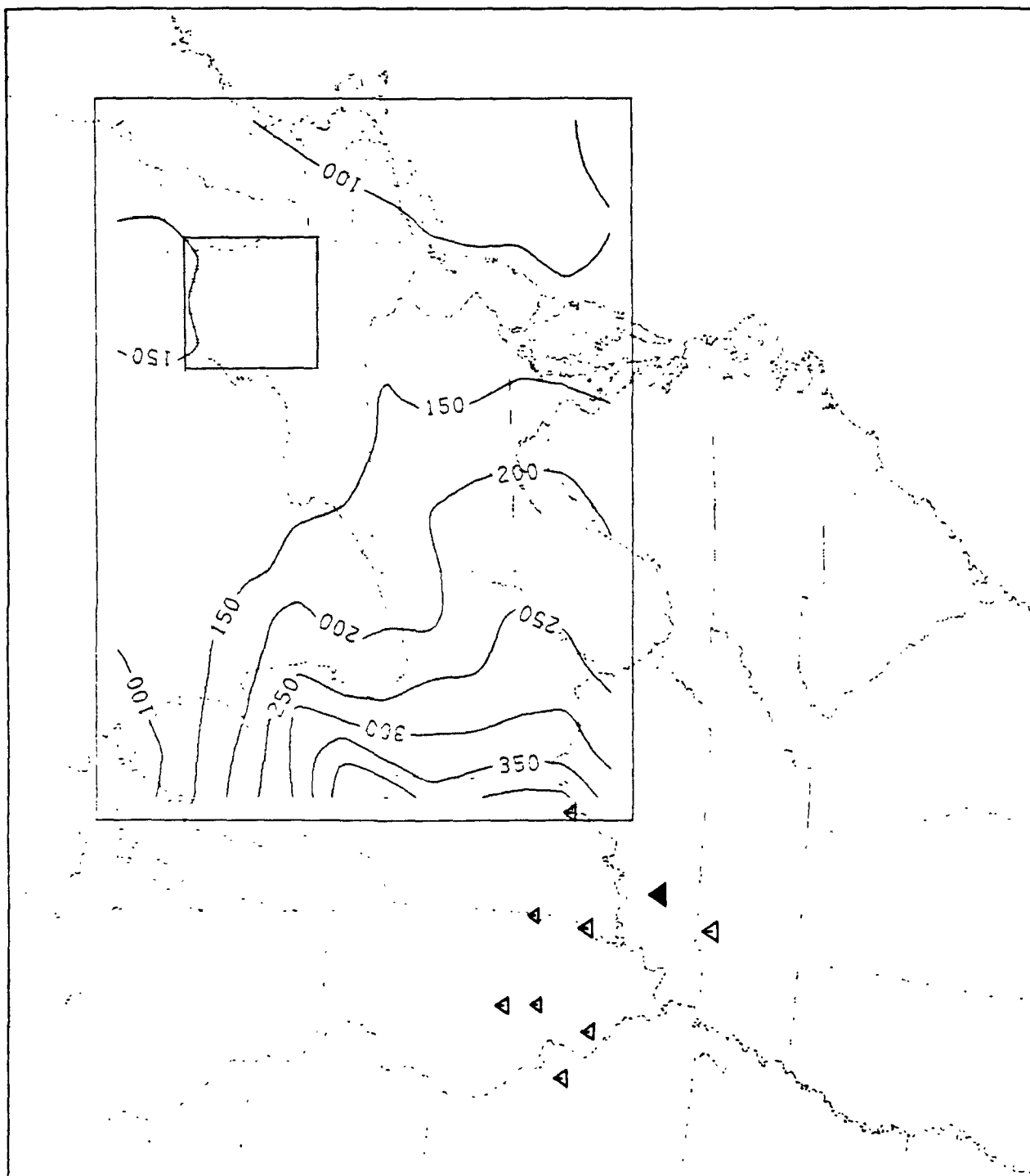


FIGURE 5-14. Geographic distribution of monthly mean x/q resulting from a continuous tracer release from the "Kentucky" cluster of point sources. (Units are 10^{-12} s/m^3)

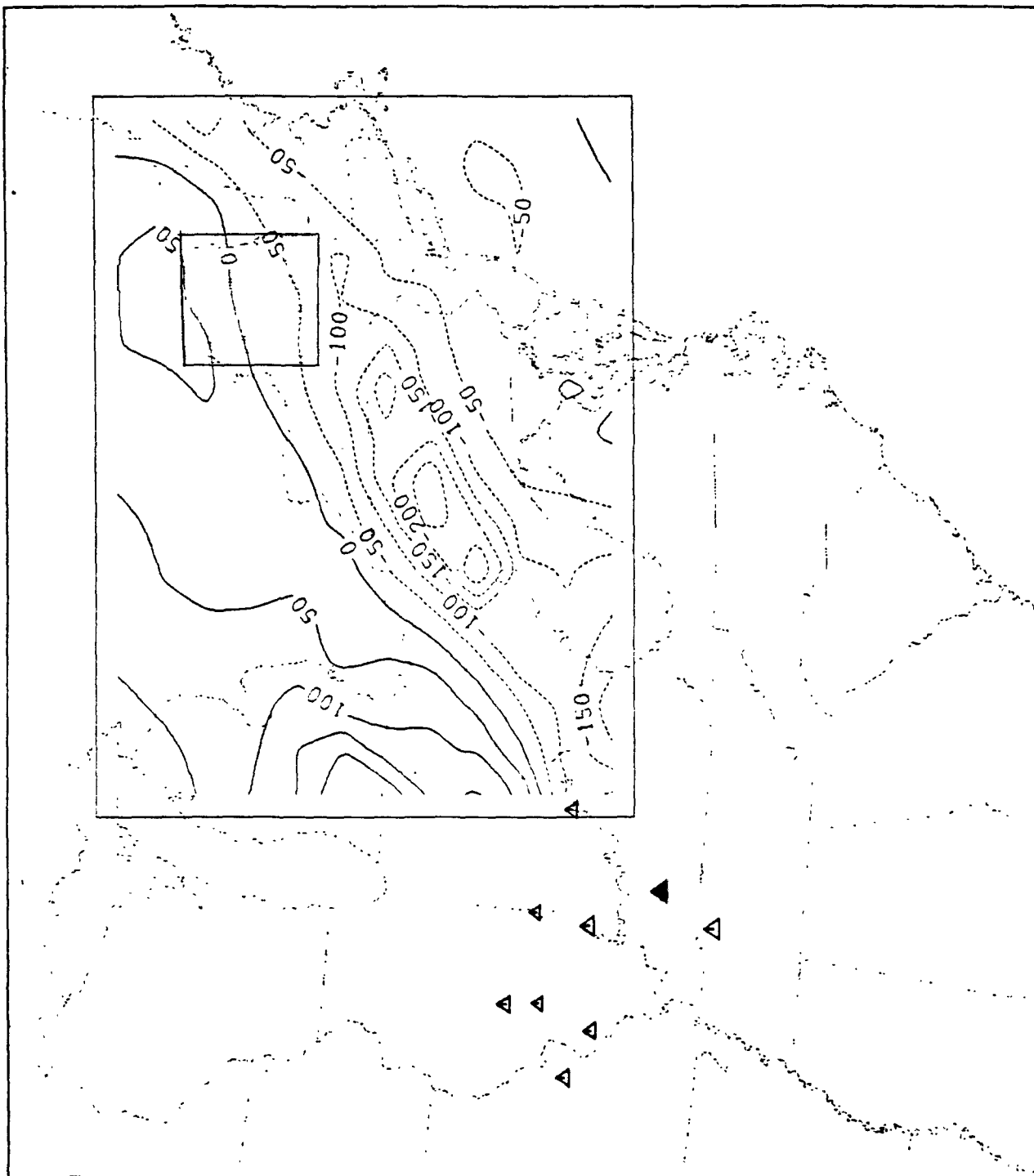


FIGURE 5-15. Geographic distribution of x/Q bias (cluster release minus major point source release) resulting from a continuous release from the "Kentucky" emission region. (Units are 10^{-12} s/m³)

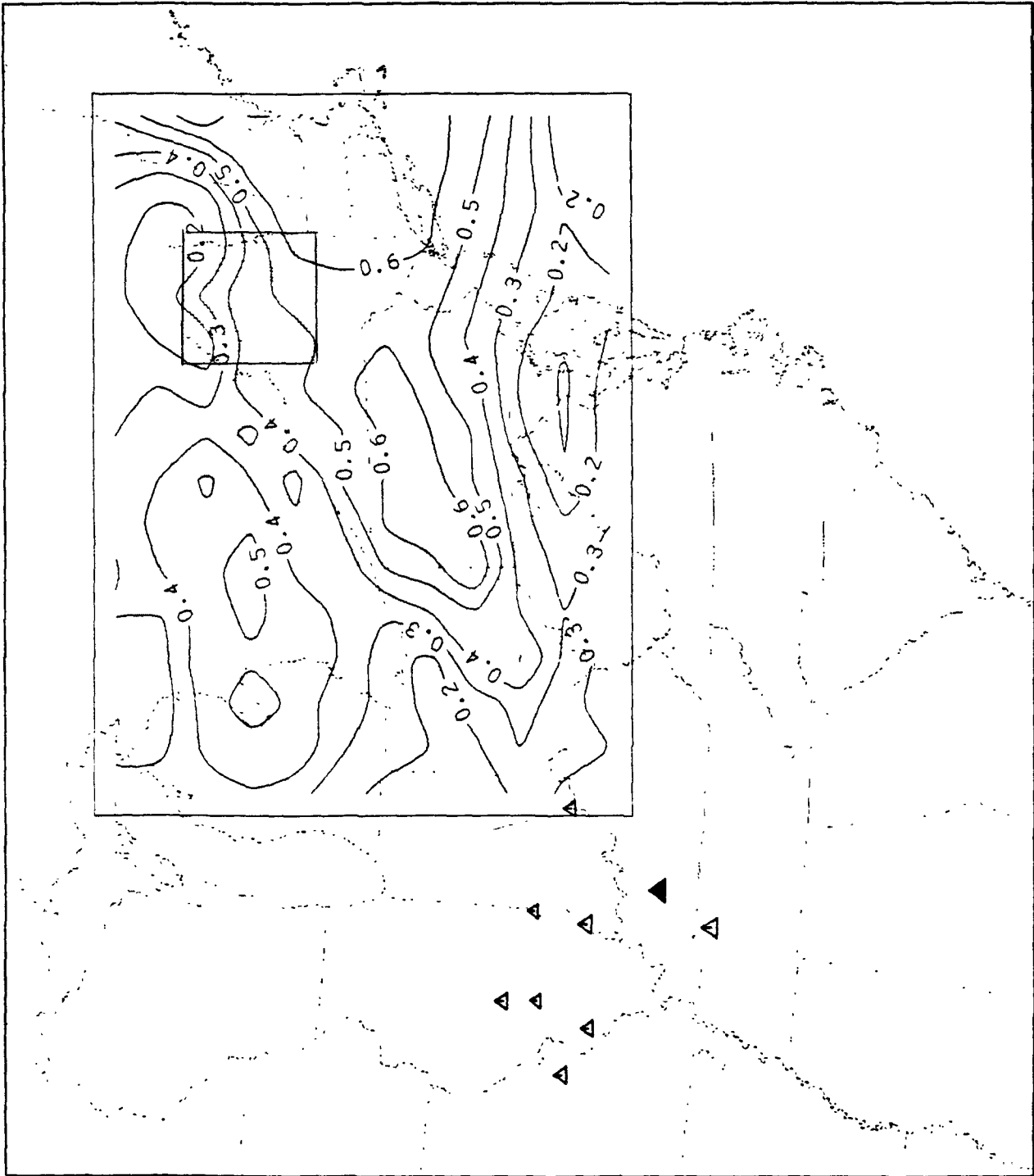


FIGURE 5-16. Geographic distribution of x/Q correlation coefficient between the "Kentucky" cluster and single major point source emission for a continuous tracer release.

correlation coefficient (Figure 5-16) averages about 0.4. The similar lack of agreement resulting from the more remote emissions is probably due to the greater angular spread of the point source cluster characteristic of the "Kentucky" emissions.

A similar analysis of tracer concentrations signals resulting from modulated emissions (one day on, two days off) was performed. Figures 5-17 through 5-19 illustrate the distributions of, respectively, monthly χ/Q mean, bias, and correlation coefficients pertaining to the modulated "Ohio" tracer emissions. With the modulated tracer release strategy, the monthly mean concentration over the Adirondacks has decreased by roughly a factor of 3. After normalization by the mean χ/Q , the bias is similar in magnitude to the continuous emissions case, whereas the correlation coefficient has fallen to approximately 0.2, despite the strong on-off nature of the emissions signal. The emissions from the more remote source region also result in largely different concentration signals depending on tracer release configuration.

From these results it appears as if single point tracer release experiments will not adequately represent the transport and dispersion associated with area-distributed emissions. While the limited simulation time may be a factor in influencing the statistics of the signals, the transport scenarios in July 1978 were favorable for strong tracer signal transmittance between the "Ohio" and "Kentucky" emission regions and the Adirondacks receptor region. Therefore, this simulation should represent a rather stringent test of alternative tracer release configurations. The analysis of this month-long simulation should be supplemented with additional simulation time to confirm the results before a final decision is made regarding tracer release strategies.

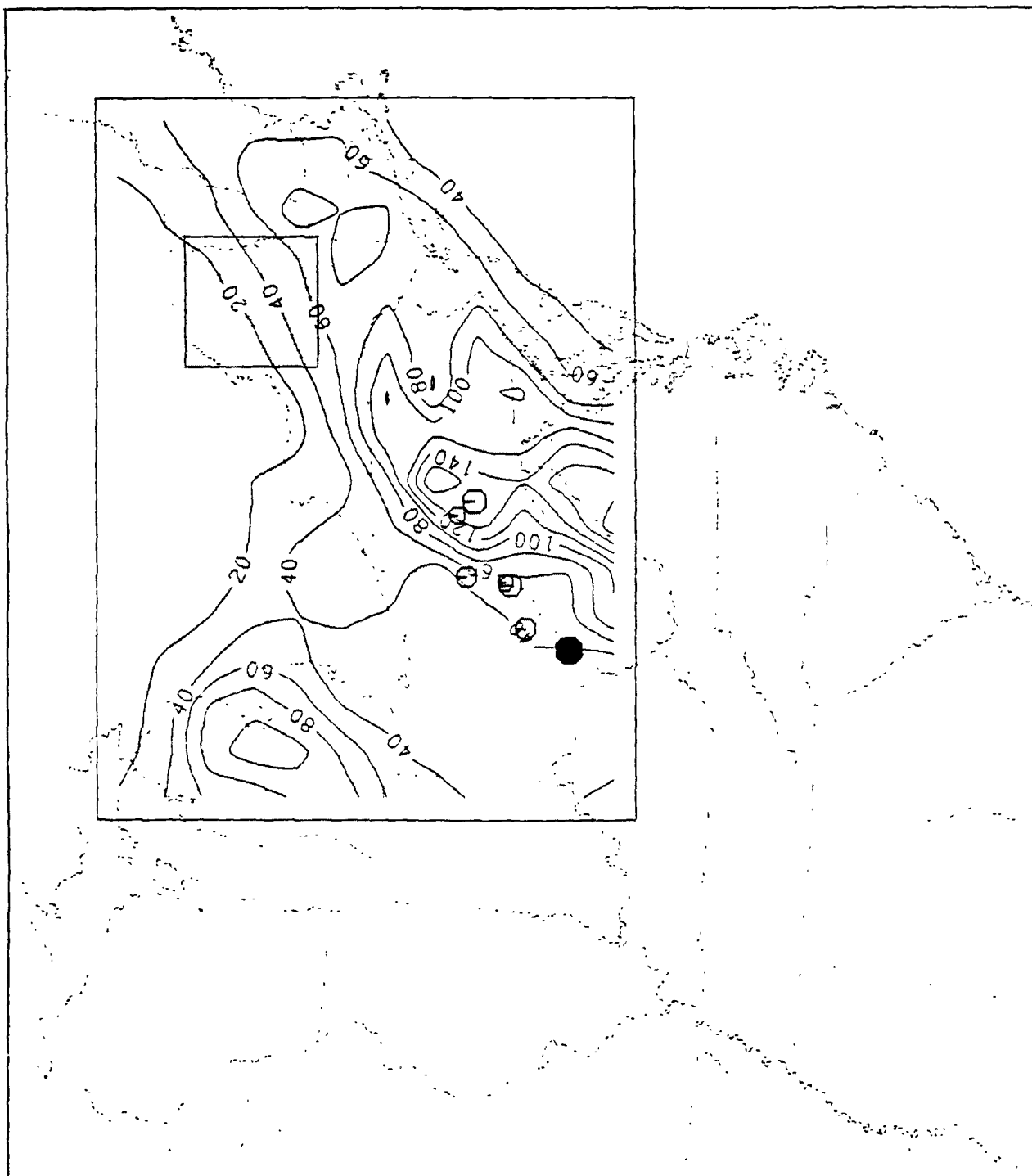


FIGURE 5-17. Geographic distribution of monthly mean X/Q resulting from a modulated tracer release from the "Ohio" cluster of point sources, (Units are 10^{-12} s/m³)

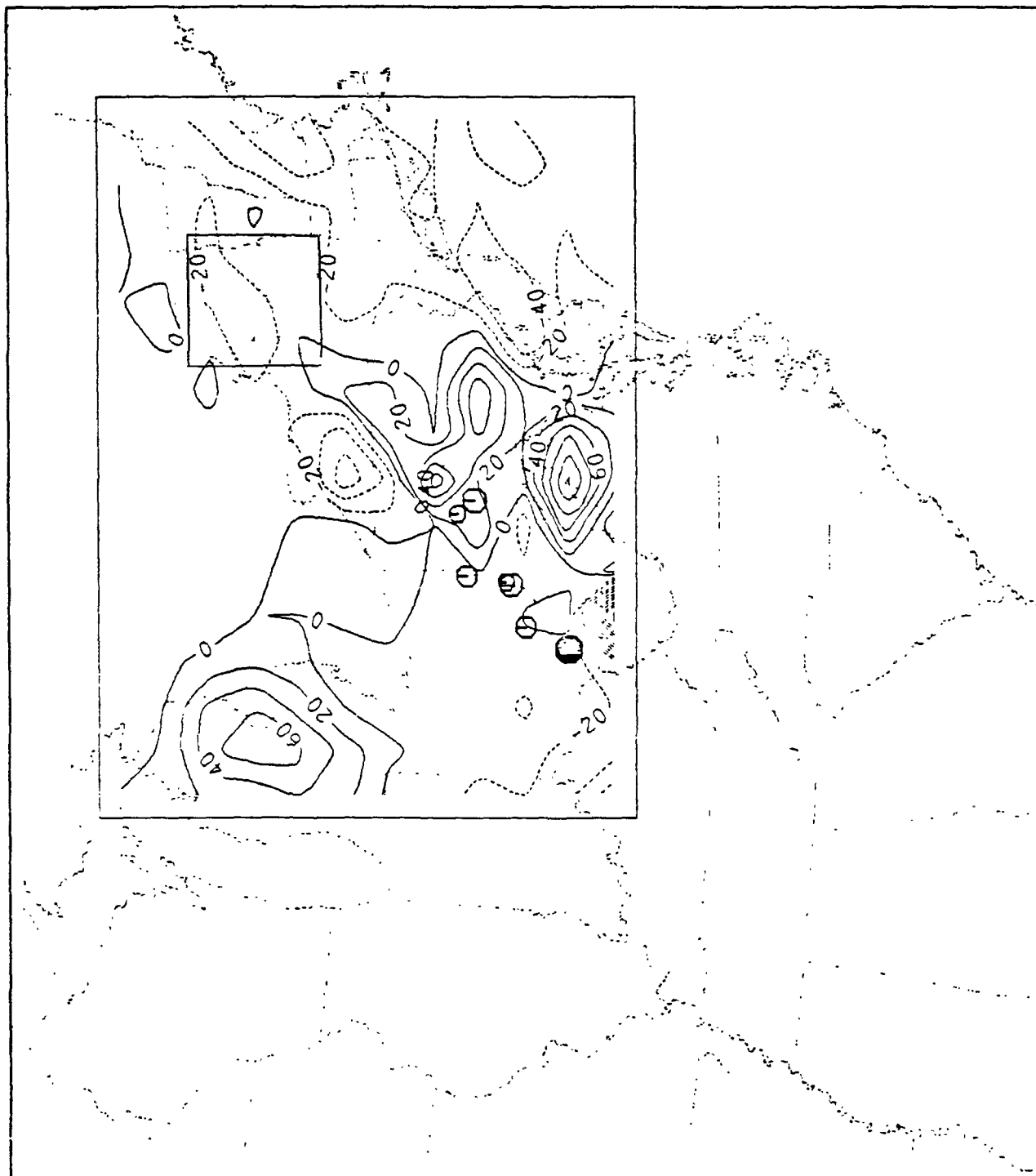


FIGURE 5-18. Geographic distribution of x/Q bias (cluster release minus major point source release) resulting from a modulated tracer release from the "Ohio" emission region. (Units are 10^{-12} s/m³)

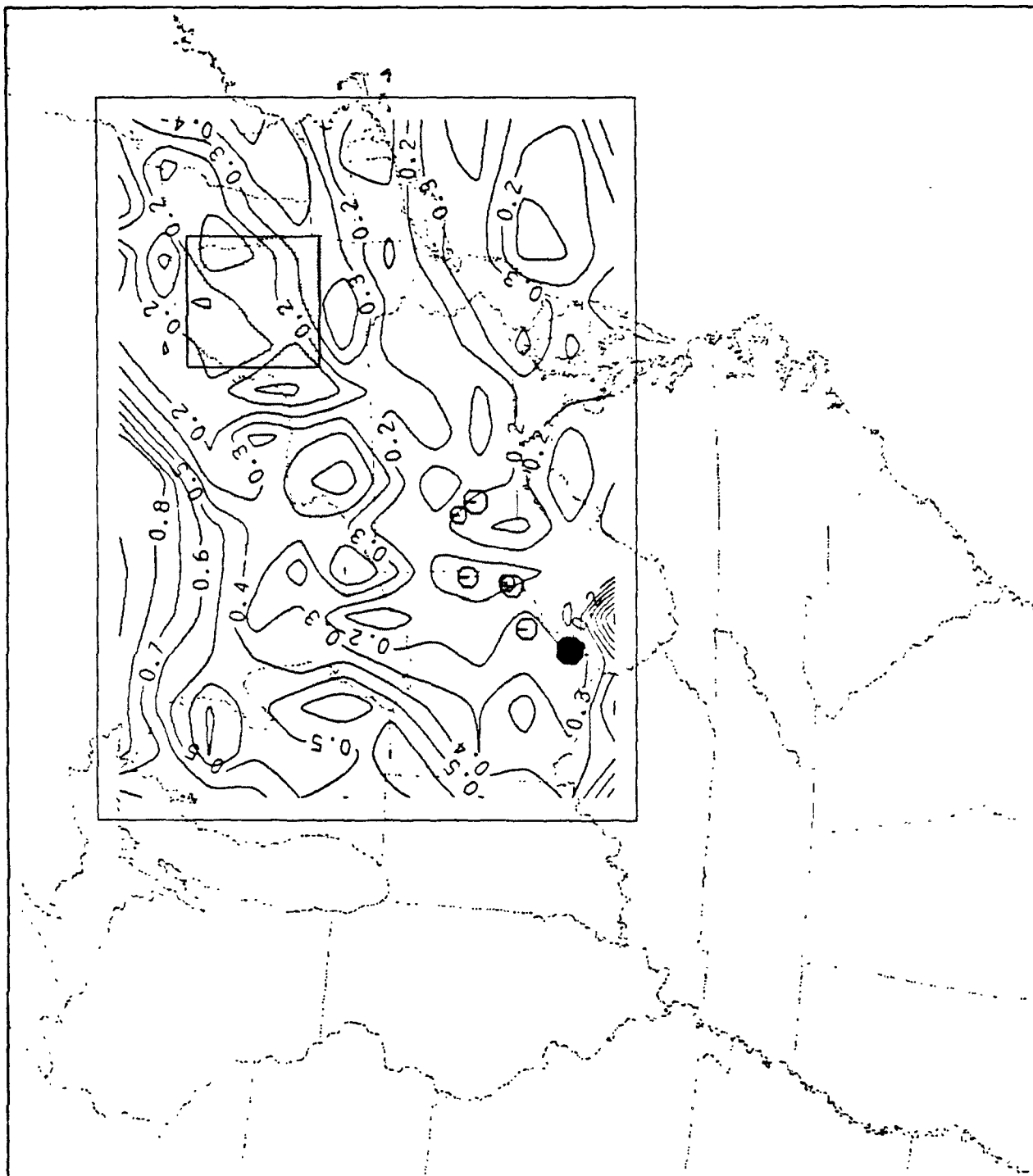


FIGURE 5-19. Geographic distribution of x/Q correlation coefficient between the "Ohio" cluster and single major point source emission for a modulated tracer release.

5.3 Uncertainties in Short-Range Experiments

The COMPEX design requires short-range experiments of two types. The first type is emission modulation experiments performed to isolate the concentration and deposition contributions from point sources situated within the mesoscale distances (less than 200 to 300 km from the Adirondack receptor region). The second type will investigate the sulfur deposition losses over a variety of surface and meteorological conditions.

Within the scope of this study it is only possible to examine a few of the key uncertainty issues associated with the design. The next two subsections focus on the issues of signal detectability for both source modulation and reactive tracer (^{34}S) experiments.

5.3.1 Local Source Modulation Experiments

The primary objective of a source modulation experiment is to evaluate the hypothesis that reductions in ambient sulfur oxide concentrations and deposition amounts will result from reduced precursor emissions. While this type of experiment is conceivable over a variety of spatial scales, preliminary modeling analyses (Morris et al., 1984) suggested that over regional scales the magnitude of the emissions modulation has to be very large to cause significant concentration differences. Other studies confirm this observation. Limited capabilities of transferring power among electrical systems and numerous socio-economic problems that would result from widespread emissions modulation require shifting the focus toward local and mesoscale studies.

As proposed under the COMPEX field study plan, a local/mesoscale source modulation field study appears to be more feasible. However, the following issues must be investigated to determine feasibility:

Are the emissions from west-central New York State of sufficient magnitude to produce detectable SO₂ and sulfate concentration and deposition signals in the Adirondacks region when modulated?

Are modulations of a detectable level possible among the emission sources, given the constraints imposed by maintaining electrical services at reasonable costs?

What type of modulation signatures are required for unambiguous data interpretation?

A preliminary feasibility analysis suggests that the west-central New York utilities appear well suited for source modulation experiments in terms of electrical power supply trade-off capabilities. However, a rigorous assessment of these capabilities is required before the experiment can be considered feasible.

Described within this section are the results of a model simulation analysis aimed at investigating the issues of the source modulation experiment, namely, the detectability of a response to continuous and modulated emissions within the Adirondack receptor region.

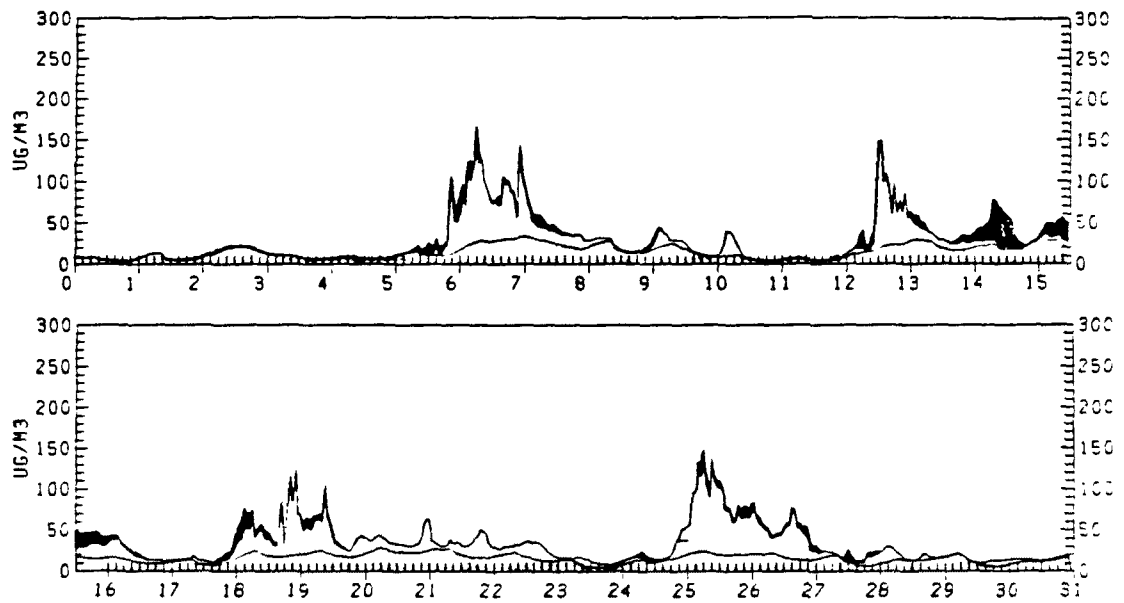
As currently envisioned, the local/mesoscale source modulation experiment would include the release of an inert tracer, such as SF₆, to determine the plume locations at all times. Therefore, measurements of SO₂ and sulfate concentration levels within the region where tracer is detectable provides the pertinent information for the New York point source impact analysis. The success of the emission modulation experiment depends on collecting sufficient concentration data within the tracer impacted region both when emissions are at full strength and when they are modulated.

For the modeling analysis, the modulation experiment is considered a pilot experiment of a one-month duration. Of key interest are the frequency with which SO₂ and sulfate concentration associated with inert tracer are detectable, and the nature of the concentration impact during full emission

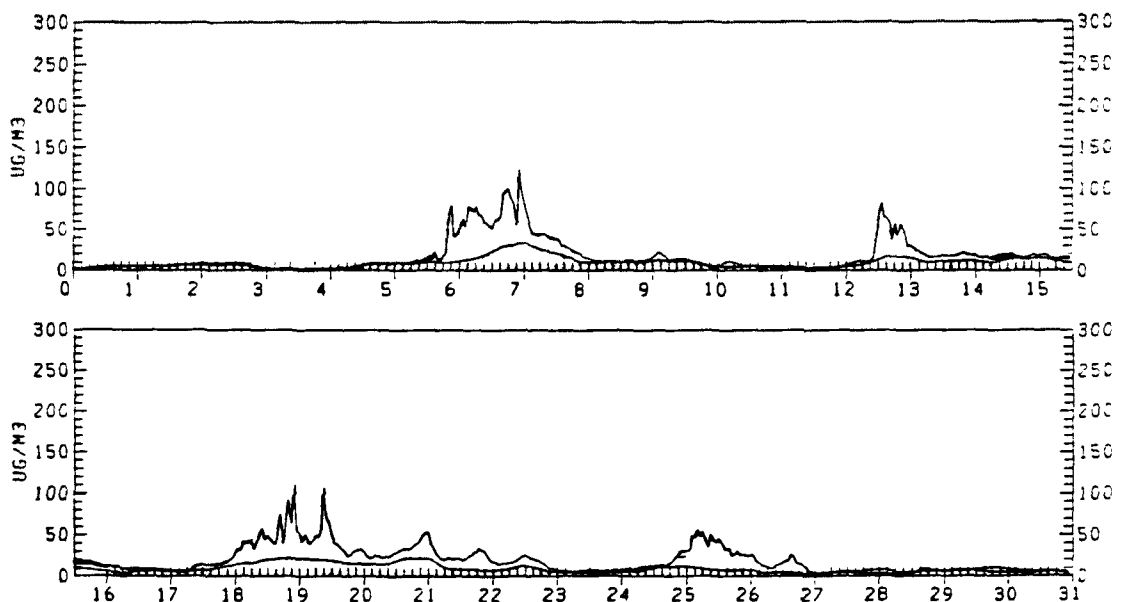
and modulated emission time periods. Since the model predicts the concentration patterns from the New York point sources separately, it is not necessary to consider inert tracer dispersion. As a conservative assumption, this analysis tacitly presumes that the tracer measurements are of sufficient detectability to continuously monitor the location of the plumes from the three New York point sources.

First, the time series of SO_2 and SO_4 concentrations due to the three candidate New York sources within the Adirondacks receptor region are examined. Figure 5-20 shows the SO_2 and SO_4 concentration time series over the southwestern portion of the receptor region for the June 1978 model simulation. The figure shows the contribution from the three New York point sources (dark shading), the contribution from the largest 21 point sources treated with the Gaussian plume segment approach (unshaded), and the contribution from the area sources and remaining point sources within the modeling region (lightly shaded). Visual inspection reveals a variable but generally small SO_2 and SO_4 concentration impacts arising from the continuous SO_2 emission of the New York point sources. The absolute SO_2 and sulfate concentration contributions from these three sources are displayed in Figure 5-21. The shaded portion of these time series represent those concentration values that would occur if the emissions were fully modulated (i.e., on and off) on a weekly basis. From the figures it is estimated that for this particular receptor point and time period, the New York point source emissions contribute to the SO_2 and sulfate concentration burden about 55 percent of the time. If the emissions are modulated, the concentration impact from these sources decrease to about 30 percent of the time.

Of course, the uncertainty associated with detecting these incremental impacts will result in a lower frequency of detection. Using 18 percent as a representative value of the precision in measuring hourly ground-level SO_2 in



(a)



(b)

FIGURE 5-20. Time series of predicted hourly July (a) SO_2 and (b) SO_4 concentrations at the centroid of the southwest 80 km grid cell within the Adirondack region. Light shading indicates the contribution from area sources and all point sources not modeled with the plume segment approach. The unshaded portion represents the contribution from the 21 large point sources treated with the plume segment modeling component. Finally the dark shading represents the contributions from the 3 New York point sources assuming continuous emission.

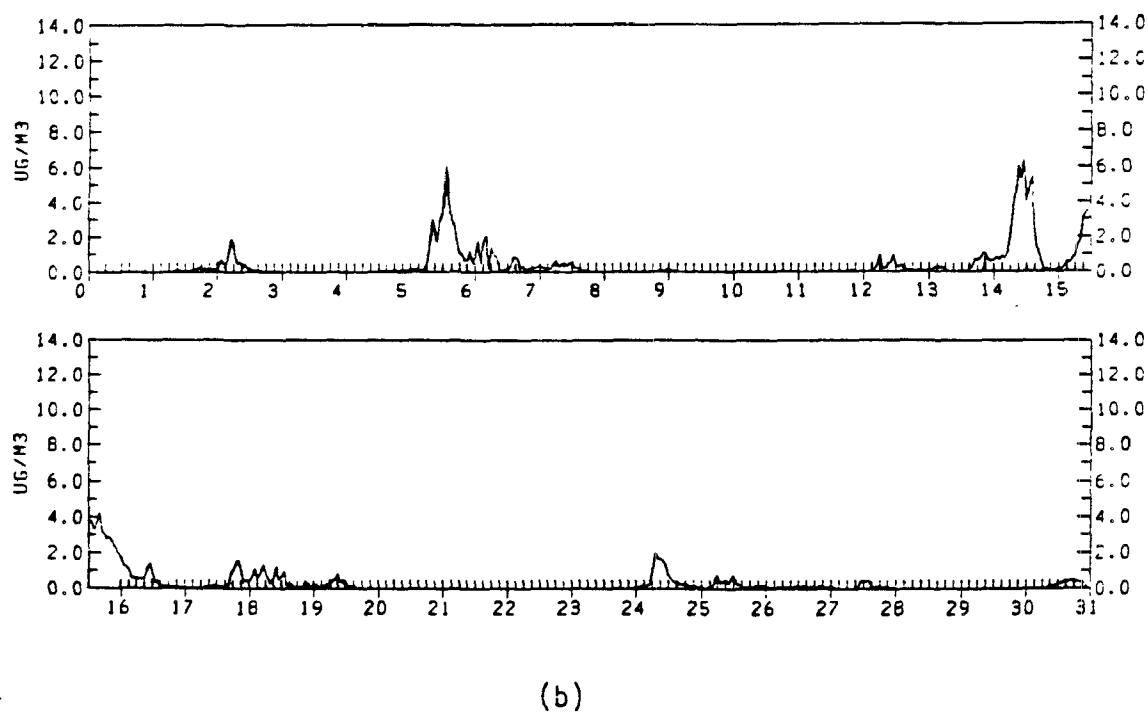
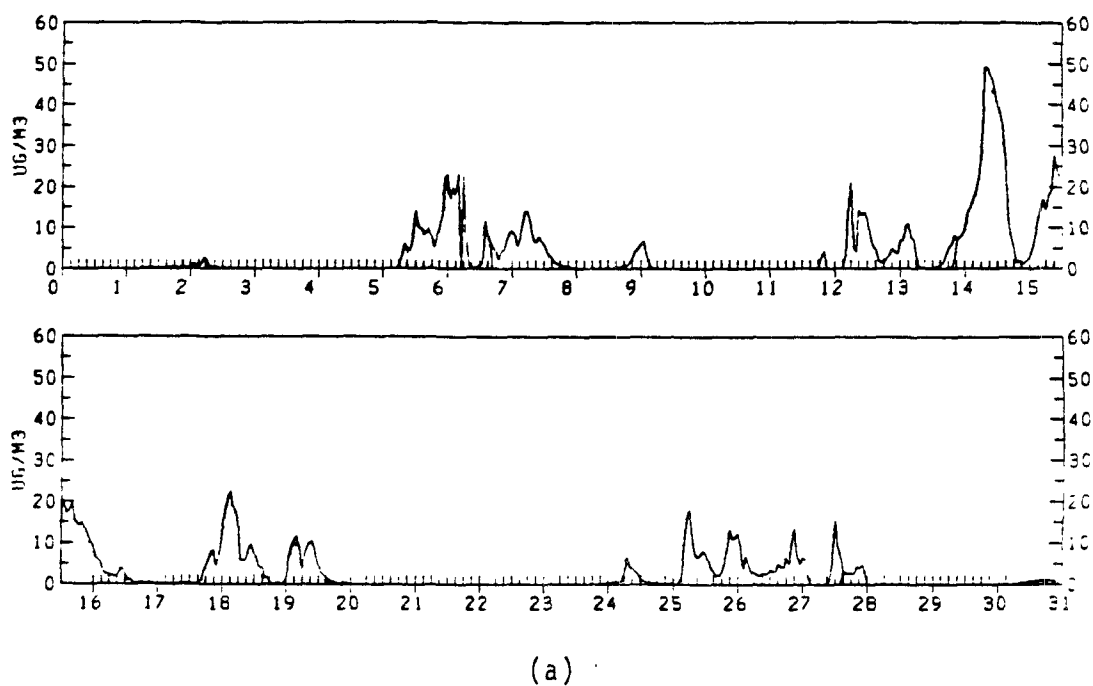
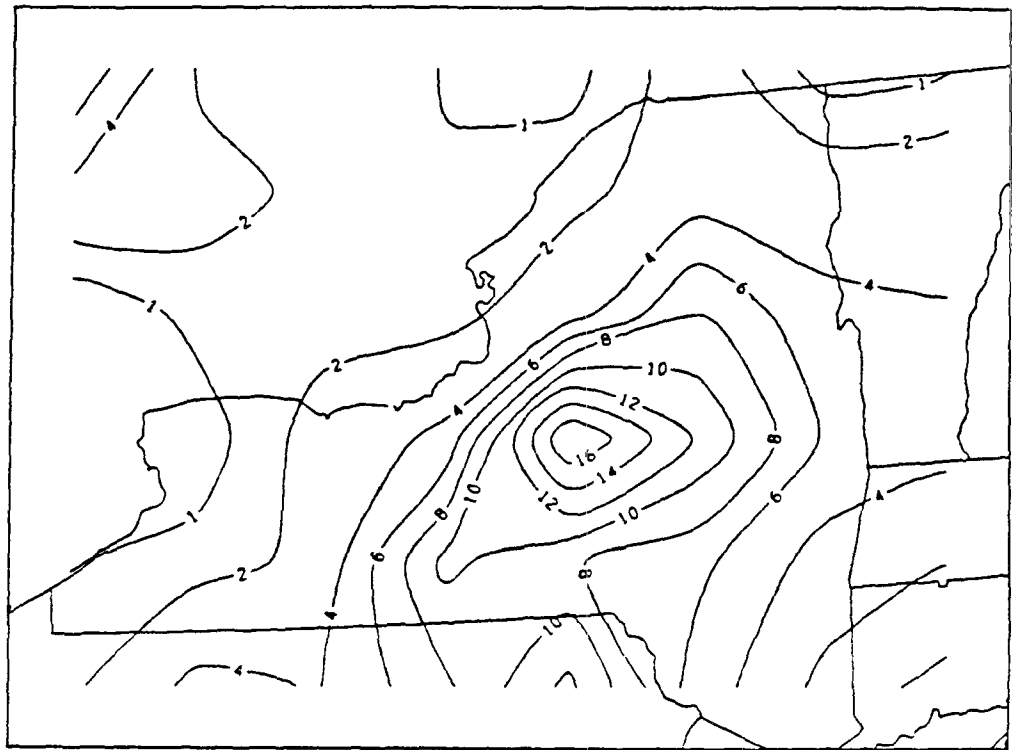


FIGURE 5-21. Predicted (a) SO_2 and (b) SO_4 concentration time series due to the three New York point source emissions only over the same receptor point as in Figure 3-23. Shaded portions refer to concentration predicted for the modulated emission configuration.

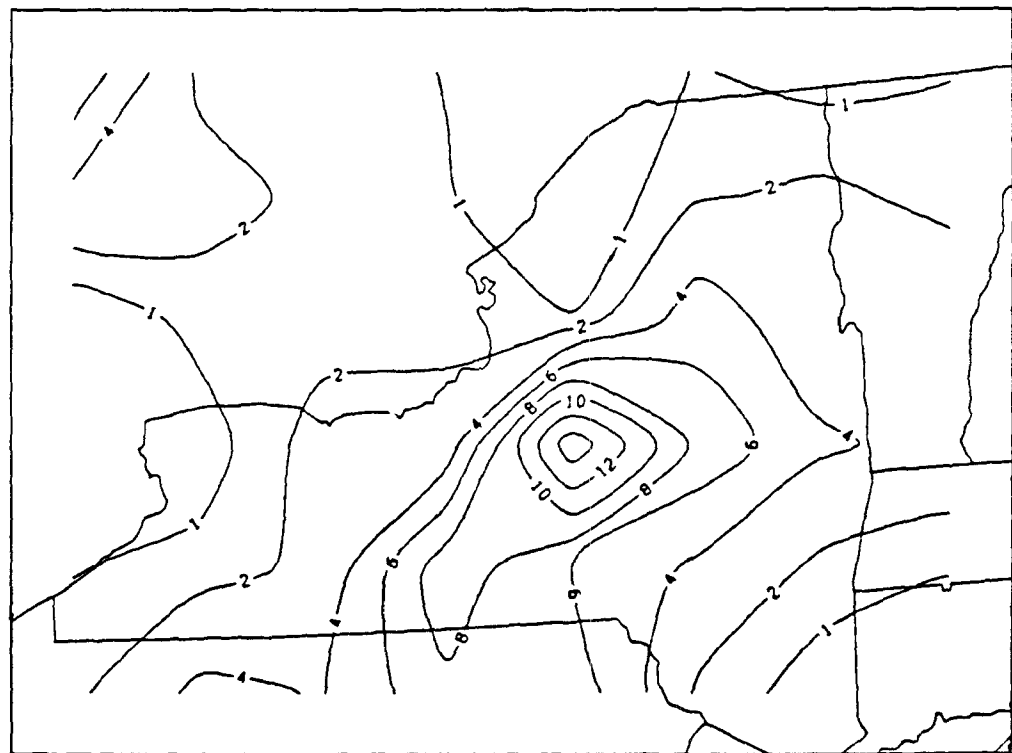
rural areas (Section 2.4), the fraction of time continuous SO₂ emissions are detectable decreases to 18 percent whereas the fraction of time modulated emissions are detected decreases to 15 percent. Similarly, if 9.7 percent is taken to be representative precision for measuring 3-hour sulfate concentrations using a sequential filter sampler, the detection frequencies decrease to 8 percent for continuous and 7 percent for modulated emissions.

These estimates of detection frequencies pertain only to the particular receptor point selected for this analysis, which is situated approximately 80 km downwind from the centroid of the three New York point sources. An indication of the spatial distribution of detectable SO₂ and sulfate concentrations resulting from the three New York point sources is provided in Figures 5-22 and 5-23. Figure 5-22 shows the percent of time (during July 1978) that SO₂ concentrations from continuous and modulated emissions are detectable above the uncertainty levels associated with the measurement technique. The maximum frequency of SO₂ detection is located at approximately the same position as that for which the time series discussed above were computed. Therefore, according to model predictions, the fraction of time the SO₂ concentration contribution from the New York point sources are detectable is roughly one third of the time that these sources contribute to the SO₂ concentration burden, assuming continuous emissions.

It is interesting to note (Figure 5-22) that for modulated emissions the detection frequency decreases by only a few percent. Upon close inspection of the SO₂ time series in Figures 5-20a and 5-21a, this fortuitous result occurs because of the concurrence of the most prominent concentration contribution from the New York point sources with the "on" phase of the emission modulation. During the remaining time, SO₂ concentrations from other sources are large enough and the New York point source contribution is small enough to preclude detection of the New York SO₂ concentration. Since

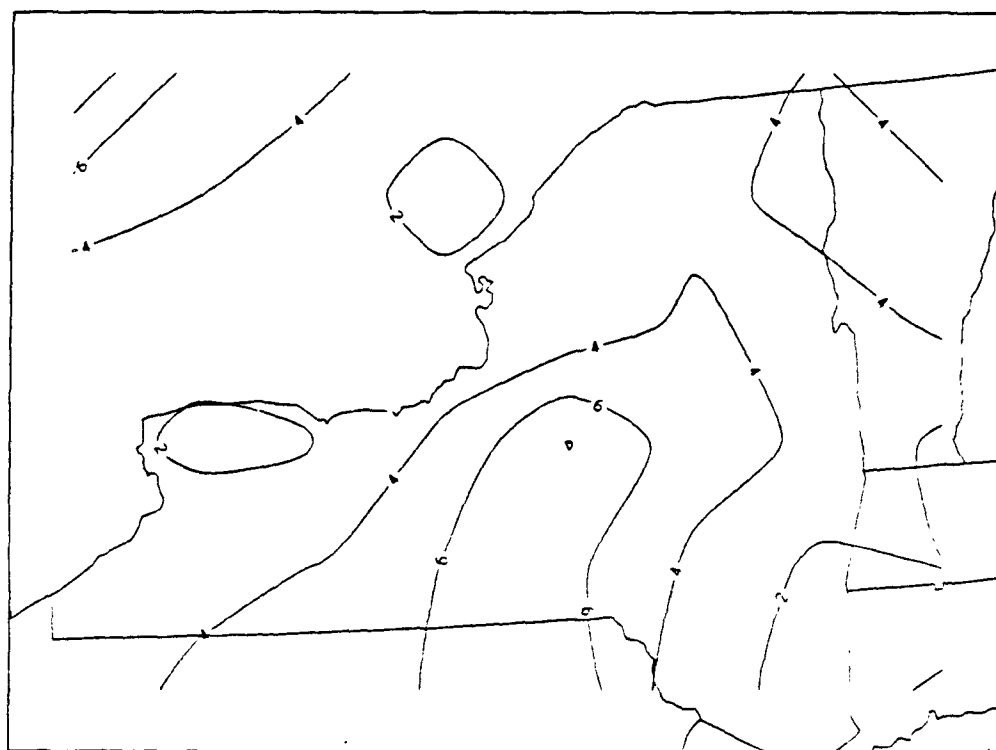


(a)



(b)

FIGURE 5-22. Percentage of time during July 1978 that SO_2 concentrations due to (a) continuous and (b) modulated SO_2 emissions from the three New York point sources are detectable.



(a)



(b)

FIGURE 5-23. Percentage of time during July 1978 that SO_4 concentrations due to (a) continuous and (b) modulated SO_2 emissions from the three New York point sources are detectable.

this period of time corresponds to the "off" phase of the modulation cycle, the lack of detectability had little effect on the detection frequency.

Figure 5-22 also suggests that the detectable SO_2 impacts arising from the New York point sources decreases considerably throughout the northeastern portion of the Adirondack receptor region during the July simulation. This tendency can be interpreted in a broad sense in terms of trajectories from the various high SO_2 emission regions. Under large-scale southwesterly flow, the background SO_2 concentration due to midwestern emissions (particularly the "Ohio" major point source cluster) are relatively high over the Adirondacks. Because we have assumed the detectability threshold is a constant fraction of the total SO_2 burden, the relatively small SO_2 impact from the New York sources becomes "lost in the noise." Clearly, the specification of instrument uncertainty plays an important role in these detectability calculations, and these results must be interpreted accordingly.

Figure 5-23 illustrates the spatial distribution of the sulfate detection frequency from the New York point sources under conditions of continuous and modulated emissions. The distribution of detection frequencies is broader than the SO_2 distribution because sulfate is a product species only* and hence its distribution is of a more regional nature. The magnitudes of sulfate detection frequencies are similar to the SO_2 detection frequencies away from the region of maximum SO_2 plume impact. Since sulfate concentrations are low close to the sources, there is no pronounced spatial maximum in the frequency of sulfate detection. The sulfate detection frequency corresponding to modulated emissions is generally 1-2 percent lower than the continuous emission configuration for reasons similar to those discussed with respect to SO_2 concentrations.

*Primary sulfate emissions were not considered in the model simulations.

The relevance of these model simulations results to the proposed short-range source modulation experiment can be summarized in the following manner. Predicted SO₂ concentration levels due to the three New York point sources are highly variable both spatially and temporally. For the month of January 1978, there is a tendency for the maximum SO₂ detectability frequency to be located east of the point sources, indicating that the amount of SO₂ concentration data useful for the local source attribution analysis is likely to be weighted by wind direction. During south-westerly flow, for example, the influence of remote SO₂ emissions may adversely affect the acquisition of pertinent data.

From the limited model simulation time period, the frequency with which weekly modulated emissions are detectable in the ground-level concentration distribution is only a few percent lower than that corresponding to continuous emissions. Assuming that the "zero SO₂" plume is identifiable using a continuously emitted inert tracer (as proposed in the preliminary experimental design), the period of time for which a detectable difference in the local source impact could be ascertained from the data is roughly one day for the entire month.

Since this short period of time results from the coincidental high correlation of the time periods of good detectability and the "on" phase of the emission modulation, it is evident that the amount of useful data acquired during a month-long experiment will be extremely sensitive to the timing of the modulation in relation to the prevailing meteorological transport.

To test this hypothesis, similar model output processing for the January 1978 simulation has been performed. The SO₂ and sulfate time series over the Adirondack receptor region (not shown here) indicate that the three New York point sources contributed less frequently to the concentration burden in January than during July. The spatial distribution of the SO₂ concentration

detectability due to continuous and modulated emissions (analogous to Figure 5-22) is shown in Figure 5-24.

This figure reveals that the different meteorological transport, chemical transformation, and deposition conditions of the January scenario result in a different location of maximum SO₂ detectability of the three point sources. Additionally, the decrease in frequency of detection accompanying a modulated emission configuration is proportional to the decrease in time that SO₂ is emitted.

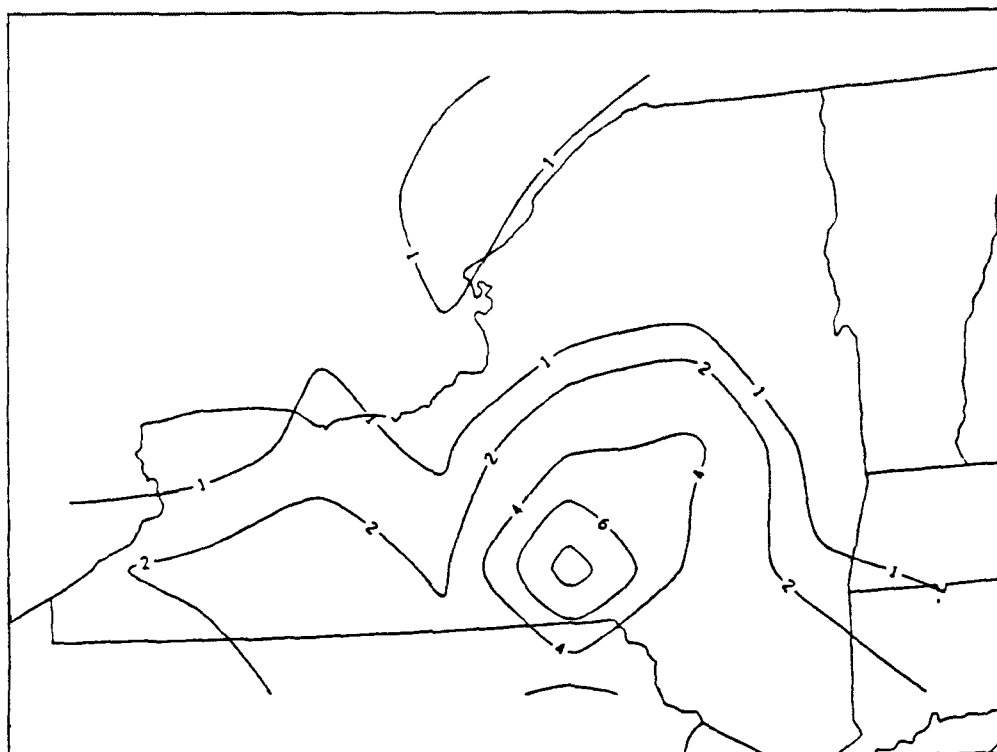
The sensitivity of pertinent data acquisition to meteorological conditions could be decreased by conducting the modulation experiment for an extended period of time (i.e., one year or longer). The concentration contribution from the three New York sources could potentially be determined by performing a spectral analysis of the measured concentration time series, focusing on the variance associated with the modulation frequency. Extended model simulations would also be useful for determining the appropriate modulation frequency (i.e., where a maximum variance differential between continuous and modulated emissions exist).

Alternatively, the sensitivity might be decreased by increasing the modulation frequency within the one-month experimental period. Further tests would be required to address this issue.

To this point, concern has been focused on the magnitude of the local source contribution and its temporal variation with and without a hypothetical emission modulation. Results from the model simulation indicate that the meteorological variability may strongly interfere with the ability to detect the modulated emissions contribution. This is examined in a different manner below, where concentration variability due to the meteorological fluctuations is more directly compared with the concentration variability due to the modulated emissions.



(a)



(b)

FIGURE 5-24. Percentage of time during January 1978 that SO₂ concentrations due to (a) continuous and (b) modulated SO₂ emissions from the three New York point sources are detectable.

Within the mesoscale region surrounding three New York point sources of interest, the 1-hour SO₂ and 3-hour sulfate ground-level concentration time series predicted by the model are analyzed in terms of time averaged mean and root-mean squared (RMS) concentration amplitudes. The four-week January simulation and four-week July simulation are subdivided into alternating weekly periods. Mean concentrations and concentration fluctuations are averaged over all odd weeks (i.e., first and third weeks of January and July) and all even weeks (i.e., second and fourth weeks of January and July). The mean and root-mean-squared SO₂ and sulfate concentrations due to continuous New York point source emissions averaged over the odd weeks are compared with those averaged over the even weeks to assess the variability in concentration mean and fluctuations due to meteorological variability over time periods consistent with the proposed modulation frequency. Figures 5-25 and 5-26 illustrate, respectively, the mean and RMS SO₂ concentration across the New York state region. Part a) of each figure illustrates the average over the odd-week; part b) the average over even-week time periods; and part c) the difference (i.e., odd-week average minus even-week average).

The mean SO₂ concentration for these two time-averaged samples show similar north-to-south concentration gradients (Figure 5-25) but a representative difference in these average concentration values near the New York point sources is several $\mu\text{g}/\text{m}^3$, and varies across the region from 0 to 7 $\mu\text{g}/\text{m}^3$. The average RMS SO₂ concentration distributions for these sample time periods is approximately 20 to 60 $\mu\text{g}/\text{m}^3$ and exhibits a similar north-to-south gradient (Figure 5-26). Typical weekly RMS concentration differences (Figure 5-26c) range from 0 to 16 $\mu\text{g}/\text{m}^3$.

For subsequent comparisons with concentration variability due to modulated emissions, the information contained in this figure can be generalized as follows:

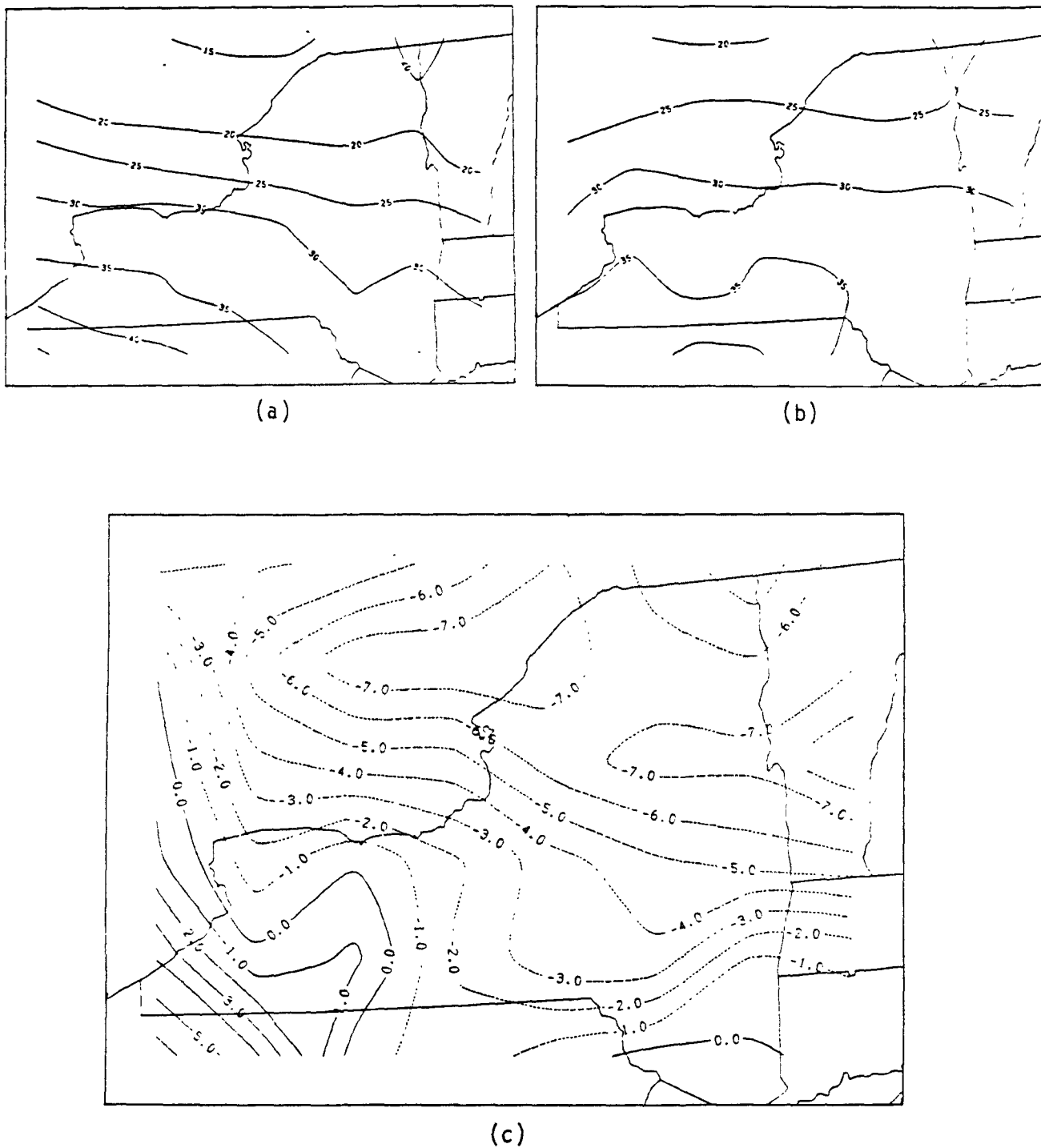
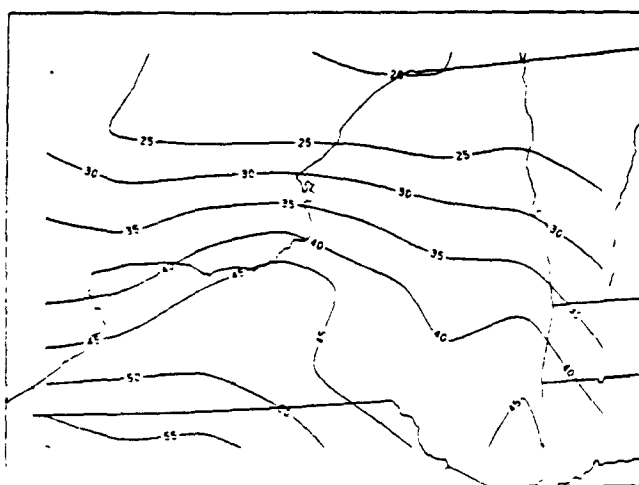
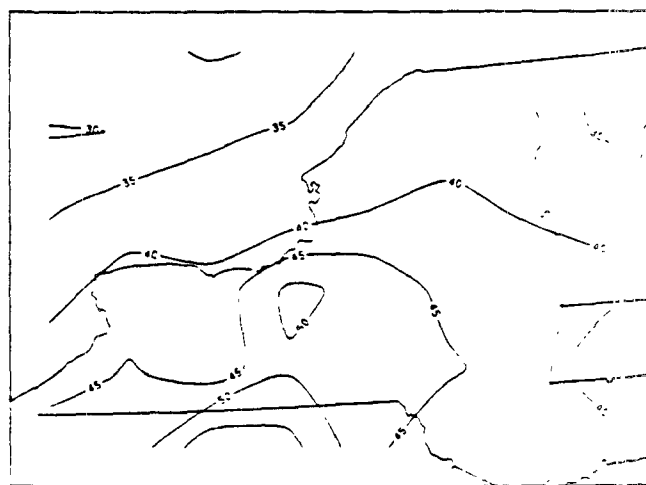


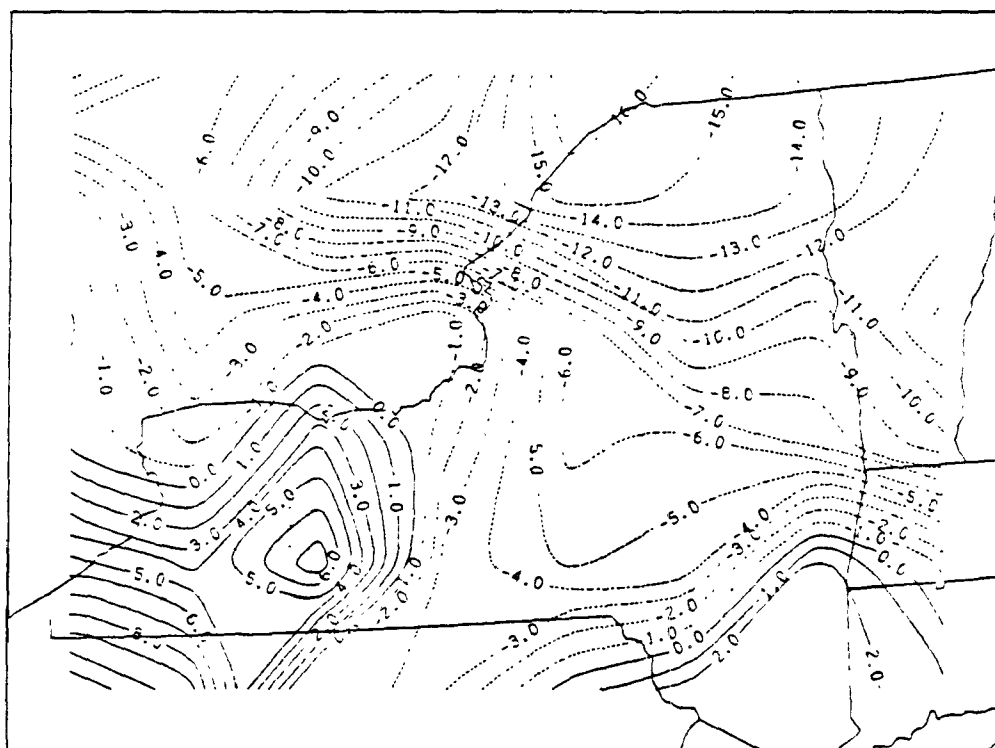
FIGURE 5-25. Predicted average SO₂ concentration distribution during the (a) odd-week and (b) even-week periods. Part "c" illustrates the difference in average SO₂ concentrations over these two samples (i.e., odd-week average minus even-week average). Units are $\mu\text{g}/\text{m}^3$.



(a)



(b)



(c)

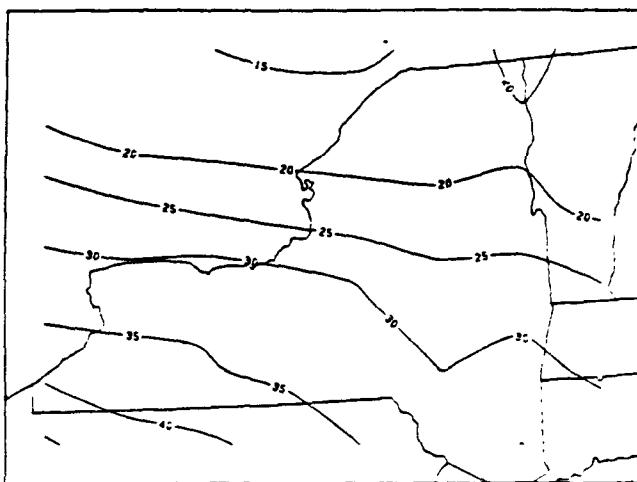
FIGURE 5-26. Predicted RMS SO_2 concentration distribution during the (a) odd-week and (b) even-week periods. Part "c" illustrates the difference in RMS SO_2 concentrations over these two samples (i.e., odd-week average minus even-week average). Units are $\mu\text{g}/\text{m}^3$.

According to the model predictions, a representative variability in mean and RMS SO₂ concentrations due to meteorological processes alone is several percent of the corresponding mean value around the central New York State region.

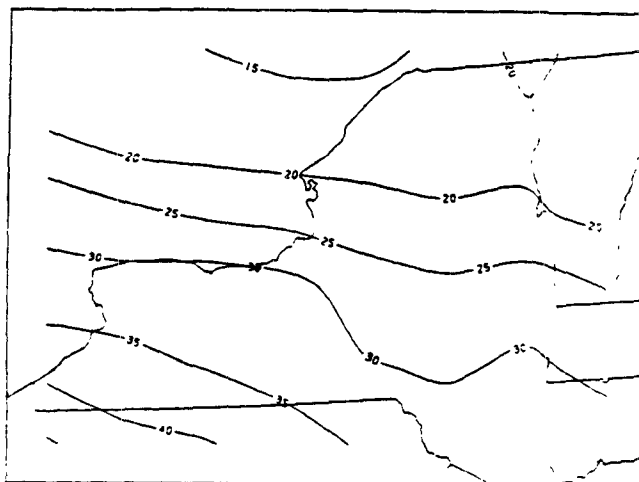
Next, the differences in the average and RMS SO₂ concentrations due to a weekly modulation of SO₂ emissions from the three New York point sources are examined. Two sets of calculations are performed. For comparison with the odd-week mean and RMS concentrations with continuous New York emissions, a parallel time series analysis is performed excluding the point source emissions. A similar comparison of mean and RMS concentration differences between the even-week sample with and without the point source emissions is also performed. From the calculations of the even-week and odd-week samples, the sample showing the maximum contribution toward average and RMS SO₂ concentrations from the New York point sources is retained for comparison with Figures 5-25 and 5-26.

Figures 5-27 and 5-28 illustrate the modulated-emission induced change in mean and RMS concentrations, respectively. Exclusion of the point source emissions results in a mean SO₂ concentration difference of, at most, 2.2 µg/m³, according to the model calculations. Throughout the region of the maximum point source contribution, the natural variability in mean SO₂ is of a greater magnitude (compare Figures 5-25 with 5-27). A similar comparison of the RMS concentration distribution (Figures 5-26 and 5-28) reveals that the effect on hourly concentration fluctuations of modulating the point source emissions is small relative to the natural variability of hourly concentration fluctuations.

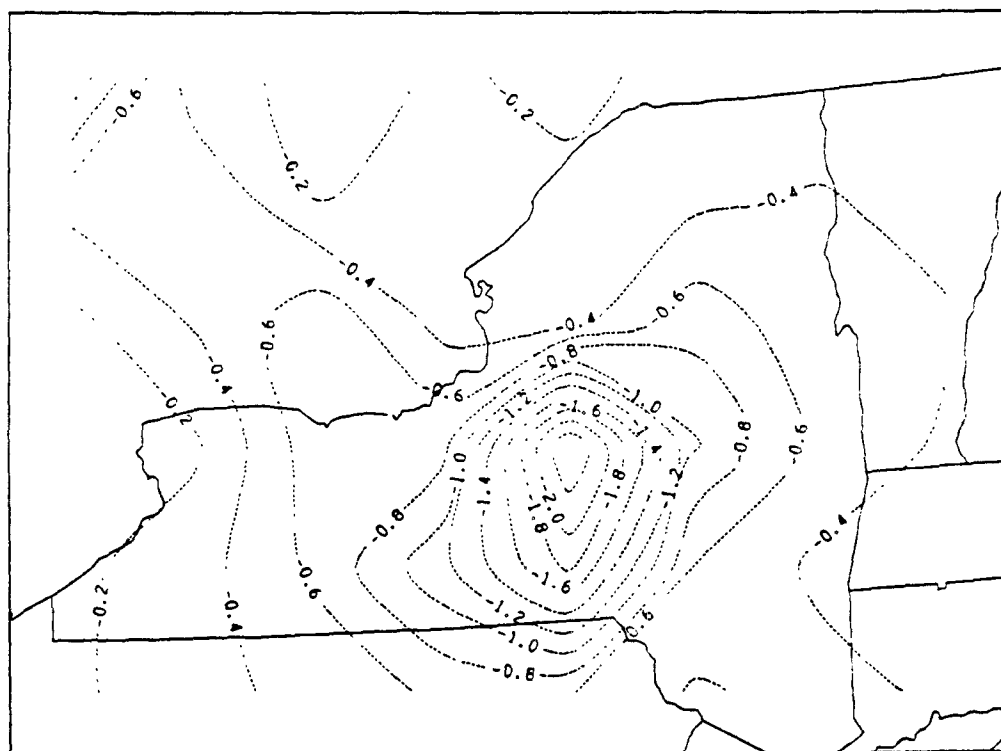
The implication of these model prediction analyses is that the weekly average and variability of the SO₂ concentration signal resulting from a



(a)

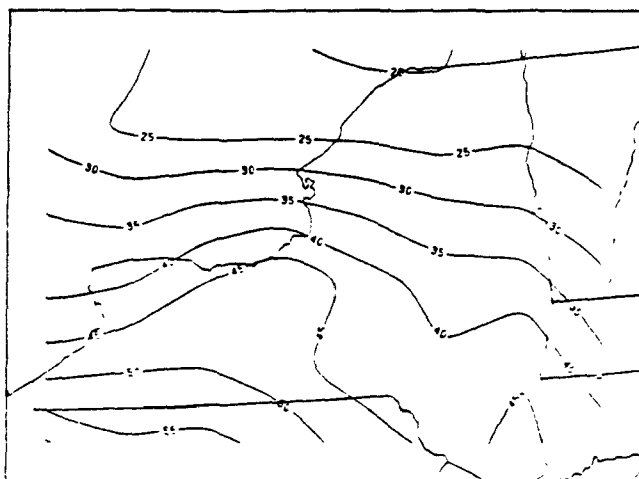


(b)

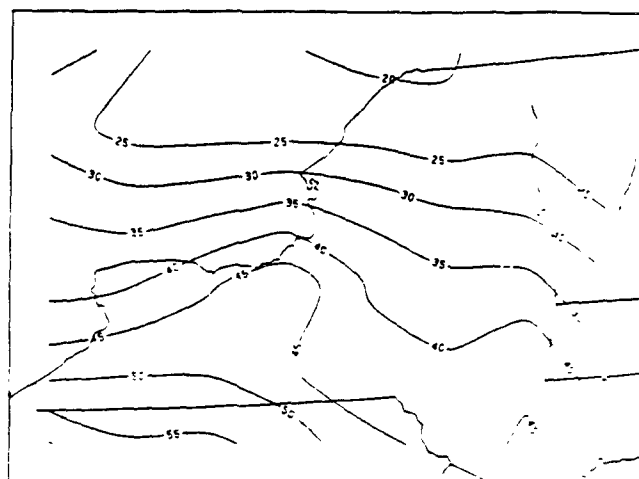


(c)

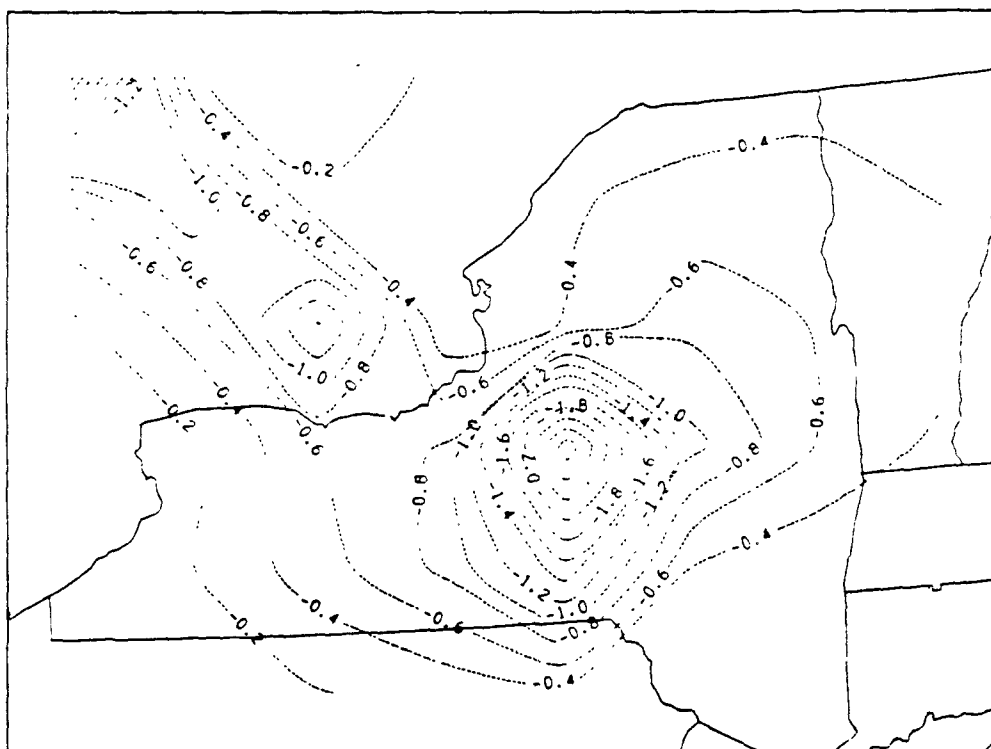
FIGURE 5-27. Predicted average SO₂ concentration distribution over the odd-week period (a) with, and (b) without the contribution from the three New York point sources. Part "c" illustrates the SO₂ concentration deficit resulting from the modulated emissions. Units are $\mu\text{g}/\text{m}^3$.



(a)



(b)



(c)

FIGURE 5-28. Predicted RMS SO_2 concentration distribution over the odd-week period (a) with, and (b) without the contribution from the three New York point sources. Part "c" illustrates the RMS SO_2 concentration deficit resulting from the modulated emission. Units are $\mu\text{g}/\text{m}^3$.

weekly emission modulation may be no greater magnitude than the week-to-week differences in SO₂ amplitude and variability caused by meteorological factors.

A similar analysis was also performed on the predicted 3-hour sulfate time series which indicates that the week-to-week differences in average and RMS sulfate concentrations due to meteorological factors exceed those due to emission modulations. The difference in odd-week and even-week average sulfate concentration levels are of the order of 1 µg/m³. Several µg/m³ difference in RMS sulfate concentrations occur due to meteorological variability. Imposing a weekly emission modulation on the three sources results in mean sulfate differences of a few tenths of a µg/m³ and a difference of similar magnitude in RMS sulfate concentrations.

Both the SO₂ and sulfate concentration analyses do not directly imply that local source contributions cannot be obtained from a source modulation experiment, but do illustrate that the signal of interest (i.e., the concentration differences between emission and no emissions) is strongly imbedded within noise of the same or larger magnitude. Furthermore, the results of the analysis of the frequency of signal detection suggest that one or two month-long modulation experiments will only give rise to a small sample of data from which to deduce the source contributions.

5.3.2 Local Reactive Tracer Experiments

The ultimate goal of the proposed reactive tracer experiments is to determine the depletion and dry deposition of SO₂ over distance scales of from 10 to 50 km. Ideally, these experiments should be performed over a variety of meteorological and surface conditions so that the transmittance factor derived from the data can be combined with the results from the long-range inert tracer experiments to determine source-receptor relationships.

The proposed design of the reactive experiment is based in part on the concepts of a plume depletion and a surface depletion approach described by Horst (1977) and Horst and co-workers (1983). The experimental design requires elevated releases of SF_6 and ^{34}S (as SO_2) with a concurrent ground-level release of a fluorocarbon tracer. Ground-level tracer monitoring is performed over an array of samplers arranged in concentric arcs with high resolution within the first 10 km of the source and lower resolution at downwind distances of from 20 to 50 km. Within 10 km of the source the concentration measurements of the two inert and one reactive tracer are used to assess the dry deposition of ^{34}S via the surface depletion approach.

Beyond 10 km, depletion of the reactive tracer is determined by calculating the reactive tracer depletion budget, making use of the downwind difference in the concentration ratios of reactive and inert tracers released from the same elevated position. The advantage of this method over a simple reactive tracer source balance approach is that measurements of the tracers need only be made below the level at which the ratio of normalized tracer concentrations differ from unity. Under non-uniform vertical tracer distributions, this level is likely to increase downwind as reactive tracer is deposited, since the resultant vertical gradient in the reactive tracer concentration near the ground will promote a downward flux of tracer from higher levels. Thus, the further downwind the tracer is sampled, the greater the importance of airborne sampling.

The uncertainties associated with measuring the y-z distribution of tracer concentrations at local distances from the point source are likely to be greater than the uncertainties in measuring the distribution farther downwind, where the pollutant distribution is spread over larger distances and is more uniform. This is due to the necessity of airborne sampling within regions of high concentration variability and intermittency. Characterizing these

uncertainties would require an extensive analysis of suitable field data, such as the EPRI PMV&D data bases and might require the use of a concentration fluctuation model as well. Such an uncertainty analysis is beyond the scope of the present effort, but is certainly of importance for planning the short-term field experiments. Within the remainder of this section, some simplifying assumptions are involved in order to examine what might be characterized as a "lowest-order" uncertainty issue; namely, to examine the relationships between the pollutant depletion over various downwind-distance increments and the uncertainties associated with measuring the mass flux of ^{34}S . The detectability of the deposition calculated by differencing the ratios of reactive to inert tracer concentration can be examined analytically if certain assumptions are made. If, for example, it is assumed that all of the tracer mass is measured at each downwind arc of receptors and, further, that the concentrations of these tracers are uniformly distributed in the vertical, then the deposition occurring between various downwind distances can be calculated by solving a simple system of mass balance equations for SO_2 and sulfate.

With the first assumption, the necessity of considering the ratio of tracers is removed so that only the sulfur species need be considered. The second assumption is a useful simplification because it permits the application of deposition and oxidation rate constants directly to the entire pollutant mass within the mixed layer, allowing the determination of simple analytic solution.

The mass conservation equation for airborne and deposited sulfur may be expressed as:

$$\frac{d}{dt} (M_1) = - (k_t + k_{d1}) M_1 \quad (5-1)$$

$$\frac{d}{dt} (M_2) = -k_{d2}M_2 + k_t M_1 \quad (5-2)$$

$$\frac{d}{dt} (R_1) = k_{d1}M_1 \quad (5-3)$$

$$\frac{d}{dt} (R_2) = k_{d2}M_2 \quad (5-4)$$

where M_1 and M_2 refer to the airborne sulfur mass as SO_2 and sulfate respectively, and R_1 and R_2 refer to the deposited sulfur mass as, respectively, SO_2 and sulfate. The SO_2 oxidation rate is given by k_t , whereas the dry deposition rates for SO_2 and sulfate is represented by k_{d1} and k_{d2} , respectively. Wet deposition has not been considered.

Using initial conditions specified by $M_1 = 1$, $M_2 = 0$, $R_1 = 0$, $R_2 = 0$, the solutions take the form:

$$M_1(t) = \exp [-(k_t + k_{d1})t] \quad (5-5)$$

$$M_2(t) = \frac{k_t}{k_t + k_{d1} - k_{d2}} \left(\exp(-k_{d2}t) - \exp[-(k_t + k_{d1})t] \right) \quad (5-6)$$

$$R_1(t) = \frac{k_{d1}}{k_t + k_{d1}} \left(1 - \exp [-(k_t + k_{d1})t] \right) \quad (5-7)$$

$$R_2(t) = \frac{k_t k_{d2}}{k_t + k_{d1} - k_{d2}} \times$$

$$\left[\frac{1}{k_{d2}} \left(1 - \exp [-k_{d2}t] \right) - \frac{1}{k_t + k_{d1}} \left(1 - \exp [-(k_t + k_{d1})t] \right) \right] \quad (5-8)$$

Under a uniform wind speed, \bar{u} , the deposition of total sulfur occurring between downwind distances $x_0 - d/2$ and $x_0 + d/2$ is given by:

$$D = \left[R_1 \left(\frac{x_o - d/2}{u} \right) + R_2 \left(\frac{x_o - d/2}{u} \right) \right] - \left[R_1 \left(\frac{x_o + d/2}{u} \right) + R_2 \left(\frac{x_o + d/2}{u} \right) \right] \quad (5-9)$$

Substituting the solution (Equations 5 through 8) into Equation 9 gives an analytic expression for the deposited sulfur as a function of downwind distance x_o , and the separation distance d .

$$D(x_o, d) = \left[2 \exp \left[-(k_t + k_{d1}) \left(\frac{x_o + d/2}{u} \right) \right] - \exp \left[-(k_t + k_{d1}) \left(\frac{x_o - d/2}{u} \right) \right] \right] + \frac{k_t}{k_t + k_{d1} - k_{d2}} \left[\exp \left[-k_{d2} \left(\frac{x_o + d/2}{u} \right) \right] - \exp \left[-k_{d2} \left(\frac{x_o - d/2}{u} \right) \right] \right] \quad (5-10)$$

Figure 5-29a illustrates the percentage of initial sulfur mass removed through dry deposition as a function travel time x_o/u , and normalized separation distance, d/x_o . For these calculations, the following oxidation and deposition rate constants were selected.

$$k_t = 0.01 \text{ h}^{-1}$$

$$k_{d1} = 0.036 \text{ h}^{-1}$$

$$k_{d2} = 0.0036 \text{ h}^{-1}$$

The dry deposition rate constants correspond to SO_2 and sulfate deposition velocities of 1 cm/s and 0.1 cm/s, respectively, and a mixing depth of 1 km. The application of these rate constants over the entire pollutant mass in the mixed layer is justified by the assumption of vertical uniformity in concentration distribution.

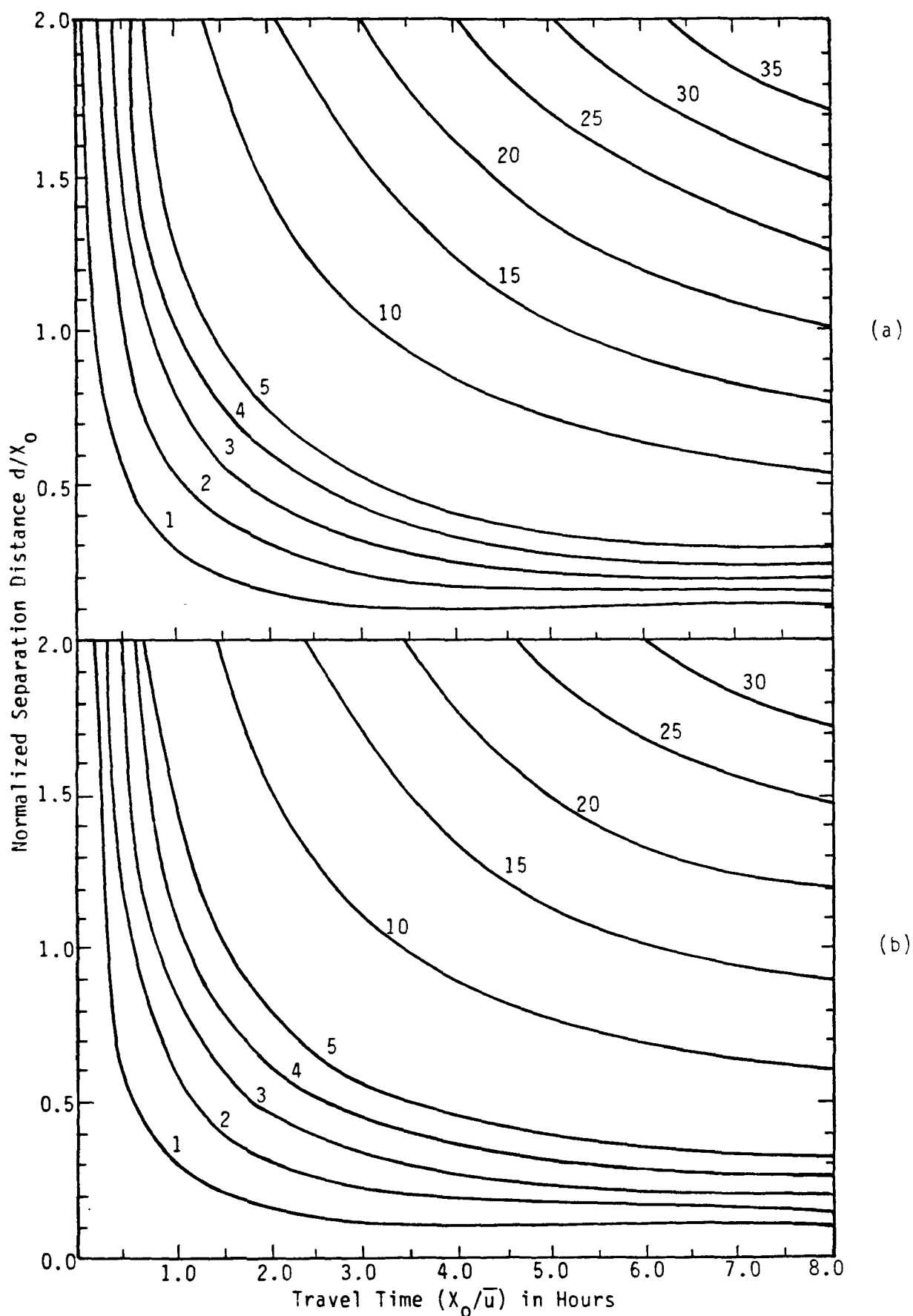


FIGURE 5-29. (a) percentage of initial sulfur mass removed through SO_2 and sulfate dry deposition; (b) Difference in percentage of initial sulfur mass removed through SO_2 and sulfate dry deposition considering the uncertainties in oxidation and dry deposition rate constant specification. See text for further details.

Recent reviews of the dry deposition and SO₂ oxidation processes (e.g., NCAR, 1983; NRC, 1983) indicate that the effective rate constants may vary over a considerable range of values. To determine the effect of different rate constants on D(x₀,d), several simple sensitivity analyses were performed. Analytic solutions to Equation 5-10 were obtained with high and low values of the three rate constants as shown below:

$$k_t = 0.005 \text{ h}^{-1} \\ = 0.02 \text{ h}^{-1}$$

$$k_{d1} = 0.018 \text{ h}^{-1} \\ 0.054 \text{ h}^{-1}$$

$$k_{d2} = 0.000 \text{ h}^{-1} \\ 0.018 \text{ h}^{-1}$$

The ranges of SO₂ and sulfate dry deposition rates correspond to deposition velocity ranges of 0.5-1.5 cm/s and 0.0-0.5 cm/s, respectively; again, a 1 km mixing height has been assumed.

The maximum sensitivity of D(x₀,d) occurs with certain combinations of oxidation rate and deposition rates. Rapid oxidation in conjunction with low deposition gives the lowest values of D(x₀,d), while slow oxidation and high deposition yields high values. The difference in the percentage of initial sulfur deposited as a function of x₀ and d, i.e., ΔD(x₀,d), corresponding to the combinations of rate constants shown in Figure 5-29b. The fact that ΔD(x₀, d) and D(x₀,d) are of comparable value throughout the range of x₀/u and d/x₀ suggests that, under these simplified assumptions, the uncertainties in oxidation and deposition rates do exert a strong influence on the optimum values of x₀ and d required to detect the deposition, as long as the rate constants are constant in time.

In fact, the mesoscale dimensions of the proposed field experiment ensure that the deposition of SO_2 dominates that of SO_4 , and hence the optimal experimental parameters, x_0 and d , are the intuitively obvious ones, namely, the largest separation distances at the farthest downwind position. For the larger-scale experiments, one might expect that the eventual SO_2 oxidation to the more slowly deposited sulfate aerosol would result in an optimal x_0 of intermediate dimensions. Several analyses of the sulfur mass deposition and deposition sensitivity to different rate constants over larger space and time scales suggest an optimal value of x_0 corresponding to travel times of about 30 hours, well beyond the range of the proposed 50 km experiment.

The simple mass balance approach is useful for establishing approximate upper limits on the measurement uncertainties (or minimum precision) required to detect sulfur deposition for various x_0 and d . In order to detect the deposition of ^{34}S from the difference of upwind and downwind mass flux measurements, the true deposition must be larger than a minimum value, which is a function of the mass flux measurement uncertainties.

In finite difference form, the measured deposition D is related to the mass flux convergence by:

$$\hat{D}/\Delta t = -(F_d - F_u)/\Delta x,$$

where F_u and F_d are the measured upwind and downwind total mass fluxes, respectively.

* Here, the assumption is made that the measured mass flux lies within the interval $F \pm \sigma F$ with approximately a 67 percent probability.

Representing the uncertainties in mass flux measurements* by σ_f , and noting $u = \Delta x / \Delta t$, yields:

$$\hat{D} = 1/\bar{u} (\bar{F}_u - \sigma_{fu}) - (\bar{F}_d + \sigma_{fd}) \quad (5-11)$$

where \bar{F}_u and \bar{F}_d are the expected (or true) values of the mass fluxes, and σ_{fu} and σ_{fd} are the corresponding measurement uncertainties, which, in the context of the proposed experiment, include individual concentration measurement uncertainties and uncertainties associated with integrating these measurements across each y-z plane. In Equation 5-11 the uncertainties have been combined with the flux measurements in such a manner as to represent the maximum likely error in the calculated deposition. Assuming no bias in the flux measurements, the true deposition is $D = 1/\bar{u} (\bar{F}_u - \bar{F}_d)$. Assuming that the normalized uncertainties associated with all mass flux measurements are equal, then:

$$D = D - 1/\bar{u} (\bar{F}_u + \bar{F}_d) C_v,$$

where C_v is the coefficient of variation of the flux measurements. A measured deposition exceeding zero therefore requires an upper limit on the flux measurement uncertainties, given by:

$$C_{v(\text{upper limit})} = \frac{D\bar{u}}{(\bar{F}_u + \bar{F}_d)} \quad (5-12)$$

Since the true mass fluxes at the upwind and downwind y-z planes are, under assumptions stated, given by:

$$\bar{F}_u = -u \left[M_1 \left(\frac{x_o - d/2}{u} \right) + M_2 \left(\frac{x_o - d/2}{u} \right) \right]$$

$$\bar{F}_d = -\bar{u} \left[M_1 \left(\frac{x_o + d/2}{u} \right) + M_2 \left(\frac{x_o - d/2}{u} \right) \right]$$

Equations 5-5, 5-6, and 5-10 can be substituted into Equation 12 to yield the upper limit on mass flux uncertainty (as a function x_o and d) necessary to detect the ^{34}S tracer. Figure 5-30a illustrates this uncertainty limit in terms of the downwind travel time, x_o/U , and normalized separation distance between flux measurements, d/x_o . The uncertainties in rate constants used in Equation 5-10 may be incorporated into the calculation of upper limits on C_v by specifying the resulting deposition uncertainty by*:

$$\sigma_d = \frac{\Delta D(x_o, d)}{3}$$

A more stringent upper limit on C_v results from this consideration, i.e.,

$$C_{v(\text{upper limit})} = \frac{(\bar{D} - \sigma_o) u}{(\bar{F}_u + \bar{F}_d)}$$

where $\bar{D} = \bar{F}_u - \bar{F}_d$.

The variations of the upper limits of C_v as a function of x_o/u and d/x_o are shown in Figure 5-30b.

Under the assumptions made thus far in the analysis, the mass flux measurement uncertainties above which the deposition of ^{34}S will not be detectable are at most about 25 percent. This minimum precision applies to a

* Here it is assumed that d is uniformly distributed in the interval $D \pm \Delta D$ with a probability of 1. To include an uncertainty in D comparable with the uncertainty in the mass flux measurements, the limits on the interval are reduced so that D occurs within $D \pm \sigma_o$ with a 2/3 probability.

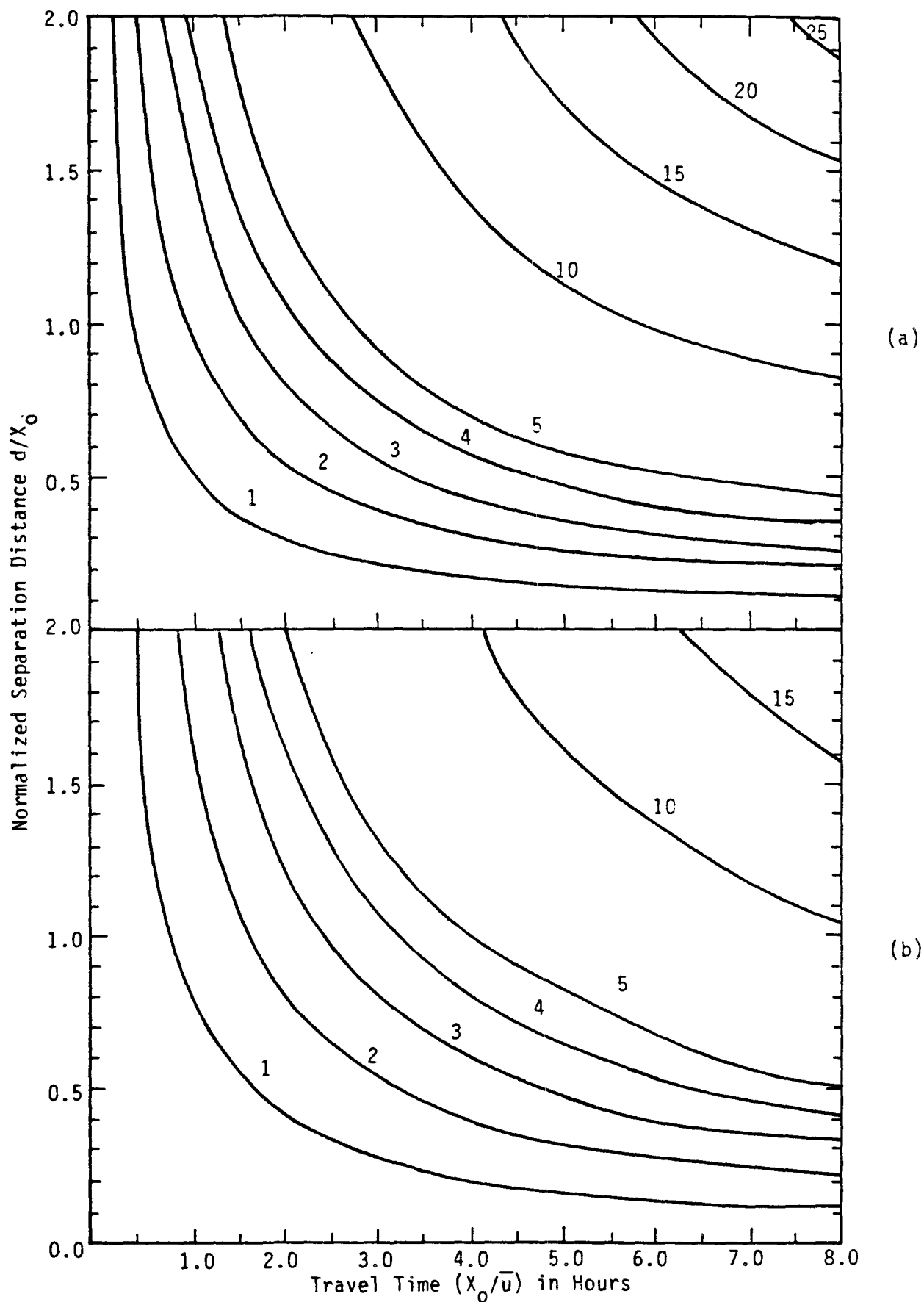


FIGURE 5-30. Minimum mass flux measurement precision (i.e., C_V -upper limit) required for sulfur deposition detection (a) without, and (b) with consideration of the uncertainties in oxidation and dry SO_2 and sulfur deposition rates. These values, expressed as a percentage, are calculated from the simple mass balance approach. See text for further details.

spatial separation distance equivalent to 16 hours of travel time (i.e., $x_0/u = 8$ hr, $d/x_0 = 2$). If uncertainties in the oxidation and deposition rate constants are factored into the analysis, the minimum precision decreases to below 20 percent (Figure 5-30b).

Over a hypothetical monitoring network configuration consisting of concentric arcs of SO_2 and sulfate monitors spaced 10 km apart at distances ranging from 10 km to 50 km, an estimate of the minimum mass flux measurement precision for all combinations of flux difference calculations can be obtained (as a function of wind speed) from Figure 5-30. For example, the minimum precision of mass fluxes determined from concentration measurements at 10 km and 50 km lies along the horizontal line corresponding to $d/x_0 = 1.33$. Since $x_0 = 30$ km, the travel time (in hours) is given by $T = 8.33/u$, where u is in m/s. The minimum mass flux measurement precision falls below 5 percent at wind speeds exceeding ~ 2.8 m/s.

As stated previously, the assumptions necessary to calculate $C_v(\text{upper limit})$ in so simple a manner have to be examined to determine whether the resulting minimum mass flux measurement precision estimates are realistic, overly conservative, or perhaps not stringent enough. The effects of these assumptions are discussed heuristically in the paragraphs that follow.

The assumption that all of the ^{34}S mass passing through a y-z plane (or equivalently, passing across a particular arc of receptors) is accounted for in the measurement is probably a very stringent assumption. Under actual dispersion conditions, one would have to measure with high spatial resolutions both the horizontal and vertical distribution of airborne ^{34}S and the wind velocity. The measurement domain would have to be extensive enough to account for the dispersive effects of vertical shear in the horizontal winds and the vertical redistribution of ^{34}S that occurs from cloud induced mass transport.

The proposed use of a conservative tracer (SF_6) in conjunction with ^{34}S is designed to circumvent the need for total mass flux determination. Measurements of the flux of the ^{34}S to SF_6 ratios at different downwind locations allows the calculation of ^{34}S depletion normalized by the mass of an inert species. The analysis presented above is now applicable with the understanding that the precision in mass flux measurements pertains to the flux of the reactive-to-inert tracer concentration ratios.

The assumptions of vertical uniformity in ^{34}S concentration distribution and stationarity of oxidation and deposition rate constants are necessary to permit analytic solutions of the simple set of mass balance equations. The uniform concentration distribution assumption introduces further liberalism into the analysis because it yields an upper bound on the calculated mass deposition, for a given deposition rate. Under this assumption, the efficient turbulent transport of pollutant toward the ground subjects the entire pollutant mass to deposition. If the aerodynamic resistance to pollutant transport was large (i.e., under stable conditions), only a fraction of the elevated plume would be efficiently removed at the ground.

An examination of the difference in deposition resulting from a source depletion approximation (equivalent to the uniform concentration distribution assumption) and a surface depletion approximation (where only a portion of the pollutant mass is removed at the surface) has been reported by Horst (1977). Horst displays graphically the overestimation of deposition computed via the source depletion relative to the surface depletion approximation. Under moderately strong deposition and stable conditions, the deposition excess can exceed a factor of 3 to 4 for downwind distances greater than 10 km. This excess deposition decreases for decreasing stability, and for conditions under which the aerodynamic resistance is low in comparison with surface resistance, the errors diminish in magnitude.

The analysis presented in this section can be modified, albeit with a loss in simplification, to reflect different stabilities and non-uniform concentration distribution but the results of Horst (1977) suggests that the minimum mass flux measurement precision would become more stringent. Thus, the analysis performed here can be viewed as a liberal estimate of the uncertainties associated with calculating deposition via mass flux differencing.

The minimum measurement precision values displayed in Figure 5-30 are dependent on the constant oxidation and deposition rates selected. In reality, these rates are spatially and temporally variable. A simplified attempt to introduce the uncertainties resulting from uncertain rate constant values has been performed. The reduction in minimum allowable mass flux measurement precision due to rate constant uncertainty (compare Figures 5-30b with 5-30a) must be viewed with a full appreciation of the assumptions involved. Certainly, a more rigorous analysis, using a time-varying model with spatially and temporally variable transport, transformation, and deposition, would serve to refine the estimates of minimum required precision.

In an attempt to refine the analysis and to confirm the assertion that the simple mass balance approach yields liberal $C_v(\text{upper limit})$ estimates, results of the model prediction of χ/Q values for ^{34}S and SF_6 at ground level receptors arranged in concentric arcs of 10 km separation are examined. Since the proposed short-range reactive tracer experiment is designed as an intensive, short-term experiment, the model results from a one-hour period characterized by well-defined transport (1500-1600, 6 July 1978) are discussed.

Figures 5-31 and 5-32 illustrate the χ/Q distributions for SF_6 and ^{34}S , respectively, out to distances of 100 km. The distribution of the ^{34}S to SF_6 relative dispersion ratios are shown in Figure 5-33. The

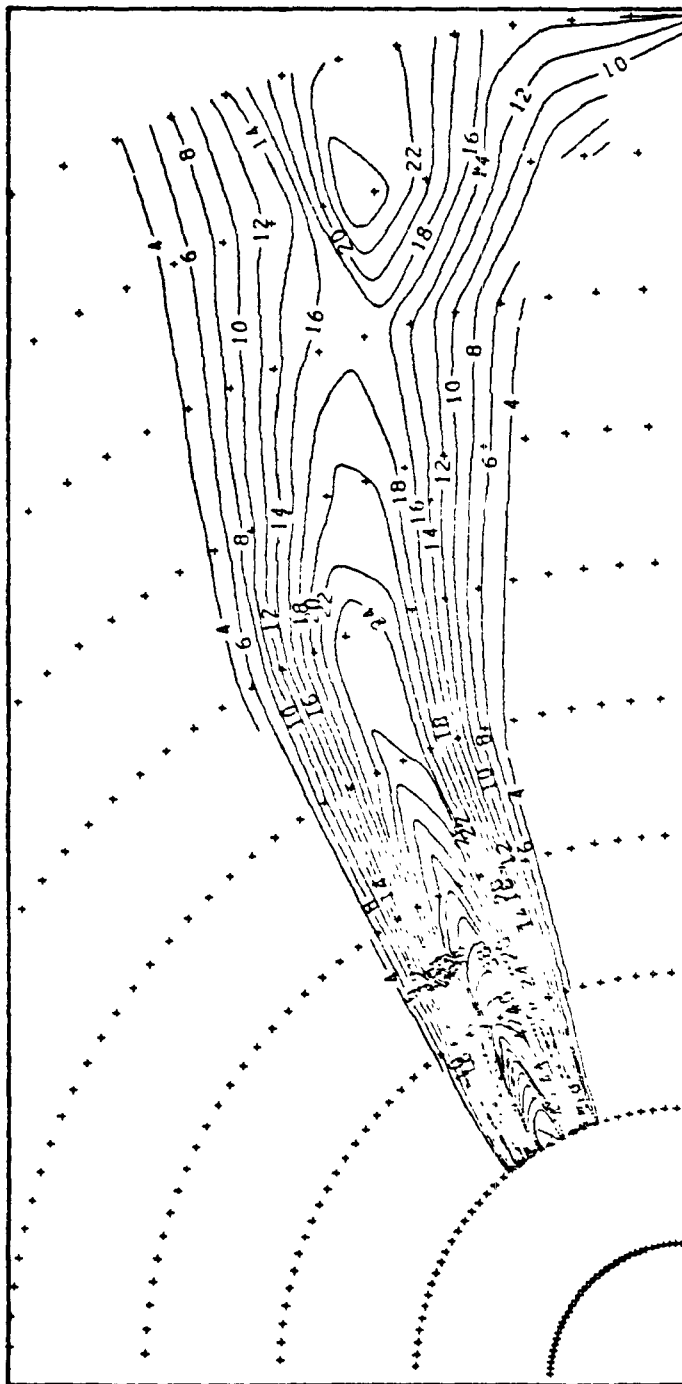


FIGURE 5-31. Spatial distribution of hourly average SF_6 χ/Q for 1500-1600 EST, July 6, 1978 (Milliken Power Plant, central New York State).

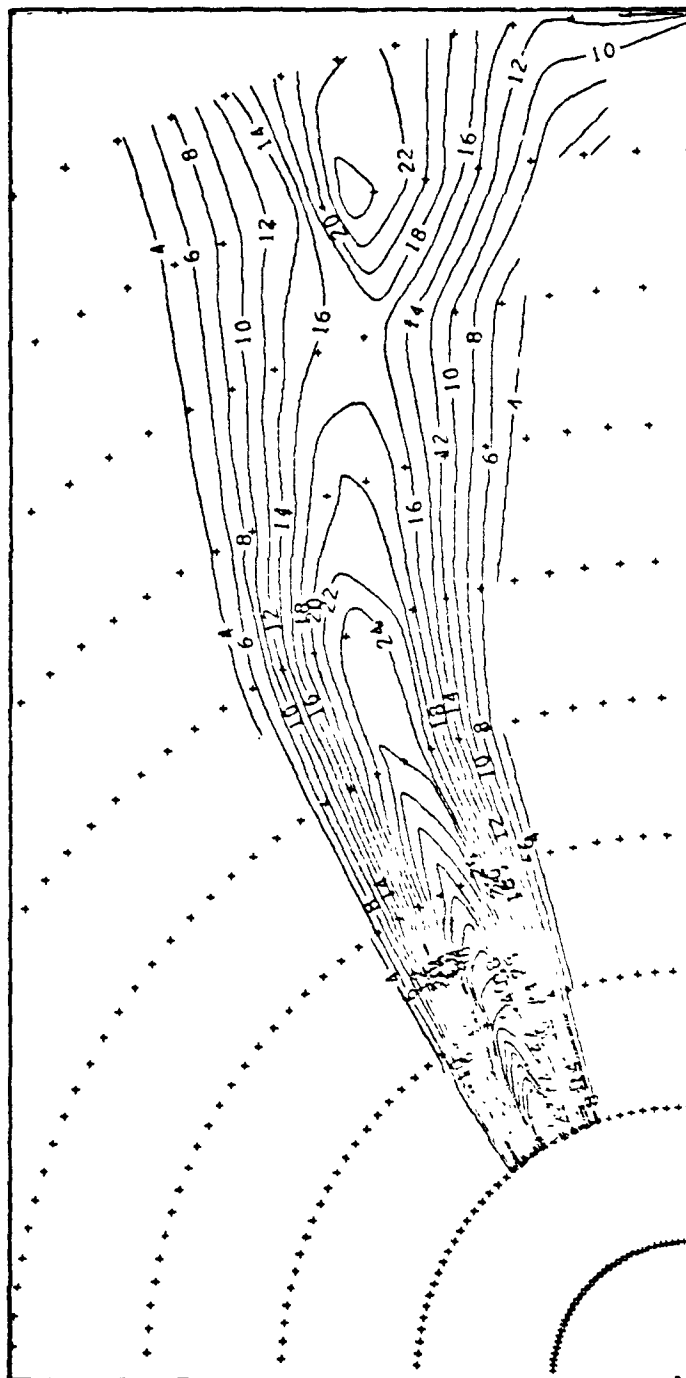


FIGURE 5-32. Spatial distribution of hourly average sulfur 34 x/Q for 1500-1600 EST, July 6, 1978 (Milliken Power Plant, central New York State).

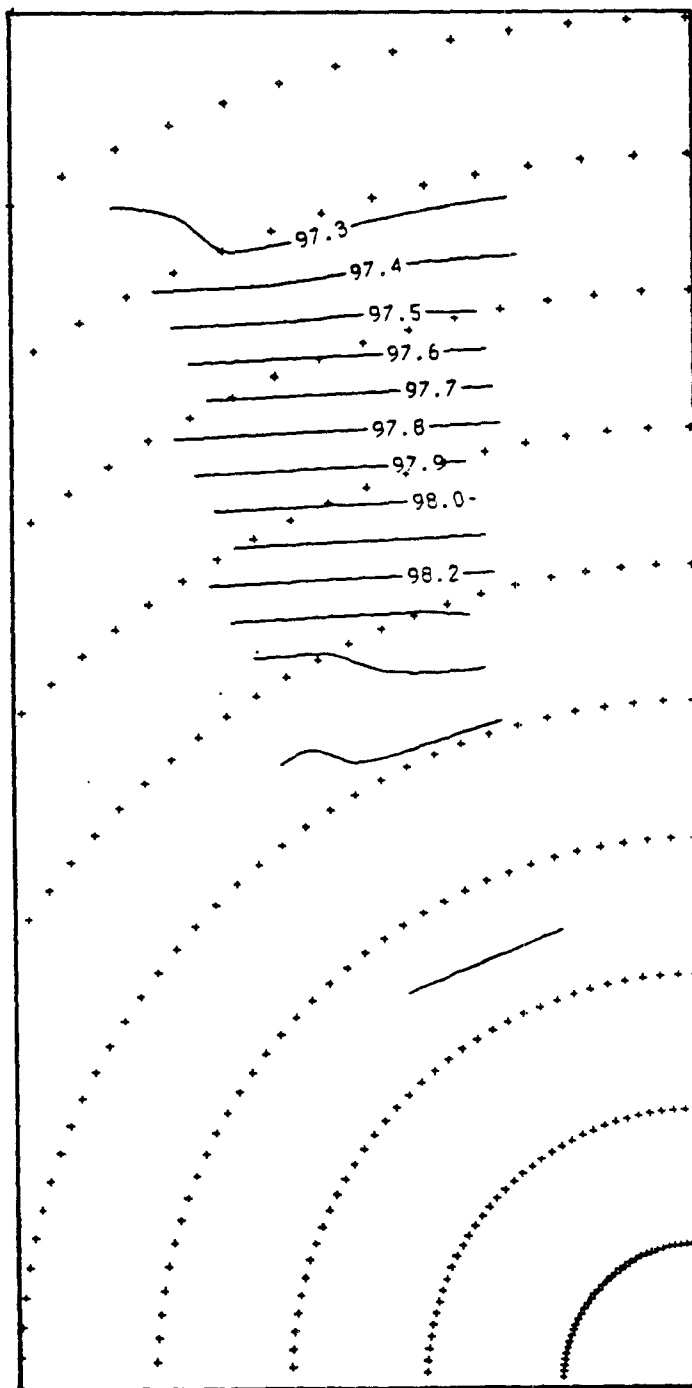


FIGURE 5-33. Spatial distribution of hourly average ratio of ^{34}S x/Q to SF_6 x/Q for 1500-1600 EST, July 6, 1978 (Milliken Power Plant, central New York State).

decreasing ratios with downwind distances are indicative of the model-calculated deposition of ^{34}S in the form of SO_2 and sulfate. Table 5-1 lists the percentage change in the χ/Q ratio (normalized by the average χ/Q ratio) across the distance interval separating the arcs where hypothetical concentration ratio measurements would be obtained.

These results suggest that less sulfur mass is deposited over these distance intervals than was calculated by the simplistic mass balance approach. The likely cause of this is the fact that in the model dry deposition is calculated from the surface layer portion of the elevated plume, not the entire plume mass. This is in accord with the surface depletion approximation.

The results of these deposition detectability estimates suggest that high precision is required in measuring the ratios of ^{34}S to SF_6 . Combining the uncertainties in measuring ^{34}S with those of measuring SF_6 , the uncertainty in measuring the ratio, R , is given by:

$$\frac{\sigma_R}{R} = \left[\left(\frac{\sigma_{^{34}\text{S}}}{[^{34}\text{S}]} \right)^2 + \left(\frac{\sigma_{\text{SF}_6}}{[\text{SF}_6]} \right)^2 \right]^{1/2}$$

where σ represents the measurement uncertainty and $[]$ represents the measured concentration.

Provided sufficient SO_2 and sulfate mass is collected at each sampling location, the uncertainty in measuring ^{34}S concentrations (Section 2.3) is negligible compared with SF_6 measurement uncertainties. Hence, the relative uncertainty in the ratio measurement is approximately equal to that associated with the SF_6 measurement. The relative fraction of airborne ^{34}S deposited between arcs therefore must exceed the relative uncertainty in measuring SF_6 . If we assume, as in the previous analysis, that the coefficient of variation of SF_6 mass flux measurements is equal to that of a single

TABLE 5-1

DIFFERENCE IN RATIOS OF NORMALIZED ^{34}S TO NORMALIZED SF_6 CONCENTRATIONS AS A FUNCTION OF THE DISTANCE BETWEEN SAMPLING ARCS. DIFFERENCES ARE EXPRESSED AS THE PERCENTAGE OF THE AVERAGE RATIO ACROSS THE INTERVAL BETWEEN ARCS.

Arc Distance (km)	Ratio	Distance Between Sampling Arcs (km)*							
		10	20	30	40	50	60	70	80
20	0.9868	--	--	--	--	--	--	--	--
30	0.9863	0.05	--	--	--	--	--	--	--
40	0.9857	0.06	0.11	--	--	--	--	--	--
50	0.9852	0.05	0.11	0.16	--	--	--	--	--
60	0.9834	0.18	0.23	0.29	0.35	--	--	--	--
70	0.9799	0.36	0.54	0.59	0.65	0.70	--	--	--
80	0.9865	0.35	0.70	0.88	0.94	1.00	1.05	--	--
90	0.9733	0.33	0.68	1.03	1.22	1.27	1.33	1.38	--
100	0.9725	0.08	0.41	0.76	1.11	1.30	1.34	1.41	1.46

* The distance between arcs is measured upwind from the arc distance listed in the left-most column.

concentration measurement (neglecting other uncertainties in integrating the concentration across a y-z plane), and further assume that this uncertainty is independent of downwind distance (i.e., SF_6 magnitude), the model-predicted relative ^{34}S deposition values listed in Table 5-1 represent the minimum SF_6 measurement precision necessary to detect ^{34}S deposition. Each of the assumptions stated above are liberal, indicating that the minimum SF_6 mass flux precision is likely to be overestimated.

If the model results are more indicative of the magnitude of ^{34}S deposited than the mass balance approach, the precision of SF_6 measurements in the field (i.e., ~10 percent) does not appear to yield detectable sulfur deposition for the proposed scale of the experiment.

From these tentative conclusions based on modeling analysis and simplified mass balance considerations, the following recommendations emerge:

1. Long-range tracer experiments designed to determine potential regional source contributions to air quality and deposition over a receptor should consider spatially distributed tracer releases rather than a single point release. Obviously, a trade-off exists between realistic simulation of source region emissions and logistical concern with coordinated tracer releases. Additional analyses are required for testing final tracer release configurations.
2. Local-source modulation experiments will probably yield more definitive estimates of source attribution if the experiments are conducted for long periods of time (longer than one month). The magnitude of the detectable signals, when coupled with limited measurement precision, is strongly embedded in noise of comparable or greater magnitude. Hence, statistical analyses of extended concentration time series might be the most appropriate method for the modulated signal isolation. Long-term model simulations would be required to further investigate this issue.
3. Because of the small magnitude of sulfur dry deposition predicted by the model and by a simplified application of the mass balance approach, an experiment designed to calculate the deposition by measuring sulfur mass fluxes over local scales appears to be a difficult undertaking. Emphasis should be on a thorough characterization of the reactive tracer mass flux, since its measurement precision is excellent. Measurements of reactive-to-inert tracer concentrations will be highly affected by the inert

tracer measurement uncertainty. A more sophisticated dry deposition analysis would be useful for verifying the modeling results presented. A detailed analysis of additional uncertainty components in mass flux characterization is warranted.

5.4 Implications in Experimental Design

A modified regional transport model was used to examine the detectability of inert and reactive tracer concentration signals and the signals resulting from local SO₂ source modulations. The uncertainties inherent in the modeling approach have not been extensively analyzed because of the monumental task of such an undertaking and the limited scope of this uncertainty survey. In most cases, however, the detectability analyses have relied on differences of model predictions rather than the absolute model predictions. While this strategy does not eliminate modeling uncertainties, it allows one to examine the relative sensitivity of detectability without being overwhelmed by the uncertainty inherent in absolute model predictions. Nevertheless, the conclusions should be regarded only as approximate indications of signal detectability.

For the proposed long-range inert tracer experiment, the regional model was exercised to provide an indication of the tracer detectability frequency, as a function of tracer emission rates, and to provide an indication of how adequately a single point tracer release serves as a surrogate for emissions from a source region. The main conclusions are as follows:

1. Qualitatively, the continuous release of perfluorocarbon tracers from either a single point source or a cluster of point sources over month-long periods yields a spatial/temporal concentration distribution over the Adirondacks that suggests the existence of an optimum emission rate. This optimum emission rate is expressed in terms of gain in detection frequency per unit increase in emissions rate. For realistic tracer emission rates, this characteristic is not found when tracers are released in an intermittent (one day on, two days off) manner. (Quantitative indications of required tracer emission rates for selected detection frequencies are presented.) Both PMCP and PMCH perfluorocarbon species were considered and release locations in the upper and lower Ohio River Valley regions were examined.

2. Simulations of inert tracer concentration distributions over the Adirondack region arising from single point and multiple point releases show sufficient bias and lack of correlation to suggest that a single point tracer release configuration is not an adequate surrogate for a spatially distributed emission region. The lack of similarity in concentration distribution is enhanced when tracers are released in an intermittent manner.

Two issues of signal detectability pertaining to the proposed short-range experiments were examined as well. First, characteristics of the SO₂ and sulfate concentration distributions attributable to continuous and modulated emissions (one week on, one week off) of three New York point sources were examined. Second, the detectability of sulfur deposition calculated by differencing local-scale mass flux measurements was analyzed. Results of these analyses are summarized below.

1. The SO₂ and sulfate concentration signals attributable to the three New York point sources are generally small relative to background concentration levels. When measurement uncertainties are considered, the frequency of 1-hour SO₂ signal detection during two one-month periods is less than 20 percent for the continuous emissions case. The frequency of detection of three-hour sulfate concentration is lower. If modulated emissions are considered, the decrease in detection frequency is highly dependent on meteorological factors, indicating that for experiments of one-month duration there is a good chance sulfur concentration data from the "non-plume" (as deduced from the inert-tracer-tagged plume) will be insufficient for source attribution analysis.
2. The above finding prompted a comparative analysis of week-to-week SO₂ and sulfate variability due to (a) natural meteorological variability and (b) weekly SO₂ emission modulation. Results indicate that the natural week-to-week variability is larger in magnitude than the modulation-induced variability. While these results should not be interpreted as suggesting that modulation-induced signals are not extractable from data, they do suggest that such a small data sample (from a one-month experiment) may be insufficient for a conclusive source attribution analysis.
3. An analytic mass balance approach was used to estimate sulfur dry deposition (as SO₂ and sulfate) as a function of the downwind distance from a source and the distance interval separating hypothetical mass flux measurement locations. Results suggest that the minimum mass flux measurement precision (expressed as the coefficient of variation) necessary to ensure a detectable

deposition is on the order of 20 percent for a distance interval equivalent to the initial 16 hours of plume travel time. (Results pertaining to other separation and downwind distances are presented graphically.) If the total sulfur mass flux is measured at each downwind distance, the measurement precision of the $^{34}\text{S}/^{32}\text{S}$ ratio is sufficiently high to offer encouragement to this type of experiment, under conditions appropriate for the validity of the mass balance approach (i.e., unstable, well-mixed conditions, high deposition velocity). If the mass flux is not completely accounted for in the measurements, the necessity of calculating sulfur flux differences by differencing the reactive-to-inert tracer concentration ratios introduces the measurement uncertainty of the inert tracer into the analysis. Since the precision of measuring SF_6 is considerably lower than the of measuring $^{34}\text{S}/^{32}\text{S}$, the experiment appears less feasible.

4. The model was exercised to examine the consequences of removing some of the assumptions invoked in the mass balance analysis. The results indicate that, conditions in which dry deposition depletes only the lower portion of the plume (e.g., high aerodynamic resistance associated with stable conditions), the minimum mass flux precision requirement decreases to 1 percent for spatial scales considered in the proposed reactive tracer experiment.

SECTION 6

ADDITIONAL UNCERTAINTY ANALYSES

Portions of the COMPEX design were evaluated through analyses of an assortment of data sets currently available. This section reviews data sets currently available from two long-range transport experiments, the SURE program, and precipitation chemistry networks. The topics considered include:

- the potential characterization of long range transport by ground-level concentration measurements;
- the climatological categorization of data for empirical analyses; and
- the frequency of source/receptor interactions.

6.1 Analysis of Long Range Pollutant Transport Using Tracer Data

The Cross-Appalachian Tracer Experiment (CAPTEX) was designed to provide data on the long range transport and dispersion of pollutants for use in evaluating long range transport models. The experiment was held in the fall of 1983 and consisted of limited releases and measurements of perfluorocarbon (PFC) tracers over the northeast. Data available from the experiment include short-term samples of the tracer on a ground level sampling network and aircraft. Meteorological data from an enhanced rawinsonde network are also available. The CAPTEX data are of interest for analysis because they show transport and dispersion patterns which are similar to those that will be studied in the combined experiment. The objectives of this review are to qualitatively examine the patterns of ground level perfluorocarbon concentrations to evaluate the likelihood of determining trajectories from tracer data and to evaluate the sampling network resolution. The combined experiments depend on both PFC sampling (on similar spatial and temporal scales) and the use of ground level samples to determine trajectories for transmittance calculations.

6.1.1 Summary of the CAPTEX Program

The CAPTEX program is described in a revised work plan written by Ferber and Heffter (1983). During September and October, 1983, a PFC tracer was released in seven experiments, five of which were made from Dayton, Ohio, and two were made from Sudbury, Ontario. The releases were generally of three hours duration over which 200 kg were released. Releases were made in the afternoon to correspond to the maximum possible convective mixing and the largest distribution of tracer in the mixed layer.

Sampling was performed by seven aircraft and a ground sampling network of approximately 100 samplers distributed over northeastern United States and Southern Ontario. The samples used for this analysis were three- and six-hour samples from the ground level network.

The aircraft data and the final CAPTEX data base were not available at the time of the analysis. As a result, the data used in the analysis did not represent a complete data set nor were they satisfactorily calibrated. This limited the usefulness of the data by an inability to specify absolute concentrations and data gaps due to sites with missing data. The problems with the data were sufficient to limit the use of the data to a qualitative analysis of the potential for determining trajectories, evaluating sampler spacing, and examining the gross features of the concentrations patterns.

Sample spacing of the ground sampling network was established by different criteria in the downwind and cross-wind directions. In the downwind direction, samplers were placed at approximately 100 km intervals starting at 300 km and continuing 500 to 1000 km. The cross-wind spacing on sampling arcs was established by estimating the expected width of tracer plumes as a function of travel time. Since two release sites were used, the final sampling grid was adjusted to provide the required resolution from both sites without overlapping sites.

6.1.2 Analysis Results

The analysis results are summarized as qualitative observations on transport and dispersion:

- Ground level tracer concentrations tend to lag the transport of the center of mass of the tracer plume or puff. In some cases, substantial delays were encountered where tracer concentrations remained in an area after the main tracer cloud was transported downwind on the sampling grid.
- In all cases studied, the progression of the tracer cloud could be observed in time sequences of spatial plots. Plotting maximum concentrations for each release episode provided a tracer trajectory. These data indicated promise in estimating trajectory positions using tracer data.
- Tracer plumes appeared to be elongated and narrow relative to the sampler spacing in a number of release events. Missing observations on the network appeared to be the significant cause of difficulty in describing the transport and dispersion of the tracer.
- Tracer data in some of the experiments indicate that tracer plumes can be split by wind shear with parts of the release being transported on significantly different paths.

6.1.3 General Observations on the CAPTEX Experiments

In addition to the questions of uncertainty and the feasibility of the techniques in the combined experiments, the CAPTEX program provided some information on the operational aspects of the experiment. Discussions with the CAPTEX participants provided the following observations on experimental design:

- CAPTEX suffered data losses due to non-functioning tracer samplers. In some tests, up to a third of the samplers were not in operation due primarily to mechanical and electronic problems. Some of the problems appeared to be weather-related and indicated a deficiency in environmental testing of the samplers. Such high data loss rates would not be acceptable in the combined experiments due to a very high reliance on the tracer data for determining transport paths.
- The combined experiments use aircraft sampling in measurements to support mass balance calculations. CAPTEX aircraft operations

were hindered by flight limitations imposed in some areas of the country and the reluctance of temporary pilots to fly in some areas of complex terrain including over the Great Lakes. One aspect of operational planning for the study is the definition and approval of strict flight patterns. In addition, it is suggested that project pilots be dedicated to the project.

- Sounding times for the standard rawinsonde network typically represent only transition times in the diurnal cycle and are, therefore, not the most representative for air quality studies.

6.2 Climatological Analysis of the Experimental Design

The main COMPEX experiments will take place over a one year period as specified by EPA. The objective of the program is to derive empirical source/receptor relationships which will require a sufficient number of experimental events to generate acceptable confidence limits on the results. This section summarizes some of the studies performed to investigate the adequacy of the experimental program. Issues considered in the analyses include:

- Characteristic durations of wet deposition events.
- Climatological categorization of data in previous studies in terms of deposition event characteristics.
- Adequacy of a one year experimental program for empirical deposition studies.

6.2.1 Duration of Wet Deposition Events

Precipitation and corresponding wet deposition events vary in duration and timing which result in difficulty selecting an adequate sampling time. This subsection briefly examines the duration of precipitation events relative to the sampling frequency proposed as part of COMPEX. The COMPEX precipitation chemistry sampling protocol is for event sampling with a daily maximum duration of sampling. Ambient pollutant concentrations are to be collected on a six hour basis.

Table 6-1 summarizes the duration of precipitation and deposition events reported by Thorp and Scott (1982). The preponderance of short-lived (<6-hour) storms in the summer would seem to indicate that precipitation chemistry samples should be collected and analyzed on a 6-hour basis in the summer. However, if most storms are separated by 40 to 60 dry hours in the summer, then a 24-hour sample would generally cover the whole storm but not more than one storm. Nonetheless, it may still might be important to collect 6-hour precipitation chemistry samples for direct comparison to the 6-hour ambient pollution concentration obtained in the summer months. Winter data showed an infrequency of short-lived (<6 hours) storms.

6.2.2 Climatological Characterization of Deposition Events

To select schemes for statistically analyzing data from acidic deposition studies it is useful to examine data from previous experiments to first understand, to the degree possible, concentration and deposition events and then to review possible schemes for analysis. Variations in sulfur deposition and concentrations are significantly influenced by variations in meteorological conditions. Raynor and Hayes (1982), Henderson and Weinggartner (1982), Niemann (1982), Mueller and Hidy (1983), and others have used several data sets to demonstrate the seasonality of airborne sulfate concentration and deposition. This dependence takes the form of summer peaks in concentrations even though precursor SO₂ emissions may not be a maximum during this period. On a shorter time scale, Tong and Batchelder (1978) demonstrated with time/distance transects of daily concentrations in the northeast that sulfate concentrations exhibit a wave-like pattern related to cyclonic migrations.

TABLE 6-1

DURATION OF PRECIPITATION/DEPOSITION EVENTS
PERCENT OF STORMS AND PERCENT OF PRECIPITATION
VERSUS STORM DURATION PERIODS, BY SEASON

	Storm Durations*			
	Summer (J,J,A)		Winter (D,J,F)	
	< 6 hrs	< 24 hrs	< 6 hrs	< 24 hrs
Percent Storms	82	100	44	86
Percent Precipitation	58	98	7	52

Storm Frequencies

Storms occur every 40 to 60 hours in summer
Storms occur every 35 to 90 hours in winter

- * Consecutive precipitation events were deemed different storms if separated by 3 dry hours in summer and 6 dry hours in winter.

Ambient Sulfate Episodes

Mueller and Hidy (1983) and Tong and Batchfelder (1978) analyzed data from the SURE program (Section 4.1) and described synoptic conditions for a total of 14 events resulting in high or low regional sulfate concentrations. Most significant peak episodes are characterized as follows:

- 1) Conditions favorable to an accumulation of SO_2 emissions in various source regions.
- 2) Conditions must be favorable for the conversion of sulfur dioxide to sulfate. High incoming solar radiation and high atmospheric moisture content have been demonstrated to greatly enhance the conversion of sulfur dioxide to sulfate in the atmosphere. Slow moving anticyclonic systems in the summer months provide the mechanism for conversion of sulfur dioxide to sulfate with clear skies and ample solar insolation. Further, as anticyclones migrate across the eastern United States, linking with the semi-permanent Bermuda high pressure system, southwesterly winds on the back side of the high pressure system advect moisture from the Gulf of Mexico into the region. Such conditions are associated with the maritime tropical air mass frequently associated with elevated sulfate events in the eastern United States during summer months.
- 3) Conditions including southwesterly winds on the back side of anticyclones. The transport wind provides a link between high emissions areas and critical receptor regions.
- 4) Conditions where enroute precipitation scavenging is small.

A useful scheme for understanding the relationship between synoptic conditions and elevated sulfate concentrations was presented by Mueller and Hidy (1983). The method is basically a classification system for describing air mass types and is reproduced in Figure 6-1. Depending on the position of the high pressure system in relation to a particular source or receptor region, vastly different air mass characteristics may be experienced. In this scheme, a high pressure system, originating in Central Canada, is centered over the Great Lakes. The air mass maintains the basic characteristics of its source region -- a continental, polar location (hence the designation "cP"). The leading edge of the high pressure system is characterized by northerly

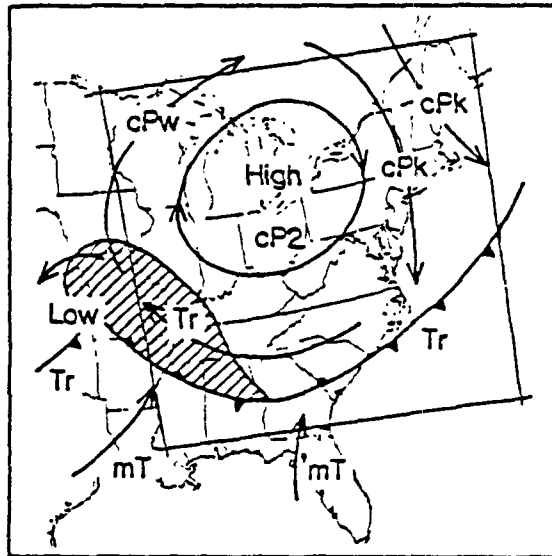


Figure 6-1. Air mass classification scheme used in SURE data analysis
SOURCE: Mueller and Hidy (1983)

wind components which advect colder air into a region (cPk - "k" for "kolder"), while southerly winds behind the center of the high advect typically warmer air (or "cPw"). The "cP2" designation is used to identify the center of the high pressure system. Two other air mass types are described in this approach. The transitional (Tr) air masses essentially describe cyclonic systems which are not stratified in terms of temperature or moisture, but rather are well mixed. All frontal systems are grouped in this category. The final category is the maritime tropical air mass (mT). Although not shown in this configuration in Figure 6-1, mT air masses frequently extend into the midwest and northeast, especially in the summer months in association with Bermuda High. The primary difference between cPw air masses result from advection of warm, continental air and are therefore drier than air advected from the Gulf as represented by the mT category.

Mueller and Hidy (1983) computed mean values for a number of parameters, including sulfate concentrations, at a number of observing stations for each air mass category (Figure 6-2). In addition, the number of sulfate events encompassing increasingly large geographic areas were compiled for each air mass category (Table 6-2).

From Figure 6-2, average ambient sulfate concentrations in the northeast were found to be highest during mT air masses, followed by cPw and cP2 air masses. In contrast, cPk air masses, which typically occur directly behind cold fronts and are characterized by northerly winds, exhibit the lowest ambient sulfate concentrations. Transitional air masses, those associated with cyclonic systems and frontal zones, also show relatively low sulfate concentrations.

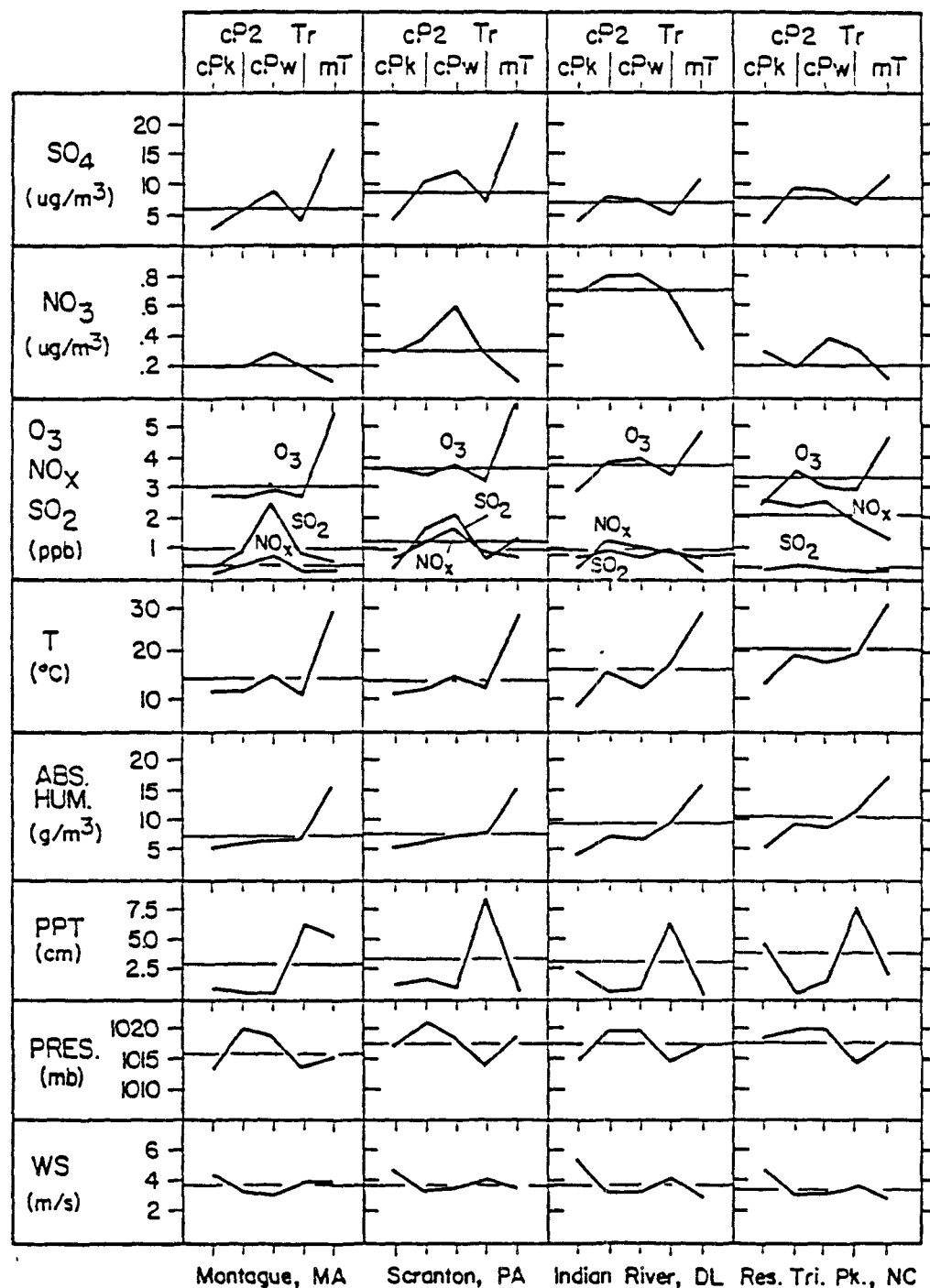


Figure 6-2. Variations of arithmetic mean values for individual areometric parameters for Class I stations in the northeast coast region. SOURCE: Mueller and Hidy (1983)

TABLE 6-2

ANNUAL PERCENTAGE OF EVENT DAYS BY AIR-MASS CATEGORY

Event Group	Air Mass Category					Annual Percentage of Days in each Event Group
	cPk	cP2	cPw	Tr	mT	
Regional	0	12	7	2	9	30
Subregional	0	4	4	4	3	15
Nonregional	2	10	2	18	0.5	32.5
No Event	6	4	0.5	12	0	22.5
Annual Percentage of Days in each air mass	8	30	13.5	36	12.5	100

Key:

Regional Event - more than 15% of sulfate recording stations in Northeast recorded concentrations greater than 15 ug/m^3 .

Subregional Event - 5-15% of stations greater than 15 ug/m^3 .

Nonregional Event - less than 5% of stations greater than 15 ug/m^3 .

No Event - no stations greater than 15 ug/m^3 .

Source: Mueller and Hidy (1983)

These findings are supported somewhat by the results shown in Table 6-2. In terms of the duration and the areal extent of each sulfate event, cP2 and mT air masses are the most frequent. In other words, elevated sulfate levels covering a large geographic area occur most frequently with cP2 and mT air masses, and do not occur at all with cPk air masses. Conversely, sulfate-clear days occur most frequently with Tr and cPk masses, and not at all during mT conditions.

Also shown in Table 6-2 is the frequency at which various air mass types occur in the SURE experimental region -- the midwest and the northeast. For example synoptic conditions dominated by cyclonic systems (Tr category) occur 36% of the time, whereas only 12.5% of the days in a year are characterized as being under maritime tropical (mT) conditions. Such climatological data are important considerations in the design of any acid deposition measurement program.

Wet Deposition Episodes

As mentioned, the amount of acid-forming substances deposited on the ground by wet processes is dependent upon both the presence of sulfates in the atmosphere and the occurrence of precipitation. Precipitation throughout the midwest and northeast can be associated with several types of synoptic systems. The passage of cyclonic systems through the regions are responsible for most of the precipitation, whether from warm, cold, or occluded fronts, or from the cyclone itself. Other rain producing events include pre-frontal squall-lines and convective thunderstorms.

Rain is much more frequently associated with the deposition of acid-forming substances than is snow. This could be due to reduced photochemical conversion of sulfur dioxide to sulfates in the winter and because snow has been found to be much less efficient than rain in scavenging

sulfate particles (Niemann, 1983). Hence, the peaks deposition events of acid forming substances through wet processes occurs primarily with precipitation in liquid form.

The amount of acid-forming substances deposited during precipitation events largely depends on the amount of precipitation occurring during the event and the trajectory of the air mass en route to the receptor region. Wilson, et al. (1982) illustrates in Figure 6-3 the amount of precipitation received at Whiteface Mountain, New York in 1978 by trajectory sector, and the resulting sulfate ion concentrations in the precipitation. Most of the precipitation (56%) received at Whiteface Mountain results from air masses that originate south and/or west of New York, and similarly, most of the sulfate ion concentration (64%) contained in the total annual precipitation amount is from the same sector. In fact, a disproportionate amount of the sulfate ions contained in the total annual precipitation at Whiteface Mountain results from the southerly through westerly sector, indicating the importance of source regions in those directions.

Raynor and Hayes (1982) have provided a description of wet deposition events at Brookhaven National Laboratory in New York as a function of synoptic conditions and types of precipitation amounts. Most of the precipitation occurring at Brookhaven occurs during warm and cold front passages, and the deposition of the various chemical species occurs during the same conditions. They note that the amount of sulfates deposited during squall line precipitation events exceeds the proportion of rainfall received in such systems implying a dependence on precipitation. They present plots of the amount of precipitation and chemical species deposited at Brookhaven as a function of precipitation type. A distinction is also made in the data

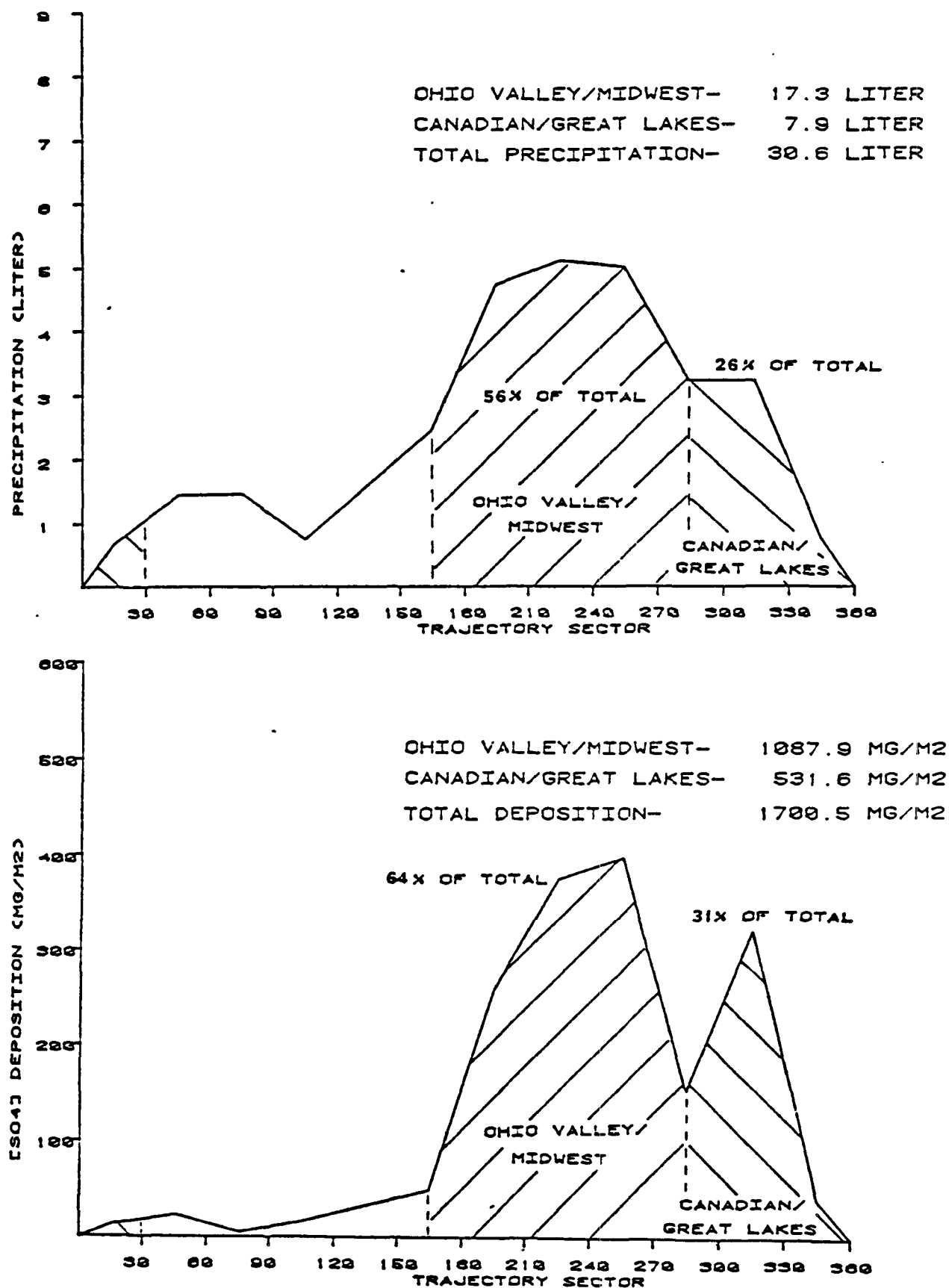


Figure 6-3. Precipitation (top) and sulfate ion concentration in precipitation (bottom) as a function of the directional sector through which the air parcel passed to reach Whiteface Mountain, New York in 1978.
SOURCE. Wilson, et al, (1982)

between deposition amount and concentration which is a function of precipitation type. For example, the concentration of sulfates in convective rains is typically higher than that of "general" rains which are presumed to mean warm frontal rains. Total deposition from convective storms was shown typically to be less because the duration of precipitation in combination with the higher concentrations in rain water were insufficient to exceed the total deposition of long steady rain events.

Niemann (1982) has provided an analysis of "exceptional episodes" of wet deposition at Whiteface Mountain and Ithaca, both in New York, based on data collected during the MAP3S program. His review indicated that 3 deposition events at Whiteface Mountain in 1978 contributed 30% of the total annual amount of sulfates deposited. At Ithaca in 1980, 3 events contributed 14% of the annual sulfate total. It is clear that acid deposition due to wet processes can be of an episodic nature. Niemann goes on to point out that such episodes tend to be localized, being on the scale of thunderstorms (about 10^4 km²).

Henderson (1982) also sheds some additional light on the episodic nature of wet acid deposition events using data collected during the MAP3S program. The average sulfate loading per precipitation event occurring with southwest trajectories at Ithaca, New York during the summers of 1978 and 1979 was found to be 720 micro-moles per square meter. However, the peak sulfate loading observed during the period was 2698 micro-moles per square meter -- almost a factor of four times higher than the mean value.

Synoptic Classification Schemes

Few classification schemes for statistical analyses have been developed due to the lack of an appropriate data base. The SURE analyses developed a classification scheme for sulfate concentrations which could be generalized to

dry deposition episodes. The scheme is based on identifying synoptic types. A limitation of the scheme is the large number of cases which fall into the transitional classification which includes most precipitation deposition events.

For meteorological and climatological studies, various other schemes have been developed but in general their orientation is directed toward large scale forecasting applications. For example, a scheme by Krick (1943) which initially appeared interesting for this study proved too specific and extensive for use. The Krick scheme included seven basic synoptic types based on location of a Pacific high. These classes were further distributed over 36 types which included seasonal effects and 10 phases or subclasses.

Perhaps the best climatological scheme for analysis may be a modification of the SURE scheme to allow allocation of transitional cases among additional cases. The transitional cases are critical in the characterization of wet deposition events. Expansion of the precipitation events as a subclass of the transitional cases could possibly be in the following categories:

- Precipitation events associated with cold fronts.
- Non-frontal precipitation.
- Warm frontal of overrunning precipitation.
- Precipitation in a cyclone without organized or distinguishable fronts.
- Precipitation in occluded systems.

In addition to the synoptic schemes several categorization schemes are possible such as by direction of trajectories. A problem in developing schemes is allocation of the limited number of events and limited data available from the field program to demonstrate this concern. Data analyses by Thorp and Scott (1982) can be considered.

The authors studied precipitation records from 77 locations covering 5 summers and 5 winter months over a 3-year period. Statistics were compiled for a total of 4516 summer and 3870 winter precipitation events. These data show that the average number of precipitation events in a given summer month is 12. In winter the average monthly number of such events is 10. Thus, in a year the total number of precipitation events at any single location is likely to be approximately 132.

During the proposed one-year monitoring program, tracer releases will be made during the first day of 120 3-day periods. No tracer will be released on the second or third days of the 3-day cycle. Since roughly one-third of the days in a year record precipitation, then only one-third of the tracer releases can be expected to be affected by precipitation. Therefore, the number of tracer releases likely to coincide with precipitation events at any single location is limited to 40. Only 15 to 20 precipitation events are likely to occur during the summer months. This is a somewhat limited data base upon which to establish relationships among measured parameters. Any additional sub-grouping of events will further reduce the number of events in any group and further decrease the significance of the statistical relationships obtained among the measured parameters.

6.2.3 Analysis of the Adequacy of a One-Year Monitoring Program

It has been noted in previous sections that the frequency of source/receptor interactions is small. Remedial modifications were made to the COMPEX design based on these observations. In the previous subsection it was noted that the combination of a low source/receptor interaction frequency of the large array of potential meteorological conditions require caution to limit the number of categories used in analyzing the data. This section

describes further the frequency of deposition events in an attempt to determine the adequacy of a one year experimental program in developing source/receptor relationships.

Tables 6-3 and 6-4 summarize an analysis of MAP3S precipitation chemistry data performed to examine the year to year variability of wet deposition data. The data show that both precipitation and deposition vary by a considerable amount from year to year. Precipitation varies by up to ± 20 percent from the 3- to 4-year mean values at four of the sites shown, and up to ± 30 to 40 percent at the Virginia site. Year to year variations in precipitation can thus range up to ± 40 percent. Meanwhile, deposition varies by up to ± 20 percent also, but the change in deposition amount does not necessarily follow the change in precipitation amount. For example, at the Brookhaven site, the June 1976 to May 1977 precipitation amount was 21 percent below the 4-year mean, while the deposition amount was 15 percent above the 4-year mean for the same period. In some instances there is a tendency for deposition to increase or decrease along with precipitation, but in others (e.g., 1978 at the 4 MAP3S sites), the two parameters exhibit opposite changes from year to year. Also noteworthy is the relatively constant deposition rate at the Penn State MAP3S site, which occurred despite the relatively large year to year changes in precipitation. Of the MAP3S sites, Penn State had the most complete set of valid precipitation and deposition data for the 3-year period of study.

A possible explanation for the lack of correlation between annual average precipitation and annual average deposition is the year-to-year variability in seasonal precipitation amounts coupled with the seasonal variability in the total sulfur concentrations in the precipitation. An example of this phenomenon is shown in Table 6-5 which results from analysis of the data obtained from the MAP3S study (MAP3S/RAINE Research Community, 1982).

TABLE 6-3

YEARLY PERCENT DEVIATIONS FROM 4-YEAR MEAN
PRECIPITATION AND SULFATE DEPOSITION AMOUNTS AT
BROOKHAVEN NATIONAL LABORATORY, UPTON, LI, NY

	Year			
	<u>6/76-5/77</u>	<u>6/77-5/78</u>	<u>6/78-5/79</u>	<u>6/79-5/80</u>
Percent Change from 4-Year Mean Precipitation	-21	+18	+17	-14
Percent Change from 4-Year Mean Deposition	+15	+10	-1	-24

TABLE 6-4

YEARLY PERCENT DEVIATION FROM 3-YEAR MEAN
PRECIPITATION AND TOTAL SULFUR DEPOSITION AMOUNTS AT
4 MAP3S LOCATIONS*

Location	Parameter	1977	1978	1979
Whiteface Mountain, NY	Precipitation	+13	-16	+3
	Deposition	+6	[+2]	-8
Ithaca, NY	Precipitation	+15	-21	+6
	Deposition	[+5]	[+2]	-7
Penn State, PA	Precipitation	-7	-11	+18
	Deposition	-2	+3	-1
Charlotte, VA	Precipitation	-28	-10	+38
	Deposition	[-20]	[+5]	[+15]

* Brackets indicate more than 2 months missing data.

TABLE 6-5

ANNUAL MEAN AND MONTHLY PERCENT DEVIATIONS FROM ANNUAL
MEAN CONCENTRATION, PRECIPITATION AND DEPOSITION VALUES FOR
CHARLOTTE, VIRGINIA, 1977-1978

Annual Mean of the Monthly Averages		Percent Deviations from the Annual Mean of the Monthly Averages										
		<u>J</u>	<u>F</u>	<u>M</u>	<u>A</u>	<u>M</u>	<u>J</u>	<u>J</u>	<u>A</u>	<u>S</u>	<u>O</u>	<u>N</u>
<u>1977</u>												
Total Sulfur Concentration ($\mu\text{m}/\text{l}$)	44.9	-	-67	-49	-51	+36	+20	+145	-4	+20	-	-
Precipitation (cm)	4.5	-	-76	+20	+15	+44	-34	-56	-5	-16	-	-
Total Sulfur Deposition ($\mu\text{m}/\text{m}^2$)	1808	-	-91	-31	-37	+120	-10	+21	+2	+13	-	-
<u>1978</u>												
Total Sulfur Concentration ($\mu\text{m}/\text{l}$)	32.1	-	-	-25	0	-	-	+21	-4	+25	+28	+15
Precipitation (cm)	7.7	-	-	+29	-28	-	-	+55	+42	-28	-72	-7
Total Sulfur Deposition ($\mu\text{m}/\text{m}^3$)	2398	-	-	+4	-26	-	-	+89	+46	-7	-63	+11

The above data and discussion show that the total annual deposition found in a one-year monitoring program may not be representative of the total annual deposition to be found in other years. Since a longer monitoring program is not contemplated, methods must be developed and used to relate the data gathered within a one year program to other years. Such methods will be discussed in the paragraphs that follow.

Since increases and decreases in precipitation amounts do not necessarily produce corresponding increases and decreases in deposition amounts, precipitation alone cannot be used to extrapolate deposition amounts found in one year to deposition amounts likely to be found in other years. Deposition amount is a function of both precipitation amount and the pollutant concentration in the precipitation (Raynor and Hayes, 1984). Year to year (and other time periods) changes in precipitation are a function of meteorological and climatological factors.

The preceding data show a number of common features of seasonal variability in both the total sulfur (or sulfate) concentration in the precipitation, and in the total sulfur deposition. Both parameters generally show their maxima in the summer and their minima in winter.

The most prominent feature of the Charlotte, Virginia data is the disparity between the 1977 and 1978 summer precipitation amounts. In 1977, the June, July, and August precipitation amounts were well below the mean for the year while the precipitation amounts for July and August in 1978 were well above the average for that year. As a result, the summer (July and August) and annual deposition amounts in 1978 were much greater than the summer (June through August) and annual deposition amounts in 1977. However, it is noteworthy that the summer 1977 rainfall deficiency did not produce an equivalent deficiency in deposition. The total sulfur concentrations were

greater in the precipitation in the summer of 1977 than in the summer of 1978, so this partially offset the lack of precipitation in 1977.

The above analysis of seasonal variability in precipitation and deposition amounts show that two years with equal precipitation amounts may not produce equal deposition totals. If the precipitation in different years is evenly distributed over all the months in the year, then the deposition patterns and totals for each year will have a greater tendency to be similar. If the precipitation in a given year occurs predominantly in the winter, then the year with the heavy summer rains will tend to have greater deposition totals than the other years.

These factors, plus variations in emissions, produce year-to-year changes in the pollutant concentrations in precipitation. Therefore, the key to relating the results of a one-year monitoring program is to first determine the categories of meteorological-climatological conditions that are associated with different types of short-term precipitation-concentration events. This link has been attempted through the integration of previous and current field study data into the COMPEX design by locating sampling sites at current or former monitoring sites.

6.3 Potential for Pollutant Transport as Indicated by Source/Receptor Pair Data

The long range tracer component of the combined experiment requires that releases be distributed within source areas and that releases from different source areas will be scheduled on the basis of trajectory predictions. The objective of this plan is to increase the chances for a tracer to affect the receptor region. An analysis of the Atlantic Coast Unique Regional Atmospheric Tracer Experiment (ACURATE), Heffter, et al. (1984), provides additional evidence on the probability of a tracer from a specific source area

influencing a specific receptor location. This analysis supports the need to devise methods to increase tracer impact frequency because the climatological probability of impact is low and decreases rapidly with distance. The ACURATE data suggest that the number of days annually available for analyses from a single source receptor pair separated by 1000 km is expected to be 47 days for continuous releases but only 15 days for the third day release schedule described for COMPEX.

The ACURATE program used Krypton 85 released from the Savannah River Project (SRP) as a tracer of opportunity. Five monitors were placed northeast of SRP at distances of 325 km to 1050 km. The four closer monitors provided 12 hour integrated samples. The fifth monitor sampled over 24-hour periods. Data were collected from March 9, 1982 through September 30, 1983 resulting in 1158 possible 12-hour sampling periods or 579 days.

Release events were identified as periods of at least 24 hours with Kr-85 releases. The events had to be separated by at least 24-hours when Kr-85 was not vented to the atmosphere. A total of 102 events were identified which contained 768 half-day periods corresponding to the 12-hour sampling period. Kr-85 releases occurred 66 percent of the time.

Kr-85 concentrations above background were counted for each sampling period and the frequency of occurrence was calculated for each monitor. The concentrations were pooled into categories of 100 times the detection limit, 10 times the detection limit and all samples above the detection limit. Data from Heffter, et al. (1984) in Figure 6-4 show the frequency of occurrence of each concentration category. These are plotted in Figure 6-4 as a function of distance from the source. The data are well behaved and straight lines were drawn on the probability graph.

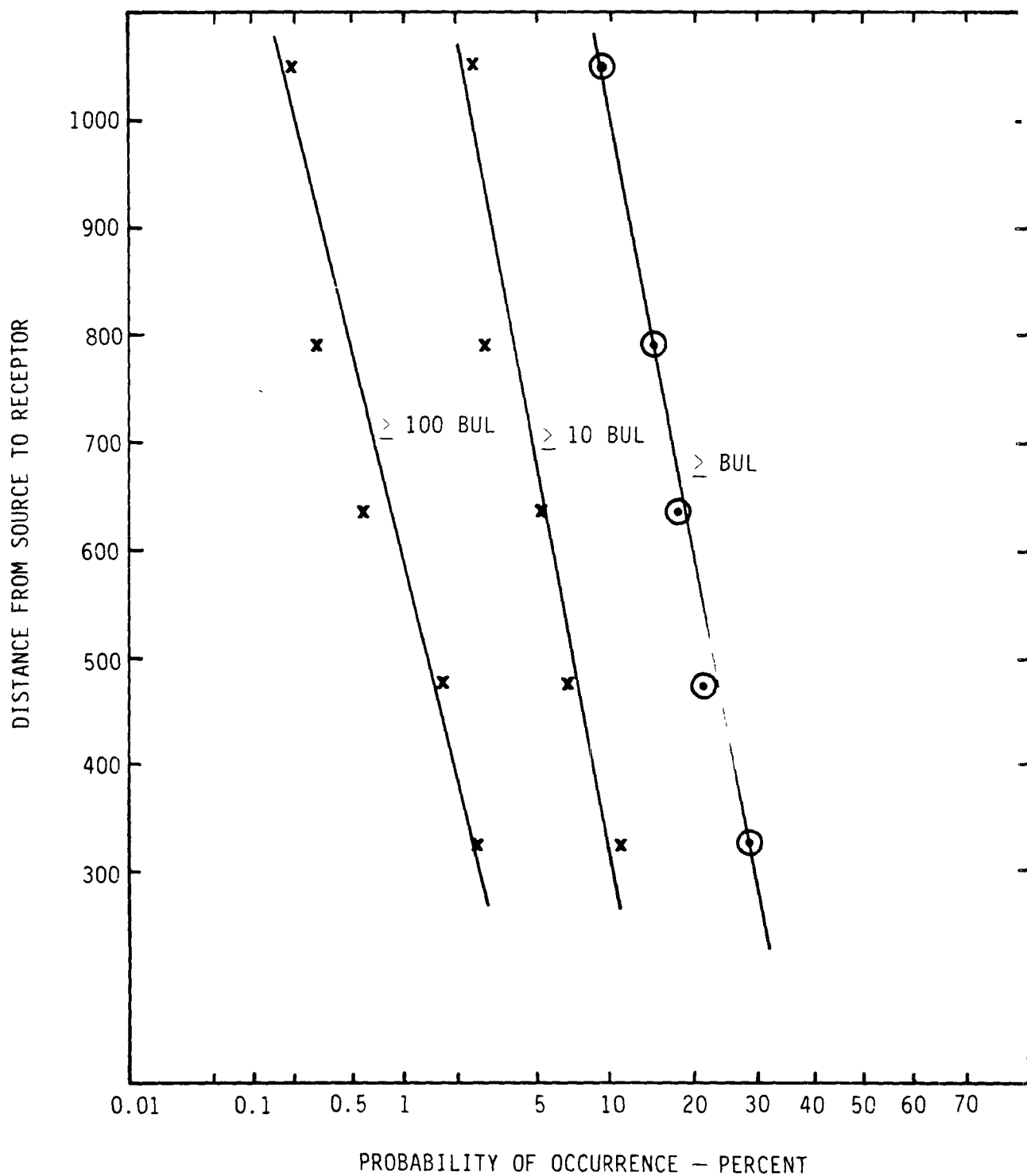


Figure 6-4. Frequency of occurrence of Krypton 85 concentrations as a function of distance for concentration levels \geq background upper limit (BUL), $\geq 10 \times \text{BUL}$ and $\geq 100 \times \text{BUL}$.

The release rates of inert tracer for the combined experiment are calculated for 10 times background concentration although 100 times background was considered. The data from Figure 6-4 provide estimates of the frequency of occurrence of impact as a function of source receptor separation. Concentrations were observed at 10 times the detection limit of the system 10 percent of the time at 300 km and 2.5 percent of the time at 1000 km. Concentrations 100 times the system's detection limit were observed 2.5 percent of the time at 300 km and about 0.2 percent of the time at 1000 km. Of course, it must be kept in mind that the source rate was not controlled and the total frequency of occurrence is a function of source term, meteorology, and distance. Tracer release on a full time basis should increase the frequency of occurrence by one third while tracer release on an every third day basis as planned for the combined experiments would decrease the frequency of occurrence to half of those shown.

An examination of the events concurrently affecting the two closest monitors was performed. The first monitor was 325 km from the source. The second monitor was 475 km from the source. Both reported concentrations above detection limit for the same, or subsequent 12 hour periods, 99 times. The number of events constituted 58 percent of the impact periods at the second monitor. A more complete analysis is required to determine if this difference in number of impacts is due to trajectories that did not pass from monitor 1 to monitor 2 or to a narrow plume that missed the second location.

ACURATE data could be used to establish uncertainties and analysis procedures for trajectories, concentrations at receptor locations, and source contributions at receptor points.

The significance of the ACURATE data is to reinforce the observation that the frequency of single point sources affecting single receptors is very low.

The long range tracer component of the combined experiment is designed to minimize this effect in three ways:

- 1) Tracer emissions are to be distributed over a relatively large area (appropriate scale: 100 km).
- 2) Sampling grid resolution was increased over initial designs.
- 3) Tracer emissions will be made from one of three pairs of tracer release sites determined by forecasts to provide the best data collection rate.

These techniques will increase the frequency of observing tracer concentrations substantially but the final expected frequency cannot be determined without data currently available. Some additional analyses of the ACURATE data may be beneficial. These are:

- 1) A study of the reduction of frequencies due to concentrations below background or detectable limits versus reductions due solely to transport.
- 2) A case study of data to characterize favorable and unfavorable transport episodes and to determine if distinguishable categories exist.
- 3) An additional case study to determine if a one year experimental period is sufficient to develop an empirical source/receptor relationship.

REFERENCES

AIHA. 1972. Air Pollution Manual Part I, Evaluation, 2nd edition. American Industrial Hygiene Association, Detroit, Michigan

Altshuller, A. P. 1976. Regional Transport and Transformation of Sulfur Dioxide and Sulfates in U.S.. Journal of the Air Pollution Control Association, 26:318-324.

Barry, P. J. 1974. Stochastic Properties of Atmospheric Diffusivity. Atomic Energy of Canada Ltd., Chalk River Nuclear Laboratories, Chalk River, Ontario. Published in The Effects of Sulfur in Canada, NRC of Canada. Ottawa, Ontario.

Bhargava, R. P. 1980. "Selection of a Subset of Pollution Stations in the Bay Area of California on the Basis of the Characteristic, 24-hour Suspended Particulate Concentrations, From the Viewpoint of Variation." Technical Report No. 37, Study on Statistics and Environmental Factors in Health, Department of Statistics, Stanford University.

Blumenthal, D. L., W. S. Keifer, and J. A. McDonald. 1981. "Aircraft Measurements of Pollutants and Meteorological Parameters During the Sulfate Program." Electric Power Research Institute, Palo Alto, CA.

REFERENCES (Continued)

Dietz, R. N., E. A. Cote, R. W. Goodrich. 1976a. "Development Application of Sulfur Hexafluoride Measurement Capabilities at Brookhaven National Laboratory, Upton, New York (BNL 21087).

Dietz, R. N., and W. F. Dabberdt. 1983. "Gaseous Tracer Technology Applications." Brookhaven National Laboratory, Upton, New York (BNL 33585).

Dietz, R. N., R. W. Goodrich, J. D. Smith and W. 1976b. "Summary Report of the Brookhaven Explosive Tagging Program." Brookhaven National Laboratory, Upton, New York (BNL 21041).

Dietz, R. N., R. W. Goodrich, E. A. Cote, G. 1983. "Passive and Programmable Samplers for with Perfluorocarbon Tracers." In preparation. Brookhaven National Laboratory, Upton, New York.

Dietz, R. N., and G. I. Senum. 1984. "Capabilities of Gaseous Tracers." Brookhaven National Laboratory, Upton, New York (BNL 35108).

Durrant

Des and
Sather
ky

REFERENCES

- AIHA. 1972. Air Pollution Manual Part I, Evaluation, 2nd edition. American Industrial Hygiene Association, Detroit, Michigan
- Altshuller, A. P. 1976. Regional Transport and Transformation of Sulfur Dioxide and Sulfates in U.S.. Journal of the Air Pollution Control Association, 26:318-324.
- Barry, P. J. 1974. Stochastic Properties of Atmospheric Diffusivity. Atomic Energy of Canada Ltd., Chalk River Nuclear Laboratories, Chalk River, Ontario. Published in The Effects of Sulfur in Canada, NRC of Canada. Ottawa, Ontario.
- Bhargava, R. P. 1980. "Selection of a Subset of Pollution Stations in the Bay Area of California on the Basis of the Characteristic, 24-hour Suspended Particulate Concentrations, From the Viewpoint of Variation." Technical Report No. 37, Study on Statistics and Environmental Factors in Health, Department of Statistics, Stanford University.
- Blumenthal, D. L., W. S. Keifer, and J. A. McDonald. 1981. "Aircraft Measurements of Pollutants and Meteorological Parameters During the Sulfate Regional Experiment (SURE) Program." Electric Power Research Institute, Palo Alto, CA. (EA-1909).
- Bowne, N. E. 1982. "A Comparison of Tracer and Sulfur Dioxide Measurements." TRC Environmental Consultants, Inc., East Hartford, Connecticut.
- Bowne, N. E., and R. J. Londergan. 1983. "Overview, Results, and Conclusions for the EPRI Plume Model Validation and Development Project: Plains Site" Electric Power Research Institute, Palo Alto, CA (EA-3074).
- Brady, P. J. 1978. Optimal sampling and analysis using two variables and modeled cross-covariance functions. J. Appl. Meteorol. 17:12-21.
- Brillinger, D. R. 1975. Time Series Data Analysis and Theory. Holt Rinehart and Winston, Inc.
- Chung, Y. S. The Distribution of Atmospheric Sulfates in Canada and Its Relationship to Long Range Transport of Air Pollutants, Atmospheric Environment, 12:1474-1480.
- Clark, T. L., G. J. Ferber, J. L. Heffter, R. R. Draxler. 1984. "Cross-Appalachian Tracer Experiment (CAPTEX'83)." Fourth Joint Conference on Applications of Air Pollution Meteorology, American Meteorological Society, Boston, MA.
- Delhomme, J. P. 1978. Kriging in the hydrosociences. Advances in Water Resources, 1:251-266.
- Dietz, R. N., and E. A. Cote. 1971. GC determination of sulfur hexafluoride for tracing air pollutants. Div. Water, Air, and Waste Chem., 11:208-215.

REFERENCES (Continued)

- Dietz, R. N., E. A. Cote, R. W. Goodrich. 1976a. "Development and Application of Sulfur Hexafluoride Measurement Capabilities at Brookhaven." Brookhaven National Laboratory, Upton, New York (BNL 21087).
- Dietz, R. N., and W. F. Dabberdt. 1983. "Gaseous Tracer Technology and Applications." Brookhaven National Laboratory, Upton, New York (BNL 33585).
- Dietz, R. N., R. W. Goodrich, J. D. Smith and W. Vogel. 1976b. "Summary Report of the Brookhaven Explosive Tagging Program." Brookhaven National Laboratory, Upton, New York (BNL 21041).
- Dietz, R. N., R. W. Goodrich, E. A. Cote, G. I. Senum and G. S. Raynor. 1983. "Passive and Programmable Samplers for Atmospheric Transport Studies with Perfluorocarbon Tracers." In preparation, Brookhaven National Laboratory, Upton, New York.
- Dietz, R. N., and G. I. Senum. 1984. "Capabilities, Needs, and Applications of Gaseous Tracers." Brookhaven National Laboratory, Upton, New York (BNL 35108).
- Durran, D., M. J. Meldgin, and M. K. Liu. 1979. A study of long-range air pollution problems related to coal development in the Northern Great Plains. Atmos. Environ., 13:1021-1037.
- EPA. 1971. Guidelines: Air Quality Surveillance Networks. U.S. Environmental Protection Agency, Research Triangle Park, North Carolina (AP-98).
- Eddy, A. 1974. An approach to the design of meteorological field experiments. Mon. Wea. Rev., 102:702-707.
- Eddy, A. 1967. The statistical objective analysis of solar data fields. J. Appl. Meteor., 6:597-609.
- Eddy, A. 1974. An approach to the design of meteorological field experiments. Mon. Wea. Rev., 102:702-707.
- Eddy, A. 1976. Optimal rainage densities and accumulation times: A decision-making procedure. J. Appl. Meteorol., 15:962-971.
- Evans, L. S., G. S. Raynor, and D. M. Jones. 1984. Frequency Distributions for Durations and Volumes of Rainfalls in the Eastern United States in Relation to Acidic Precipitation. Water, Air and Soil Pollution, 23:187-195.
- Ferber, G. and J. Heffter. 1983. CAPTEX '83 Cross Appalachian Tracer Experiments: Revised Plan, NOAA ARL, Rockville, MD.
- Ferber, G. F., K. Telegadas, J. L. Heffter, C. R. Dickson, R. N. Dietz, P. W. Krey. 1981. "Demonstration of a Long-range Atmospheric Tracer System Using Perfluorocarbons." Air Resources Laboratories, Silver Spring, Maryland (ERL ARL-101).
- Forrest, J. and L. Newman. 1973. Sampling and analysis of atmospheric sulfur compounds for isotope ratio studies. Atmos. Environ., 7:561-573.

REFERENCES (Continued)

- Fowler, M. M. and S. Barr. 1983. A long-range atmospheric tracer field test. Atmos. Environ., 17(9):1677-1686.
- Freeman, D. L., N. R. Robinson, J. G. Watson, and R. T. Egami. 1984. "Propagation of Measurement Uncertainties in Gaussian Plume Models: An Application to Experimental Data." Fourth Joint Conference on Applications of Air Pollution Meteorology. American Meteorological Society, Boston, Mass.
- Gandin, L. S. 1965. "Objective Analysis of Meteorological Fields." Israel Program for Scientific Translations, Jerusalem (translated from Russian; originally published 1963, Leningrad).
- Geogapoulos, P. G., and J. H. Scenfield. 1982. Statistical Distributions of Air Pollutant Concentrations, Environmental Science and Technology, 16:401A-416A.
- Hanna, S. R. 1984. Concentration fluctuations in a smoke plume. Atmos. Environ., 18(6):1091-1106.
- Heffter, J. L., J. F. Schubert, and G. A. Mead. 1984. Atlantic Coast Unique Regional Atmospheric Tracer Experiment (ACURATE). NOAA Technical Memorandum (ERL ARL-130).
- Henderson, R. G., and K. Weingartner. 1982. Trajectory Analysis of MAP3S Precip. Chemistry Data at Ithaca, NY, Atmospheric Environment, 16:1647-1666.
- Hicks, B. B. 1984. "Background Notes on the Use of Sulfur Isotopes in Long-Range Tracer Experiments." National Oceanic and Atmospheric Administration, Oak Ridge, Tennessee.
- Hidy, G. M., P. Mueller, and E. Tong. 1978. Spatial and Temporal Distribution of Airborne Sulfate in Parts of the U.S. Atmospheric Environment, 12:735-752.
- Hitchcock, D. R., and M. S. Black. 1984. $^{34}\text{S}/^{32}\text{S}$ evidence of biogenic sulfur oxides in a salt marsh atmosphere. Atmos. Environ., 18(1):1-17.
- Horst, T. W. 1977. A surface depletion model for deposition from a Gaussian Plume. Atmos. Environ., 11:41-46.
- Horst, T. W., J. C. Doran, and P. W. Nickola. 1983. "Dual Tracer Measurements of Plume Depletion." In Precipitation Scavenging, Dry Deposition, and Resuspension. Elsevier Science, The Netherlands.
- Huijbregts, C. J. 1975. "Regionalized Variables and Quantitative Analyses of Spatial Data. In Display and Analysis of Spatial Data, J. Davis and M. McCullagh, eds., Wiley, London.
- Kaplan, I. R., and S. C. Rittenberg. 1964. Microbiological fractionation of sulphur isotopes. J. Gen. Microbiol., 24:195-212.

REFERENCES (Continued)

- Klein, W. H. 1957. Principal Tracks and Mean Frequencies of Cyclones and Anticyclone in the Northern Hemisphere. Research Paper No. 40, U.S. Weather Bureau, Wash. DC, 60 pages.
- Korshover, J. 1976. Climatology of Stagnating Anticyclones East of the Rocky Mountains 1936-1975. ERL-ARL-55, NOAA Technical Memorandum Silver Springs, MD.
- Krick, I. P. 1943. Synoptic Weather Types of North America. NOAA Technical Memorandum.
- Lamb, R. G. 1984. Air pollution models as descriptors of cause-effect relationships. Atmos. Environ., 18(3):591-606.
- Langstaff, J., C. Seigneur, T. Myers, G. Whitten, and M. K. Liu. 1984. "Design of an Optimum Air Monitoring Network to Support Toxic Exposure Assessment." Systems Applications, Inc., San Rafael, California (SYSAPP-84/175).
- Leaderer, B. P., and Stalwyk, J. A. 1981. Seasonal Visibility and Pollutant Sources in Northeast U.S., Environmental Science and Technology, 15:305-309.
- Liu, M. K., D. A. Stewart, and D. Henderson. 1982. A mathematical model for the analysis of acid deposition. J. Appl. Meteorol., 21:859-873.
- Manowitz, B., L. Newman, W. D. Tucker, and others. 1970. "The Atmospheric Diagnostics Program at Brookhaven National Laboratory, Third Status Report." Brookhaven National Laboratory, Upton, New York (BNL 50280).
- MAP3S/RAINE Research Community. 1982. The MAP3S/RAINE Precipitation Chemistry Network: Statistical Overview for the Period 1976-1980. Atmos. Environ., 16(7):1603-1631.
- McNaughton, D. J., and N. E. Bowne et al. 1984. "Comprehensive Field Study Plan to Relate Pollutant Sources to Acidic Deposition." TRC Environmental Consultants, Inc., East Hartford, CT.
- Morris, M. D., and S. F. Ebey. 1984. An interesting property of the sample mean under a first-order autoregressive model. Amer. Statistician, 38(2):127-128.
- Morris, R. E., D. A. Stewart, S. M. Greenfield, and M. K. Liu. 1984. "A Preliminary Test of the Ability of Emission Modulation to Establish Empirical Source-Receptor Relationships." Systems Applications, Inc., San Rafael, CA (SYSAPP-84/096).
- Mueller, P. K., and G. M. Hidy. 1979. "Implementation and Coordination of the Sulfate Regional Experiment (SURE) and Related Research Programs." Electric Power Research Institute, Palo Alto, CA (EA-1066).
- Mueller, P. K., and G. M. Hidy. 1982. "The Sulfate Regional Experiment: Documentation of SURE Sampling Sites." Electric Power Research Institute, Palo Alto, CA (EA-1902).

REFERENCES (Continued)

Mueller, P. K., and G. M. Hidy. 1983. "The Sulfate Regional Experiment: Reporting of Findings," 3 vols. Electric Power Research Insititute, Palo Alto, CA (EA-1901).

Mueller, P. K. and J. G. Watson. 1982. "Eastern Regional Air Quality Measurements," Volume 1. Electric Power Research Institute, Palo Alto, CA (EA-1914).

NCAR. 1983. "Regional Acid Deposition: Models and Physical Processes." National Center for Atmospheric Research, Boulder, CO (Technical Note NCAR/TN-214+STR).

NRC. 1983. Acid Deposition: Atmospheric Processes in Eastern North America. National Research Council. National Academy Press, Washington, DC.

Nakamori, Y., S. Ikeda, and Y. Sawaragi. 1979. Design of air pollutant monitoring system by spatial sample stratification. Atmos. Environ., 13:97-103.

Netterville, D. D. J. 1979. "Concentration Fluctuations in Plumes." Syncrude Canada Ltd (Environmental Research Monograph 1979-4).

Newman, L., et al. 1971. A tracer method using stable isotopes of sulfur. Proc. American Nuclear Society Topical Meeting on Nuclear Methods in Environmental Research.

Newman, L., J. Forrest, and B. Manowitz. 1975a. The application of an isotopic ratio technique to a study of the atmospheric oxidation of sulfur dioxide in the plume from an oil-fired power plant. Atmos. Environ., 9:959-968.

Newman, L., J. Forrest, and B. Manowitz. 1975b. The application of an isotopic ratio technique to a study of the atmospheric oxidation of sulfur dioxide in the plume from a coal-fired power plant. Atmos. Environ., 9:969-977.

Niemann, B. L. 1982. An Analysis of Regional Acid Deposition Episodes and the Feasibility of Their Deterministic Simulation. U.S. Environmental Protection Agency, Washington, DC. 19 pages.

Niemann, B. L. 1983. Further Analysis of Relationships Between Scavenging Ratios for Exceptional Episodes and Air Quality and Storm Parameters. U.S. Environmental Protection Agency, Washington, DC, 14 pages.

Meteorological Aspects of Acid Rain, C. Bhumralkar (ed.) Ann Arbor Science.

Niemann, B. L. 1982. Analysis of Wind and Precipitation Data for Assessments of Transboundary Transport and Acid Deposition between Canada and the United States.

Niemann, B. L. and P. M. Mayerhofer. 1978. "A Climatology and Meteorological Parameters for Short Range Dispersion and Long Range Transport," in Proceedings of the 9th Int'l Technical Meeting on Air Pollution Modeling and Its Applications (Brussels, Belgium NATO 1978).

REFERENCES (Continued)

- O'Conner, J. F. 1961. Mean Circulation Patterns based on 12 years of recent North. Hemis. data. Mon. Wenth. Review, 89:211-227.
- Pack, D. H., et al, 1978. Meteorology of Long Range Transport, Atmospheric Environment, 12:425-444.
- Papoulis, A. 1965. Probability, Random Variables, and Stochastic Processes. McGraw-Hill, New York.
- Pickett, E. E., and R. G. Whiting. 1981. The design of cost-effective air quality monitoring networks. Env. Monitor. Assess., 1:59-74.
- Raynor, G. S., and J. V. Hayes. 1982. Variation in Chemical Wet Deposition with Meteorological Conditions. Atmospheric Environment, 16(7):1647-1656.
- Sloane, C. S. 1983. Summertime Visibility Declines: Meteorological Influences. Atmospheric Environment, 17:763-774.
- Smith, F., C. E. Decker, R. B. Strong, J. H. White, F. K. Arey, and W. D. Bach. 1983. "Estimates of Uncertainty for the Plume Model Validation and Development Project Field Measurements -- Plains Site." Electric Power Research Institute, Palo Alto, CA (EA-3081).
- Smith, F. B. 1981. The Significance of Wet and Dry Synoptic Regions on Long Range Transport of Pollution and its Deposition, Atmospheric Environment, 15(5):863-873.
- Stern, A. C. 1968. Air Pollution, 2nd edition. Academic Press, New York.
- Stewart, D. A., R. E. Morris, A. B. Hudischewskj, M. K. Liu, and D. Henderson. 1983a. "Evaluation of Episodic Regional Transport Models of Interest to the National Park Service." Systems Applications, Inc., San Rafael, CA (SYSAPP-83/020).
- Stewart, D. A., R. E. Morris, M. K. Liu. 1983b. "Evaluation of Long-Term Regional Transport Models of Interest to the National Park Service." Systems Applications, Inc., San Rafael, CA (SYSAPP-83/215).
- Sullivan, P. J. 1984. "Whence the Fluctuations in Measured Values of Mean-Square Fluctuations?" Fourth Joint Conference on Applications of Air Pollution Meteorology. American Meteorological Society, Boston, Mass.
- Thiebaut, H. J., and F. W. Zwiers. 1984. The interpretation and estimation of effective sample size. J. Climate Appl. Meteor., 23:800-811.
- Thorp, J. M., and B. C. Scott. 1982. Preliminary Calculations of Average Storm Duration and Seasonal Precipitation Rates for the Northeast Sector of the United States. Atmos. Environ., 16(7):1763-1774.

REFERENCES (Continued)

Tong, E. Y., M. T. Mills, and B. L. Niemann. 1979. Characterization of Regional Episodes of Particulate Sulfates and Ozone Over the Eastern United States and Canada. Presented at the WMO Symposium on the Long Range Transport of Pollutants and Its Relation to General Circulation Including Stratospheric/Tropospheric Exchange Processes.

Tong, E. Y., and R. B. Batchelder. 1978. Aerometric Data Compilation and Analysis for Regional Sulfate Modeling. Teknekron, Inc., Berkeley, California, 135 pages.

Tijonis, J. and K. Yuan. 1978. Visibility in the Northeast United States, U.S. Environmental Protection Agency, (EPA-600/3-78-075).

Venkatram, A. 1983. Uncertainty in predictions from air quality models. Boundary-Layer Meteor., 27:185-196.

Wilson, J. W., V. A. Mohnen, and J. Kadlecsek. 1982. Wet Deposition Variability as Observed by MAP3S. Atmospheric Environment, 16:1657-1666.

Yerg, M. C. 1973. "An Optimal Sampling and Analysis Methodology." University of Oklahoma, Department of Meteorology Report.